A STUDY ON STRENGTH AND DEFORMATION BEHAVIOUR OF GLASS FIBRE-REINFORCED CLAYEY AND SANDY SOILS UNDER VARYING MOULDED STATES

A Thesis

Submitted in Partial Fulfillment of the Requirements

for the Degree of

DOCTOR OF PHILOSOPHY

by

SUCHIT KUMAR PATEL

DEPARTMENT OF CIVIL ENGINEERING

INDIAN INSTITUTE OF TECHNOLOGY GUWAHATI

DECEMBER 2017

Dedicated to my Parents whose blessings brought me to this stage

STATEMENT

I do hereby declare that the matter embodied in this thesis is the result of investigations carried out by me in the Department of Civil Engineering, Indian Institute of Technology Guwahati, Guwahati, Assam, India.

In keeping with the general practice of reporting scientific observations, due acknowledgements have been made wherever the work described is based on findings of other investigators.

IIT Guwahati Suchit Kumar Patel

Date:

CERTIFICATE

This is to certify that the thesis entitled **"A Study on Strength and Deformation Behaviour of Glass Fibre-Reinforced Clayey and Sandy Soils Under Varying Moulded States"** submitted by Suchit Kumar Patel (Roll No. 126104037), to the Indian Institute of Technology Guwahati, for the award of degree of Doctor of Philosophy in Civil Engineering, is a record of bonafide research work carried out by him under my supervision and guidance. The thesis work, in my opinion, has reached the requisite standard fulfilling the requirement for the degree of Doctor of Philosophy. The results contained in this thesis have not been submitted in part or full to any other University or Institute for award of any degree or diploma.

Date:

Dr. Baleshwar Singh
Professor
Department of Civil Engineering
Indian Institute of Technology Guwahati
Guwahati-781039
India

ACKNOWLEDGEMENTS

I would like to express my sincere gratitude and respect to my supervisor, Prof. Baleshwar Singh, for his unconditional guidance, support and advice throughout this research. Working with Prof. Singh has been an invaluable learning experience for me. This research would not have been possible without his support and guidance. I am also thankful to my doctoral committee members, Prof. Arbind Kumar Singh, Dr. T. V. Bharat and Dr. Karuna Kalita for their advice and encouragement during my research.

I express my heartfelt gratitude and thanks to the technical officer of Geotechnical Engineering Laboratory Mr. Samarjyoti Kalita, for extending all possible support for my experiments. I also acknowledge the unconditional and invaluable help of Mr. Hari Ram Upadhyaya and Mr. Siva Kalita during my experimental works. Furthermore, I would like to thank the staff of Civil Engineering Department office, for their support in official works.

I also want to thank my fellow research scholars and postgraduate friends for their love, timely help, moral support, and friendship. In particular, Shiv Shankar, Tanmoy, Pawan, Chandra Bhanu, Ansel, Kumar Abhishek, Arya, Krishanu, and Argdeep Biswas, who have offered their generous help with my research and made my life enjoyable here.

Last, but most importantly I am very grateful to my parents whose unconditional love, faith and patience encouraged me throughout the journey to achieve this. I am thankful to my wife (Menka Patel), younger brother (Abhay) and sister (Sulekha) who are always beside me for everything.

Suchit Kumar Patel

ABSTRACT

The strength of available soils in the field may not be sufficient for various construction activities, and it can also differ due to the variation of environmental conditions of moisture content and temperature. Moisture variation is mainly due to local factors that include precipitation, drainage condition, soil permeability, water table and capillary action. The variation in moisture content may have both short and long term effects on the strength and deformation characteristics of the soil.

Among the several techniques that are currently in use to improve the engineering properties of soils, soil reinforcement method is getting increasing favour of practising engineers due to its simplicity, ease of construction and overall economy. After the earliest reinforcement in the form of galvanized steel strips of high tensile modulus, use of synthetic materials named as geosynthetics in different forms (geogrid, geotextile, geocomposite etc.), and of natural products (bamboo, jute and coir) are being adopted in the form of sheets or meshes. In most applications, the conventional method of soil reinforcement is in a continuous planer form introduced within the soil mass in a definite pattern. The one-dimensional orientation of reinforcement is installed sequentially in alternating layers as per the design requirements of the structure.

Other than conventional method of reinforcement, soils can be reinforced with discrete fibres. The concept of fibre-reinforced soil originated in ancient times, when natural fibre materials including straw and plant roots were added to soil bricks to provide integrity to the soil matrix by arresting the development of cracks. The use of natural fibres in composite construction can be seen even today in the rural areas of India where mud houses are made by using natural reinforcement. Fibre reinforcement technique can also be used successfully in the structures where implementation of traditional planer reinforcement is difficult due to geometric constraints of limited space. The arrangement of fibres in the fibre-

reinforced soil is basically three-dimensional, though it is dependent on the quality of mixing and placement. Fibres can be classified as natural fibres and synthetic fibres. Most natural fibres are the byproducts of plants and vegetation whereas synthetic fibres are artificially made from synthesized polymers.

In spite of several advantages, field applications of fibre-reinforced soil have been rather limited and are still lagging behind the traditional planer reinforcement method. There is ample scope to increase field applications of fibre reinforcement in both cohesive and cohesionless soils. In the present study, the strength and deformation behaviour of two soil types, a clayey soil and a sandy soil, reinforced with glass fibres, were studied through a systematic series of laboratory tests. Glass fibre was considered as reinforcing material due to its high strength, stiffness, light weight and non-biodegradable characteristics, which makes it beneficial for long-term soil reinforcement. This study may also encourage the use in soil reinforcement of recycled glass fibres derived from industrial glass wastes.

Glass fibres of 0.15 mm diameter and of different lengths (10, 20 and 30 mm) were mixed randomly up to 1% content with the clayey soil and up to 4% content with the sandy soil. The reinforced clayey soil specimens were moulded at different combinations of dry unit weight and moisture content, close to the maximum dry unit weight and optimum moisture content of the unreinforced soil, whereas the reinforced sandy soil specimens were moulded at relative densities ranging from 35% to 85%.

Unconfined compression tests, California Bearing Ratio tests and consolidated undrained triaxial tests were conducted on reinforced clayey soil specimens, whereas only consolidated drained triaxial tests were carried out on reinforced sandy soil specimens. The soaking period in CBR tests was extended up to 40 days from the standard 4 days. The laboratory results were analysed to evaluate the effect of the glass fibres on the compressive strength, CBR, shear strength, failure axial strain, specimen deformation and failure modes,

secant modulus and energy absorption capability. The contribution of fibres to the soil strength improvement under varying moulded states has been examined, and a comparison has been made on the behaviour of glass fibre-reinforced clayey soil and sandy soil. For the materials used in the study, representative equations have been developed to predict the major principal stress at failure of glass fibre-reinforced soils.

TABLE OF CONTENTS

LIST OF TABLES

LIST OF FIGURES

ABBREVIATIONS AND NOTATIONS

ANOVA	analysis of variance
BPR	bearing pressure ratio
CBR	California Bearing Ratio
C_c	coefficient of curvature
C_u	coefficient of uniformity
c'	cohesion intercept (kPa)
D	specimen diameter (mm)
DR	deformation ratio (dimensionless)
DSR	deviator stress ratio (dimensionless)
D_r	relative density (%)
d	fibre diameter (mm)
df	degrees of freedom (dimensionless)
EAC	energy absorption capability (kJ/m^3)
$(EAC)_f$	energy dissipated in soil-fibre interaction and fibre stretching (kJ/m^3)
f_c	fibre content (%)
G_s	specific gravity of soil solid (dimensionless)
G_f	specific gravity of fibre (dimensionless)
I_B	brittleness index (dimensionless)
I_{CBR}	CBR improvement factor (dimensionless)
k_s	secant subgrade modulus (MN/m^3)
L	fibre length (mm)
L/d	fibre aspect ratio (dimensionless)
MDU	maximum dry unit weight (kN/m^3)
OMC	optimum moisture content (%)
SR	strength ratio (dimensionless)
UCS	unconfined compressive strength (kPa)
W_f	weight of fibres
W_s	weight of dry soil
w	moisture content (%)
V	volume of specimen

γ_d	dry unit weight (kN/m^3)
σ_3	confining pressure (kPa)
σ_{1f}	major principal stress at failure (kPa)
$\sigma_{d,fibre}$	failure deviator stress of reinforced soil (kPa)
$\sigma_{d,un}$	failure deviator stress of unreinforced soil (kPa)
σ_n	normal stress (kPa)
τ	shear stress (kPa)
η	fibre aspect ratio
χ	Volumetric fibre content
ϕ'	friction angle (˚)
δ	fibre skin friction angle (˚)
Δ_r	failure strain of fibre-reinforced soil (%)
Δ_u	failure strain of unreinforced soil (%)

CHAPTER 1

INTRODUCTION

1.1 INTRODUCTION

With rapid worldwide development, there is an increasing demand for the construction of new roads, embankments, slopes, retaining structures and foundations. As competent soil conditions do not exist everywhere, utilization of marginal land and soft ground is a must, after improving the strength and stiffness of the soils by adopting any suitable modification technique. The soil strength in the field can differ due to the variation of environmental conditions of moisture content and temperature. Moisture variation is mainly due to local factors that include precipitation, drainage condition, soil permeability, water table and capillary action. The variation in moisture content may have both short and long term effects on the strength and deformation characteristics of the soil.

Several techniques are currently in use to improve the engineering properties of soils. These methods include soil stabilization using lime or cement, mechanical modification using external compaction, pre-consolidation using vertical drains, modification by inclusion of stone column and soil nails, soil reinforcement, grouting and mechanical mixing. The application of any method depends on the field requirement and economic constraints which can vary from site to site. The soil reinforcement method is getting the favour of the practising engineers, primarily due to its simplicity, ease of construction and overall economy.

1.2 SOIL REINFORCEMENT

Soil reinforcement is a method where various types and forms of tension resisting elements are embedded in the soil mass to improve its engineering properties. This method is

being used widely and effectively in the construction practice of civil engineering projects, including retaining structures, pavements, embankments, slopes and foundations. Soil reinforcement can be done by either incorporating continuous reinforcement inclusions within soil in some definite patterns, or by mixing discrete fibres randomly within soil mass before their placement and compaction.

Soil-reinforcement method has got establishment in modern era after the pioneering work by Vidal (1969) where the reinforcement in the form of inextensible steel/metal strips within soil was used. This led to the first development of principles for design and analysis of earth structures reinforced with planar geosynthetics, and this reinforced soil was named as Reinforced Earth (Schlosser and Long 1974). After the earliest reinforcement in the form of galvanized steel strips of high tensile modulus, use of synthetic materials named as geosynthetics in different forms (geogrid, geotextile, geocomposite etc.), and of natural products (bamboo, jute and coir) are being adopted in the form of sheets or meshes. The soil reinforced with extensible reinforcement is also termed as geosynthetic-reinforced soil (or as ply soil by McGown et al. 1978).

In most applications, the conventional method of soil reinforcement is in a continuous planer form introduced within the soil mass in a definite pattern, resulting in the systematically reinforced soil (Koerner 1998, Shukla 2002). The one-dimensional orientation of reinforcement is installed sequentially in alternating layers as per the design requirements of the structure.

1.3 FIBRE-REINFORCED SOIL

Other than conventional method of reinforcement, soils can be reinforced with discrete fibres. In fibre-reinforced soil, fibres of the desired type and quantity are added to the soil, mixed randomly and laid in the position after compaction. The arrangement of fibres in

the fibre-reinforced soil is basically three-dimensional, though it is dependent on the quality of mixing and placement.

The concept of fibre-reinforced soil originated in ancient times, when natural fibre materials including straw and plant roots were added to soil bricks to provide integrity to the soil matrix by arresting the crack development (Hoover et al. 1982). The Ziggurats of Babylon were built 3000 years ago using reeds in the form of woven mats, and in the Great Wall of China completed about 200BC, tamarisk branches were mixed with clay and gravel (Sarsby 2007). The use of natural fibres in composite construction can be seen even today in the rural areas of India where mud houses are made by using natural reinforcement.

However, the understanding of mechanism of fibre-reinforced soils began in the 1970s when Waldron (1977) made an attempt to estimate the influence of plant and tree roots on the stability of earth slopes. The mechanism of fibre-reinforced soil is similar to that of root-reinforced soil, where the plant roots enhance the shear strength of the soil by mobilizing additional cohesion (Wu et al. 1979, Waldron and Dakessian 1981, Greenwood et al. 2004, Abdullah et al. 2011), as typically shown in Fig. 1.1. In the last 30-35 years, fibre-reinforced soils have attracted increasing attention in the field applications of geotechnical engineering (Shukla 2017).

Fibres can be classified as natural fibres and synthetic fibres. Most natural fibres are the byproducts of plants and vegetation while synthetic fibres are artificially made from synthesized polymers. Various types of natural fibres available in India are: coir, sisal, jute, bhabar, hemp, munja, bamboo and banana. Typical natural and synthetic fibres are shown in Fig. 1.2. Most of the natural fibres lose their strength under changing environmental conditions of alternate wetting and drying, and exposure of sunlight. As they are biodegradable and have poor resistance to alkaline environment, they can be used as soil

reinforcement with suitable chemical treatment. Among the natural fibres, coir fibres are strong and have high resistance to biodegradation.

Fig. 1.1 Slope protection using vegetation for Dora bridge abutment in Assam, India (http://www.chhajedgarden.com/blog/vetiver-planting-for-slope-stabilization/)

Fig. 1.2 Typical fibre types used in soil reinforcement: (a) coir fibre; (b) jute fibre; (c) polypropylene fibre; (d) glass fibre

On the other hand, synthetic fibres (polypropylene, nylon, plastic, glass, asbestos etc.) have higher tensile strength and are non-biodegradable. Most of them are resistant to harsh

chemical environment and environmental conditions (heat, cold, moisture variation and sunlight). Synthetic fibres can be produced according to desired specifications as per field requirements. For example, their geometry can be controlled, and their shape and surface conditions can be altered in order to enhance the frictional properties.

1.4 ADVANTAGES OF FIBRE-REINFORCED SOIL

Fibre-reinforced soil is similar to the conventional soil stabilization method in its preparation where additive (lime, cement or any chemical) is mixed into the soil and then compacted. Randomly mixed fibres within soil makes it a homogeneous mass and provides an isotropic strength improvement of the soil composites (Tang et al. 2007) by evading the development of any weak plane, such as parallel to oriented reinforcement. This method can be used in any type of soil (sand, silt and clay). Unlike lime, cement and other chemical stabilization methods, the construction using fibre reinforcement is not significantly affected by weather conditions. This reinforcement technique can also be used successfully in the structures where implementation of traditional planer reinforcement is difficult due to geometric constraints of limited space as in repairing of localized slope failure and reinforcement of thin soil veneers (Zornberg et al. 2002, Najjar et al. 2013). Fibres are not easily damaged during field applications, and the inclusion of fibres only changes the physical properties of soil and has no impact on environment (Li et al. 2014). Fibres of desired strength and stiffness can also be manufactured as per the requirements.

Among different fibres that are usable, glass fibre has high strength and stiffness (Lutz et al. 2002), and its ready availability and non-biodegradable characteristics make it more attractive for long-term soil reinforcement material (Mujah et al. 2013). Glass fibre also retains 70-75% of its original elastic modulus and tensile strength even under 450°C temperature (Ahmad et al. (2012).

In spite of the above advantages, field applications of fibre-reinforced soil have been rather limited and are still lagging behind the traditional planer reinforcement method. There is ample scope to increase field applications of fibre reinforcement in both clayey and sandy soils.

1.5 OBJECTIVE AND SCOPE OF THE STUDY

In earlier studies on fibre-reinforced soil, the effect of specimen moulded states on strength behaviour has not been covered, especially for clayey soil. In this study, glass fibre is considered as reinforcing material due to its high strength, stiffness, high ratio of surface area to weight, dimensional stability, ready availability, lightweight and non-biodegradable characteristics (Mujah et al. 2013), which makes it more beneficial for long-term soil reinforcement. Glass fibre also retains its tensile strength and elastic modulus at 70-75% of that of original fibres even under 450 °C temperature (Ahmad et al. 2012). With glass fibre reinforcement, a wide range of tensile strength suitable for specific sites can be achieved (Lutz & Grossman 2001). This study may also encourage the use in soil reinforcement of recycled glass fibres derived from industrial glass wastes.

Therefore, the main objective of the present study is to understand the effect of randomly distributed glass fibres on the strength and deformation behaviour of a clayey soil and a sandy soil, especially under varying moulded states, by conducting different laboratory tests. This will provide a better insight for the field application of glass fibre-reinforced soils with varying moulding states.

The scope of the present work can be summarized as follows:

1. To characterize the soil materials used in this study, and to determine the required moulded states of the specimens of clayey soil and sandy soil, respectively through compaction tests and relative density tests.

2. To conduct unconfined compression tests on the glass fibre-reinforced clayey soil, and to evaluate the effects of fibre content, fibre length, moulding moisture content and dry unit weight variation on unconfined strength and deformation behaviour.
3. To carry out California Bearing Ratio tests on the glass fibre-reinforced clayey soil, and to study the effects of fibre content, fibre length, moulding moisture content and soaking period variation on bearing capacity behaviour.
4. To conduct consolidated undrained triaxial tests on the glass fibre-reinforced clayey soil, and to analyse the effects of fibre content, fibre length and moulding dry unit weight variation on stress-strain response, pore pressure response, deformation and failure modes of the soil specimens.
5. To carry out consolidated drained triaxial tests on glass fibre-reinforced sandy soil, and to study the effects of fibre content, fibre length and relative density variation on stress-strain response, volume change response, deformation and specimen failure modes.

1.6 ORGANIZATION OF THE THESIS

The thesis is organized in eight chapters, including the present introductory one. Chapter 2 presents a review of literature on fibre-reinforced soils under different sections, summarizing the works of various researchers based on the materials used, the experimental methods and the analysis approaches adopted. Chapter 3 describes the details of the soil types and the fibres used, types of laboratory tests, and specimen preparation procedures. Chapter 4 deals with the testing programme, experimental details, and results of unconfined compression test on glass fibre-reinforced clayey soil. In Chapter 5, the testing programme, experimental details and results of California Bearing Ratio tests on glass fibre-reinforced clayey soil are presented and discussed. Chapter 6 presents the testing programme,

experimental details and the performance improvement of glass fibre-reinforced clayey soil under undrained triaxial compression tests. Subsequently, a representative equation for predicting the shear strength of clayey soils due to glass fibre reinforcement is brought out. Chapter 7 brings out the testing details and results of drained triaxial compression tests on fibre-reinforced sandy soil, and a representative equation for predicting the shear strength performance improvement of sandy soils due to glass fibre reinforcements is brought out. Chapter 8 summarizes the results obtained and conclusions drawn from the present study.

CHAPTER 2

LITERATURE REVIEW

2.1 INTRODUCTION

A brief review of the literature is presented in this chapter. The available literature is grouped in different sections: laboratory tests along with soil type, field tests, fibre-reinforced soil models and some numerical studies, and applications of fibre-reinforced soils. In the last section, a summary of the literature review is brought out based on which the scope of the present study is defined.

2.2 SHEAR STRENGTH BEHAVIOUR OF FIBRE-REINFORCED SOILS

2.2.1 Direct Shear Tests on Sandy Soils

Initial work on fibre-reinforced soil was carried out by Gray and Ohashi (1983). They conducted direct shear tests on dry sand reinforced with natural fibres, synthetic fibres and copper wires. Fibres were placed in regular patterns in loose sand (D_r = 20%) and dense sand (D_r = 100%) in either perpendicular orientation or in inclined orientations of 30˚, 60˚, 120˚ and 150˚ with shear surface. Increase in shear strength was the maximum for fibre orientation of 60˚, and the improvement was directly proportional to the fibre area ratio, while it increased with fibre length up to a point. The shear strength increment was same irrespective of specimen density. Shear strength envelopes for the fibre-reinforced sand clearly showed the existence of a threshold confining stress below which the fibres tended to slip or pull out. Above this threshold stress, parallel envelopes indicated that the fibres did not affect the angle of internal friction of the sand. They compared the experimental observations of the shear strength for fibre-reinforced sand with theoretical predictions based on a force-equilibrium model proposed by them.

Shewbridge and Sitar (1989) performed a series of direct shear tests in order to examine the mechanism of shear zone development in reinforced sands and to quantify their deformation characteristics. Different types of reinforcements were used in the tests: bungy cord, parachute cord, wood dowelling, aluminium rod and steel rod. Tests results showed that the width of shear zone increased for reinforced soil, and it further widened with increasing stiffness of the composite due to any combination of increased reinforcement concentration, stiffness, and reinforcement-soil bond strength.

Nataraj and McManis (1997) compared the strength and deformation characteristics of a sand (SP) and a clay (CL) reinforced with randomly distributed polypropylene fibrillated fibres, by means of direct shear tests at normal stresses ranging from 20.7 to 462 kPa. Peak shear strength of the sand and clay increased with fibre content, with reduction in post-peak loss of shear strength. The peak friction angle and cohesion values were 33.5˚ and 0 kPa for the unreinforced sand, and 19.5˚ and 84 kPa for the unreinforced clay. They increased with fibre content and reached maximum values of 38˚ and 9.6 kPa for the sand and 32˚ and 122.5 kPa for the clay, when reinforced with 0.3% fibres.

Kaniraj and Havanagi (2001) conducted direct shear tests on fly ash reinforced with polyester fibres. Inclusion of fibres increased the failure displacement from 1.2 to 4 mm of unreinforced specimens to more than 4 mm of reinforced specimens which even exceeded 10 mm at higher normal stress, indicating that fibre reinforcement imparted ductility to the fly ash-soil specimens. At failure, the corresponding vertical displacement was greater and the shear strength of fibre-reinforced specimens was significantly higher than that of unreinforced specimens.

Yetimoglu and Salbas (2003) conducted direct shear tests on clean oven-dried uniform river sand, reinforced with 20 mm long polypropylene fibres at relative density of 70%. The results revealed that with fibre content varying from 0.1 to 1%, the initial stiffness,

failure displacement and peak shear strength of the sand were not significantly affected by fibre reinforcement. However, the brittleness of the specimen was reduced with smaller loss of post-peak strength, indicating an increase in residual shear strength.

Lovisa et al. (2010) conducted direct shear tests to investigate the effect of water content on the shear strength of a poorly graded sand reinforced with randomly distributed glass fibres of 0.25% content. It was found that the peak friction angle of fibre-reinforced moist sand was 3˚ less than that of dry reinforced specimen at relative density higher than 50%. However, the induced peak cohesion of reinforced specimens remained the same for both dry and moist conditions. At the ultimate state, the shear strength parameters of both unreinforced and reinforced specimens were observed to be independent of both water content and relative density.

Sadek et al. (2010) conducted direct shear tests on a coarse sand and a fine sand reinforced with nylon fishing wire fibres of three diameters. Inclusion of fibres led to an increase of the initial stiffness and peak stress of the reinforced soils, and also consistently increased the tendency for dilation at all normal stresses. The dilatancy was noted to be more for specimens reinforced with longer fibres. Increase in shear strength was noted to be limited for coarse sand compared to the fine sand with fibre content less than 0.75%, but it was noted to be significant for higher fibre dose for both sands. This indicated that the relative dimensions of the reinforced sand grains and the reinforcing fibre diameters have an important effect on the extent of improvement by fibre inclusion in sands.

Falorca and Pinto (2011) investigated the shear strength behaviour of a poorly graded sand and a low plastic clay reinforced with polypropylene fibre by performing direct shear tests. The inclusion of fibres decreased the initial stiffness of the sand while there was no significant change in stiffness of the clay. It was found that the shear strength of the soils increased with fibre content and fibre length in terms of both cohesion and angle of friction.

The soil-fibre interfacial interaction was studied with optical and scanning electron microscopes. It was found that the there was no rupture of fibres during shearing, though the fibres were stretched and damaged by soil particle indentations which caused adhesion to develop within reinforced specimen.

Claria and Vettorelo (2016) studied the effect of randomly oriented polypropylene fibres in both mesh and smooth forms on the behaviour of an alluvial fine to medium sand in a loose state. The study focused on the characterization of the influence that the fibre addition has on the shear strength and on the deformational modulus corresponding to low, medium, and large strain levels of the reinforced sand. The initial modulus of sand was noted to decrease with fibre content. The shear strength of specimen increased with fibre content up to 2%. The shear strength increment was slightly higher with mesh fibres than those with smooth fibres. When the strain selected as the failure criterion was reduced, the improvement of the resultant internal friction angle decreased.

Eldesouky et al. (2016) investigated the effects of the fibre reinforcement and moisture content on the shear strength and volumetric change behaviour of sand with varying relative density, and also the usability of dry fibre-reinforced sand as an alternative to heavily compacted unreinforced moist sand. The peak and post-peak shear strengths and dilation of sand were found to increase with fibre inclusion, but they were suppressed by the presence of moisture. Dry loose fibre-reinforced sand achieved the same shear strength of heavily compacted unreinforced moist sand, though at more than double the horizontal displacement.

2.2.2 Direct Shear Tests on Clayey Soils

Cetin et al. (2006) investigated the geotechnical properties of a cohesive clayey soil (CL type) reinforced with fine tyre-chips (under 0.425 mm size) and coarse tyre-chips (between 2 mm and 4.75 mm size) through direct shear test and other tests. Cohesion increased with tyre-chips up to 40% for both fine and coarse tyre-chips, while the angle of

internal friction angle decreased with any tyre-chips content. However, the shear strength increased with up to 30% and 20% for fine tyre-chips and coarse tyre-chips mixtures, respectively.

Falorca et al. (2006) performed direct shear and ring shear tests on sandy clay of medium plasticity (CL), reinforced with randomly oriented polypropylene fibres. The shear strength of fibre-reinforced soil was unaffected by fibres at initial small deformation. The increase in shear strength of soils due to fibres depended on the shear displacement induced.

Ozkul and Baykal (2006) evaluated the shear strength of tyre fibres-reinforced clay soil by conducting drained and undrained direct shear tests. The drained shear strength of clay was found to be essentially unchanged by the inclusion of the fibres in both standard and modified compaction states. Undrained strength was also not changed when standard compaction energy was used, but decreased slightly with more ductile failure when modified energy was employed. At standard compaction energy, the vertical displacements of the composite samples were consistently less than those of clay for all displacements and all confinement stresses. In contrast, at modified compaction energy, the composite samples had a consistently greater vertical displacement than those of the clay samples.

Tang et al. (2007) conducted direct shear tests and other tests on a clayey soil with inclusion of different contents of 12 mm long polypropylene fibres and ordinary Portland cement. All the test specimens were compacted at their respective maximum dry unit weight and optimum water content. Specimens treated with cement were cured for 7, 14 and 28 days. It was observed that the cohesion and friction angle values increased with fibre content. The reinforcement benefit was controlled by friction at the soil-fibre interface in uncemented soil and by the bond strength in cemented soil.

Pradhan et al. (2012) conducted direct shear tests and other tests on cohesive soil (CL) reinforced with 0.2 mm diameter polypropylene fibres of three aspect ratios (l/d = 75, 100

and 125) and varying contents (0-1% by weight of oven-dried soil). Both peak and residual shear strength increased with aspect ratio up to 100 and fibre content up to 0.4%. Both peak and residual angle of internal friction were increased by respective maximum factors of 1.76 and 1.71, and that of peak and residual cohesion by maximum factors of 3.2 and 2.4.

Zaimoglu and Yetimoglu (2012) carried out direct shear test and other tests to investigate the effect of randomly distributed polypropylene fibres (0.25 to 1% by dry weight) on the strength behaviour of high plasticity silt (MH). They found an increase in initial stiffness of the fibre-reinforced soil under 50 kPa normal stress, while it remained unaffected at 100 and 200 kPa normal stresses. The shear strength increased with fibre content up to 0.75% fibres. The shear strength development was mainly due to increase in induced cohesion with increasing fibre content, while the friction angle did not change significantly.

Qu et al. (2013) studied the effect of fibre length (5, 10, 15 and 20 mm) and fibre content (0.1-0.4% of by weight of oven-dried soil) of wheat straw fibres on shear strength behaviour of clayey soil specimens, compacted to standard Proctor's maximum density at four different normal stresses (50, 100, 150, 200 kPa). The peak shear stress of soil was noted to be unaffected by fibres under 100 kPa normal stress. Above 100 kPa normal stress, it increased significantly with fibre content and fibre length. The maximum increase in shear strength occurred approximately at 0.3% wheat straw content of 15-20 mm length.

Anagnostopoulos et al. (2014) conducted consolidated drained and undrained direct shear tests on unreinforced and reinforced sandy silt and silty clay specimens, to investigate the influence of certain parameters (the strength properties of the fibre, the relative size of the fibres and grains, and the rate of shear) on the shear strength. Two types of polypropylene fibres with different mechanical indices were used. The fibre content was varied between

0.3% and 1.1% by weight of dry soil. The reinforcing effect was more noticeable for soil with lower grain size and also with the lower shear rate of undrained condition.

2.2.3 Triaxial Tests on Sandy Soils

Gray and Al-Refeai (1986) performed triaxial compression tests to compare the stress-strain response of a dry sand reinforced with randomly distributed, discrete fibres as opposed to continuous, oriented fabric layers. Both natural reed fibres and glass fibres were used. The inclusion of fibres up to 2% by dry weight of soil was found to increase the strength of the sand, expressed as the major principal stress at failure. The strength improvement was proportional to the fibre aspect ratio, and the fibre roughness was more effective than the stiffness property in increasing strength. Fibre-reinforced sand failed along a classic planar shear plane, whereas fabric-reinforced sand failed by bulging between layers. The existence of a critical confining stress was common to both types of reinforcement.

Maher and Gray (1990) conducted triaxial compression tests to determine the static stress-strain response of dry sands reinforced with discrete, randomly distributed fibres (rubber fibres, natural fibres and glass fibres), and to observe the influence of various fibre properties, soil properties, and test variables. The increase of stiffness and ultimate strength due to the fibre inclusions was found to be a function of sand granulometry (gradation, particle size and shape) and fibre properties (weight fraction, aspect ratio and modulus). The reinforced sands had either a curved linear or a bilinear failure envelope, with the break occurring at a critical confining stress. In addition to the experimental program, a model was developed, based on a statistical theory of strength for composites, to predict the fibre contribution to strength under static loads. The predicted strength increases from fibre reinforcement using the theoretical model agreed reasonably well with measured values.

Al-Refeai (1991) investigated through triaxial compression tests the load-deformation behaviour of fine sand with subrounded particles and medium sand with subangular particles,

reinforced with glass fibres and polypropylene pulp and mesh elements. Results indicated that shorter inclusions required a greater confining stress to prevent bond failure. Soil-inclusion friction interaction depended mainly on the extensibility of the inclusions. The mesh elements were superior to glass fibres in improving sand strength especially in the case of fine sand. The fine sand showed a more favourable response to fibre reinforcement than the medium sand. At constant fibre content, the increase in principal stress at failure and secant modulus were proportional to fibre length.

Maher and Ho (1993) investigated the effect of randomly distributed glass fibre reinforcement on cemented sand through triaxial static compression, cyclic compression and splitting tension tests. The inclusion of fibres significantly increased the peak compressive strength of the cemented sand. The increase was more pronounced at higher fibre contents and lengths, and at lower confining stresses. The post-peak strength loss of the cemented sand increased with increasing fibre content and length, and reduced with increasing confining stress. However, fibre addition increased peak internal friction angle, peak cohesion intercept and energy absorption capacity of the cemented sand.

Ranjan et al. (1994) carried out triaxial compression tests on a fine sand (SP) reinforced with plastic fibres and observed the influence of fibre properties (weight fraction and aspect ratio) and confining stress. Fibre inclusion increased the peak shear strength of the sand and reduced post-peak strength loss. It was found that the strength envelopes for the fibre-reinforced sand had a curvilinear or bilinear shape with a change of slope at a certain critical confining stress. The critical confining stress decreased with increasing fibre aspect ratio.

Consoli et al. (1998, 2002, 2007 and 2009b) investigated the effects of fibre inclusion (glass, polyethylene terephthalate and polypropylene fibres) on both uncemented and cemented sands (silty sand and fine grained Osorio sand) under drained conditions. Fibre

reinforcement decreased stiffness, increased both peak and residual shear strengths, and changed the cemented soil's brittle behaviour to a more ductile one. Addition of fibres increased the initial contraction at low strain level and decreased the subsequent dilation of specimen at higher strain level, and both the effects were more prominent with increasing confining pressure.

Consoli et al. (2004) found that the behaviour of fibre-reinforced uncemented and cemented fine sand specimens was influenced by the stiffness (elastic modulus) of the fibre type (polypropylene, polyester and glass fibres). Inclusion of relatively stiff fibres (polyester and glass) slightly reduced the stiffness and increased the peak friction angle of both the cemented and uncemented sand, and also slightly reduced the peak cohesive intercept and brittleness of the cemented composite. On the other hand, relatively flexible polypropylene fibre reinforcement dramatically reduced the stiffness and brittleness (changing the mode of failure of the cemented sand from brittle to ductile for longer fibres), while increasing the ultimate strength of the cemented composite.

Later, Consoli et al. (2009c) reported the effect of aspect ratio (120 to 2174) of polypropylene fibres by varying fibre length (12 to 50 mm) and diameter (from 0.023 to 0.1 mm) on stress-strain behaviour of the uncemented sand. It was found that fibres with high aspect ratios (above about 300) produced higher strengths and strain-hardening behaviour. They suggested the usability of such mixtures as geomaterial for structures like embankments over soft soil which withstands large deformations without losing its strength. However, very thin fibres (such as 0.023 mm diameter), longer than 24 mm, tangled during mixing, and were found to significantly reduce the effects of the fibres on the soil behaviour.

Michalowski and Cermak (2002) conducted drained triaxial compression tests to investigate the role of the inclination of monofilament polyamide and galvanized steel fibres in the increase in strength of sandy soils. Two sands were used, one with grains significantly

smaller than the fibre diameter, and the second with grains larger than the fibre diameter. The contribution of the fibres to the soil strength was the largest when they were placed in the direction of largest extension (horizontal direction) of the fibre-reinforced soil. Vertical fibres under compression had an adverse effect on the initial stiffness of the reinforced soil specimen and did not contribute to the strength. Specimens with a random distribution of fibres exhibited a smaller increase in strength than those with horizontal fibres, because a portion of randomly distributed fibres was subjected to compression.

Later, Michalowski and Cermak (2003) reported the effects of fibre concentration, aspect ratio and the relative size of the grains with fibre length. The effect of reinforcement was more in fine sand than that of coarse sand at low fibre content (0.5%) and vice versa at higher fibre content (1.5%). The reinforcement was also more effective when the fibre length was large compared to the size of the grains, to be at least one order of magnitude larger than the size of the grains, to gain the reinforcement benefit. They introduced the concept of macroscopic internal friction angle to describe the failure criterion of fibre-reinforced sand. Further, they presented a model for prediction of the failure stress in triaxial compression, in which the failure envelope has two segments: a linear part associated with fibre slip, and a nonlinear one related to yielding of the fibre material. Their analysis indicated that yielding of fibres would take place well beyond the stress range actually occurring in practice.

Ahmad et al. (2010) conducted both drained and undrained triaxial tests on specimens of silty sand reinforced with oil palm empty fruit bunch fibres. Both uncoated and coated (with acrylic butadiene styrene thermoplastic) fibres of different lengths (15, 30 and 45 mm) and varying content (0.25 and 0.5%) were used. Inclusion of the fibres significantly increased the peak shear stress and failure strain. Coated fibres increased the shear strength of the soil much more compared to uncoated fibres, as the coating increased interface friction between fibre and soil particles by increasing the surface area. Reinforced silty sand containing 0.5%

coated fibres of 30 mm length exhibited approximately 25% increase in friction angle and 35% in cohesion under undrained loading conditions compared to those of unreinforced soil.

Sivakumar Babu and Chouksey (2011) conducted consolidated undrained triaxial test and other tests on a fine sand and a cohesive red soil reinforced with plastic chips (12 mm long and 4 mm wide), obtained from waste plastic water bottles. It was found that the addition of plastic chips (0.5, 0.75 and 1.0% by dry weight of soil) significantly increased the shear strength of the soils in terms of increased friction angle, and their compressibility reduced significantly.

Hamidi and Hooresfand (2013) conducted conventional triaxial compression tests to investigate the effect of polypropylene fibres on cemented sand of 50% and 70% relative densities. The cement content was 3% (dry weight of the soil) and specimens were cured for seven days. Fibres of 12 mm in length and 0.023 mm thick were added at 0.5% and 1% (dry weight) of the sand-cement mixture. The initial stiffness of the cemented sand was noted to decrease with fibre content. The addition of fibres increased peak and residual shear strengths of cemented soil and changed its brittle behaviour to a more ductile one. With increasing fibre content, the compressive volumetric strain increased and residual dilation decreased. The effectiveness of fibres in shear strength improvement was greater at 70% relative density.

Li and Zornberg (2013) conducted triaxial compression and fibre pullout tests to evaluate how the fibre tension was mobilized with varying shear strain levels for sand specimens of varying relative densities. It was found that comparatively high strain was required for full mobilization of fibre-induced tension. Based on these results, they proposed a refinement of the discrete framework of Zornberg (2002) for prediction of the equivalent shear strength of fibre-reinforced soil, by calculating the equivalent shear strength twice, at strain levels corresponding to both the peak and residual shear strength of the soil matrix. The

equivalent shear strength of the fibre-reinforced soil corresponds to the maximum of these two values.

2.2.4 Triaxial Tests on Clayey Soils

Prabakar and Sridhar (2002) studied the inclusion of sisal fibres of varying length (5, 10, 20 and 25 mm) and content (0.25, 0.5, 0.75 and 1%), on the shear strength of a low plastic clayey soil compacted at OMC and MDU of the soil, by means of undrained triaxial tests. It was found that the shear strength increased nonlinearly with increasing fibre length up to 20 mm and fibre content up to 0.75%, respectively. While the induced cohesion increased linearly with fibre length, no specific trend was noted on friction angle variation with fibre length.

Ozkul and Baykal (2007) conducted both drained and undrained triaxial compression tests on tyre fibres-reinforced clayey soil, at effective confining stresses ranging from 50 to 300 kPa. The peak strength of reinforced specimen appeared at higher axial strain under drained condition, while it appeared at lower axial strain under undrained condition. The contribution of the fibres to the strength of clay decreased with increasing confinement level, and a limiting confining pressure existed beyond which the presence of fibres tended to degrade the strength of the clay. For the soil tested, this limiting confining stress was between 200 and 300 kPa.

Sivakumar Babu and Vasudevan (2008a) found that the strength and stiffness of a tropical soil reinforced with coir fibre (1-2%) of different sizes (diameter and length) improved significantly. The maximum increase of deviator stress was 3.5 times that of plain soil when the fibre length was between 15 to 25 mm (i.e. 40 to 60%) of the least lateral dimension (38 mm) of the specimen.

Later, Sivakumar Babu et al. (2008b) investigated the effect of the same coir fibres on the engineering properties of expansive black cotton soil by conducting undrained triaxial

compression tests. The maximum increase of major principal stress at failure was found to be 1.30 times over the unreinforced soil. Both friction angle and cohesion of soil increased with fibre content as well as with increase in fibre diameter. The coir fibres were effective in reducing the swell potential of the expansive soil.

Freilich et al. (2010) conducted both consolidated drained and consolidated undrained tests (with pore pressure measurement) on fibrillated polypropylene fibre-reinforced clayey soil compacted at MDU and at water contents approximately 2% dry of OMC. The (long term) effective shear strength values of the fibre-reinforced clay soil from both the undrained and drained tests were determined and then compared. The shear strength determined from the drained tests was found to be lower than that obtained from the undrained tests, and it was concluded that the generated pore pressure in the presence of fibres during undrained testing might have given a higher estimation of effective strength.

Estabragh et al. (2011) conducted consolidated undrained triaxial tests on samples of unreinforced and reinforced clay with different percentages (10, 20 and 30%) of randomly distributed short nylon fibres (4.0 mm length, 2.0 mm width and 0.4 mm thickness). The fibres were found to restrain the volumetric dilation of soil and this led to an increase of the excess pore water pressure. Both the stiffness and shear strength of soil increased with increasing the fibre content. Later, Estabragh et al. (2013) reported similar findings when natural palm fibres (water absorption capacity of 170% after 24 hours) were used to reinforce the same soil.

2.3 UNCONFINED COMPRESSIVE STRENGTH BEHAVIOUR OF FIBRE-REINFORCED SOILS

Freitag (1986) investigated the effects of three different synthetic fibres (spun nylon string, polypropylene rope fibre and polypropylene olefin concrete reinforcement fibre) randomly distributed in a lean sandy clay (CL), through unconfined compression tests. The

fibres had different diameters (0.1 to 0.2 mm) but same length of 20 mm, and 1% volumetric content was used in all specimens. The plain and reinforced specimens were compacted over a sufficiently wide range of water content to define the compaction curve. The maximum strength occurred somewhat dry of optimum. However, greater contribution of the fibres to the strength was observed for the specimens compacted wet of optimum compared to those compacted dry of optimum.

Maher and Ho (1994) conducted UC test and other tests on a kaolinite clay reinforced with different types of fibres (glass, polypropylene and softwood pulp) of varying tensile strength and elastic modulus. The inclusion of fibres increased the peak compressive strength and ductility of the clay, with the increase being more pronounced at lower-composite water contents. Increase in fibre length reduced the contribution of fibres to peak compressive strength, while increasing the contribution to energy absorption or ductility. This is opposite to the effect of increased fibre length on the strength of fibre-reinforced granular soils (Maher and Gray 1990) as observed from triaxial compression tests.

Nataraj and McManis (1997) investigated the influence of moisture content, specimen size and amount of reinforcement on the UCS of 25 mm long polypropylene fibrillated fibre-reinforced clayey soil. The strength reached maximum values at the optimum moisture content, and then decreased with a further increase in moisture content in all cases. The strength increased with an increase in specimen diameter from 33 to 70 mm, with or without reinforcement and thereafter, slightly decreased with 100 mm diameter. The post-peak strength loss was less for specimens prepared wet of the optimum moisture content, when compared with that of specimens prepared dry of the optimum. The unreinforced specimens revealed a shear failure plane, and with the addition of fibres, the specimens bulged in compression.

Puppala and Musenda (2000) investigated the influence of polypropylene fibre reinforcement on expansive soil stabilization. Two expansive soils, two types of fibres and three fibre dosages (0.3, 0.6, and 0.9 percent by dry weight of soil) were used in the testing program. Results indicated that the fibre reinforcement enhanced the UCS of the soil and reduced both volumetric shrinkage strains and swell pressures of the expansive clays. The fibre treatment also increased the free swell potential of the soils. The axial strain at peak shear strength of the fibre-reinforced soils was 1 to 4 percent more than that of raw soil, and this axial strain increased with the fibre dosage.

Ang and Loehr (2003) performed unconfined compression tests on compacted fibrillated polypropylene fibre-reinforced silty clay to evaluate how the specimen size affects the measured strength and stress-strain properties. Four different diameters (38 to 152 mm) of cylindrical specimens were compacted at moisture contents of 12, 14, 16, 18, and 20 % (from 4 % dry to 4 % wet of standard Proctor optimum moisture content) and at fibre contents of 0.0, 0.2, and 0.4 % of the dry weight of soil. Specimen size effects were most significant for specimens compacted at water contents dry of the optimum moisture content, and were almost negligible for specimens compacted wet of the optimum. While no clear threshold size could be established, it appeared as though use of specimens with diameters of 70 mm or greater would produce strengths that are reasonably representative of the true "mass" strengths for fibre-reinforced soils.

Akbulut et al. (2007) investigated the suitability of the inclusion of different fibres (scrap tyre rubber, polyethylene and polypropylene) on the geotechnical behaviour of three clayey soils (CH). Three different diameters (35, 50 and 80 mm) of cylindrical specimens were used. The UCS values increased with increasing tyre rubber fibres up to 2% content and then decreased, and with polyethylene and polypropylene fibres up to 0.2%. For maximum

improvement of the UCS values, the fibre length had to be increased with the sample dimension.

Tang et al. (2007) conducted UC tests on uncemented and cemented polypropylene fibre-reinforced clayey soil with different fibre contents (0.05%, 0.15% and 0.25% by weight of soil) of 12 mm length. The unconfined compressive strength for both cemented and uncemented specimens increased with fibre content, along with reduction in loss of post-peak strength. The addition of fibres reduced the width of tension cracks developed at failure by impeding the opening and development of cracks, and thereby changing the brittle behaviour to ductile behaviour.

Attom et al. (2009) investigated the effect of nylon (0.2 mm diameter) and palmyra (0.4 mm diameter) fibres on the mechanical properties of three clayey soils of varying plasticity index and clay content. Fibres of aspect ratios equal to 75 and varying volumetric content (1, 2, 3, 4 and 5%) were used as reinforcement. The stiffness, UCS and ductility of the clay-fibre mixture increased with fibre content. The post-peak softening decreased with increasing fibre content. For all fibre contents, Palmyra fibres showed a higher increase in the relative UCS than nylon fibres when mixed with the soils. Further, the strength improvement with fibre reinforcement was greater for the clayey soil of higher activity index.

Jiang et al. (2010) investigated the effect of polypropylene fibre content (0.1, 0.2, 0.3 and 0.4% by weight), fibre length (10, 15, 20 and 25 mm) and soil aggregate size on the UCS of a clayey soil. The UCS of the fibre-reinforced soil showed an initial increase followed by a rapid decrease with increasing fibre content and fibre length, and the optimal fibre content and length were found to be 0.3% and 15 mm, respectively. The strength of both unreinforced and fibre-reinforced soil decreased continuously with an increase in aggregate size.

Mirzababaei et al. (2013) conducted UC tests on carpet waste fibre-reinforced clayey soils at variable conditions of moisture content and dry unit weight. At a constant dry unit

weight, increasing the fibre content resulted in a significant increase in UCS value. At a constant fibre content and moisture content, an increase in dry unit weight of the reinforced specimens led to a significant increase in UCS. At the same fibre content and dry unit weight, an increase in moisture content of the reinforced specimens caused a reduction in UCS. However, at aconstant fibre content, a combined increase in dry unit weight and moisture content resulted in an increase in the UCS.

Only a few studies related to UC tests on fibre-reinforced sands have been found in the literature. Santoni et al. (2001) conducted unconfined compression tests on six different sands ranging from a fine sand to a coarse sand, reinforced with four different types of polypropylene fibres. Five primary conclusions were obtained. First, the inclusion of fibres significantly improved the unconfined compressive strength of the sands. The performance of the various fibre types from best to worst was fabrillated, tape, monofilament and mesh. Second, an optimum fibre length of 51 mm (2 in.) was identified for the reinforcement of sand specimens. Third, a maximum performance was achieved at a fibre dosage rate between 0.6 and 1.0% dry weight. Fourth, specimen performance was enhanced in both wet and dry of optimum conditions. Finally, the inclusion of up to 8% of silt did not affect the performance of the fibre reinforcement.

Park (2009) examined the effect of concentration and distribution of polyvinyl alcohol fibre reinforcement of the same overall specimen fibre content of 1% on the UCS of artificially cemented sand (4% cement). The randomly distributed fibres were placed only at predetermined layers (1, 3 and 5 layers) among five compacted layers of the specimens (70 mm diameter and 140 mm length). The results showed that the UCS of the reinforced soil increased gradually as the number of fibre inclusion layers increased. A fibre-reinforced specimen, where fibres were evenly distributed throughout the five layers, was twice as strong as an unreinforced cemented specimen. A specimen with five fibre inclusion layers

was 1.5 times stronger than a specimen with one fibre inclusion layer at the middle of the specimen.

2.4 BEARING CAPACITY OF FIBRE-REINFORCED SOIL

2.4.1 Based on California Bearing Ratio Tests

Hoover et al. (1982) conducted CBR tests to investigate into the potential of improving soils of varying gradation through polypropylene fibre reinforcement. The fibre reinforcement was found to be more effective in sandy soils than in fine-grained soils. The CBR value increased to a maximum of six times that of unreinforced soil.

Fletcher and Humphries (1991) conducted CBR tests on specimens of a residual silt reinforced with polypropylene fibres of varying content (0.09 to 1.5%), length (19 and 25 mm) and diameter (0.38 and 0.76 mm). The specimens were compacted at the standard Proctor maximum dry unit weight. The CBR of the soil increased by 65% when reinforced with 0.09% fibres of 19 mm length and 0.38 mm diameter, and by 133% when reinforced with 1% fibres of 25 mm length and 0.76 mm diameter.

Benson and Khire (1994) performed CBR tests to investigate the feasibility of using strips of reclaimed high-density polyethylene of varying aspect ratio (4, 8 and 12) and fibre content (1, 2, 3 and 4%) as reinforcing material in a uniformly graded medium sand. The CBR, secant modulus and deformation behaviour of the soil were substantially improved with fibre reinforcement, and the maximum increase in CBR was by a factor of 5 with 4% strip content having aspect ratio of 8.

Al-Refeai and Al-Suhaibani (1998) performed CBR tests on uniform fine subrounded dune sand reinforced with two fibrillated polypropylene fibres of varying contents (0.2, 0.4, 0.6, 0.8 and 1%). The inclusion of fibres increased the CBR values, and the improvement in the CBR was observed over a larger penetration depth than with unreinforced sand. The optimum fibre content was approximately 0.4%.

Kumar et al. (1999) conducted CBR tests on silty sand and pond ash specimens reinforced with polyester fibres (0.1, 0.2, 0.3 and 0.4%), and concluded that the fibres increased the CBR value and ductility of the specimens. The optimum fibre content for both the silty sand and pond ash was approximately 0.3 to 0.4% of dry unit weight of soil.

Tingle et al. (2002) conducted dynamic cone penetrometer (DCP) tests in two full-scale field test sections to validate the performance of fibre-reinforced sands for low-volume roads based on the laboratory UC test results of Santoni et al. (2001). The DCP data were converted to CBR values. The objectives were to verify the structural load bearing capacity of the fibre-reinforced sands under actual traffic conditions, and to develop guidance for constructing and maintaining the fibre-stabilized pavements. Among the four types of polypropylene fibres used, the fibrillated fibres provided the best rut resistance, followed by the monofilament, the tape and then the mesh elements of 51 mm length. The improvement was found to be up to a limiting fibre fraction value of 0.8% by dry weight of soil. It was concluded that the discrete fibre stabilization of sand was a viable alternative to traditional stabilization techniques for low-volume road applications.

Kumar et al. (2005) conducted both laboratory CBR and field CBR tests on fly ash reinforced with polypropylene fibres (0.5, 1, 1.5 and 2%). The lab CBR value of fly ash at 5.0 mm penetration was more compared to 2.5 mm penetration, whereas the field CBR value at 2.5 mm penetration was greater than at 5.0 mm penetration. With 0.5% fibre content, the lab soaked CBR of flyash was 31.5%, whereas the field CBR was 25.71%. The fly ash with 0.5% fibre content was found to be suitable for pavement subbase for traffic up to 2 msa (IRC 37-2001).

Yetimoglu et al. (2005) conducted CBR tests to investigate the load-penetration behaviour of sand fill reinforced with polypropylene fibres and overlying soft clay. The stiffness, bearing capacity and ductility of the fibre-reinforced sand fill-soft clay system was

determined. The initial stiffness of load-penetration curves was not significantly affected by fibre reinforcement. Fibre inclusions resulted in an appreciable increase in the peak piston load, and the reinforcement benefit increased with an increase in fibre content. The penetration value at which the piston load was the highest also tended to increase with increasing fibre content. However, increasing fibre content caused an increase in the brittleness of the system as observed from a higher loss of post-peak strength.

Kumar and Singh (2008) conducted both lab and field CBR tests on fly ash reinforced with polypropylene fibre of aspect ratios 60, 80, 100, and 120 with varying fibre content (0.1, 0.2, 0.3, 0.4 and 0.5%). Field CBR tests are conducted to confirm the lab CBR tests. The field soaked CBR values of fly ash with 0.2, 0.3 and 0.4% fibre contents were found to be 16.6, 23.2 and 27.4%, respectively. Thus, fly ash with 0.2% fibres was found to be suitable for subbase material of rural roads with low traffic (IRC SP 20-2000), whereas fly ash with 0.3 and 0.4% fibres was found to be suitable for rural road subbase with higher traffic (IRC 37-2001).

Hazirbaba and Gullu (2010) presented results on the improvement of the CBR performance of a low plasticity silt (ML) by the separate or combined addition of polypropylene fibres (fibrillated or tape) and a synthetic fluid, under both unsoaked and soaked conditions. The tests were conducted for freezing and thawing conditions in addition to non-freezing conditions. For unsoaked condition, significant improvement in the CBR was noted for samples treated with fibres and synthetic fluid together. For soaked condition, the best performance was obtained from the samples treated with fibres only. For unsoaked samples, the addition of synthetic fluid alone was not very effective against the detrimental impact of freeze-thaw, but the addition of fibres together with synthetic fluid was generally successful in providing resistance against freeze-thaw weakening. Similarly, soaked samples subjected to a freeze-thaw cycle showed poor CBR performance for treatments involving

synthetic fluid, while samples improved with fibres alone generally produced better performance.

Pradhan et al. (2012) investigated the CBR of clayey soil (CL) with randomly reinforced polypropylene fibres and found that the CBR value increased with fibre content up to 0.8-0.9% for all lengths (15, 20 and 25 mm), while the CBR values increased with fibre length up to 20 mm and then decreased with longer fibres. Compared to unreinforced soil, the soaked CBR value of fibre-reinforced soil was increased to maximum by a factor 3.0 for 20 mm fibre length (L/d = 100) at optimum fibre content of 0.8%.

Rao and Nasr (2012) conducted CBR tests and other tests on silty sand reinforced with linen fibres of various contents (0.25, 0.5, 0.75 and 1%) and aspect ratios (50, 100 and 150). The fibre addition up to 1.0% fibre content and 100 aspect ratio was found to give the optimum CBR value and thereafter the CBR value decreased with higher aspect ratio of 150.

Zaimoglu and Yetimoglu (2012) investigated the effect of polypropylene fibres (0.25, 0.5, 0.75 and 1% by dry weight) of 12 mm length reinforcement on the soaked CBR of high plasticity silt (MH). The inclusion of the randomly distributed fibres caused a significant increase of soaked CBR up to 0.75% fibre content, and the CBR value remained more or less constant thereafter. The CBR value of 14% for the unreinforced soil increased maximum to 25% for the reinforced soil.

Muntohar et al. (2013) investigated the engineering behaviour of the lime (12% by dry weight of soil) and rice husk ash (12% by dry weight) stabilized clayey soil (MH) reinforced with randomly distributed discrete polypropylene plastic waste fibres (0.1, 0.2, 0.4, 0.8 and 1.2%) through CBR test and other tests. The CBR value of the unreinforced soil increased from 6.2% to a maximum of 22.5% on addition of lime/RHA. However, the CBR value increased considerably up to 53.8% by adding 0.8% plastic-waste fibres which met the requirement of subbase and base course materials.

Edincliler and Cagatay (2013) presented the CBR results of sand reinforced with granulated rubber (aspect ratio of 1) and rubber fibres (aspect ratios of 4 and 8) of varying content (5, 10, 20, 30 and 40% by weight). The CBR of sand was affected by three factors: rubber shape, aspect ratio and content. The addition of the rubber fibres increased the CBR value of the mixture, but the addition of granulated rubber decreased it. The use of rubber fibres with a higher aspect ratio resulted in a higher CBR value. The addition to sand of 30% rubber fibres having aspect ratio of 8 increased the CBR value from 8 to 16, and the addition of fibres having aspect ratio of 4 resulted in an increase of the CBR value from 8 to almost 12.

Jha et al. (2014) found that the addition of waste plastic strips (12, 24 and 36 mm length; 12 mm width; 0.4 mm thickness) of varying content (0.25, 0.5, 1, 2 and 4%) to three industrial wastes (fly ash, stone dust and waste recycled product obtained by recycling of blast furnace slag) caused an appreciable increase of CBR and secant subgrade modulus. The maximum increase in CBR and subgrade modulus was with 4% strip content having an aspect ratio of 3. The addition of 4% strip content having an aspect ratio 3 to fly ash, increased the CBR value of fly ash approximately by 8.0 times, whereas for the same reinforcement condition, the increase in CBR value for stone dust and waste recycled product were 7.0 times and 2.4 times their unreinforced values, respectively.

Sarbaz et al. (2014) presented CBR test results of a fine sand (SP) reinforced with uncoated and bitumen-coated date palm fibres (20 and 40 mm length; 0.5, 1 and 2% content) under both unsaturated and submerged conditions. Submergence of specimens caused a reduction in the CBR strength of both unreinforced and reinforced specimens. It was found that the CBR increased maximum by 56% under moist condition and by 41% under submerged condition when reinforced with 1% uncoated fibres of 40 mm length. With

bitumen coating of fibres, the CBR slightly decreased. It was observed that even 12 dried and wetted cycles and semi-saturation condition of specimens had no effect on CBR strength.

2.4.2 Based on Laboratory or Field Model Tests

Wasti and Butun (1996) performed laboratory model tests using strip footing plate (20 mm thick, 50 mm wide and 250 mm long) placed over sand beds reinforced with randomly distributed polypropylene fibre and mesh elements. Two sizes of mesh elements (30 × 50 mm and 50 x 100 mm) having the same opening size (10 × 10 mm) and one size of fibre element (50 mm length) cut from the meshes, were used in varying inclusion amounts (0.075, 0.10 and 0.15% by dry weight). In general, the reinforcement of sand by randomly distributed inclusions caused an increase in the ultimate bearing capacity values and the settlement at the ultimate load. A larger mesh size was found to be superior to the other inclusions, in terms of increase in ultimate bearing capacity. Though the mesh elements had an optimum percentage of inclusion, the fibres exhibited a linearly increasing trend of bearing capacity, for the range of fibre contents used.

Consoli et al. (2003a) carried out field plate load tests (300 mm diameter, 25 mm thickness) on a thick homogeneous stratum (1200 mm thickness) of compacted low plasticity silty sand-clayey sand, with and without polypropylene fibre reinforcement. In addition to the field test program, laboratory triaxial compression tests were performed to determine the static stress-strain response of the compacted soil reinforced with the randomly distributed polypropylene fibres. The plate load test on reinforced soil stratum was performed to relatively high pressures, and gave a noticeable stiffer response than that carried out on the non-reinforced stratum. The laboratory test results also showed that the strength increased continuously regardless of the confining pressure applied, and did not reach an asymptotic upper limit, even at axial strains as large as 25%.

Consoli et al. (2003b) reported the results of field plate load tests (300 mm diameter, 25 mm thickness) carried out directly on a homogeneous residual soil stratum (low plasticity sand silty red clay), as well as on a layered system formed with two different top layers of 300 mm thick sand-cement (7% content) and sand-cement-polypropylene fibres (24 mm length and 0.5% content) overlaying the residual soil stratum. The utilization of a cemented top layer increased the bearing capacity, reduced displacement at failure, and changed soil behaviour to a noticeable brittle behaviour. The addition of fibre to the cemented top layer maintained roughly the same bearing capacity but changed the post-failure behaviour to a ductile behaviour. A punching failure mechanism was observed in the field for the load test bearing on the sand-cement top layer, with tension cracks being formed from the bottom to the top of the layer. In the case of the sand-cement-fibre top layer, a completely distinct mechanism was observed with the failure occurring through the formation of a thick shear band around the border of the plate, which allowed the stresses to spread through a larger area over the residual soil stratum

Consoli et al. (2009a) also reported the results of plate load tests carried out on both unreinforced and reinforced Osorio sand with polypropylene fibres (24 mm long, 0.5% by dry weight), compacted at relative densities (D_r) of 30, 50 and 90%. The soil load-settlement behaviour was significantly influenced by the fibre inclusion, changing the kinematics of failure. For the densest (D_r = 90%) fibre-sand mixture, a significant change in the load-settlement behaviour was observed at very small (almost zero) displacement. However, for the loose to medium dense sand (D_r = 30% and 50%), significant settlements (50 mm and 30 mm respectively) were required for the differences in the load-settlement responses to appear. The overall behaviour seemed to support the argument that inclusion of fibres increases strength of sandy soil by a mechanism that involves the partial suppression of dilation (and

hence produces an increase in effective confining pressure, and a consequent increase in shear strength).

Hataf and Rahimi (2006) carried out laboratory model tests to investigate the effects of content and aspect ratio of waste tyre shreds as reinforcement on the bearing capacity of sand. Tyre shreds of rectangular shape and widths of 2 and 3 cm with four aspect ratios (2, 3, 4 and 5) were mixed with the sand at five contents (10, 20, 30, 40 and 50%) by volume. Addition of tyre shreds to sand increased BCR (bearing capacity ratio) between 1.17 to 3.9. The BCR was found to increase with shred content only up to an optimum volume. For a given shred width, shred content and soil density it seemed that aspect ratio of 4 gave higher BCR. The maximum BCR of 3.9 was attained at shred content of 40% and dimensions of 3 × 12 cm.

Tafreshi and Norouzi (2012) carried out laboratory tests to obtain the bearing capacity of a square footing (100 × 100 mm in size and 20 mm thick) resting on a sand bed (600 mm height) in a test tank (700 x 700 mm in plan). The sand bed consisted of an unreinforced cap layer underlain by an intermediate layer reinforced with tyre shreds (2.5, 5 and 7.5% by volume) followed by another unreinforced layer. The efficiency of reinforcement was noted to vary with tyre shred content, thickness of the reinforced soil layer and thickness of the soil cap. At footing settlement level equal to 5% footing width, the maximum improvement in bearing capacity of reinforced bed was 2.68 times of the unreinforced bed. This optimum value of improvement was with tyre shred content of 5%, thickness of reinforced layer equal to 0.5 times of footing width and thickness of soil cap equal to 0.25 times of footing width.

Nasr (2014) conducted physical model tests to investigate the behaviour of a strip footing (100 mm width, 499 mm length and 25 mm thickness) resting on fibre-reinforced cemented sand in the active zone of a cantilever sheet pile wall, and compared the test results with the observations from two-dimensional non-linear finite element analyses. Fibre

inclusion (0.25 to 1% content) and cement kiln dust (3 to 12% content) into the soil caused an increase in ultimate bearing capacity of footing and significant reduction in the lateral deflection of the sheet pile wall. At high fibre content above 0.75%, the increase in bearing capacity and reduction in lateral deflection were 42% and 51%, respectively. The addition of fibres increased the vertical surface settlement obtained at the ultimate bearing capacity.

2.5 MODELS OF FIBRE-REINFORCED SOILS

2.5.1 Force Equilibrium Models

Waldron (1977) conducted direct shear tests on 25 cm diameter root-permeated soil columns obtained from soil slopes, to measure the stabilizing effect of the plant roots acting as mechanical reinforcement of the slopes. The root types were alfalfa, barley and yellow pine, whereas the soil type was silty clay loam. Alfalfa roots were found to be most effective followed by barley roots and then the pine roots in increasing the resistance to shearing.

Based on the test results, he evaluated the tensile stress developed at the shear plane of root-permeated soil as shown in Fig. 2.1, and presented a model based on force equilibrium method. The following assumptions were made in this model: (i) soil shearing occurs in a horizontal zone of thickness, Z, which is penetrated by vertical roots (Fig. 2.1a) and Z does not change during shear; (ii) the roots are flexible and of uniform diameter and are linearly elastic; (iii) the soil friction angle, φ, is unaffected by roots. The Mohr-Coulomb equation in its modified form for root-permeated soil is:

$$s_f = c + \sigma_n \tan\phi + \Delta s_f \tag{2.1}$$

where c = cohesion of soil, σ_n = normal stress acting on shear plane, and ϕ = soil friction angle. Δs_f is the increase in shear strength due to presence of roots in soil, expressed as:

$$\Delta s_f = a_f K (\sec\theta - 1)^{1/2} (\sin\theta + \cos\theta \tan\phi) \tag{2.2}$$

where $a_f = \frac{A_f}{A}$ = root area ratio, A_f = area of roots in shear, A = total area of soil in shear, θ = root distortion angle (Fig. 2.1b), and K = a constant.

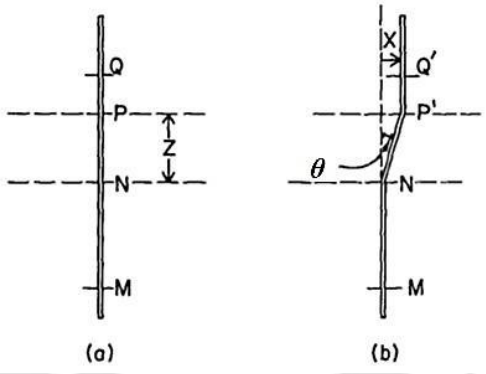

Fig. 2.1 Model of flexible elastic root extending vertically across horizontal shear zone: (a) undisturbed soil; (b) displaced root and soil (after Waldron 1977)

Gray and Ohashi (1983) extended the work of Waldron (1977) to describe the deformation and the failure mechanism of fibre-reinforced sand and to estimate the contribution of fibre reinforcement to increasing the soil shear strength. They developed a model of fibre-reinforced sand by conducting direct shear tests on dry sand reinforced with different types of fibres placed at both vertical and inclined orientations (Fig. 2.2). The model consists of a long, elastic fibre extending an equal length over either side of a potential shear plane in the sand. Shearing of the sand along the shear plane is assumed to cause fibre distortion, which mobilizes its tensile resistance. The shear strength increment, (Δs_f) due to fibre reinforcement is:

For perpendicular fibre: $\Delta s_f = t_f(\sin\theta + \cos\theta \tan\phi)$ (2.3)

For inclined fibre: $\Delta s_f = t_f(\sin(90^\circ - \psi) + \cos(90^\circ - \psi)\tan\phi)$ (2.4)

where t_f = mobilized tensile strength of fibre per unit area of soil, $\psi = \tan^{-1}[\frac{1}{k + (\tan^{-1} i)^{-1}}]$, i = initial fibre orientation, and $k = \frac{x}{z}$ = shear distortion ratio.

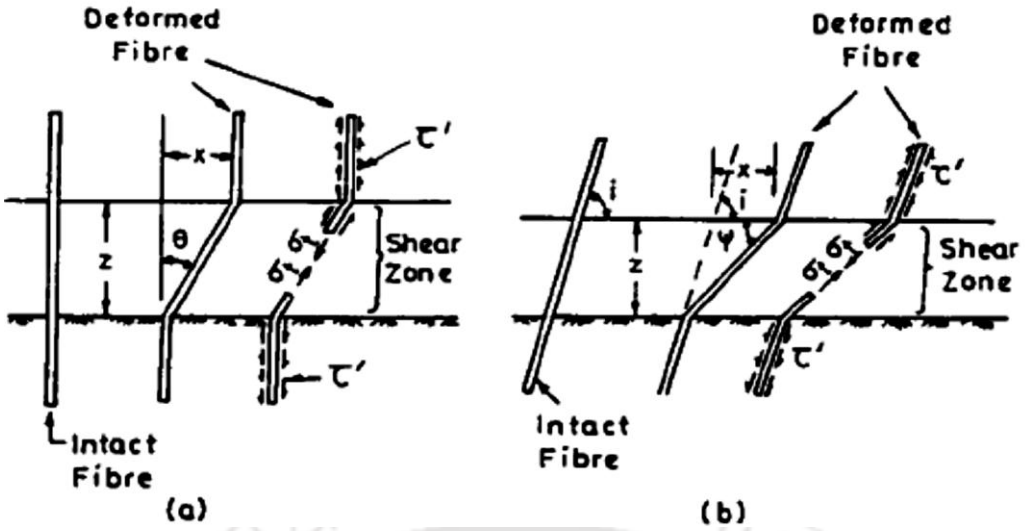

Fig. 2.2 Fibre reinforcement model: (a) fibre perpendicular to shear plane; (b) fibre inclined to shear plane (after Gray and Ohashi 1983)

In addition to triaxial compression tests on randomly distributed fibre-reinforced sand, Maher and Gray (1990) carried out a statistical analysis by adapting the force equilibrium approach of Waldron (1972), Gray and Ohashi (1983), and Gray and Al-Refeai (1986), and proposed a model to predict the fibre contribution to strength under static loads. Figure 2.3 shows a single fibre crossing the potential shear zone of a sand-fibre specimen under triaxial compression load.

In the model, they considered a bilinear failure envelope with a break occurring at a threshold confining stress called critical confining pressure (σ_{crit}), which is determined empirically from the experimental measurements. At confining stress less than the critical, the fibres slip during deformation, and at confining stress (σ_{conf}) higher than the critical, they stretch or yield. Assuming a Mohr-Coulomb yield criterion, the reinforced soil envelope is parallel to that of unreinforced soil above the critical confining stress.

The shear strength increments (ΔS_f) under different confining ranges are:

For $0 < \sigma_{conf} < \sigma_{crit,}$

$$\Delta S_f = N_s(\pi \frac{d^2}{4})(2\eta\sigma_{conf} \tan\delta)(sin\omega + cos\omega \tan\phi)(\xi) \qquad (2.5)$$

and for $\sigma_{conf} > \sigma_{crit}$,

$$\Delta S_f = N_s(\pi \frac{d^2}{4})(2\eta\sigma_{crit} \tan\delta)(sin\omega + cos\omega \tan\phi)(\xi) \quad (2.6)$$

where d = diameter of fibre, N_s = average number of fibres per unit area of the shear plane, η = aspect ratio of fibres, ω = angle of shear distortion, δ = fibre skin friction angle, and ξ = empirical coefficient accounting for the influence of sand granulometry and fibre properties. It was found that predicted strength increases using the theoretical model agreed reasonably well with measured values.

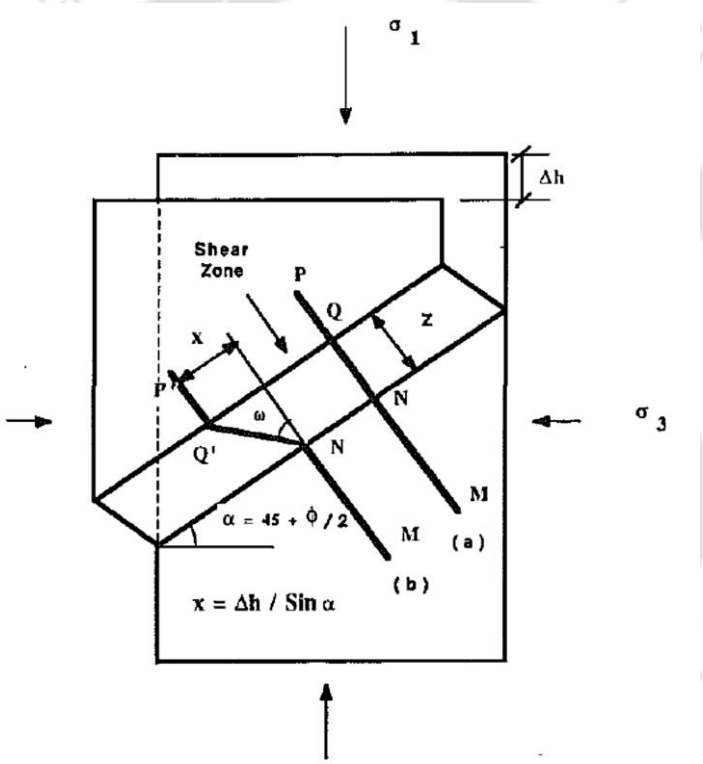

Fig. 2.3 Characterization of single fibre crossing shear zone during deformation in triaxial compression tests: (a) Intact fibre; (b) Deformed fibre (after Maher and Gray 1990)

Shukla et al. (2010) proposed a simple analytical model for predicting the shear strength behaviour of fibre-reinforced granular soils under high confining stresses, where it can be assumed that pullout of fibres does not take place. The analytical expression of the model shows that inclusion of fibres in the granular soil induces apparent cohesion, as well as increase in normal stress on the shear failure plane, and both of them are proportional to the

fibre content and aspect ratio. However, it was observed that the increase in shear strength of the fibre-reinforced granular soil was significantly contributed by the apparent cohesion, and the contribution from the increase in normal stress was limited.

The shear strength (s_f) of the fibre-reinforced granular soil is expressed as:

$$s_f = c_f + \sigma_{n,f} \tan\phi \tag{2.7}$$

where c_f = apparent cohesion developed due to fibre inclusion, and $\sigma_{n,f}$ = improved confining normal stress on fibre-reinforced soil, given as:

$$c_f = \sigma_n[2(\frac{A_f}{A})\{\frac{1-\sin\phi\sin(\phi-2i)}{\cos^2\phi}\}\eta\tan\delta\sin i\cos\psi] \tag{2.8}$$

$$\sigma_{n,f} = \sigma_n[1+2(\frac{A_f}{A})\{\frac{1-\sin\phi\sin(\phi-2i)}{\cos^2\phi}\}\eta\tan\delta\sin i\cos\psi] \tag{2.9}$$

where i = inclination of fibre to horizontal.

2.5.2 Models Based on Statistical Analysis

Based on triaxial tests on cohesionless soils, Ranjan et al. (1996) developed a mathematical model to define the strength characteristics of fibre-reinforced soil. The test results indicated that the principal stress (σ_{1f}) envelopes of soil-fibre composites had a curvilinear failure envelope, with a transition occurring at a certain confining stress, termed as critical confining stress, below which the fibres tended to slip. The model represented the principal stress mathematically as a function of weight fraction of fibres (f_c), fibre aspect ratio (L/d), surface friction coefficient (f^*), coefficient of friction (f) and confining pressure (σ_3), as follows:

$$\sigma_{1f} = f(f_c, \frac{L}{d}, f^*, f, \sigma_3) \tag{2.10}$$

The developed mathematical equations are:

$$\text{For } \sigma_3 \le \sigma_{crit}, \quad \sigma_{1f} = 12.3(f_c)^{0.4}\left(\frac{L}{d}\right)^{0.28}(f^*)^{0.27}(f)^{1.1}(\sigma_3)^{0.68} \tag{2.11}$$

$$\text{For } \sigma_3 \ge \sigma_{crit}, \quad \sigma_{1f} = 8.78(f_c)^{0.35}\left(\frac{L}{d}\right)^{0.26}(f^*)^{0.06}(f)^{0.84}(\sigma_3)^{0.73} \tag{2.12}$$

Based on the test results of conventional triaxial testing of a tropical soil mixed with coir fibres, Sivakumar Babu and Vasudevan (2008a) presented a statistical regression model for predicting the strength of coir fibre-reinforced soil. The model is capable of quantifying the major principal stress at failure, cohesion, friction angle and initial stiffness of coir fibre-reinforced soil, as follows:

$$\sigma_{1f} = 159.1 + 3.96\sigma_3 - 0.0083\sigma_3^2 - 2959d + 4866.5d^2 - 37.01f_c + 17.35f_c^2 + 58.8L$$
$$-1.69L^2 + 2.69\sigma_3 d + 548.61df_c + 6.21f_cL - 0.016L\sigma_3 \tag{2.13}$$

$$c_f = 76.5 + 156.4d - 102.1d^2 + 126.1f_c - 39.3f_c^2 - 20.2df_c \tag{2.14}$$

$$\phi = 23.1 - 78.55d + 191.1d^2 + 7.03f_c + 2.38f_c^2 - 15.02df_c \tag{2.15}$$

$$E_i = 8992.2 + 64.94\sigma_3 - 0.14\sigma_3^2 - 94612d + 186594d^2 - 1744.9f_c + 1167.8f_c^2$$
$$+1765.1L - 52.1L^2 + 33.3\sigma_3 d + 11707.7df_c + 129.77f_cL - 0.47L\sigma_3 \tag{2.16}$$

where σ_{1f} = major principal stress at failure (kPa), σ_3 = confining pressure (kPa), f_c = fibre content in percentage by dry weight of soil, d = diameter of fibre (mm), L = length of fibre (mm), c_f = cohesion of fibre-reinforced soil (kPa), ϕ = angle of internal friction (degree), and E_i = initial stiffness modulus of coir fibre-reinforced soil (kPa).

2.5.3 Energy-Based Homogenization Model

Michalowski and Zhao (1996) used an energy-based homogenization technique to calculate the macroscopic (average) failure stress of fibrous granular composite materials at failure. The fibre-soil mixture was considered as isotropic. The model assumes that the fibres contribute to the strength of the composite only if they are subjected to tension, whereas their influence in the compressive regime is neglected due to possible buckling and kinking. The

strength of the granular matrix is quantified by the internal friction angle, whereas fibres are characterised by volumetric concentration, aspect ratio, yield point and fibre-soil interface friction angle.

In this model, failure criterion for fibre-reinforced granular soil is described mathematically in terms of in-plane variants q (radius of the Mohr circle representing the state of stress) and p (mean principal stress) in a macroscopic stress space as stated below:

$$\frac{q}{\chi\sigma_{f,ult}} = \frac{p}{\chi\sigma_{f,ult}}\sin\phi + \frac{1}{3}M\left(1-\frac{1}{4\eta\chi}\frac{\cot\delta}{\frac{p}{\chi\sigma_{f,ult}}}\right) \tag{2.17}$$

where $M = \frac{1}{\pi}\cos\phi + \left(\frac{1}{2}+\frac{\phi}{\pi}\right)\sin\phi$ (2.18)

$$q = \frac{\sigma_1 - \sigma_3}{2} \tag{2.19}$$

$$p = \frac{\sigma_1 + \sigma_3}{2} \tag{2.20}$$

and χ = volumetric fibre content

Failure of a single fibre in the deforming composite can occur due to fibre slip or tensile rupture (Fig. 2.4). However, even if a tensile rupture occurs, the end of the fibre slips as the tensile strength of fibre material cannot be mobilized throughout the entyre fibre length.

For pure slip failure, the failure criterion takes the following form:

$$\frac{q}{\chi\sigma_{f,ult}} = \frac{p}{\chi\sigma_{f,ult}}\left(\sin\phi + \frac{1}{3}M\chi\eta\tan\delta\right) \tag{2.21}$$

When no fibres are present, both Eqns. (2.17) and (2.21) reduce to the standard Mohr-Coulomb failure criterion for granular material as:

$$q = p\sin\phi \tag{2.22}$$

The failure criteria derived are directly applicable in numerical methods for solving boundary value problems, but are limited to isotropic mixtures.

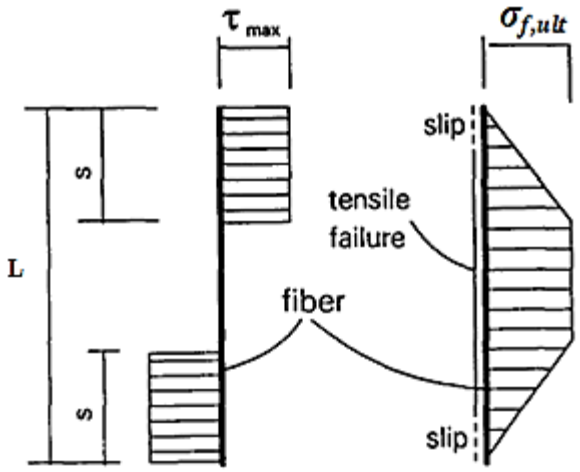

Fig. 2.4 Shear stress and axial stress of fibre in reinforced soil (after Michalowski and Zhao 1996)

2.5.4 Discrete Framework Model

Zornberg (2002) proposed a discrete model for predicting the shear strength of fibre-reinforced soil based on the independent properties of fibres and soil (e.g. fibre content, fibre aspect ratio and shear strength of unreinforced soil), originally for the design of fibre-reinforced soil slopes. The main objective of the discrete framework was to avoid the need of conducting non-conventional shear strength tests on fibre-reinforced specimens, in order to perform limit equilibrium analysis.

In this model, the failure mode of fibres changes from pullout to breakage at a critical normal stress ($\sigma_{n,crit}$), defined as:

$$\sigma_{n,crit} = \frac{\sigma_{f,ult} - \eta c_{i,c} c}{\eta c_{i,c} \tan\phi} \tag{2.23}$$

where $\eta = L/d$ = fibre aspect ratio, c = cohesion of unreinforced soil, and ϕ = friction angle of unreinforced soil. $c_{i,c}$ and $c_{i,\phi}$ are interaction coefficients defined as:

$$c_{i,c} = \frac{a}{c} \quad \text{and} \quad c_{i,\phi} = \frac{\tan\delta}{\tan\phi}$$

where a = adhesive component of the interface shear strength between soil and fibre.

For pullout failure, the fibre-induced distributed tension is a function of the volumetric fibre content, interface shear strength and fibre aspect ratio. When failure is governed by fibre breakage, the fibre-induced distributed tension is a function of the volumetric fibre content and tensile strength of individual fibre.

The equivalent shear strength of fibre-reinforced soil for fibre pullout failure is defined as:

$$s_{eq,p} = c_{eq,p} + (\tan\phi)_{eq,p}\,\sigma_n \tag{2.24}$$

where $c_{eq,t} = c(1+\alpha\eta\chi c_{i,c})$, $(\tan\varphi)_{eq,p} = (1+\alpha\eta\chi c_{i,\phi})\tan\phi$, α = empirical coefficient for the effect of fibre orientation and χ = volumetric fibre content.

The equivalent shear strength of fibre-reinforced soil for fibre breakage failure is given as:

$$s_{eq,t} = c_{eq,t} + (\tan\phi)_{eq,t}\,\sigma_n \tag{2.25}$$

where $c_{eq,t} = c + \alpha\chi\sigma_{f,ult}$ and $(\tan\phi)_{eq,t} = \tan\phi$

2.5.5 Other Models and Numerical Studies

Michalowski and Cermak (2002) derived a failure criterion for fibre-reinforced sand with an anisotropic distribution of fibre orientation, by considering contribution of a single fibre to the work dissipation during failure of the reinforced sand and integrating this dissipation over all fibres in a reinforced sand element. A deformation-induced anisotropy was detected in triaxial experiments conducted by them. Specimens with initially isotropic distribution of fibre orientation exhibited a kinematic hardening effect. The evolution of fibre orientation in the deformation process was found to have been the cause of the anisotropic

hardening. The derived failure criterion can be applied directly in methods for solving stability problems of fibre-reinforced sand.

Michalowski and Cermak (2003) developed a model for prediction of the failure stress of fibre-reinforced sand based on drained triaxial compression tests. This model is limited to cylindrical monofilament fibres with an isotropic distribution of their orientation. Five parameters (volumetric fibre concentration (χ), fibre aspect ratio (η), fibre yield stress ($\sigma_{f,ult}$), internal friction angle of soil (ϕ) and soil-fibre interface friction angle (δ) are needed to theoretically predict the failure stress. The failure envelope has two segments: a linear part associated with fibre slip up to a critical confining stress, and a nonlinear one related to yielding of the fibre material beyond that critical stress. The analysis of their experimental results indicated that yielding of fibres would occur in a stress range well beyond that is encountered in practice. The critical confining stress is defined as:

$$\sigma_{3,crit} = \frac{6 - N\eta\chi \tan\delta}{6(1+K_p)\eta \tan\delta}\sigma_{f,ult} \tag{2.26}$$

As the initial part of the failure condition is linear, they approximated the influence of the fibres by introducing the concept of macroscopic equivalent friction angle to describe the fibre-reinforced sand, which is expressed as:

$$\bar{\phi} = 2\tan^{-1}\sqrt{\left(\frac{N\eta\chi \tan\delta + 6K_p}{6 - N\eta\chi \tan\delta}\right)} - \frac{\pi}{2} \tag{2.27}$$

where $K_p = \tan^2\left(\frac{\pi}{4} + \frac{\phi}{2}\right)$, $N = K_p \sin\theta_o$, and $\theta_o = \tan^{-1}\sqrt{\frac{K_p}{2}}$, and θ_0 = inclination angle of surface to the horizontal below which all fibres are in compression.

Michalowski (2008) presented the development of an anisotropic yield condition for fibre-reinforced sand with ellipsoidal distribution of fibres. The maximum shear stress is represented as a function of the inclination of the principal stress direction and the in-plane mean stress. He introduced a term called as distribution ratio which varied between 0 and 1.

If the fibre-reinforced soil behaved as an isotropic material, the ratio was equal to 1. The developed yield condition was used in the kinematic approach of limit analysis. As the material is anisotropic, the internal friction angle is not unique. This angle can be represented as a function of the major principal stress (or strain rate) direction, but it cannot be determined as a unique function of orientation in space. However, for a given boundary value problem the principal strain rate directions can be incurred from the kinematics of the mechanism, and a unique value of internal friction angle can be found iteratively along all velocity discontinuities.

Two examples were presented to illustrate the use of the kinematic approach for anisotropic frictional materials. Solutions to a rough retaining wall loading and the bearing capacity of a strip footing indicated that the addition of fibres reduced the load on the retaining walls, and increased the bearing capacity. In both cases, the contribution of the fibres was enhanced by anisotropic distribution of their orientation.

2.6 APPLICATIONS OF FIBRE-REINFORCED SOIL

Crockford et al. (1993) presented laboratory and field results indicating that discrete, fibrillated fibres (2.54 cm long, 0.254 cm wide and 1000 denier) mixed with cement or lime stabilized sand or clay soils improved the life of pavement layers. From the lab tests, the improvement could be seen in axial compression stress-strain curves as an increase in modulus, strength and strain energy. In some cases, the fibres appeared to alter the material response by moving from a strain-softening response toward a response analogous to strain-hardening. In the field, qualitative as well as quantitative observations suggested that fibres alone could not completely replace chemical stabilizers in certain relatively high-stress pavement applications. However, it was apparent that the tested fibres enhanced the performance of chemically stabilized materials.

Santoni and Webster (2001) conducted laboratory unconfined compression tests and field load tests on a poorly graded (SP) sand reinforced with monofilament polypropylene fibres (51 mm length). The laboratory tests showed optimum fibre content of 1% (by dry weight). Field test sections were constructed and traffic tested using simulated C-130 aircraft traffic with a 13,608 kg tyre load at 690 kPa tyre pressure and a 4,536 kg military cargo truck loaded to a gross weight of 18,870 kg. Test results showed that sand-fibre stabilization over a sand subgrade supported over 1,000 passes of a C-130 tyre load with less than 51 mm of rutting. When the top 102 mm of the sand-fibre layer was lightly stabilized with tree resin to prevent fibre segregation and to provide a wearing surface, substantial amounts of military truck traffic could be supported.

Later, Tingle et al. (2002) reported the performance of fibre-reinforced sand in low volume roads based on laboratory and full scale field tests. The laboratory results of Santoni et al. (2001) were used to design two full-scale field test sections to validate the performance of fibre-reinforced sands for low-volume roads. Other than rut resistance, performance based on construction and maintenance was also checked. It was found that the fibrillated fibres provided the best rut resistance, followed by the monofilament, the tape, and then the Netlon mesh elements. The use of 0.8% fibres of 51 mm length was optimum for maximum performance improvement in terms of reducing rutting and enhancing the serviceability of the road. The effect of different deniers of the same fibre on rut resistance was not that significant. The test sections demonstrated the need for a surfacing for fibre-stabilized layers to keep the tyre friction from pulling the fibres out of the sand.

Zhang et al. (2003) evaluated two methods for repairing slope surface failures of clayey soil embankments. One method involved reinforcing the cohesive soils with randomly oriented fibrillated polypropylene fibres of 25.4 mm length, and the other method incorporated non-woven geotextiles. The performance of soils reinforced using these two

methods was studied in the laboratory and in the field. In the laboratory, a large direct shear and a standard triaxial apparatus were used to evaluate the shear strengths of the reinforced materials. The laboratory results indicated that, in the short term, the fibre reinforcement compensated the loss of soil shear strength caused by the increase in moisture content, and the best results were achieved with 0.1% fibre content by weight. To investigate the long term stability in the field, seven experimental slope sections with fibre and geotextile reinforcements were constructed at various compaction efforts and moisture contents. The performance of these slopes was monitored and the results indicated that repairing failed slopes with the non-woven geotextile was a better option to battle repetitive surface failures in slopes of high plastic soils.

Park and Tan (2005) performed full-scale wall tests to evaluate the effects of polypropylene fibres (60 mm length and 0.2% content) in sandy silt (SM) soil, with and without geogrid reinforcement, for application as a railway embankment vertical wall in Korea. The test results were compared with those obtained from finite element method (FEM) modelling. The results showed that inclusion of short fibres helped to produce a backfill that was stronger and stiffer than the unreinforced compacted backfill. The fibres in the soil decreased the earth pressures and displacements of the wall and increased its stability. The effect of fibres was more significant when used in combination with geogrids.

Yoon et al. (2006) evaluated the feasibility of using tyre shred-sand mixtures as a fill material in embankment construction. A test embankment (2.1 m height, 20 m length and 17.7 m width) constructed using a 50:50 mixture, by volume of tyre shreds (38 and 76 mm length) and a uniformly graded sand, was instrumented and monitored to determine total and differential settlements as well as lateral movement for a period of 1 year. After 200 days of road traffic, the settlement stabilized at small values and the maximum settlement observed was approximately 12 mm. The maximum relative lateral movement with reference to the

bottom of the embankment was only about 2 mm. No evidence of significant differential settlement was observed.

Gregory (2011) investigated the performance of fibre-reinforced soil for repairing side slope failures of road embankments with fibre-reinforced soil. The fibre reinforcement consisted of individual polypropylene fibres, approximately 78 mm long. The fibres were mixed into the soil to increase the shear strength as the soil was placed and compacted in the embankment. This method allowed the existing clay soils in the embankments to be excavated, mixed with fibres, and recompacted into the fill without importing select fill or disposing of the existing fill (i.e., the spoil). The extent of the areas requiring repairs included approximately 2,100 m along the embankments. The embankment repairs were performed in two phases, and completed in 2004 and 2007. The fibre-reinforced soil embankments performed well to-date.

Falorca et al. (2011) reported the results of a full-scale experiment on a trial embankment (50 m length and 10 m width) constructed using a silty sand reinforced with randomly distributed polypropylene fibres (75 mm length). Different sections of the embankment were reinforced with different reinforcing characteristics (0.1, 0.25 or 0.5% fibre content; 6 or 15 denier diameter) to verify the feasibility of this type of construction, and to study the most suitable procedures on site for both embankment construction and soil-fibre mixing. In the laboratory, samples were prepared by manually mixing thin layers of fibres spread in thin layers of hydrated soil. In the field, various mixing techniques were tried in order to achieve an acceptable random and homogeneous mixture along the entyre area of the embankment, as well as for the whole thickness of each embankment layer. They recommended that the water content of the soil should be about half the OMC obtained in the modified Proctor test, so as to facilitate pulverisation of the soil particles. The reinforced soil layers must be ready for compaction immediately after placement, with no need for levelling

procedures. Soil reinforced with thicker fibres showed lower compressibility when compared with unreinforced soil or soil reinforced with thinner fibres.

2.7 SUMMARY OF LITERATURE REVIEW

In general, it has been noted that the modification of engineering properties of soil due to the random inclusion of discrete fibres is a function of a large number of parameters related to soil and fibre characteristics, fibre concentration and orientation, the presence of any cementing material, and both test and field conditions. It has been noted that proper inclusion of fibres within soil can significantly improve the shear strength, compressive strength and bearing capacity. Some key points which have been observed while reviewing the literature, regarding the behaviour of fibre-reinforced soils, are as follows:

1. For proper mixing of fibres in cohesionless soils, the use of a little amount of moisture (less than 5% water content) is sufficient. However, to produce effective fibre-soil mixing in cohesive soils, the use of water content above OMC may be required.
2. Fibre-reinforced cohesionless soil exhibits either curved-linear or bilinear principal stress or failure envelope, as observed from direct shear and triaxial test results. The break in the bilinear curve occurs at a threshold confining stress, termed as critical confining stress. Below the critical confining pressure, fibres tend to slip out at failure condition, and above the critical confining pressure, fibres tend to get stretched till rupture occurs.
3. Keeping other factors constant, the critical confining stress decreases with a better gradation or an increase in coefficient of uniformity of the cohesionless soil.
4. For pullout failure, the fibre-induced distributed tension increases linearly with fibre content and fibre aspect ratio.
5. The contribution of fibres to the shear strength of soil is dependent on the direction of fibre placement in the specimen. For the same fibre content, isotropic distribution of fibres exhibit smaller increase in strength compared to that of anisotropic distribution, in

which the fibres are mainly in the direction of largest extension of reinforced soil specimen (i.e horizontal direction). Vertical fibres have an adverse effect on initial stiffness and have no contribution to the strength.

6. Addition of randomly distributed fibres increases peak deviator stress but the post-peak deviator stress depends on the cementation level of the soil. However, the contribution of fibres is effective after a certain level of shear strain depending on the soil type and fibres used.
7. Both compressive and shear strengths are observed to increase with fibre content up to certain limiting fibre contents, beyond which the strength remains constant or decreases.
8. The increase of shear strength is not only dependent on the fibre content but also on the relative size of fibres and soil grains. At small fibre content, the improvement in shear strength is slightly greater in reinforced fine sands compared to reinforced coarse sands. In contrast, at high fibre content, the relative increase in strength of coarse sand is greater.
9. Field tests indicate that fibre inclusions improve load bearing capacity by increasing the mechanical confinement of soil particles. Fibres do not prevent the formation of cracks, but they control directly the crack propagation and improve the post-cracking properties.
10. Fibre-reinforced soil models based on the approaches of force-equilibrium and superposition of the effects of soil and fibres can be used to estimate the engineering properties of all reinforced soil types, whereas the model based on energy dissipation approach is usable for reinforced cohesionless soils. However, statistical models may not be used as generalized expressions of fibre-reinforced soils.
11. Fibre-reinforced soil structures can be designed by using the composite or discrete approach. As the discrete approach requires independent testing of soil and of fibres, but not of the fibre-reinforced soil, the results obtained are more realistic. Additionally the

fibres can be optimized in terms of their quality, content, aspect ratio, etc. for obtaining a cost-effective design.

It has been noted that studies on fibre-reinforced soil have been carried out mostly on specimens compacted at some specific moisture content and dry unit weight or relative density. In the present study, the strength and deformation behaviour of glass fibre-reinforced clayey and sandy soil specimens under varying moulded states are being investigated.

CHAPTER 3

MATERIALS AND METHODS

3.1 INTRODUCTION

This chapter summarizes the materials and procedures used in performing the investigation. The different sections are for the materials used and their properties, for the laboratory test procedures, for the preparation of test specimens of various mixes with different proportions and for the mixing efficiency. Two types of local soils were used in the present study: a clayey soil and a sandy soil. They are found in abundance within the city of Guwahati in Assam state.

3.2 MATERIALS USED

3.2.1 Clayey Soil

The clayey soil was procured from a nearby hill, as shown in Figure 3.1a, by excavating with a shovel from a depth of 0.4 m below the surface to avoid humus and roots. The properties of the soil are tabulated in Table 3.1. Wet sieve analysis (ASTM D6913-04) and hydrometer analysis (ASTM D422-07) were performed to determine particle size distribution of the soil grains, as presented in Fig. 3.2. The soil has 25% sand size, 54% silt size and 21% clay size particles.

The specific gravity of soil particles is 2.63 as per ASTM D854-10. The values of liquid and plastic limits are 46% and 25%, respectively (ASTM D4318-10). As per Unified Soil Classification System (ASTM D2487-11), the soil is classified as clay of low plasticity (CL). The optimum moisture content (OMC) and maximum dry unit weight (MDU) of the soil are 19.4% and 16.80 kN/m^3, respectively, as per standard Proctor compaction test.

3.2.2 Sandy Soil

The sand was collected from the nearby bank location of Brahmaputra River, as shown in Figure 3.1b. The properties of the sandy soil are also summarized in Table 3.1. The specific gravity (G_s) of the sand particles is 2.69. Dry sieve analysis (ASTM D6913-09) was conducted to determine the grain size distribution of the soil, as shown in Fig. 3.2. The coefficient of uniformity (C_u) and coefficient of curvature (C_c) of the soil are 1.58 and 0.97, respectively. The soil is classified as poorly graded silty sand (SP-SM) as per ASTM D2487-11. The minimum ($\gamma_{d,min}$) and maximum ($\gamma_{d,max}$) dry unit weights of the soil are 13.66 and 16.52 kN/m^3, respectively. For the experimental study, soil at three relative densities of 35, 65 and 85%, corresponding to dry unit weights of 14.55, 15.40 and 16.02 kN/m^3, respectively were used for both unreinforced and fibre-reinforced specimens.

(a) (b)

Fig. 3.1 Soil sampling locations: (a) clayey soil from a nearby hill; (b) sandy soil from nearby bank of Brahmaputra River

3.2.3 Glass Fibres

Commercially available glass fibres of 0.15 mm diameter were used after cutting them into three different lengths of 10, 20 and 30 mm (Fig. 3.3). Its specific gravity is 2.57, determined as per ASTM D792-08. The ultimate tensile strength, modulus of elasticity and

elongation at break of the glass fibre are 1.53 GN/m^2, 112.3 GN/m^2 and 1.8%, respectively as given by the supplier. The water absorption capacity of the glass fibres is nil.

Table 3.1 Engineering properties of soils

Properties	**Clayey soil**	**Sandy soil**
Specific gravity of soil solid (G_s)	2.63	2.69
Grain size analysis		
Coarse sand content (2 – 4.75 mm) (%)	-	0.2
Medium sand content (0.425 – 2 mm) (%)	-	3
Fine sand content (0.075 – 0.425 mm) (%)	21	92.8
Silt content (0.002 – 0.075 mm) (%)	54	4
Clay content (< 0.002 mm) (%)	25	0
Mean size, D_{50} (mm)	0.023	0.21
Effective size, D_{10} (mm)	-	0.145
Uniformity coefficient, C_u	-	1.58
Coefficient of curvature, C_c	-	0.97
Atterberg limits		
Liquid limit (%)	46	-
Plastic limit (%)	25	-
Plasticity index (%)	21	Non-plastic
Soil classification		
USCS soil classification	CL	SP-SM
Description	Low plasticity clay	Poorly graded silty sand
Compaction parameters		
Optimum moisture content (%)	19.4	-
Maximum dry unit weight (kN/m^3)	16.80	-
Relative density		
Minimum dry unit weight (kN/m^3)	-	13.66
Maximum dry unit weight (kN/m^3)	-	16.52

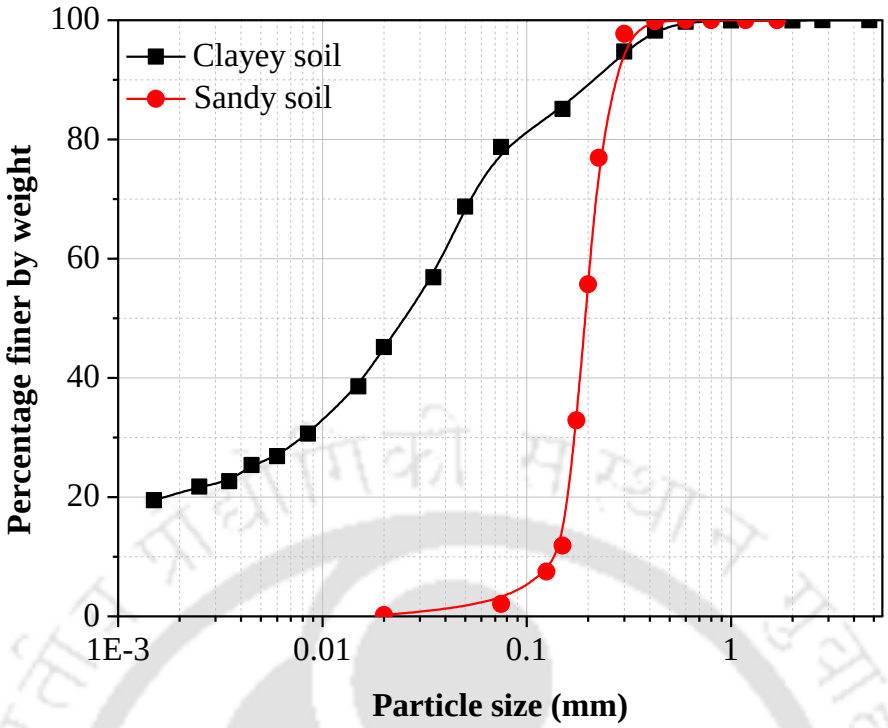

Fig. 3.2 Particle size distribution curve of soils

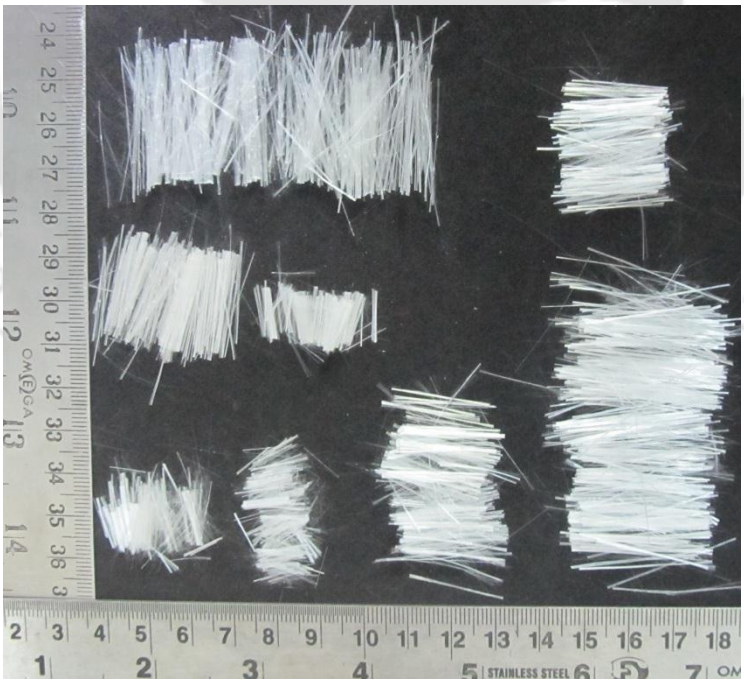

Fig. 3.3 Glass fibres of 0.15 mm diameter as cut in three lengths of 10, 20 and 30 mm

3.3 LABORATORY TESTS CONDUCTED

3.3.1 Compaction Tests

Standard Proctor compaction tests were performed as per ASTM D698-12 to determine the maximum dry unit weight (MDU) and optimum moisture content (OMC) of the clayey soil and soil-fibre mixes. The test results of both unreinforced and reinforced clayey soil specimens, with different combinations of fibre content and fibre length, are shown in Fig. 3.4, and their OMC and MDU values are summarized in Table 3.2. The OMC and MDU of the unreinforced soil are 19.4% and 16.80 kN/m^3. With increasing fibre content, there is a marginal increase in OMC value from 19.4% to 19.7% and a very small reduction in MDU from 16.80 to 16.75 kN/m^3.

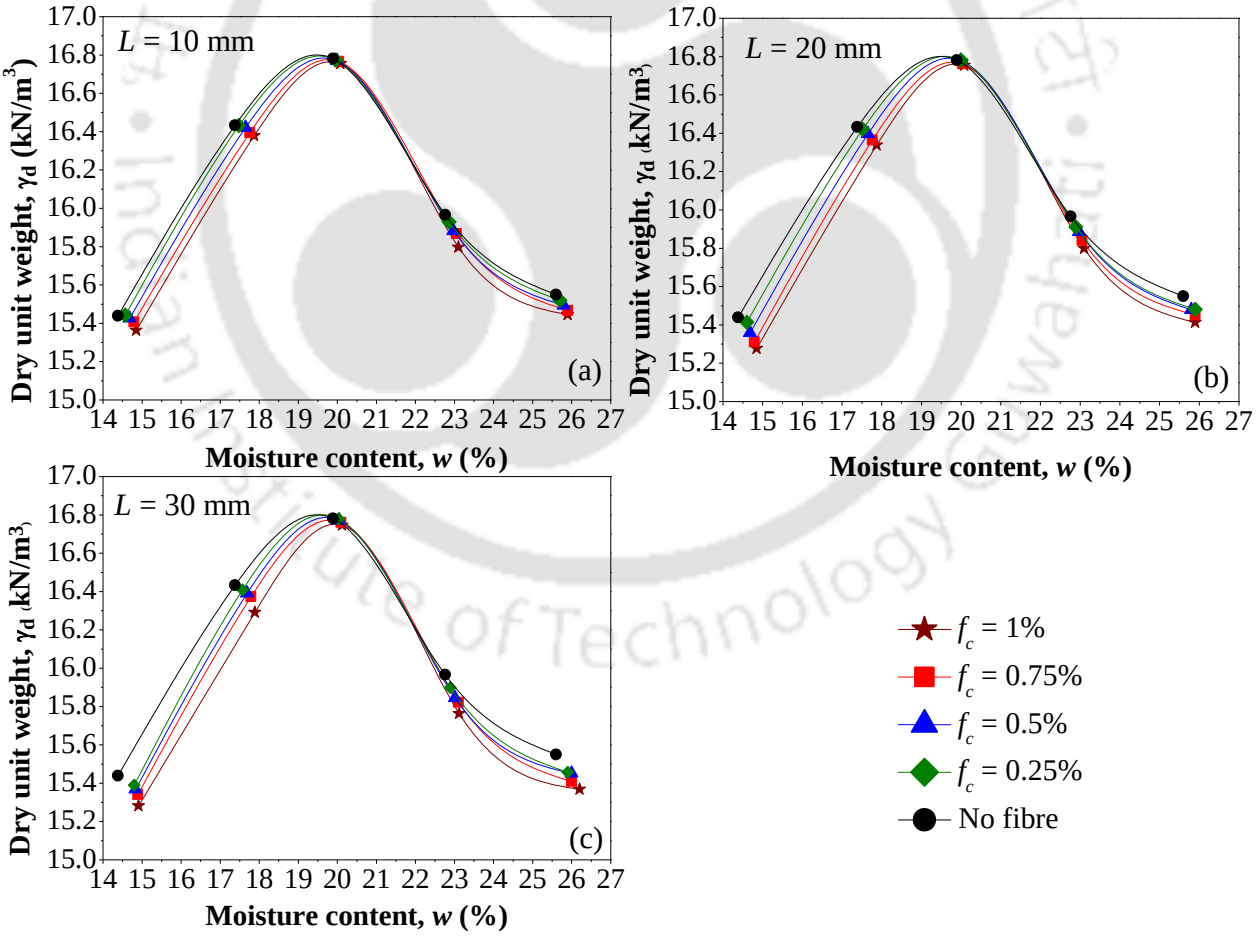

Fig. 3.4 Standard proctor compaction curves of glass fibre-reinforced clayey soil with different fibre lengths: (a) L = 10 mm; (b) L = 20 mm; (c) L = 30 mm

Table 3.2 Proctor compaction test results of fibre-reinforced clayey soil

f_c (%)	L = 10 mm		L = 20 mm		L = 30 mm	
	OMC (%)	MDU (kN/m^3)	OMC (%)	MDU (kN/m^3)	OMC (%)	MDU (kN/m^3)
0	19.4	16.80	19.4	16.80	19.4	16.80
0.25	19.4	16.80	19.4	16.80	19.4	16.80
0.5	19.5	16.79	19.5	16.79	19.5	16.79
0.75	19.5	16.79	19.6	16.78	19.6	16.77
1	19.6	16.78	19.7	16.77	19.7	16.75

3.3.2 Relative Density Tests

The minimum and maximum dry unit weights of the sandy soil were determined as per ASTM D4254-06. A minimum of five trials were conducted and the average values have been considered.

3.3.3 Unconfined Compression Tests

The unconfined compression (UC) tests on the unreinforced and reinforced clayey soil specimens were conducted as per ASTM D2166/D2166M-13. This test is widely used as a quick and economical method for obtaining the compressive strength of the clayey soils and their mixes with other materials. A minimum of three specimens were prepared for each combination of variables. The specimens were compressed at a deformation rate of 1.25 mm/min until a definite failure pattern was developed, or an axial strain of 15% was reached. The axial load and deformation were measured with proving ring and dial gauge, respectively.

3.3.4 California Bearing Ratio Tests

The CBR tests were performed in accordance with ASTM D1883-16 on both unreinforced and fibre-reinforced clayey soil specimens, under unsoaked and soaked conditions. After placing the CBR mould in position under a surcharge weight of 4.54 kg, load was applied to the penetration plunger of 50 mm diameter, at a penetration rate of 1.25

mm/min. Axial load and penetration were measured with proving ring and dial gauge, respectively up to 12.70 mm penetration depth (**Fig. 3.5**).

Fig. 3.5 Details of CBR testing equipment

3.3.5 Triaxial Compression Tests

Consolidated undrained (CU) triaxial tests on clayey soil specimens and consolidated drained (CD) triaxial tests on sandy soil specimens were conducted as per ASTM D4767-11. The triaxial testing equipment had a pneumatic pressure loading system along with an electronic data recording system (Fig. 3.6).

The moulded specimen was first mounted on the pedestal of the triaxial cell along with rubber membrane and rubber O-ring, and the confining pressure and back pressure lines were then connected with pressure control unit. Thereafter, the specimen was saturated using back pressure method with incremental confining and back pressures by maintaining a 20 kPa positive difference between them, while keeping the confining pressure higher. At every increment of confining pressure, the Skempton's pore water pressure parameter B was calculated to check the saturation level of specimen. Specimen was saturated till the parameter B value reached a minimum value of 0.95.

Subsequently, the specimen was consolidated under effective confining pressures (σ_3) of 100, 200, 300 and 400 kPa. The clayey soil specimens were then sheared under undrained condition whereas the sandy soil specimens were sheared under drained condition, at axial strain rates of 0.12 mm/min and 0.03 mm/min, respectively.

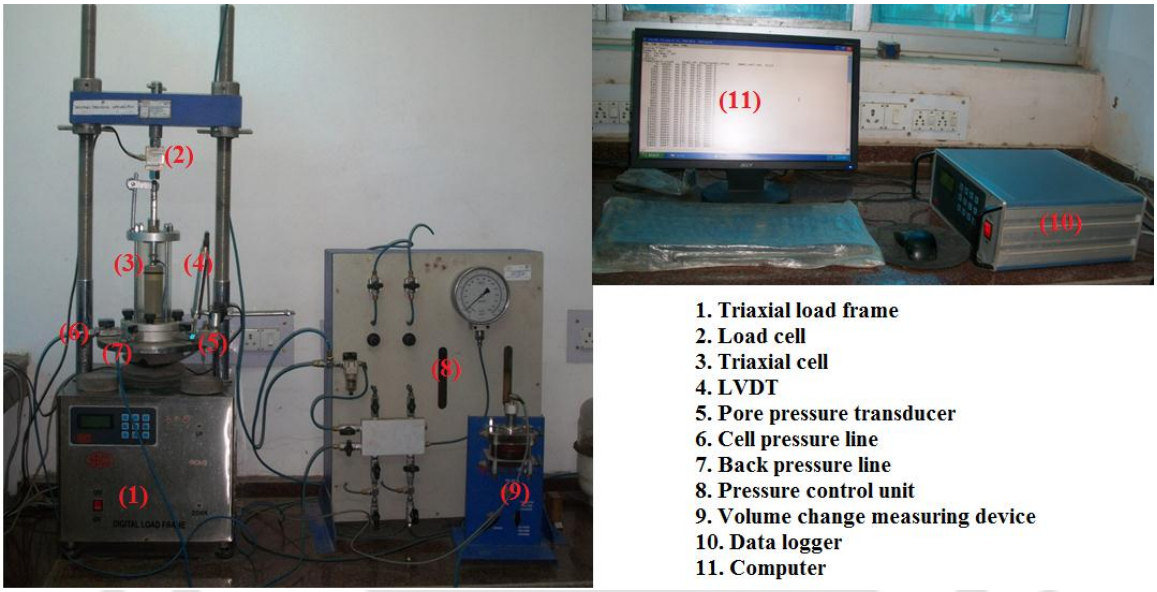

Fig. 3.6 Details of triaxial testing equipment

Specimen shearing was continued either up to a minimum 5% additional axial strain after peak deviator stress or up to 20% axial strain, whichever was reached first (ASTM D4767-11). Load, axial deformation and pore pressure during the test were electronically measured with a load cell of 5 kN capacity of with 0.01 kN sensitivity, LVDT of capacity ±20 mm with 0.01 mm sensitivity and pore pressure transducers with 0.01 kg/cm^2 sensitivity, respectively.

3.4 PREPARATION OF TEST SPECIMENS

The fibres added to both the soil types were considered as a part of solids fraction in the soil matrix. The fibre content (f_c) of the specimen is the ratio of weight of fibres (W_f) to the weight of the dry soil solids (W_s). For a given dry unit weight of specimen (γ_d), the total weight (W) of the specimen moulded in the fixed volume (V) is

$$W = W_s + W_f = \gamma_d \times V \tag{3.1}$$

For any particular fibre content (f_c), the weight of dry soil solids is

$$W_s = \frac{W}{1+ f_c} \tag{3.2}$$

3.4.1 Clayey Soil-Fibre Specimens

For preparing specimens for UC and CU tests, the required quantity of water was first added to the specified weight of dry soil. Once the water was uniformly mixed with the soil, the desired weight of fibres was then added in small increments manually. The mixing of water and fibres was done with proper care until a homogeneous mixture was obtained. The soil-fibre mix was then transferred to a polythene bag and kept in a desiccator for 24 hrs to ensure moisture equilibrium. Thereafter, the soil-fibre mix was moulded in a cylindrical mould of 38 mm inner diameter having detachable collars at both ends (Fig. 3.7). For this, the entire quantity of moist soil-fibre mixture was transferred into the mould from one end, after fixing the collar at the other end. Thereafter, pressure was applied from both ends by giving simultaneous equal rotation to the collars till the specimen length of 76 mm was obtained. Then, the specimen of 38 mm diameter and 76 mm length was extracted from the mould with the help of an extruder.

It was noted that with increasing fibre content of 1%, uniform mixing of fibres became difficult as the fibres started to stick together and form lumps. Therefore, it was decided to restrict the maximum fibre content to 1%. Four different fibre contents (f_c = 0.25, 0.5, 0.75 and 1%) and three different fibre lengths (L = 10, 20 and 30 mm) corresponding to aspect ratios of 67, 133 and 200 were chosen to mould the specimens at different moisture content and dry unit weight combinations, close to the OMC and MDU of the unreinforced clayey soil.

For CBR test specimens, the mixing of soil, water and fibres was carried out in a similar manner, prior to compaction into moulds of 152 mm internal diameter and 178 mm height, using standard Proctor compaction energy.

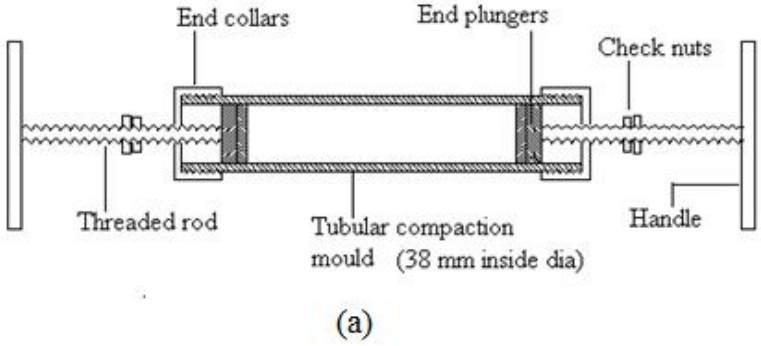

(a)

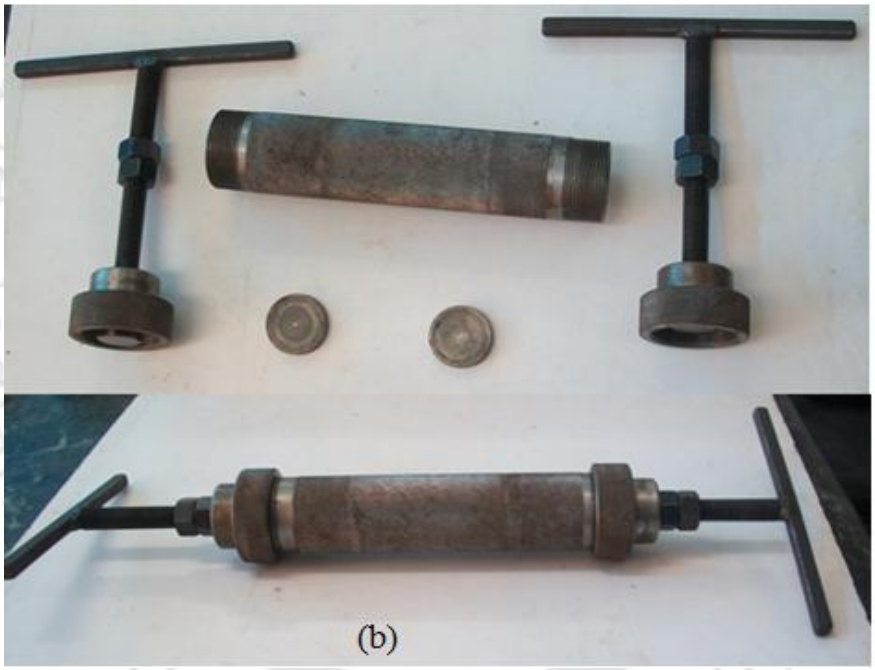

(b)

Fig. 3.7 Static compaction mould used for preparing clayey soil specimens: (a) line diagram; (b) picture

3.4.2 Sandy Soil-Fibre Specimens

For each specimen, dry soil of specified weight was first mixed with a minimal water content of 2%, in order to restrict fibre segregation. Once the water was uniformly mixed with the soil, the desired weight of fibres was then added in small increments manually, and a sand-fibre homogeneous mixture was prepared with proper care (Fig. 3.8a).

The homogeneous mixture was then poured in three equal layers in a rubber membrane kept within a split mould sampler of 38 mm internal diameter, fixed at the pedestal of the triaxial cell (Fig. 3.8b). Proper compaction was given to each of the layers by adopting the undercompaction method (Ladd 1978). Once the specimen was moulded to desired height of 76 mm, the split sampler was removed. Both unreinforced and fibre-reinforced sand specimens were prepared in the same manner (Fig. 3.8c).

For the sand specimens, at fibre content of 5%, uniform mixing of fibres became problematic due to the lumping. Hence, the maximum fibre content was restricted to 4%. Five different fibre contents (f_c = 0.5, 1, 2, 3, and 4%) and three different fibre lengths (L = 10, 20 and 30 mm) corresponding to aspect ratios of 67, 133 and 200 were chosen to mould the specimens at three different relative densities (D_r = 35%, 65% and 85%) of the sandy soil.

(a) (b) (c)

Fig. 3.8 Typical pictures of (a) sand-fibre homogeneous mix, (b) specimen preparation with split mould, and (c) test specimen

3.6 SUMMARY

The details of the materials used in the laboratory tests are presented in this chapter. The characterization of the material properties has been carried out using the standard procedures as per the ASTM codes of practice. Test procedures and specimen preparation methods for different laboratory tests are discussed.

CHAPTER 4

UNCONFINED COMPRESSIVE STRENGTH BEHAVIOUR OF FIBRE-REINFORCED CLAYEY SOIL

4.1 INTRODUCTION

Unconfined compressive strength (UCS) behaviour of unreinforced and fibre-reinforced clayey soil has been investigated by conducting several series of unconfined compressive strength tests. The effects of specimen moulded states (moisture content and dry unit weight), fibre content and fibre length on the unconfined strength, failure deformation, failure secant modulus and energy absorption capability (*EAC*) have been evaluated.

4.2 EXPERIMENTAL PROGRAMME

The unconfined compression (UC) tests were carried out on different soil-fibre mixes with varying parameters. The details of the test specimens are presented in Table 4.1. The specimens were prepared for three series of UC tests. The values of moisture content and dry unit weight were selected to include moulded states other than the OMC and MDU of the unreinforced soil, so as to examine its influence on unconfined compressive strength.

For the first test series (Series 1), the specimens were moulded at 19.4% moisture content (OMC of the unreinforced soil) and at 16.8 kN/m^3 dry unit weight (MDU of the unreinforced soil), with various combinations of fibre content (f_c = 0.25, 0.5, 0.75 and 1%) and fibre length (L = 10, 20 and 30 mm having corresponding aspect ratio of 67, 133 and 200). For the second test series (Series 2), specimens were prepared at moisture contents different from the OMC while keeping dry unit weight equal to MDU, for all the above combinations of fibre content and fibre length. For the third test series (Series 3), specimens were moulded at all moisture contents (including OMC) and dry unit weights (other than the MDU), with all fibre contents of only 20 mm length.

Thus, for the entire three test series combined together, there are four variable moisture contents (15.4, 17.4, 19.4 and 21.4%) with two values lower than OMC and one value above OMC, and five variable dry unit weights of 14.3, 15.1, 16.0, 16.8 and 17.6 kN/m^3 corresponding to 85, 90, 95, 100 and 105% of the MDU of the unreinforced soil. The UC tests were conducted as per ASTM D2166/D2166M (2013) at an axial strain rate of 1.2 mm/min. The test was carried out till specimen failure or up to 15% axial strain deformation, whichever reached first. For each set of parameters, three specimens were tested and the results were analyzed to evaluate the repeatability of the test results. For each soil-fibre mix, the reported values of UCS, failure strain, failure secant modulus and energy absorption capability are the average of the three specimens tested.

Table 4.1: Summary of UC test specimens of clayey soil

Series	**Moisture content, *w* (%)**	**Dry unit weight, γ_d (kN/m^3)**	**Fibre content, f_c (%)**	**Fibre length, *L* (mm)**
1	19.4	16.8	0, 0.25, 0.5, 0.75, 1	10, 20, 30
2	15.4, 17.4, 21.4	16.8	-do-	-do-
3	15.4, 17.4, 19.4, 21.4	14.3, 15.1, 16.0, 17.6	-do-	20

4.3 RESULTS AND DISCUSSION

4.3.1 Strength Characteristics

4.3.1.1 Unreinforced Soil

Stress-strain responses of all unreinforced soil specimens from the three test series are presented in Fig. 4.1a for constant dry unit weight equal to MDU and in Fig. 4.1b for constant moisture content equal to OMC. From Fig. 4.1a, it can be noted that with increasing moisture content from 15.4% to OMC, both the initial stiffness and peak compressive stress increase. The sudden drop in stress after peak indicates brittle nature of the unreinforced soil. At the higher moisture content of 21.4% (wetter state) above OMC, both the initial stiffness and

peak compressive stress are found to be the minimum, whereas the failure strain is the maximum.

As the dry unit weight of unreinforced specimen is varied over the entire range from 14.3 to 17.6 kN/m^3 with moisture content equal to OMC, both the peak stress and failure strain increase (Fig. 4.1b), and the increase in peak stress is about 2.2 times from 84 to 184 kPa. However, the initial stiffness is found to be the minimum for the specimen with the highest dry unit weight.

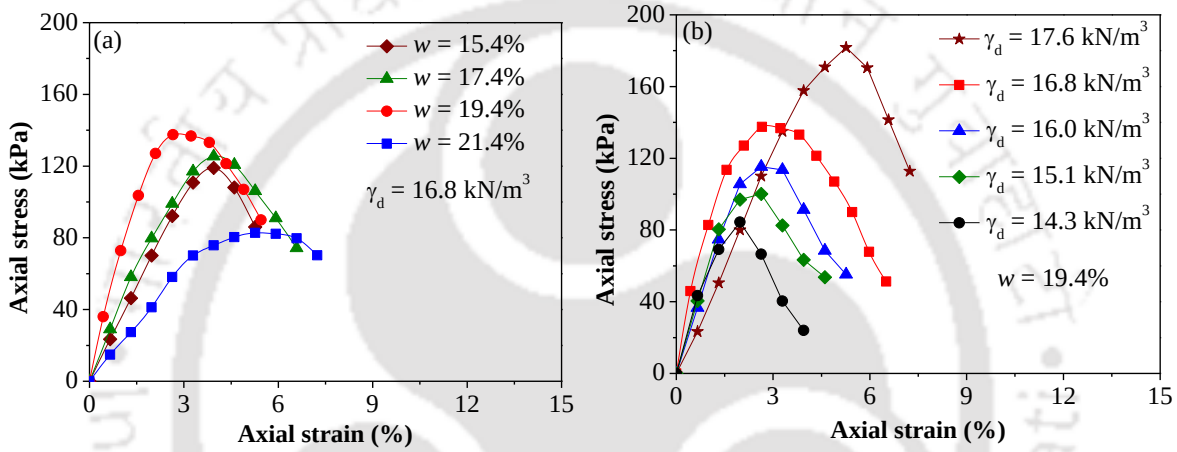

Fig. 4.1 Typical compressive curves of all unreinforced soil specimens: (a) effect of moisture content variation at MDU; (b) effect of dry unit weight variation at OMC

4.3.1.2 Effect of Fibres on Specimens Moulded at OMC and MDU

Figure 4.2 presents unconfined compression results showing the effect of fibre content for all reinforced specimens tested in Series 1. As fibres are added to the soil, the stress-strain behaviour has changed significantly in terms of both increased peak stress and failure strain. This is followed by reduction of post-peak stress loss, showing inducement of plasticity to the unreinforced soil and transformation of the nature gradually from brittle to ductile.

With 10 mm fibres length, the peak stress for 0.75% and 1% fibres are comparable (Fig. 4.2a), though the failure strain with 1% fibres is considerably higher. With 20 and 30 mm fibre lengths (Figs. 4.2b & 4.2c), the peak stress is found out to be the maximum for

0.75% fibres, and addition of more fibres results in reduction of strength. This indicates that there is an optimum fibre content at which reinforcement benefit is the maximum in terms of bond strength and friction between soil particles and fibres. With increased number of fibres in soil at 1% fibre content, the availability of soil matrix quantity for holding the fibres may not be sufficient to develop optimum bond between all soil-fibre interfaces. Consequently, the tensile strength of all fibres is not fully mobilized resulting in drop of peak strength at 1% fibre content. However, the UCS of reinforced specimen with 1% fibres is greater than that of the specimen with 0.5% fibres. Fibre reinforcement benefit is mainly influenced by the bond strength and friction between soil particles and fibres (Tang et al. 2007). It was also noted that at the time of specimen preparation with 1% fibres, uniform mixing of fibres became difficult and formation of fibre lumps started to appear which hindered the specimen uniformity (Section 3.4.1).

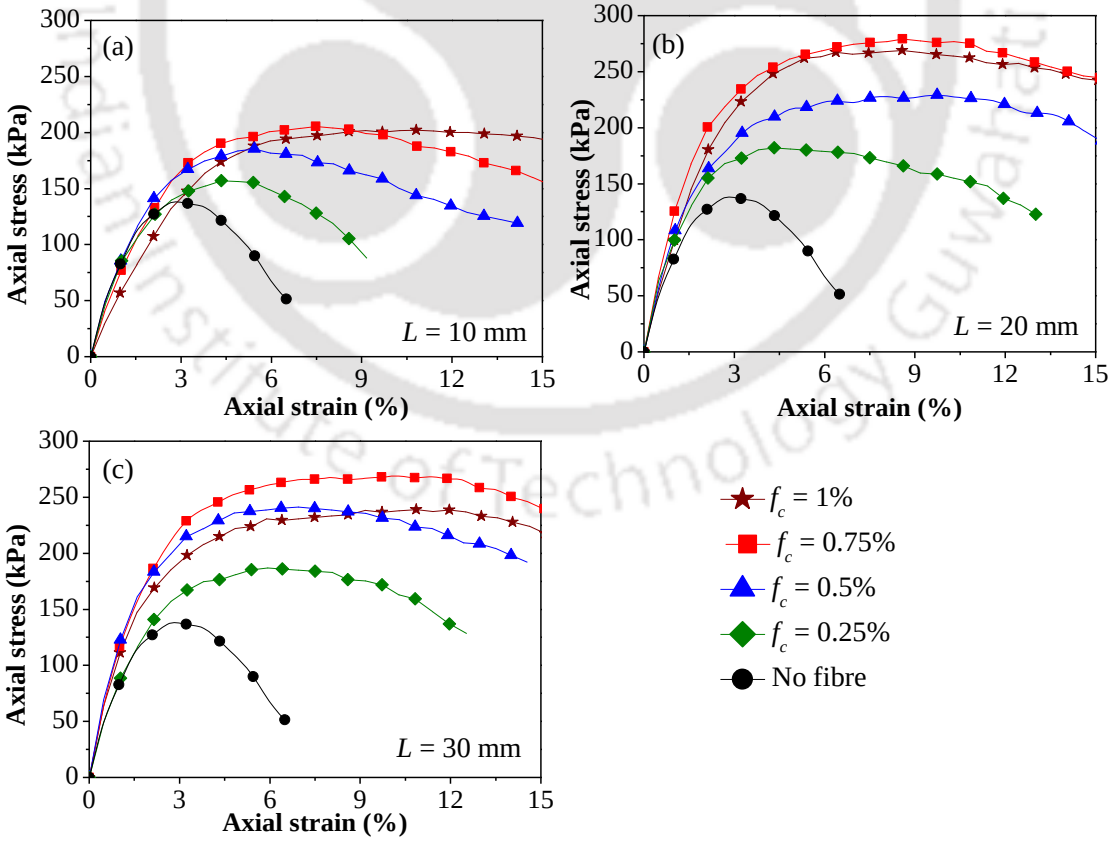

Fig. 4.2 Typical compressive curves of all reinforced specimens of Series 1 with different fibre lengths: (a) L = 10 mm; (b) L = 20 mm; (c) L = 30 mm

The unconfined strength of fibre-reinforced clayey soil depends on the cohesion of the unreinforced soil and also on the interfacial mechanical interactions of adhesion and friction between the soil matrix and fibres. With gradual deformation of the specimen due to the applied load, there is greater soil-fibre interfacial interaction, and the fibres get stretched resulting in development of tensile stress resistance. The observed increase in the strength of the reinforced soil specimen can also be attributed to the fibres interlocking and interweaving with the soil particles.

Figure 4.3 presents unconfined compression test results showing the effect of fibre length for all reinforced specimens tested in Series 1. At all fibre contents, with the increase of fibre length from 10 to 30 mm, the increase in peak stress is noticeably significant whereas the increase in failure axial strain is marginal. For 0.25% fibre content, the peak stress is the maximum with 30 mm length (Figs. 4.3a), whereas for 0.5%, 0.75% and 1% fibre contents, the peak stress is the maximum with 20 mm length (Figs. 4.3b, 4.3c & 4.3d).

For the same fibre content, the peak stress with 30 mm fibres is always greater than that with 10 mm fibres. It was also noted during specimen preparation that there was more folding and bending of fibres at the cylindrical surface of the specimen of 38 mm diameter when 30 mm fibres were added. This indicates that at the time of compressive loading, there is partial utilization of the entire 30 mm fibre length for soil-fibre interfacial interaction, though the fibre contribution still exists from interlocking and interweaving. The observed maximum UCS with 20 mm fibres at higher fibre contents indicates that there is an optimum magnitude of straight fibre length depending on the specimen diameter or size for full mobilization of fibre strength.

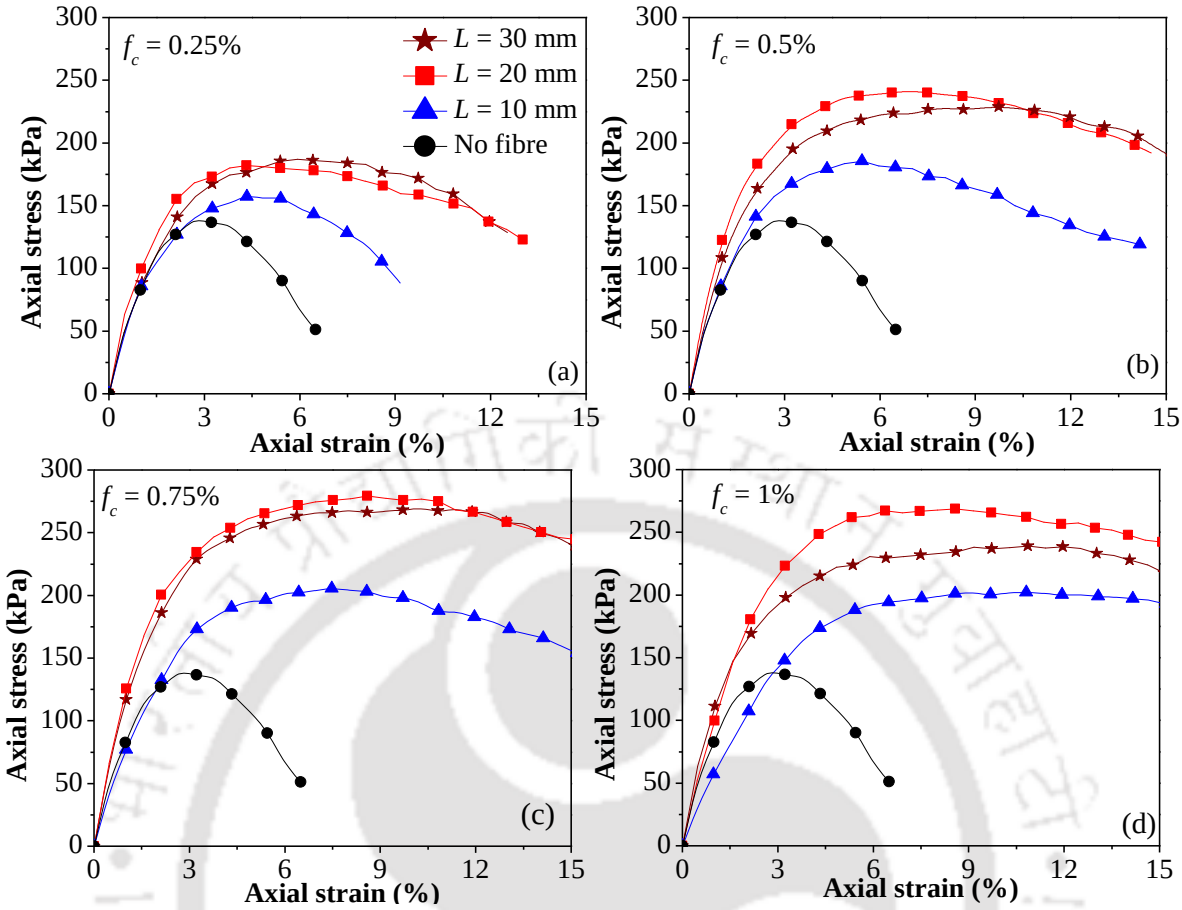

Fig. 4.3 Typical compressive curves of all reinforced specimens of Series 1 with different fibre contents: (a) f_c = 0.25%; (b) f_c = 0.5%; (c) f_c = 0.75%; (d) f_c = 1%

Gray and Ohashi (1983) and Santoni et al. (2001) also reported that increasing the length of fibre reinforcement increases the shear strength of the fibre-reinforced soil composite only up to a certain length. Further, Ang and Loehr (2003) found that the use of specimen diameter greater than 1.4 times the fibre length produces results which are reasonably representative of the true strength of specimen.

The average UCS values with their standard deviation and the average failure strain of the three specimens for any soil-fibre mix of Series 1 are listed in Table 4.2, and the UCS trends are depicted in Fig. 4.4. The UCS is noted to increase with fibre content up to 0.75%, and then decreases with 1% fibres. Further, at any fibre content the UCS is found to be the maximum with 20 mm fibres followed by 30 mm and 10 mm fibres.

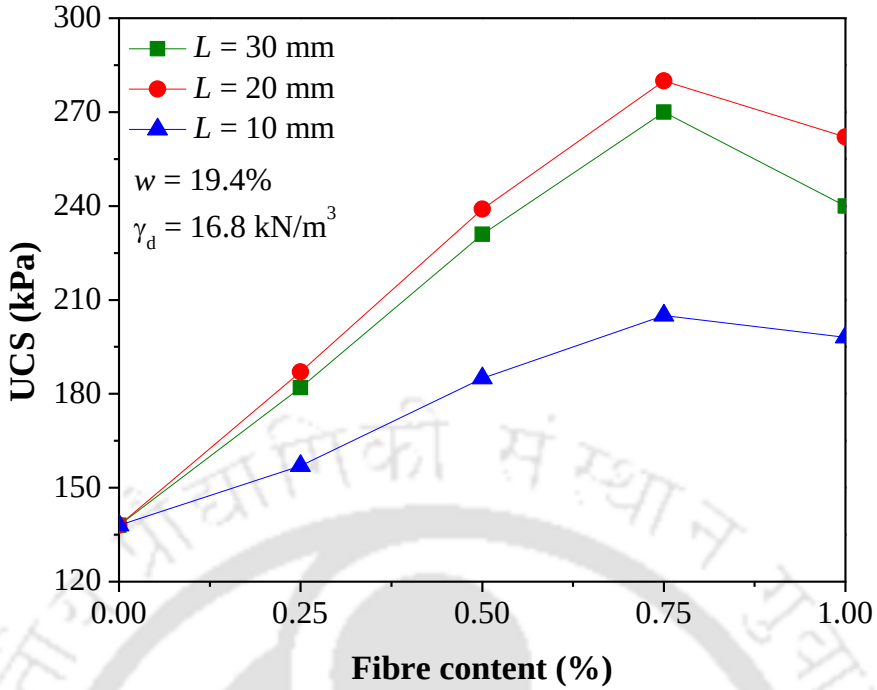

Fig. 4.4 Effect of fibre content and fibre length variation on UCS of all reinforced specimens of Series 1

The UCS of the unreinforced soil is 138 kPa, whereas the corresponding maximum UCS values of the reinforced soil are 205, 280 and 259 kPa with 0.75% fibres of 10, 20 and 30 mm lengths, respectively (Table 4.2). For Series 1, the maximum fibre contribution to UCS is 142 kPa (from 138 kPa to 280 kPa) with 0.75% fibres of 20 mm length. However, the maximum failure strain is found out to be 13.18% for the specimen reinforced with 1% fibres of 30 mm length, which is 4.71 times that of 2.67% for the unreinforced soil specimen. Thus, it can be concluded that the glass fibre-reinforced clayey soil can sustain external loading up to large axial deformation prior to failure.

It has been reported by many researchers that the strength of unreinforced and reinforced soil specimens improves with increase in confining pressure in triaxial tests (Al-Refeai 1991; Ranjan et al. 1996; Michalowski and Zhao 1996) and also with higher normal stresses in direct shear tests (Gray and Ohashi 1983; Yetimoglu and Salbas 2003; Zaimoglu and Yetimoglu 2012). It can be inferred that an increase in fibre content of the reinforced

specimen has internal interlocking effect in unconfined compression tests similar to an increase in confining pressure in triaxial tests and an increase in normal stress in direct shear tests. The presence of fibres restrains the horizontal deformation of specimen and results in strength improvement in unconfined compression tests (Park 2011).

It was observed during and after the tests that different failure characteristics developed in specimens of varying soil-fibre mix. Based on the specimen failure patterns, an attempt has been made to interpret the separate effects of fibre content and fibre length. Fig. 4.5 shows typical effect of fibre content on failure patterns of specimens with 20 mm fibres and moulded at OMC and MDU (Series 1). For the unreinforced soil specimen (Fig. 4.5a), at initial strain during loading, two diagonal shear planes started to appear simultaneously from the top and bottom along the length of specimen, and they joined together to form a single dominant inclined shear plane at failure, indicating brittle behaviour. This brittle behaviour of unreinforced specimen can also be observed from the stress-strain curve (Fig. 4.2), where a sudden drop in stress is noted after peak.

In contrast, the reinforced specimens with 0.25% and 0.5% fibre contents develop distinct multi-shear planes in a part of the specimen (Figs. 4.5b & 4.5c). At higher fibre contents of 0.75% and 1%, failure of the specimens involves predominantly bulging with the formation of smaller fissures (Figs. 4.5d & 4.5e). The restriction of development of shear planes or fissures is due to the bridging effect of the fibres, which results in redistribution of stresses inside the reinforced soil specimen. As can be observed from the stress-strain curves in Fig. 4.2, specimen failure occurs at increasingly greater axial strain with higher fibre content showing the inducement of ductility.

Table 4.2 Summary of UCS test results for all specimens moulded at OMC and MDU (Series 1)

γ_d (kN/m^3)	w (%)	L (mm)	f_c (%)	Average UCS (kPa)	Standard deviation (± kPa)	Fibre contribution to UCS (kPa)	Average failure strain (%)	*SR*	*DR*	Average *EAC* (kJ/m^3)
16.8	19.4	0	0	138	4	--	2.65	--	--	318
		10	0.25	157	4	19	4.61	1.14	1.74	626
			0.5	185	2	47	5.44	1.34	2.05	842
			0.75	205	5	67	7.47	1.48	2.82	1269
			1	198	5	60	10.81	1.43	4.08	1827
		20	0.25	182	1	44	5.26	1.32	1.98	843
			0.5	239	6	101	7.89	1.73	2.98	1456
			0.75	280	3	142	9.86	2.03	3.72	2080
			1	262	6	124	11.36	1.89	4.29	2818
		30	0.25	187	7	49	5.92	1.35	2.23	925
			0.5	231	3	93	6.92	1.67	2.61	1625
			0.75	270	5	132	11.18	1.96	4.22	2449
			1	240	7	102	13.18	1.74	4.71	3095

(a) (b) (c) (d) (e)

Fig. 4.5 Effect of fibre content on failure patterns of specimens reinforced with 20 mm fibres and moulded at OMC and MDU (Series 1): (a) Unreinforced; (b) f_c = 0.25%; (c) f_c = 0.5%; (d) f_c = 0.75%; (e) f_c = 1%

Fig. 4.6 indicates the typical effect of fibre length on failure patterns of specimens with 0.75% fibre content and moulded at OMC and MDU (Series 1). In contrast to the single dominant shear plane at failure of the unreinforced specimen (Fig. 4.6a), the failure of the reinforced specimen with short fibres of 10 mm length involves multi-shear planes in a significant part of the specimen without a distinct failure plane (Fig. 4.6b).

With further increase of fibre length to 20 mm and 30 mm at the same fibre content, drum-shaped ductile failure occurs with minor fissures (Figs. 4.6c & 4.6d). Due to its shorter length, 10 mm long fibres have allowed the bulging only up to a relatively small lateral deformation, after which formation of fissures takes place with the fibres across them getting pulled out. Longer fibres have adequate length which provides more surficial interaction and they sufficiently restrict the development of fissures, as the bulging increases. As can be noted from the stress-strain curves (Fig. 4.3), the reinforced specimens are capable of undergoing greater pre-failure deformation than that of unreinforced soil specimens. Similar trends in the failure patterns were also observed for other reinforced specimens of Series 1 with different fibre contents and fibre lengths.

(a) (b) (c) (d)

Fig. 4.6 Effect of fibre length on failure patterns of specimens reinforced with 0.75% fibres and moulded at OMC and MDU (Series 1): (a) Unreinforced; (b) L = 10 mm; (c) L = 20 mm; (d) L = 30 mm

4.3.1.3 Effect of Fibres on Specimens Moulded with Varying Moisture Content and at MDU

The effect of variation of moisture content on stress-strain behaviour of specimens with the same dry unit weight is shown in Fig. 4.7, only for those reinforced with 20 mm fibres. Overall results showing the effect of moulded moisture content variation are summarized in Table 4.3 for all specimens of Series 1 & 2.

The initial stiffness and peak stress increase with the increase in moulded moisture content up to a limiting value of 19.4% (OMC) with post-peak strain-softening behaviour. At the wetter state of 21.4% moisture content (higher than OMC), the initial stiffness and peak stress decrease substantially with post-peak strain-hardening behaviour.

Increase in moisture content up to OMC results in flocculated rearrangement of soil particles at the time of specimen preparation, and results in a stronger specimen with better interaction among soil particles and fibres, and the stress-strain response of the specimen is improved (Fig. 4.7). At moisture content above OMC, the arrangement of soil particles is more oriented. Also the extra moisture causes lubrication effect between soil-fibre interfaces,

and this leads to a gradual development of tensile strength of fibres within the specimen up to a large strain at the time of axial loading.

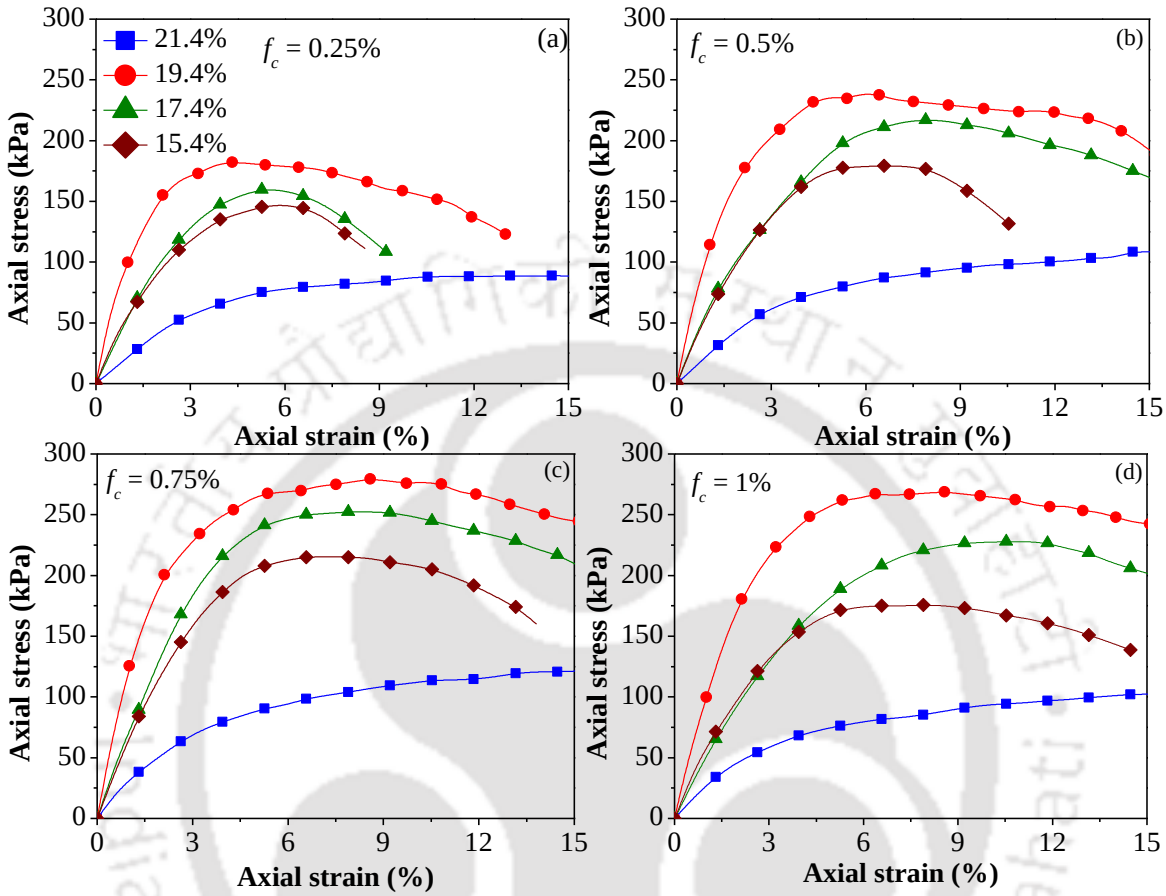

Fig. 4.7 Typical compressive curves of specimens reinforced with 20 mm fibres and moulded with varying moisture content and at MDU (Series 1 & 2): (a) f_c = 0.25%; (b) f_c = 0.5%; (c) f_c = 0.75%; (d) f_c = 1%

In Fig. 4.8, the variation of UCS with moisture content is depicted for all reinforced specimens with 20 mm fibre length (Series 1 & 2). For all fibre contents, as the moisture content increases from 15.4%, the UCS value shows a continuous increase up to 19.4% (OMC) and then decreases to a minimum at 21.4%. At any moisture content, the UCS is found to be highest for the specimen reinforced with 0.75% fibres followed by 1.0% fibres. The same trends were also observed for specimens with 10 and 30 mm fibre lengths (Table 4.3).

However, the fibre contribution to UCS in Series 2 is the highest for the specimen reinforced with 0.75% fibres of 20 mm length (Table 4.3), and the maximum fibre contribution values for specimens moulded at 15.4, 17.4, 19.4 and 21.4% moisture contents are 107, 126, 142 and 53 kPa, respectively.

Similar effect of moisture content was reported by Nataraj and McManis (1997) for clayey soil reinforced with polypropylene fibres, whereas Mirzababaei et al. (2013) reported a dissimilar effect of the peak strength decreasing with increase in moisture content on the dry side of OMC for clay soils moulded at the same dry unit weight and reinforced with carpet waste fibres.

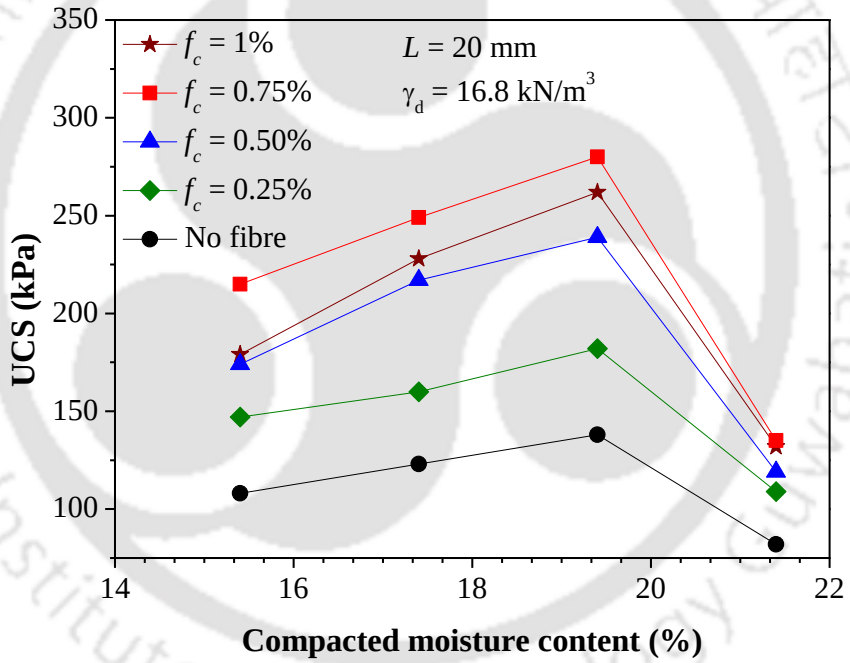

Fig. 4.8 Effect of moulding moisture content variation on UCS of all reinforced specimens with 20 mm fibres (Series 1 & 2)

Table 4.3 Summary of UCS test results for all specimens moulded with varying moisture content and at MDU (Series 1 & 2)

***L* (mm)**	**f_c (%)**	***w* (%)**	**Average UCS (kPa)**	**Standard deviation (± kPa)**	**Fibre contribution to UCS (kPa)**	**Average failure strain (%)**	***SR***	***DR***	**Average *EAC* (kJ/m^3)**
10	0	15.4	108	2	--	2.21	--	--	201
		17.4	123	2	--	2.47	--	--	242
		19.4	138	4	--	2.65	--	--	318
		21.4	82	2	--	5.26	--	--	323
	0.25	15.4	130	4	22	3.29	1.2	1.49	337
		17.4	138	3	15	4.35	1.12	1.76	458
		19.4	157	4	19	4.61	1.14	1.74	573
		21.4	91	2	9	6.92	1.11	1.32	603
	0.5	15.4	149	4	41	3.59	1.38	1.62	403
		17.4	161	3	38	5.26	1.31	1.81	666
		19.4	185	2	47	5.44	1.34	2.05	840
		21.4	109	3	27	7.89	1.33	1.50	862
	0.75	15.4	160	4	52	3.94	1.48	1.78	476
		17.4	185	4	62	6.14	1.5	2.11	884
		19.4	205	5	67	7.47	1.48	2.82	1154
		21.4	121	2	39	9.86	1.47	1.87	1272
	1	15.4	151	4	43	4.57	1.4	2.07	482
		17.4	167	3	44	7.89	1.36	2.71	1066
		19.4	198	5	60	10.81	1.43	4.08	1717
		21.4	112	2	30	11.18	1.36	2.13	1827
20	0.25	15.4	147	3	39	3.74	1.36	1.69	398
		17.4	164	3	41	4.85	1.33	1.96	502
		19.4	182	1	44	5.26	1.32	1.98	856
		21.4	109	2	27	20.0	1.33	3.80	1081

Table 4.3 (Contd.)

L (mm)	f_c (%)	*w* (%)	Average UCS (kPa)	Standard deviation (± kPa)	Fibre contribution to UCS (kPa)	Average failure strain (%)	*SR*	*DR*	Average *EAC* (kJ/m^3)
20	0.5	15.4	179	3	71	4.26	1.66	1.93	564
		17.4	217	4	94	5.91	1.76	2.39	896
		19.4	239	6	101	7.89	1.73	2.98	1623
		21.4	119	3	37	20.0	1.45	3.80	1815
	0.75	15.4	215	6	107	4.62	1.99	2.09	698
		17.4	249	4	126	8.59	2.02	3.48	1782
		19.4	280	3	142	9.86	2.03	3.72	2383
		21.4	135	3	53	20.0	1.65	3.80	2687
	1	15.4	186	4	78	5.92	1.72	2.68	806
		17.4	228	3	105	11.18	1.85	3.84	2016
		19.4	262	6	124	11.36	1.89	4.29	2695
		21.4	132	3	50	20.00	1.61	3.80	2818
30	0.25	15.4	127	3	19	4.11	1.18	1.86	369
		17.4	164	2	41	5.39	1.33	2.18	659
		19.4	187	7	49	5.92	1.35	2.23	920
		21.4	97	2	15	20.00	1.18	3.80	1149
	0.5	15.4	151	3	43	4.61	1.40	2.08	504
		17.4	213	3	90	6.92	1.73	2.80	1074
		19.4	231	3	93	8.55	1.67	3.23	1831
		21.4	110	3	28	20.00	1.34	3.80	2086
	0.75	15.4	185	5	77	5.26	1.71	2.38	660
		17.4	237	5	114	10.26	1.93	4.15	2006
		19.4	270	5	132	11.18	1.96	4.22	2681
		21.4	121	4	39	20.00	1.47	3.80	2912
	1	15.4	158	3	50	5.92	1.46	2.68	750
		17.4	212	4	89	11.36	1.72	4.60	2141
		19.4	240	7	102	13.18	1.74	4.97	2719
		21.4	115	3	33	20.00	1.40	3.80	3095

Fig. 4.9 presents the effect of moisture content on failure patterns of specimens moulded at 16.8 kN/m^3 dry unit weight with 0.75% fibres of 20 mm length (Series 1 & 2). At moisture contents of 15.4% and 17.4% lower than OMC, there is localized appearance of wide multiple surface cracks all around the specimen surface leading to peeling of soil at failure condition (Figs. 4.9a & 4.9b). This is because at low moisture content, the soil cohesion is less resulting in easy disturbance and flaking of soil under loading. As the moisture content is increased to 19.4% (OMC), the surficial cracks no longer appear and the reinforced specimen undergoes bulging failure with small fissures (Fig. 4.9c). At the wetter state of 21.4% moisture content, no failure is observed even up to 15% axial strain and the reinforced specimen continues to bulge (Fig. 4.9d). The strain-hardening behaviour at 21.4% moisture content can also be seen from the stress-strain curves (Fig. 4.7).

(a) (b) (c) (d)

Fig. 4.9 Effect of moulding moisture content variation on failure patterns of specimens reinforced with 0.75% fibres of 20 mm length (Series 1 & 2): (a) w = 15.4%; (b) w = 17.4%; (c) w = 19.4%; (d) w = 21.4%

4.3.1.4 Effect of Fibres on Specimens with Different Dry Unit Weights at Varying Moisture Content

The effect of variation of dry unit weight at different moisture contents (Series 1 & 3) on the stress-strain behaviour of fibre-reinforced soil (0.75% fibres of 20 mm length) is presented in Fig 4.10. At any moisture content, it can be observed that the initial stiffness,

failure axial strain and peak strength of the reinforced specimens are observed to increase gradually with dry unit weight up to 16.8 kN/m^3 (MDU). However, at the higher dry unit weight of 17.6 kN/m^3, only the peak strength is observed to increase further whereas the initial stiffness and failure axial strain are noted to decrease. An increase in dry unit weight of specimen leads to more surficial contacts and improved interfacial mechanical interaction between soil particles and fibres, which increases the pullout resistance of fibres and increases the overall strength of specimen. Similar trends were observed for all other reinforced specimens of Series 3 with different fibre contents of 20 mm length.

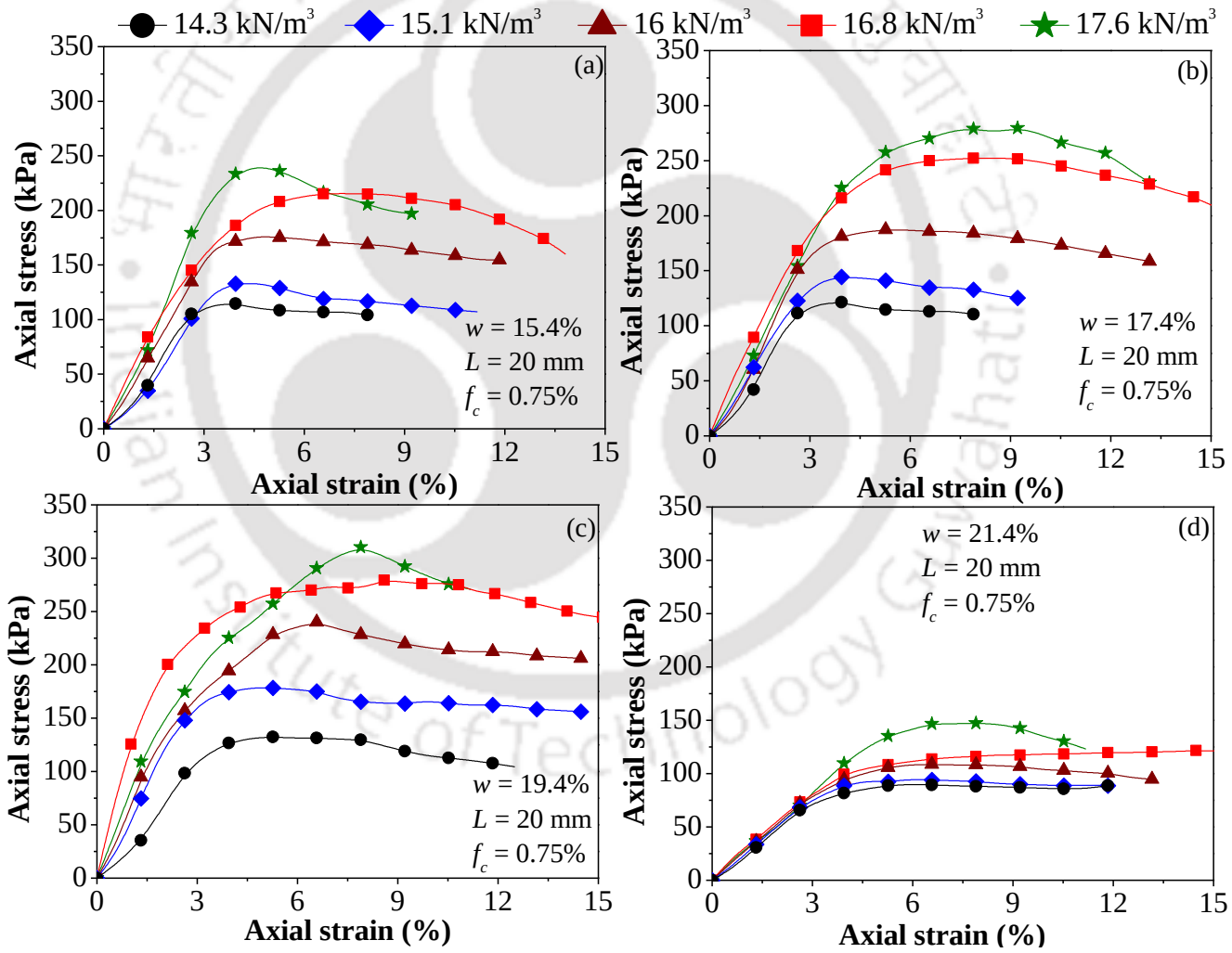

Fig. 4.10 Typical compressive curves of specimens reinforced with 0.75% fibres of 20 mm length and moulded at different dry unit weights and moisture contents (Series 1& 3): (a) w = 15.4%; (b) w = 17.4%; (c) w = 19.4%; (d) w = 21.4%

In Fig. 4.11, the effect of dry unit weight on the variation of UCS is depicted for all reinforced specimens with 20 mm fibre length and moulded at OMC. With any fibre content, the UCS value shows a continuous increase with an increase in dry unit weight. For the specimens with 20 mm fibre length and moulded at other moisture contents, similar trends can be noted (See Fig. 4.12). At the time of specimen preparation, more energy was applied to achieve higher dry unit weight leading to more contacts between soil-fibre interfaces. Mirzababaei et al. (2013) also noted significant improvement in UCS with increase in dry unit weight of reinforced clay soil specimens prepared at a constant carpet waste fibre content and moisture content.

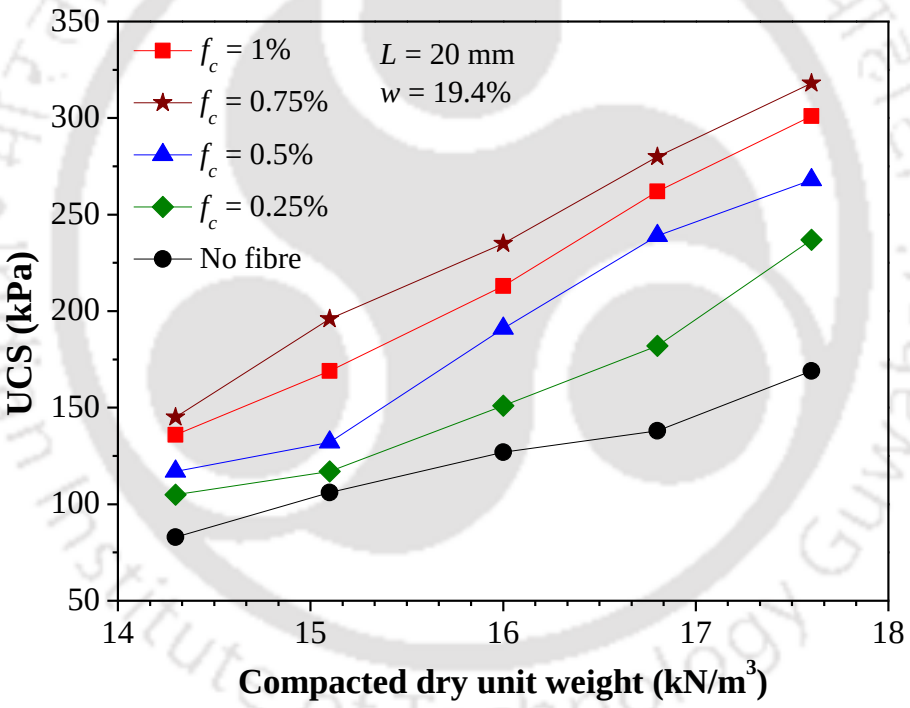

Fig. 4.11 Effect of dry unit weight variation on UCS of specimens reinforced with 20 mm fibres and moulded at OMC (Series 1 & 3)

Tang et al. (2010) conducted single fibre pullout tests on polypropylene fibre-reinforced cohesive soil, and reported that the interfacial shear strength between fibre surface and soil matrix increased by 220.5% as moulded dry unit weight increased from 14 to 17 kN/m^3. From single particle shear tests, Dove and Frost (1999) observed that the effective

contact area between a smooth geomembrane and sand particles directly influenced the internal friction and adhesion. The development of interfacial shear strength between soil and reinforcement was found to be dependent on soil properties, material surface roughness and effective contact area of interface during pullout tests of corrugated geotextile strips in sand (Racana et al. 2003) and of extruded geogrids embedded in a moulded granular soil (Moraci and Recalcati 2006).

Overall results showing the effect of dry unit weight variation (Series 1 & 3) on the average UCS values of fibre-reinforced specimens, with 20 mm fibres and moulded at the same moisture content (OMC), are summarized in Table 4.4. For any dry unit weight, UCS increases with fibre content up to 0.75% fibre content and decreases with higher fibre content of 1%. (Fig. 4.11 & Table 4.4). In general, the increase in UCS with fibre inclusion is small for reinforced specimens moulded at lower dry unit weight, and it gradually increases with increasing dry unit weight similar to the variation of UCS of the unreinforced specimens. For specimens with 14.3 kN/m^3 dry unit weight, the UCS of unreinforced soil is 86 kPa which increases maximum to 196 kPa with fibre contribution of 110 kPa. For specimens with 17.6 kN/m^3 dry unit weight, the corresponding increase in UCS value is from 169 kPa to 318 kPa with fibre contribution of 149 kPa, which is the maximum value in Table 4.4.

Figs. 4.12a to 4.12d show the effect of dry unit weight variation on the average UCS values of all reinforced specimens of Series 1 & 3, moulded at all moisture contents. For any particular fibre content, the variation in UCS with increasing moisture content is relatively smaller for specimens of lower dry unit weights (14.3 and 15.1 kN/m^3) compared to that of specimens of higher dry unit weights (16.0, 16.8 and 17.6 kN/m^3). For the specimens of lower dry unit weights, the UCS values are the maximum with 1% fibres (Fig. 4.12d). In contrast, for the specimens of higher dry unit weights, the maximum UCS values are with 0.75% fibres (Fig. 4.12c).

Table 4.4 Summary of UCS test results for specimens reinforced with 20 mm fibres and moulded at only OMC and different dry unit weights (Series 1 & 3)

f_c (%)	γ_d (kN/m^3)	Average UCS (kPa)	Standard deviation (± kPa)	Contribution of fibre to UCS (kPa)	Average Failure strain (%)	*SR*	*DR*	Average *EAC* (kJ/m^3)
0	14.3	86	4	-	1.97	-	-	135
	15.1	110	2	-	2.23	-	-	203
	16.0	127	4	-	2.47	-	-	237
	16.8	138	4	-	2.65	-	-	318
	17.6	169	5	-	4.60	-	-	538
0.25	14.3	105	5	19	2.63	1.09	1.33	268
	15.1	117	3	7	3.28	1.06	1.47	292
	16.0	151	6	24	3.28	1.19	1.33	379
	16.8	182	1	44	4.85	1.32	1.83	773
	17.6	237	5	68	5.92	1.40	1.29	894
0.5	14.3	117	3	31	3.28	1.22	1.66	302
	15.1	132	4	22	3.94	1.2	1.77	430
	16.0	191	7	64	4.60	1.50	1.86	622
	16.8	239	6	101	5.91	1.73	2.23	1132
	17.6	268	5	99	6.57	1.58	1.43	1176
0.75	14.3	145	3	59	4.60	1.51	2.33	469
	15.1	186	5	76	4.85	1.69	2.17	603
	16.0	225	5	98	5.26	1.77	2.13	739
	16.8	280	3	142	8.59	2.03	3.24	2070
	17.6	318	4	149	7.23	1.88	1.57	1570
1	14.3	140	3	54	5.26	1.46	2.67	519
	15.1	169	4	59	5.39	1.53	2.42	757
	16.0	213	2	86	5.92	1.68	2.40	852
	16.8	262	5	124	11.36	1.90	4.29	2418
	17.6	310	4	141	7.89	1.83	1.72	1764

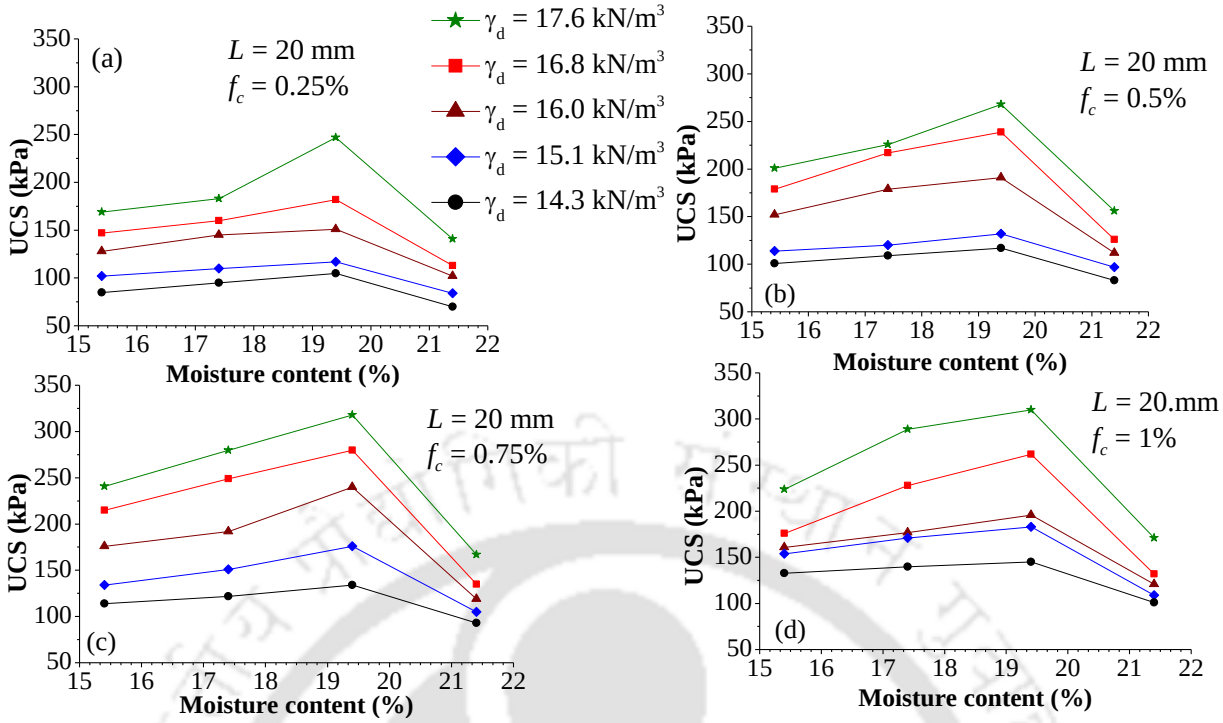

Fig. 4.12 Effect of dry unit weight and moisture content variation on UCS of all reinforced specimens of Series 1 & 3: (a) f_c = 0.25%; (b) f_c = 0.5%; (c) f_c = 0.75%; (d) f_c = 1%

Fig. 4.13 shows the effect of dry unit weight on typical failure patterns of specimens moulded at 19.4% moisture content with 0.75% fibres of 20 mm length (Series 1 & 3). At lower dry unit weights of 14.3 & 15.1 kN/m^3, there is specimen bulging with the appearance of prominent multiple shear cracks around the failure zone but there is no peeling of specimen surface at failure (Figs. 4.13a & 4.13b). As the dry unit weight is increased to 16.0 and 16.8 kN/m^3, the specimen undergoes more bulging and the shear cracks become smaller (Figs. 4.13c & 4.13d). This is because as the dry unit weight increases, the soil-fibre interaction increases which effectively bridges the developing shear cracks. As the dry unit weight is increased further to17.6 kN/m^3 above MDU, no bulging of the reinforced specimen is noted and a proper shear band is observed at failure (Fig. 4.13e). The brittle failure at 17.6 kN/m^3 dry unit weight can also be noted from the stress-strain curves (Fig. 4.10).

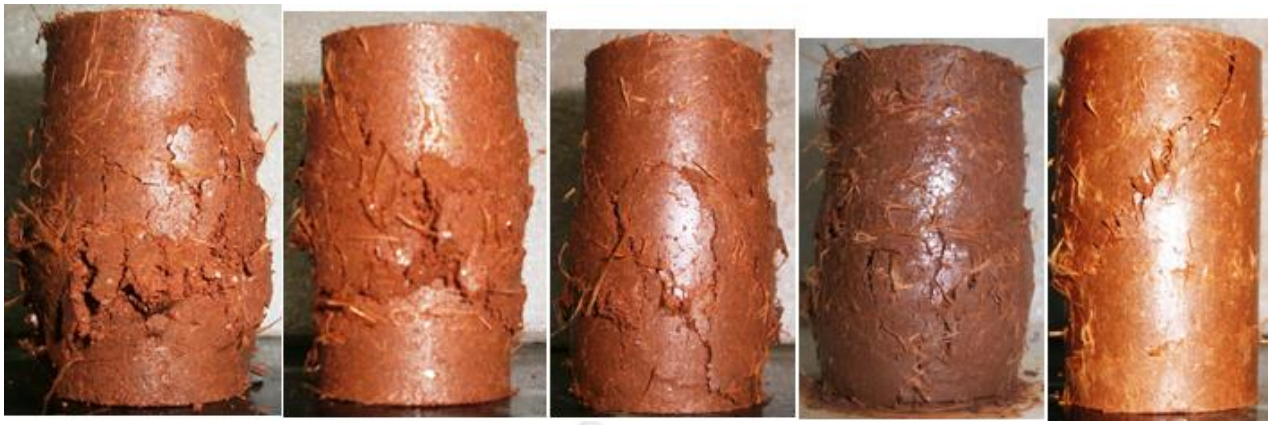

(a) (b) (c) (d) (e)

Fig. 4.13 Variation of failure pattern with dry unit weight for specimens reinforced with 0.75% fibres of 20 mm length and moulded at OMC (Series 1 & 3): (a) γ_d = 14.3 kN/m^3; (b) γ_d = 15.1 kN/m^3; (c) γ_d = 16.0 kN/m^3; (d) γ_d = 16.8kN/m^3; (e) γ_d = 17.6 kN/m^3

4.3.2 Strength Ratio

The improvement in UCS due to fibre reinforcement can be quantified in terms of strength ratio (*SR*) defined as:

$$SR = \frac{UCS_{fr}}{UCS_{ur}} \tag{4.1}$$

where UCS_{fr} is UCS of fibre-reinforced soil and UCS_{ur} is UCS of unreinforced soil.

The *SR* values for specimens moulded at OMC and MDU (Series 1) are given in Table 4.2. In this series, for any fixed fibre length, the *SR* of reinforced soil increases up to 0.75% fibre content, and the maximum *SR* values obtained with 10, 20 and 30 mm fibres are 1.48, 2.03 and 1.96, respectively. This indicates that 0.75% fibre content is the optimum among the used fibre contents, whereas 20 mm fibre length is the optimum among the used fibre lengths, for this particular specimen diameter of 38 mm.

Fig. 4.14 shows the effect of moisture content on *SR* of specimens moulded at MDU with different fibre contents of only 20 mm length (Series 1 & 2), whereas the *SR* values of all specimens of this series are summarized in Table 4.3. At any moisture content, the *SR*

increases with fibre length up to 20 mm and then decreases with 30 mm fibres. However, the *SR* of specimens reinforced with 30 mm fibres is greater than that with 10 mm fibres at any fibre content and moisture content. For 15.4% moisture content, the maximum *SR* values with different fibre lengths of 10, 20 and 30 mm are 1.48, 1.99 and 1.71, and they increase to 1.50, 2.02 and 1.93 with 17.4% moisture content and to 1.52, 2.03 and 1.96 with 19.4% moisture content. As the specimens get wetter with 21.4% moisture content, the *SR* values decrease to 1.47, 1.65 and 1.47 for 10, 20 and 30 mm fibres. With 0.75% fibres of 20 mm length, the maximum values of *SR* in Series 1 & 2 are 1.99, 2.02, 2.03 and 1.65 corresponding to moisture contents of 15.4, 17.4, 19.4 and 21.4%. Thus, the maximum fibre contribution to UCS is 142 kPa when moulded at OMC and MDU.

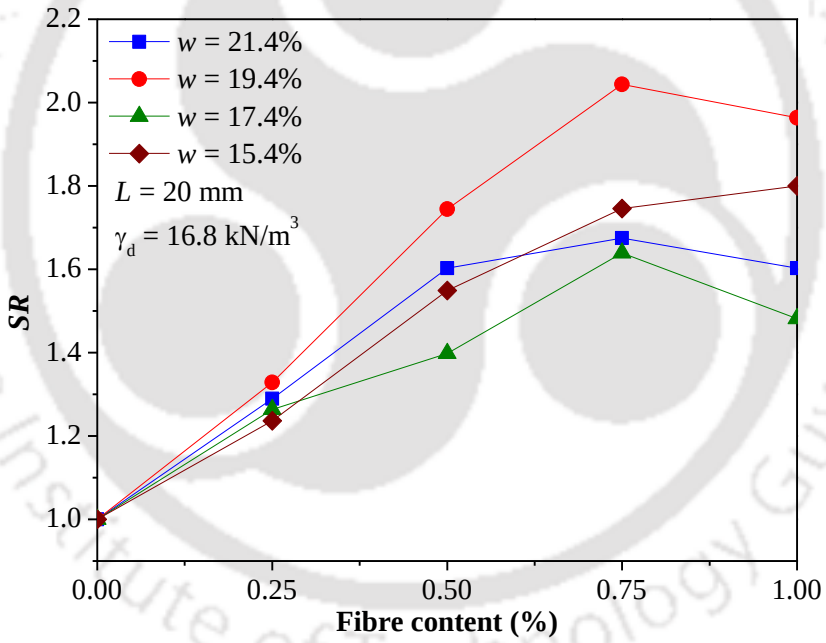

Fig. 4.14 Variation of strength ratio with fibre content and moisture content for specimens reinforced with 20 mm fibres and moulded at MDU (Series 1 & 2)

The *SR* values are tabulated in Table 4.4 for specimens of Series 1 & 3 reinforced with 20 mm fibres and moulded at OMC with different dry unit weights. At lower dry unit weights of 14.3 and 15.1 kN/m^3, the *SR* increases with fibre content up to 1% fibres, with corresponding maximum values of 1.51 and 1.78. At higher dry unit weights of 16.0, 16.8

and 17.6 kN/m^3, the *SR* increases up to 0.75% fibre content, with the respective maximum values of 1.77, 2.03 and 1.88. Among all the specimens of Series 1 & 3, the highest *SR* value of 2.03 is with 16.8 kN/m^3 dry unit weight, for which the fibre contribution to UCS is 142 kPa. However, the maximum fibre contribution to UCS is 149 kPa when moulded at OMC and at 17.6 kN/m^3 above MDU.

4.3.3 Deformation Characteristics

The deformation behaviour of unreinforced and reinforced specimens has been studied from the axial failure strains obtained from the stress-strain plots of Series 1 to 3. The failure axial strain of glass fibre-reinforced soil increases with fibre content for the same fibre length (Fig. 4.2), with fibre length for the same fibre content (Fig. 4.3), and with moisture content for the same fibre content and length (Fig. 4.7), indicating that fibre inclusion progressively increases ductile behaviour. The average failure axial strain values of the specimens have been presented in Tables 4.2 to 4.4.

It can be noted that for the unreinforced specimen of Series 1, the UCS and failure axial strain values are 138 kPa and 2.65%. The reinforcement of 0.75% fibres of 20 mm length has given maximum UCS of 280 kPa (fibre contribution of 142kPa) with corresponding increase in failure axial strain from 2.65% to 9.86% (Table 4.2). However, the maximum failure axial strain is 13.18% with UCS of 240 kPa for the specimen reinforced with 1% fibres of 30 mm length.

In triaxial testing, the brittleness of specimen can be expressed in terms of brittleness index (Maher and Ho 1993), defined as the ratio of the difference between failure deviator stress and residual state deviator stress to that of the residual state deviator stress. In triaxial test, the residual state stress can always be obtained if the specimen is subjected to axial strain much beyond the peak strength. In unconfined compression testing, the specimen does not reach residual state as it is not able to bear any further axial load beyond peak stress.

Therefore, for unconfined compression test, the performance of fibre-reinforced specimen can be quantified in terms of ductility, which is a measure of the reinforced specimen's ability to undergo deformation prior to failure without a significant loss in resistance. Increase in failure strain indicates that the soil specimen is becoming more ductile. The deformation characteristics of the specimens have been investigated by comparing the failure strains due to fibre reinforcement in terms of ductility ratio (*DR*) defined as follows:

$$DR = \frac{\Delta_r}{\Delta_u} \tag{4.2}$$

where Δ_r is failure strain of fibre-reinforced soil and Δ_u is failure strain of unreinforced soil. The *DR* values of the specimens have been summarized in Tables 4.2 to 4.4.

In Table 4.2, the variation of *DR* with fibre content and fibre length is depicted for all specimens of Series 1.With an increase in fibre content, the *DR* value shows a continuous increase up to the highest content of 1.0%, and the same trend is observed in the three groups of specimens differing in fibre length with the maximum *DR* values obtained for 30 mm fibre length (Fig. 4.15). It can be noted that at the four fibre contents of 0.25, 0.5, 0.75 and 1%, the corresponding maximum *DR* values are 2.23, 2.98, 4.22 and 4.71.

From Table 4.3, the failure strain of both unreinforced and reinforced specimens moulded at 16.8 kN/m^3 dry unit weight (Series 1 & 2) is found to increase with moisture content for any fibre content-fibre length combination, indicating that increasing moulded moisture content induces ductility in the specimen. For all fibre contents, the *DR* values show an increasing trend with an increase in moisture content only up to 19.4% (OMC). At any moisture content, the maximum *DR* value is found with 1% fibre content of any length. At the four different moisture contents of 15.4, 17.4, 19.4 and 21.4%, the corresponding maximum *DR* values are 2.68, 4.60, 4.97 and 3.80, respectively with 1% fibres of 30 mm length.

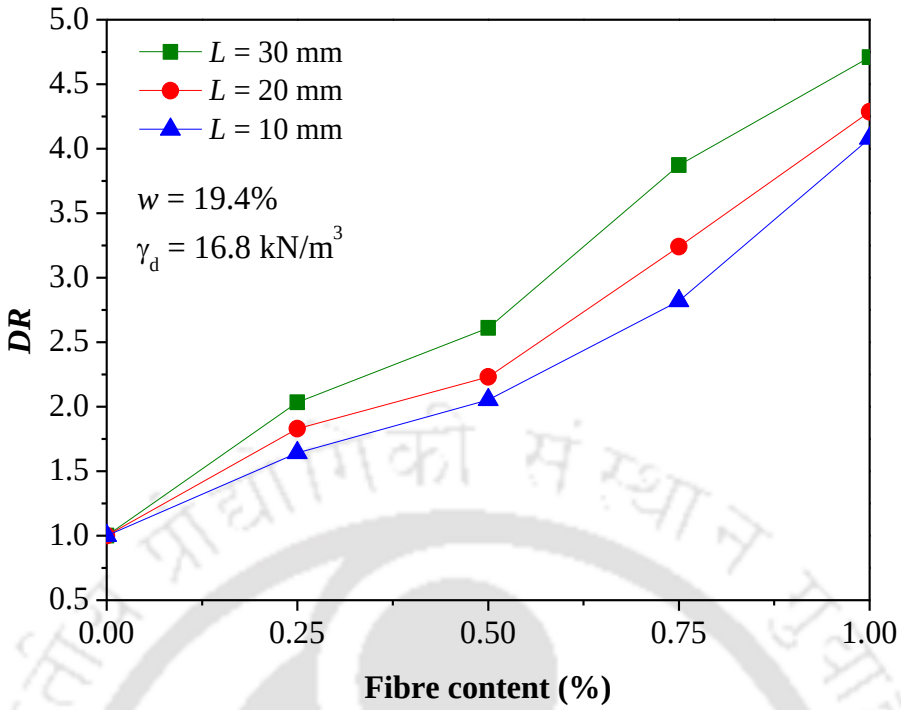

Fig. 4.15 Variation of ductility ratio (*DR*) for all reinforced specimens moulded at OMC and MDU (Series 1)

From Table 4.4, the failure strain of both unreinforced and reinforced soil specimens moulded at OMC (Series 1 & 3) is observed to increase with increasing dry unit weight. For lower fibre contents of 0.25% and 0.5%, the failure strain increases continuously with dry unit weight. For higher fibre contents of 0.75% and 1%, the failure strain is found to increase with dry unit weight only up to 16.8 kN/m^3 (MDU), and then decreases at higher dry unit weight of 17.6 kN/m^3. However, for all fibre contents, the *DR* value shows an increasing trend with an increase in dry unit weight up to 16.8 kN/m^3 (MDU) and then reduces to a minimum value at 17.6 kN/m^3.

4.3.4 Failure Secant Modulus

The stiffness of both unreinforced and reinforced specimens at failure condition can be compared in terms of the failure secant modulus, defined as the ratio of peak strength to the failure axial strain as illustrated in Fig. 4.16. In field applications, the actual applied load

level should remain lower than the peak compressive strength so that the failure axial strain is never reached. Hence, it is appropriate to specify the stiffness of the fibre-reinforced soil in terms of the failure secant modulus.

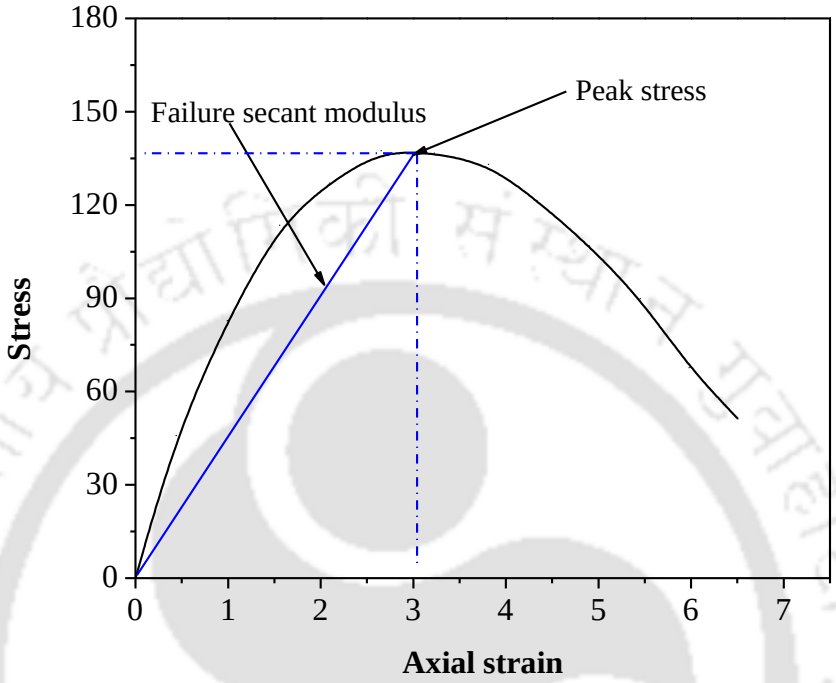

Fig. 4.16 Typical illustration of failure secant modulus calculation from axial stress-axial strain plot of UC test

In Fig. 4.17, the variation of failure secant modulus with fibre content and fibre length is depicted for all specimens of Series 1. With an increase in fibre content, the failure secant modulus value shows a continuous decrease up to the highest content of 1%, and the same trend is observed in the three groups of specimens differing in fibre length. At any fibre content, the failure secant modulus is the maximum for the specimen with 20 mm fibre length, followed by the specimens with 10 mm length and 30 mm length. It can also be noted that at the four fibre contents of 0.25, 0.5, 0.75 and 1%, the corresponding minimum failure secant modulus values are 3.49, 3.17, 2.62 and 1.83 MPa for 30 mm fibre length. The failure secant modulus of unreinforced specimen is 5.18 MPa, whereas those of reinforced

specimens with 1% fibre reinforcement are 2.07, 2.57 and 1.83 MPa for 10, 20 and 30 mm fibre lengths, respectively.

In Fig. 4.18, the variation of failure secant modulus with moisture content is depicted for all reinforced specimens with 20 mm fibre length (Series 1 & 2). With an increase in moisture content, the failure secant modulus value initially increases followed by a decrease, and the maximum value of the failure secant modulus is found at 19.4% moisture content (OMC). Same trends are observed for the four groups of specimens with different fibre contents, but the stiffness is noted to be the minimum for the highest fibre content at any moisture content. From Fig. 4.17, it can be noted that at the four variable moisture contents of 15.4, 17.4, 19.4, and 21.4%, the minimum failure secant modulus values are 2.22, 2.04, 2.57 and 0.67 MPa for the 1% fibre-reinforced specimens.

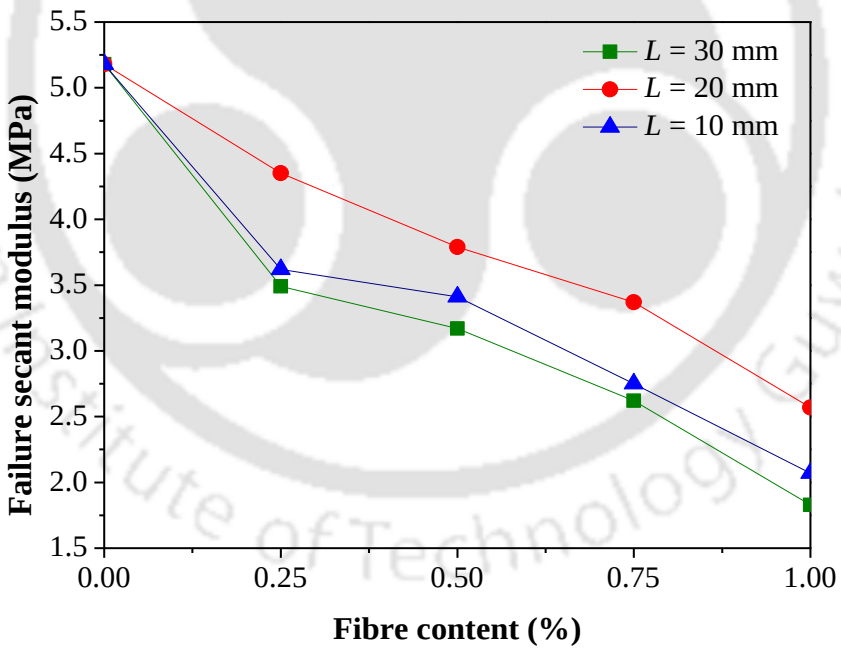

Fig. 4.17 Variation of failure secant modulus for all reinforced specimens moulded at OMC and MDU (Series 1)

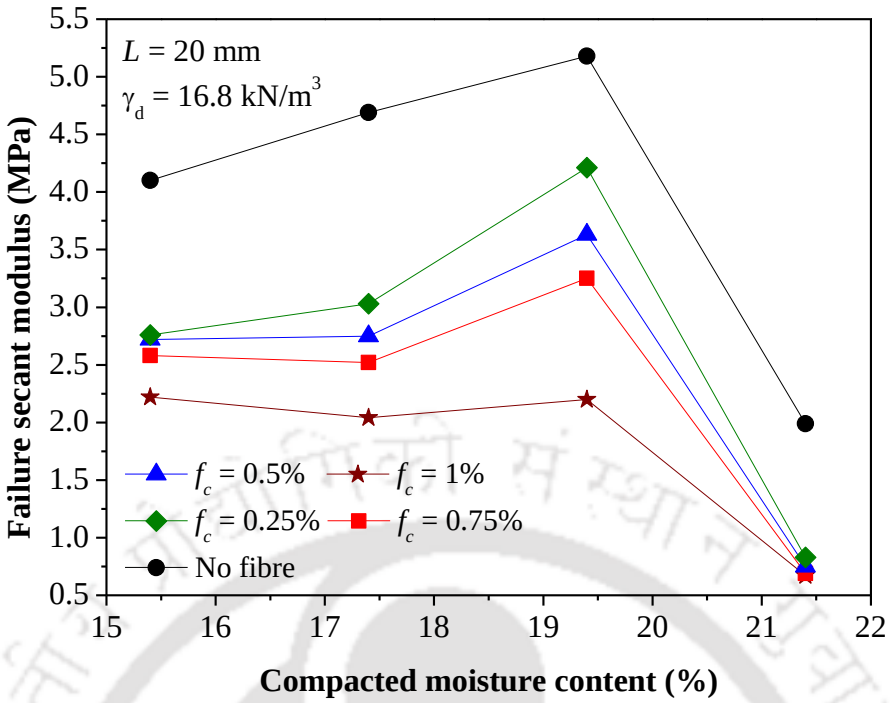

Fig. 4.18 Variation of failure secant modulus with moisture content for specimens reinforced with fibres of 20 mm length and moulded at MDU (Series 1 & 2)

In Fig. 4.19, the effect of dry unit weight on the variation of failure secant modulus is presented for all reinforced specimens with 20 mm fibre length (Series 1 & 3). With an increase in dry unit weight up to 16.0 kN/m^3, the failure secant modulus value of reinforced specimens shows a continuous increase followed by a decrease at 16.8 kN/m^3, after which there is an increase again. The same trends are found in the four groups of specimens differing in fibre content, and the failure secant modulus is observed to be the minimum for the highest fibre content at any dry unit weight. From Fig. 4.18, it can be seen that at the five dry unit weights of 14.3, 15.1, 16.0, 16.8, and 17.6 kN/m^3, the minimum failure secant modulus values of the reinforced specimens are 2.76, 3.04, 3.60, 2.31 and 3.93 MPa for the 1% fibre-reinforced specimens.

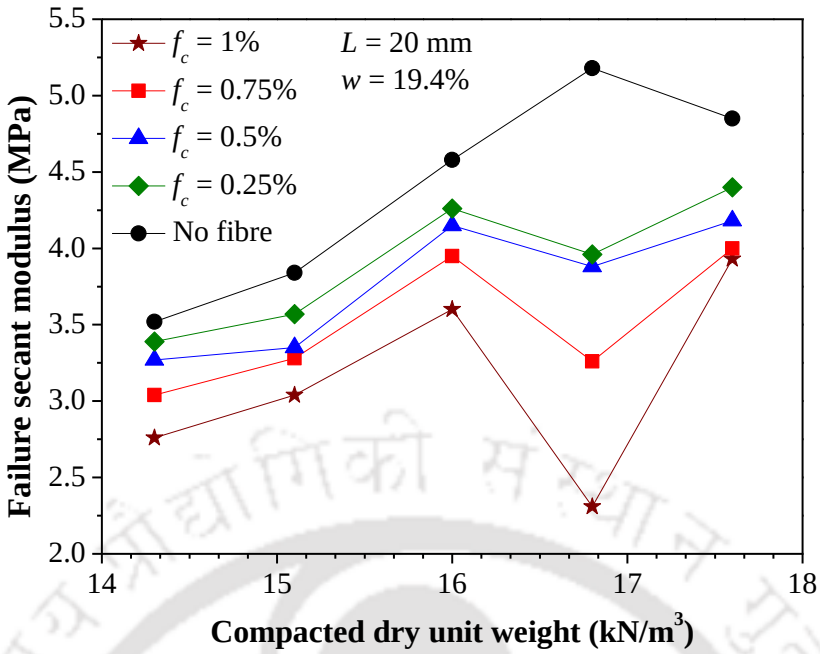

Fig. 4.19 Variation of failure secant modulus with dry unit weight for specimens reinforced with fibres of 20 mm length and moulded at OMC (Series 1 & 3)

4.3.5 Energy Absorption Capability

The area under the stress-strain curve gives the energy absorption capability (*EAC*) of the soil specimen in triaxial compression (Consoli et al. 2002). In a similar manner, the *EAC* values of both unreinforced and fibre-reinforced specimens under unconfined compression have been calculated up to failure axial strain and then compared. A typical representation of *EAC* calculation from stress-strain plot of UC test is shown in Fig. 4.20. The shaded area under stress-strain curve up to peak stress is used for calculating *EAC* of the specimen. An increase in *EAC* with fibre reinforcement is the indication of increase in peak strength or failure strain or both.

The effects of fibre content and fibre length on the *EAC* values have been summarized in Table 4.2 for the specimens of Series 1, and the trends are depicted in Fig. 4.21. It can be noted that the *EAC* of reinforced specimen improves with both fibre content and fibre length. This indicates that the fibres distributed within the soil specimen have caused continuous energy absorption prior to specimen failure. The maximum *EAC* value is found as 3074 kJ/m^3

for the specimen reinforced with 1% fibre content and 30 mm length, with UCS of 240 kPa and axial failure strain of 13.18%. However, among all reinforced specimens of Series 1, the maximum UCS value of 280 kPa (at axial failure strain of 9.86%) is for the specimen reinforced with 0.75% fibre content and 20 mm length (Table 4.2), and the corresponding *EAC* value is 2080 kJ/m^3.

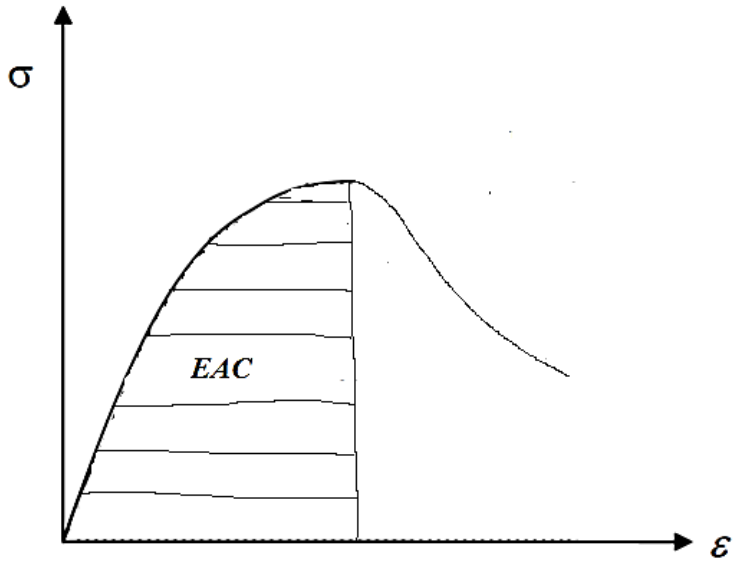

Fig. 4.20 Typical representation of energy absorption capability calculation from axial stress-axial strain plot of UC test

The *EAC* values of specimens tested in Series 1& 2, as tabulated in Table 4.3, are observed to increase with increasing moisture content. Typical effect of moulded moisture content on *EAC* for specimens reinforced with 20 mm fibre of varying fibre content is shown in Fig. 4.22. It can be noted that the *EAC* increases with moisture content at any fibre content and also increases with fibre content at any moisture content. Among all reinforced specimens of Series 1 & 2, the maximum *EAC* value is found for the specimen reinforced with the uppermost fibre content (1%), greatest fibre length (30 mm) and the highest moulding moisture content (21.4%). This maximum value is 3095 kJ/m^3, with UCS value of 115 kPa (Table 4.3). For any fibre content-fibre length combination, although the UCS value of specimen moulded at the wettest state of 21.4% moisture content is the minimum, whereas

the corresponding *EAC* value is the maximum due to the failure axial strain being much larger than at other moisture contents.

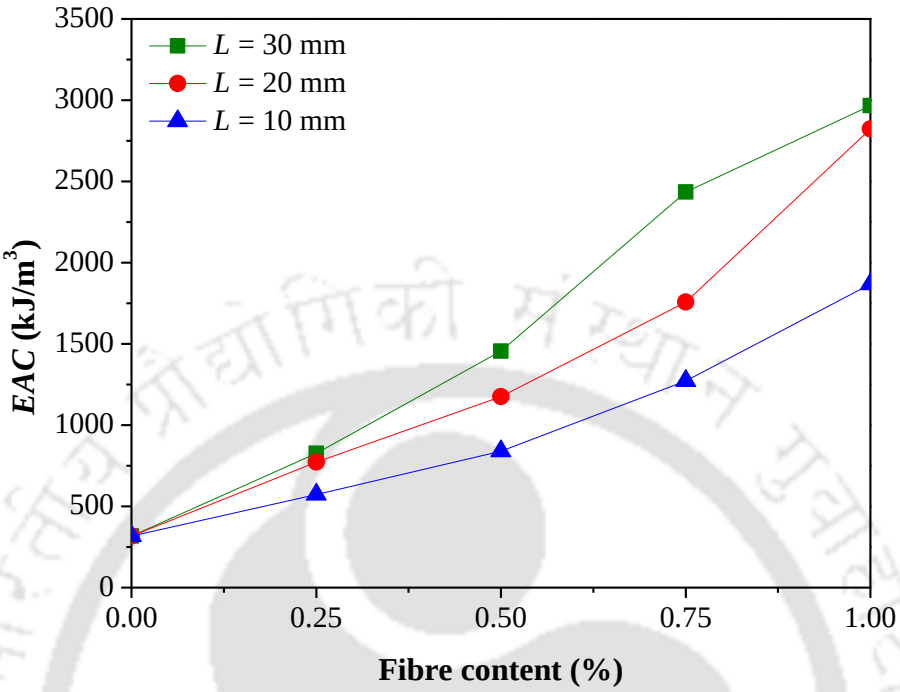

Fig. 4.21 Variation of energy absorption capability for all reinforced specimens moulded at OMC and MDU (Series 1)

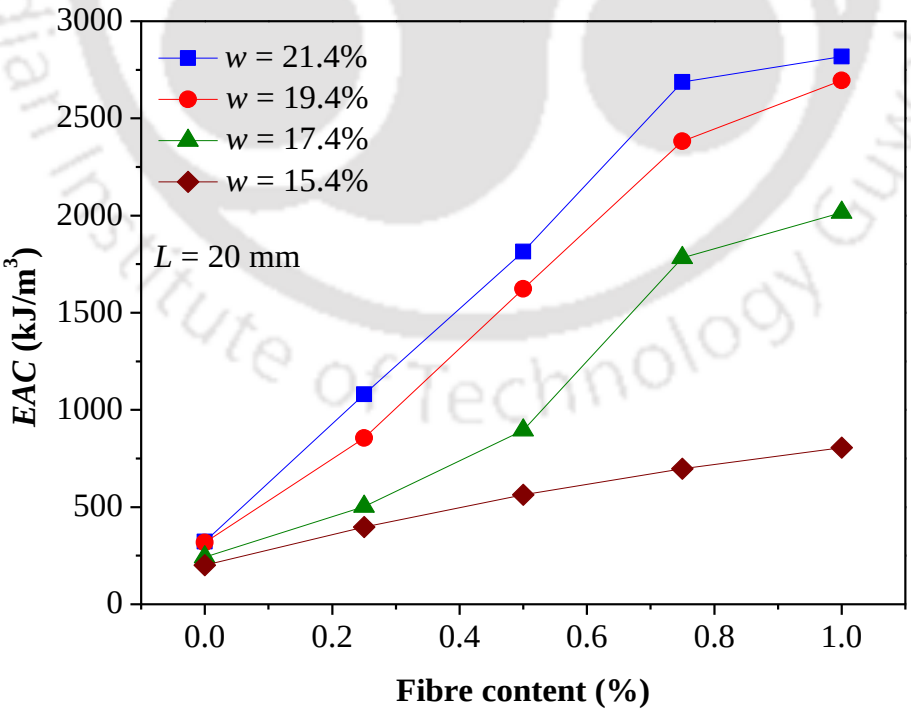

Fig. 4.22 Variation of energy absorption capability with moisture content for specimens reinforced with fibres of 20 mm length and moulded at MDU (Series 1 & 2)

The *EAC* values of specimens tested in Series 1 & 3 have been tabulated in Table 4.4, and typical effect of dry unit weight on *EAC* of specimens reinforced with 20 mm fibres of varying content is shown in Fig. 4.23. At fibre contents up to 0.5%, the *EAC* value shows a continuous increase with dry unit weight up to 17.6 kN/m^3. However, at higher fibre contents of 0.75 and 1%, the *EAC* value is the maximum for the specimen with 16.8 kN/m^3. At any dry unit weight, the *EAC* is found to be the greatest for specimen reinforced with 1% fibre content. Among all reinforced specimens of Series 1 & 3, the maximum *EAC* value of 2418 kJ/m^3 is with 1% fibres of 20 mm length, and moulded at OMC and MDD.

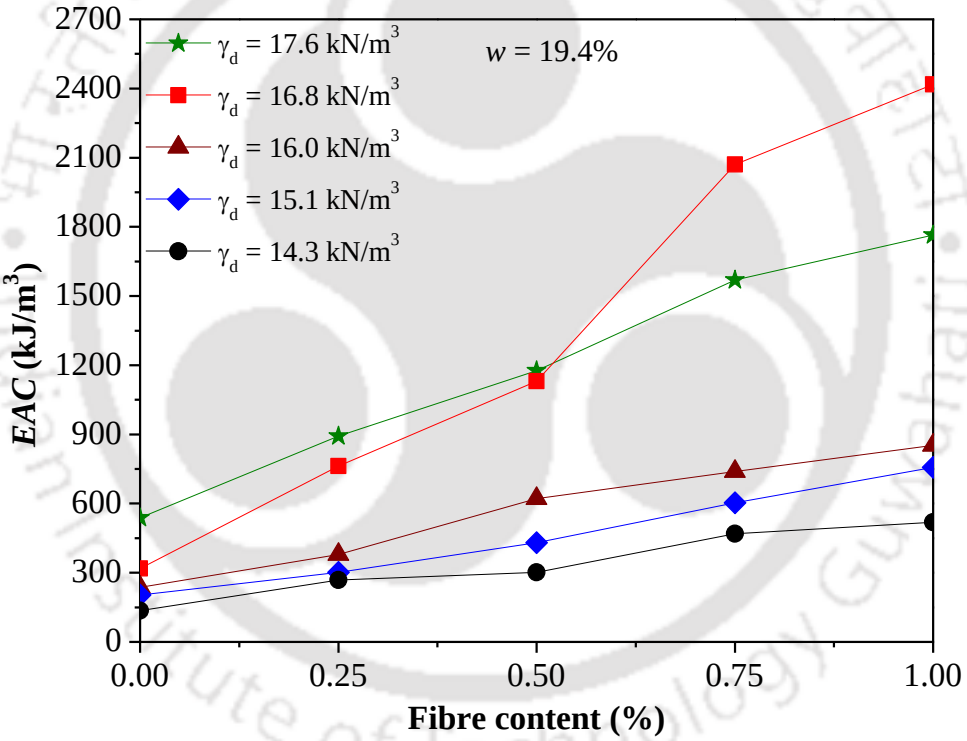

Fig. 4.23 Variation of energy absorption capability with dry unit weight for specimens reinforced with fibres of 20 mm length and moulded at OMC (Series 1 & 3)

4.4. SUMMARY

The effect of glass fibre reinforcement on clayey soil specimens at varying moulded states was studied through UC tests. The specimens were moulded at varying dry unit weight

other than MDU and moisture content other than OMC along with different fibre lengths and fibre contents. The effect of fibre reinforcement and moulding states variation on stress-strain response, specimen failure mode, peak stress, failure strain, failure secant modulus, and *EAC* beahviour was investigated. The following conclusions have been drawn from the test results:

1. At any moulded state (moisture content and dry unit weight) of reinforced clayey soil specimens, the unconfined clayey strength (UCS) increases with fibre content for any length to reach maximum value with 0.75% fibres, and also with fibre length for any content to reach highest value with 20 mm fibres.
2. At any dry unit weight, an increase in moulding moisture content up to OMC results in an increase of UCS of reinforced specimens, whereas moisture content above OMC leads to a reduction of UCS. In contrast, at any moulding moisture content, an increase in dry unit weight always results in increase of UCS.
3. At any dry unit weight, the failure axial strain of reinforced specimens always increases with the increase of any of fibre content, fibre length or moisture content keeping the others constant. At any moulding moisture content, with lower fibre contents of 0.25% and 0.5%, the failure strain increases continuously with dry unit weight. For higher fibre contents of 0.75% and 1%, the failure strain is found to increase with dry unit weight only up to 16.8 kN/m^3 (MDU), and then decreases at higher dry unit weight of 17.6 kN/m^3.
4. At any moulded state of the reinforced specimens, the secant modulus at failure strain level decreases with increasing fibre content keeping the fibre length constant. However, at any dry unit weight, the secant modulus at failure strain level increases with increasing moisture content only up to OMC and then decreases.
5. For constant dry unit weight of the reinforced specimens, the energy absorption capability (*EAC*) increases with higher fibre content or fibre length or moisture content keeping the

others unchanged. However, at constant moisture content, the *EAC* value increases with higher dry unit weight only up to MDU and then decreases.

6. For unreinforced soil specimens, the failure pattern is characterized by a single distinct shear plane. With reinforcement of low fibre contents (f_c = 0.25 & 0.5%) and of any length, the failure pattern consists of mainly multi-shear planes along with barrelling in a part of the specimen. With higher contents (f_c = 0.75 & 1%) of any fibre length, the failure pattern is gradually transformed to predominantly plastic bulging with a network of minor fissures.
7. At low moulding moisture contents (w = 15.4 & 17.4%), the failure pattern of the reinforced specimen is characterized with localized appearance of multiple cracks around the specimen surface leading to flaking of soil at failure condition. At higher moisture contents (w = 19.4 & 21.4%), the surficial cracks disappear and the reinforced specimen undergoes bulging failure with small fissures.
8. At low dry unit weights (γ_d = 14.3 & 15.1 kN/m^3), the failure pattern of the reinforced specimen is characterized with bulging and the appearance of prominent multiple shear cracks. At higher dry unit weights (γ_d = 16.0 & 16.8 kN/m^3), the reinforced specimen undergoes more plastic bulging and the shear cracks become smaller. However, at the highest dry unit weight (γ_d = 17.6 kN/m^3), the reinforced specimen undergoes distinct shear failure.
9. With the optimum glass fibre reinforcement of 0.75% content and 20 mm length, the maximum UCS of the reinforced specimen is noted at moulding moisture content equal to OMC, with the fibre contribution being 0.51, 0.78, 0.77, 1.03 and 0.88 times, over and above that of the corresponding unreinforced specimen at 14.3, 15.1, 16.0, 16.8 and 17.6 kN/m^3 dry unit weights.

CHAPTER 5

CALIFORNIA BEARING RATIO OF FIBRE-REINFORCED CLAYEY SOIL

5.1 INTRODUCTION

California Bearing Ratio (CBR) test method is most frequently used to evaluate the potential strength of subgrade materials for their applications in road and airfield pavements design, due to its economy and simplicity (Al-Refeai and Al-Suhaibani 1998). The pavement structure constitutes nearly one-third to one-half of the total cost of the road (IRC: SP 20-2002), and subgrade strength is one of the key design parameters which affect the overall pavement thickness. In extreme environmental conditions such as during prolonged and intense periods of rainfall, embankments of roads or railways may undergo failure. Abbott (2017) has reported such a case study of a cohesive soil embankment of rail network in the United Kingdom that underwent catastrophic failure during the winter of 2013-2014. Therefore, to evaluate the effect of environmental condition variation on CBR strength, both unsaturated and saturated specimens were tested by varying moulding water content (17.4%, 19.4% and 21.4%) and soaking period (4 to 40 days), while keeping dry unit weight constant.

5.2 EXPERIMENTAL PROGRAMME

An experimental programme was carried out to investigate the CBR strength variation of the glass fibre-reinforced clayey soil**,** in accordance with ASTM D1883-16. The effects of fibre content, fibre length, moulded moisture content and soaking time on CBR and secant subgrade modulus of the fibre-reinforced specimens have been evaluated.

CBR strength was investigated under two test series, and the details are presented in Table 5.1. All specimens had dry unit weight equal to MDU (16.8 kN/m^3). In Series 1, unsoaked specimens with varying moulding moisture content (17.4 to 21.4%) were tested. In

Series 2, specimens moulded only at OMC (19.4%) were tested after different soaking periods. Glass fibres of different contents (f_c = 0, 0.25, 0.5, 0.75 and 1% by dry weight of soil) and three lengths (10, 20 and 30 mm) having corresponding aspect ratios (67, 133 and 200) were used as reinforcement. The results of the tests are presented as load-penetration plots, from which the CBR and secant subgrade modulus have been determined at five penetrations depths (2.54, 5.08, 7.62, 10.16 and 12.70 mm).

Table 5.1 Summary of CBR testing programme

Series	Dry unit weight, γ_d (kN/m^3)	Moisture content, w (%)	Fibre content, f_c (%)	Fibre length, L (mm)	Soaking days
1	16.8	17.4, 19.4, 21.4	0, 0.25, 0.5, 0.75, 1	10, 20, 30	Unsoaked
2	16.8	19.4	0, 0.25, 0.5, 0.75, 1	10, 20, 30	4, 20, 40

5.3 RESULTS AND DISCUSSION

5.3.1 Load-Penetration Response

Typical load-penetration curves of the CBR tests on unreinforced and reinforced soil specimens with varying fibre content of 20 mm length and moulded at OMC and MDU are shown in Fig. 5.1 for both unsoaked condition and soaked condition (4 days soaking). The load bearing capacity of the specimens increases with fibre content up to 0.75% for both conditions, indicating that fibres can improve the load-penetration behaviour. The load capacity of the specimens increases with penetration depth up to 12.70 mm with all fibre contents, indicating clearly that the peak strength of specimen has not been reached even at 12.70 mm penetration, and that the fibres are still in tension without complete pullout or rupture. With higher penetration, the slope of the curves reduces indicating that the rate of bearing capacity improvement is decreasing.

The interfacial interaction between fibres and soil restricts the movement of soil particles and the fibre indentations caused by the soil particles allow to develop adhesion

within soil (Falorca and Pinto 2011), resulting in improved load bearing capacity of the reinforced soil. Tang et al. (2007) reported that distributed discrete fibres act as a spatial three-dimensional network which interlocks soil grains, helps grains to form a unitary coherent matrix and restricts the movement improving the stretching resistance between soil and fibres, resulting in improved strength. Also, the tensile restraint in the fibres induces additional soil confinement (Al-Refeai and Al-Suhaibani 1998) and results in enhancement of specimen strength.

The initial stiffness of the specimen has increased with reinforcement up to 0.75% fibre content under both soaking conditions (Fig. 5.1), whereas a reduction of initial stiffness is noted at 1% fibre content. This drop in stiffness is due to the change in soil fabric produced by the higher fibre content, which creates non-uniform voids within the specimen and prevents dense packing (Chandra et al. 2008). Yetimoglu et al. (2005) reported that the initial stiffness is not significantly affected by fibre reinforcement in CBR tests, whereas Gray and Al-Refeai (1986) and Consoli et al. (1998) reported that increasing fibre content cause reduction of soil stiffness in triaxial tests.

Under unsoaked condition (Fig. 5.1a), the penetration resistance rate is noted to decrease after 5.08 mm penetration depth. However, in soaked condition (Fig. 5.1b), the load penetration response of reinforced specimen continues to increase uniformly till 12.70 mm penetration depth for all fibre contents. For the same piston penetration depth, the load bearing capacity of unsoaked specimen is much higher than that of the corresponding soaked specimen. The presence of extra water in the voids of soil-fibre specimen results in lubrication effect, resulting in easier slippage between soil particles and fibres. Thus the mobilization of tensile strength of fibres is restricted resulting in low strength enhancement.

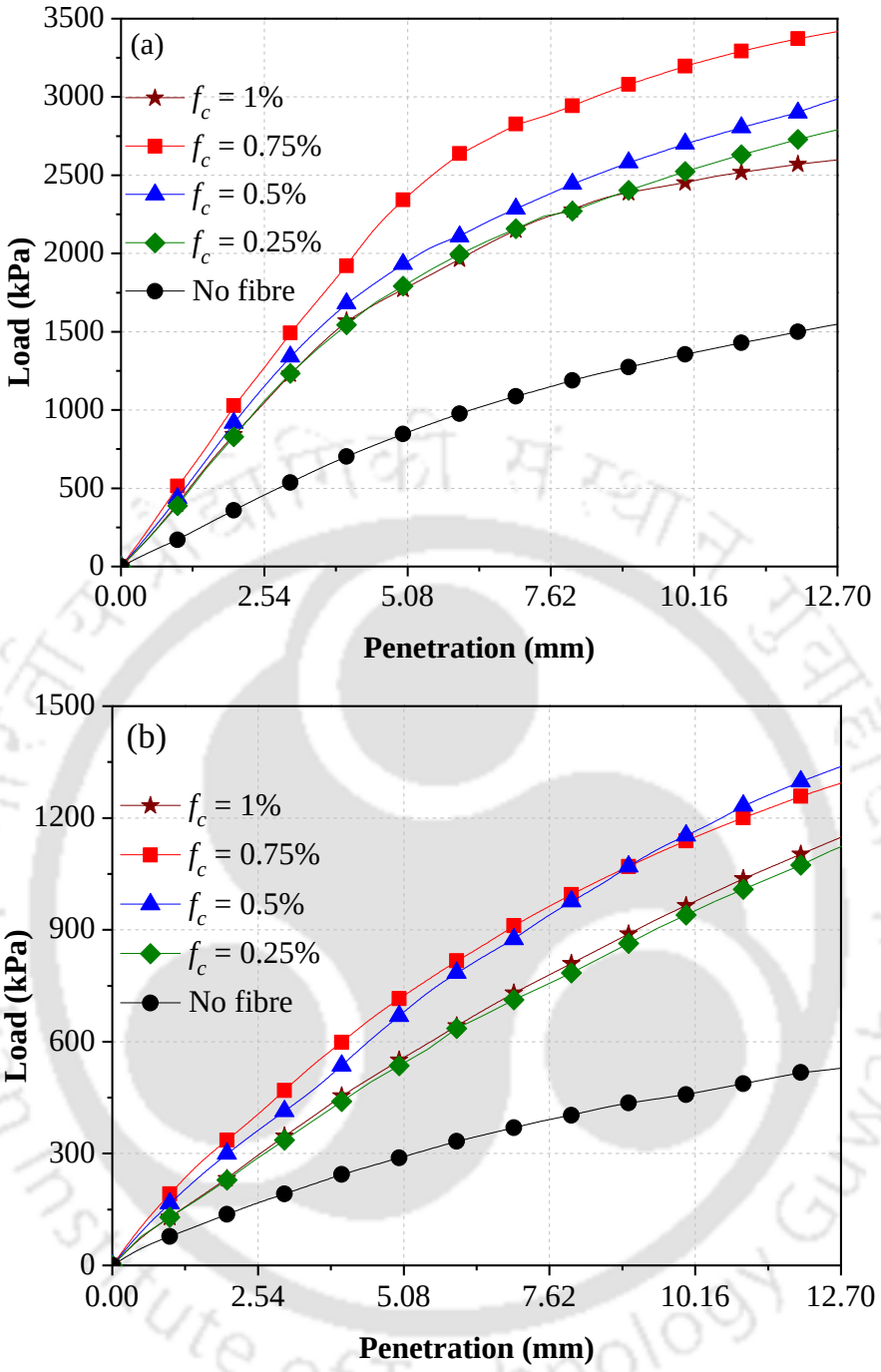

Fig. 5.1 Effect of fibre content on load-penetration response of specimens reinforced with fibres of 20 mm length and moulded at OMC and MDU: (a) unsoaked condition; (b) soaked condition (4 days)

5.3.2 California Bearing Ratio

The CBR values were calculated from the load-penetration curves of all specimens of Series 1 & 2, for different penetration values ranging from 2.54 mm to 12.70 mm. In common

practice, the higher CBR value corresponding to either 2.54 mm or 5.08 mm penetration, is considered for design purpose. However, for fibre-reinforced soils, these two penetration values may not be truly representative of full mobilization of strength under field conditions (Take et al. 1997), and higher resistance can be observed at greater depths of penetration because reinforcing fibres need some deformation to fully mobilize its tensile strength at the time of axial loading. Considering this point, the CBR value has been evaluated also at additional penetration depths up to 12.70 mm.

For checking the reproducibility and reliability of the CBR results, three specimens for every single soil-fibre mix of similar moulded state were tested. Since for all the specimens considered in the present study, CBR values at 5.08 mm penetration were observed to be higher than that of 2.54 mm penetration even on repetition, the CBR values at 5.08 mm penetration have been considered for obtaining the optimum soil-fibre mix. The average value of three tests has been reported in this study, as per IRC: 37-2001. Yoder and Witczak (1995) considered two specimens for the repeatability and reliability of test results.

5.3.2.1 Effect of Fibres on CBR of Specimens Moulded at OMC and MDU

The variations of CBR values with fibre content and fibre length are respectively presented in Fig. 5.2 and Fig. 5.3, for all soil specimens moulded at OMC and MDU (Series 1 & 2). CBR value increases gradually with fibre content under both unsoaked and soaked conditions up to 0.75% and thereafter decreases at 1% fibres. Zaimoglu and Yetimoglu (2012) reported that the soaked CBR of polypropylene fibre-reinforced highly plastic silt soil increased only up to a limiting fibre content of 0.75%.

The improvement in CBR with fibres can be attributed to the tensile strength mobilization of the randomly distributed fibres within the soil at the time of loading. With increased number of fibres, the chance of fibre-fibre interaction exceeds that of soil-fibre interaction. At 1% fibre content, the number of fibres in a fixed volume of specimen is

higher. If the soil-fibre interfacial friction is higher than that of fibre-fibre interfacial friction, this causes reduction in strength improvement.

Under unsoaked condition, the CBR value increases with penetration depth up to 5.08 mm and then decreases gradually (Fig. 5.2a). However, under soaked condition, the CBR value increases with penetration depth up to 12.70 mm penetration, although the improvement after 7.62 mm penetration is marginal (Fig. 5.2b). This can be attributed to the extra moisture present in the soil voids facilitating a gradual pullout of the indented fibres in the soaked condition. At 5.08 mm penetration, the unsoaked CBR value improves from 8.06% for the unreinforced specimen to 22.31% for the reinforced specimen with 0.75% fibres (Fig. 5.2a). After 4 days soaking, the corresponding soaked CBR values are 2.89% and 8.23% (Fig. 5.2b).

For the same fibre content of 0.75%, the CBR value of the reinforced soil improves noticeably with fibre length from 10 to 20 mm and then decreases with 30 mm fibres (Fig. 5.3), for both unsoaked and soaked conditions. Specimen reinforced with 20 mm fibres has shown the optimum improvement. In case of shorter fibres (L = 10 mm), the fibre length is probably insufficient for developing full friction at the ends and only a small tensile force can be developed prior to pullout resulting in small improvement of CBR value. Although longer fibres (L = 30 mm) can develop higher tensile force within the specimen at the time of piston loading, the number of fibres for supporting the tensile strength is small and the strength tends to decrease.

Similar to the variation with fibre contents, for all fibre lengths, the improvement in unsoaked CBR is up to 5.08 mm penetration and then decreases with penetration depth (Fig. 5.3a). In soaked condition, the CBR increases up to 7.62 mm penetration and varies marginally at higher penetration depths (Fig. 5.3b).

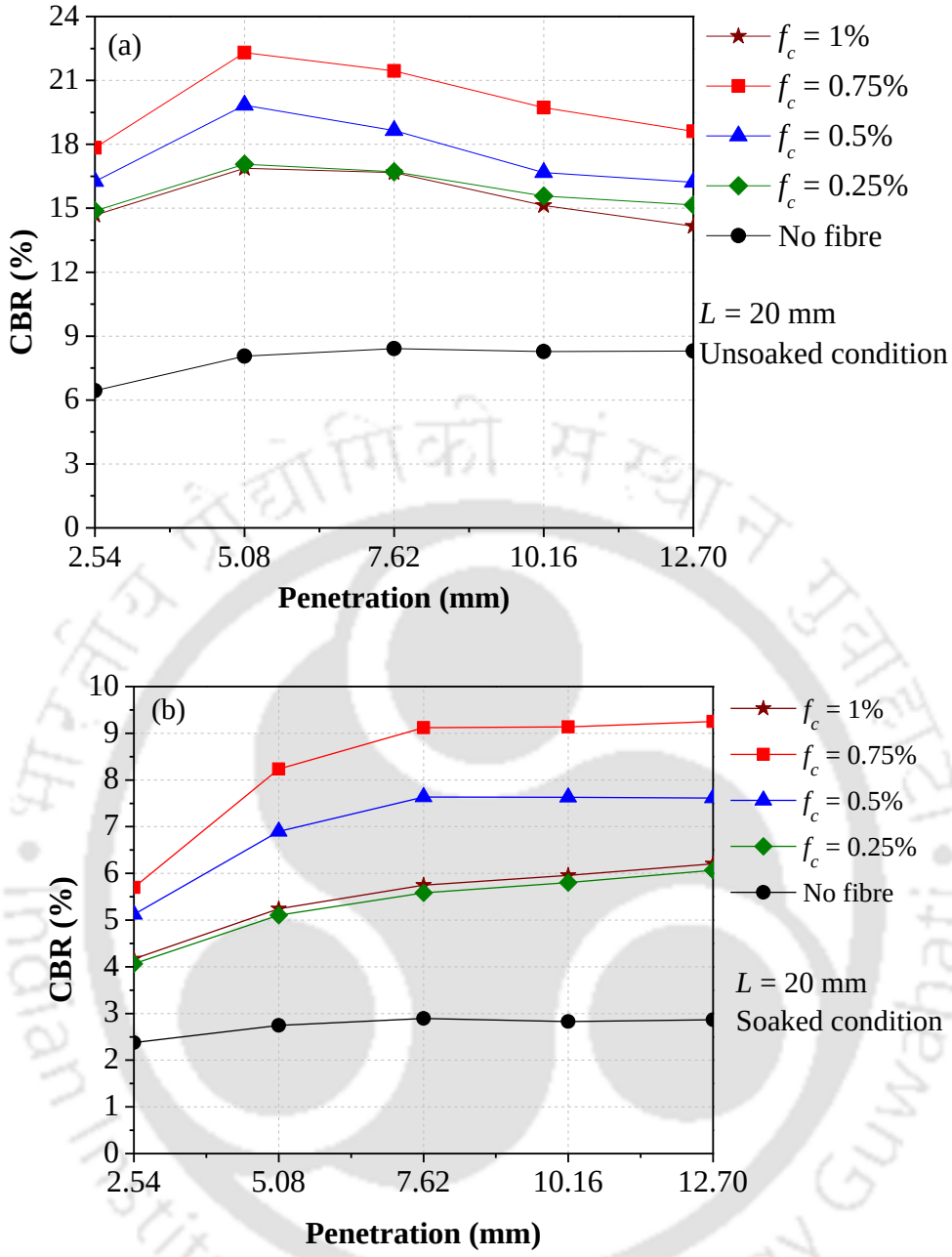

Fig. 5.2 Effect of fibre content on CBR values variation at different penetration depths for specimens reinforced with 20 mm fibres and moulded at OMC and MDU: (a) unsoaked condition; (b) soaked for 4 days

Similar trend was reported by Pradhan et al. (2012), where CBR value of polypropylene fibre-reinforced clayey soil increased with fibre length up to 20 mm and then decreased with 25 mm fibres. Ayyappan et al. (2010) observed that the soaked CBR value of

polypropylene fibre-reinforced soil-fly ash specimen improved with fibre length up to 12 mm and reduced with 24 mm.

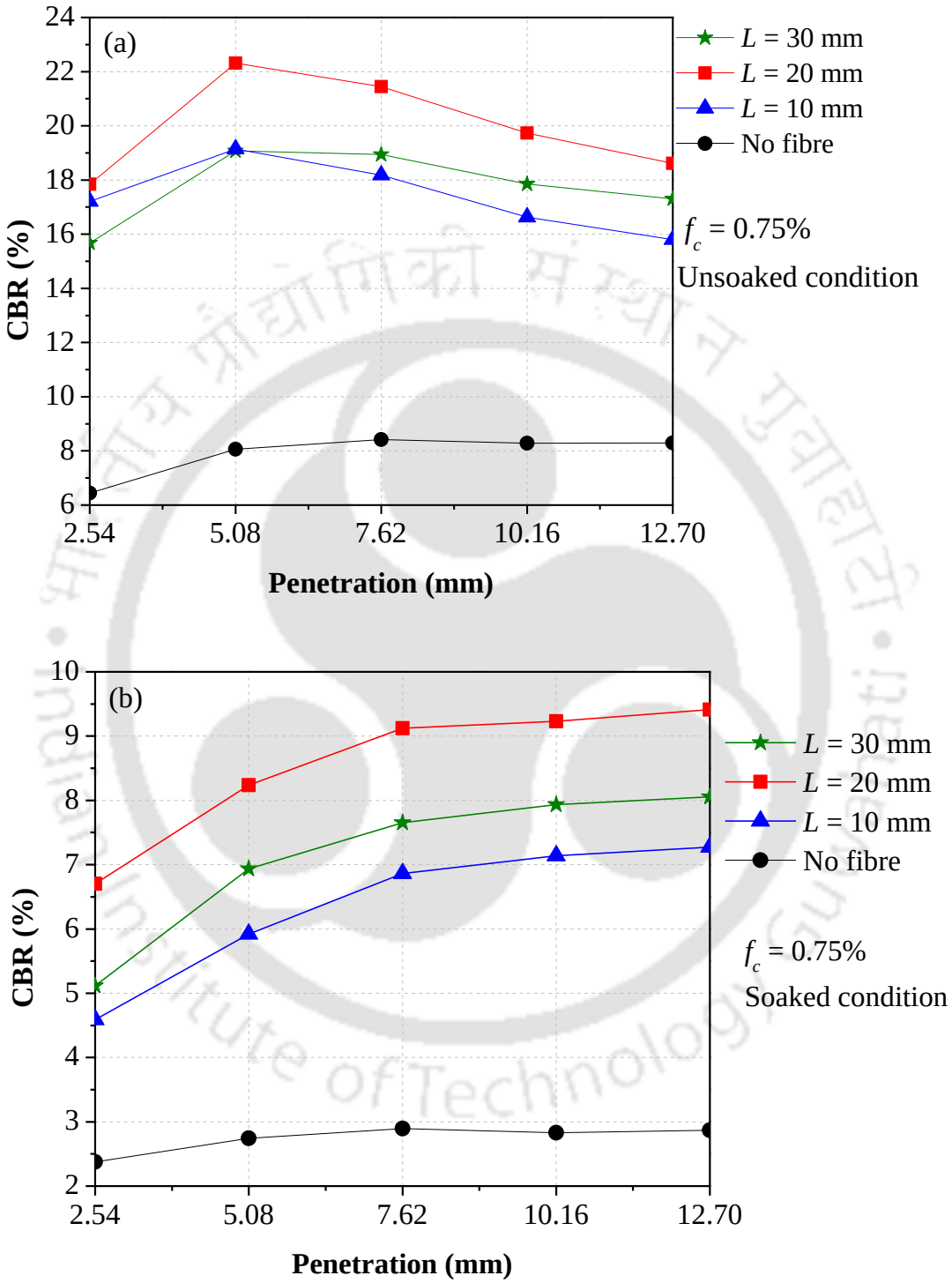

Fig. 5.3 Effect of fibre length on CBR variation at different penetration depths for specimens reinforced with 0.75% fibres and moulded at OMC and MDU: (a) unsoaked condition; (b) soaked for 4 days

The contribution of glass fibres to bearing capacity improvement of the clayey soil can be quantified in terms of CBR improvement factor (I_{CBR}) defined as:

$$I_{CBR} = \frac{CBR_r}{CBR_u} - 1 \tag{5.1}$$

where CBR_r is the CBR value of reinforced specimen and CBR_u is the CBR value of unreinforced specimen.

The CBR values, fibre contribution values and improvement factors for all specimens, calculated for 5.08 mm penetration depth, are summarised in Tables 5.2 and 5.3, respectively for unsoaked and soaked conditions.

Maximum enhancement in CBR for any fibre length is with 0.75% fibre content (Tables 5.2 & 5.3). The maximum improvement of bearing capacity with 10, 20 and 30 mm fibres are 1.37, 1.77 and 1.36 times for the unsoaked condition at OMC, and 1.05, 1.85 and 1.40 times for 4 days soaking condition.

For field applications, the determination of optimum soil-fibre combination is essential. Under 4 days soaked condition, the CBR value of the unreinforced specimen is 2.89%, and the maximum CBR value of 8.23% is obtained with 0.75% fibres of 20 mm length (Table 5.3). Thus, as per IRC:SP:72-2007, the unreinforced soil is classified as very poor quality subgrade material (soaked CBR less than 3%), which can be modified to that of good quality (soaked CBR between 7% and 9%). However, as per IRC: 37-2001, a minimum soaked CBR value of 6% is necessary for use in the subgrade layer of low-volume flexible pavements. The soil mix with 0.5, 0.75% and 1% glass fibres of 20 mm length (having corresponding CBR values of 6.89%, 8.23% and 7.62%), and with 0.75% and 1% fibres of 30 mm length (having corresponding CBR of 6.93% and 6.36%) can be used in practice (See Table 5.3).

Table 5.2 Summary of unsoaked CBR value at 5.08 mm penetration depth, fibre contribution and improvement factor for all specimens moulded at MDU and varying moisture content (Series 1)

L (mm)	f_c (%)	w = 17.4%			w = 19.4% (OMC)			w = 21.4%		
		Unsoaked CBR (%)	Fibre contribution to CBR (%)	I_{CBR}	CBR (%)	Fibre contribution to CBR (%)	I_{CBR}	CBR (%)	Fibre contribution to CBR (%)	I_{CBR}
0	0	6.45	--	--	8.06	--	--	4.67	--	--
10	0.25	12.26	5.81	0.90	12.95	4.89	0.61	9.76	5.09	1.09
	0.5	15.56	9.11	1.41	16.80	8.74	1.08	11.71	7.04	1.51
	0.75	17.90	11.45	1.77	19.14	11.08	1.37	14.81	10.14	2.17
	1	14.46	8.01	1.24	15.15	7.09	0.88	13.43	8.76	1.87
20	0.25	15.98	9.53	1.48	17.06	9.00	1.11	12.58	7.91	2.12
	0.5	16.67	10.22	1.58	18.40	10.34	1.29	14.94	10.27	2.20
	0.75	18.94	12.49	1.94	22.31	14.25	1.77	16.67	12.00	2.57
	1	16.04	9.59	1.49	16.87	8.81	1.09	13.84	9.17	1.96
30	0.25	10.91	4.46	0.69	11.57	3.51	0.43	9.67	5.00	1.07
	0.5	14.84	8.39	1.30	16.39	8.33	1.03	12.39	7.72	1.65
	0.75	15.53	9.08	1.41	19.07	11.01	1.36	13.77	9.10	1.95
	1	11.64	5.19	0.80	12.46	4.40	0.54	10.53	5.86	1.25

Table 5.3 Summary of soaked CBR value at 5.08 mm penetration depth, fibre contribution and improvement factor for all specimens moulded at OMC and MDU, and soaked for different periods (Series 2)

L (mm)	f_c (%)	4 days soaking			20 days soaking			40 days soaking		
		Soaked CBR (%)	Fibre contribution to CBR (%)	I_{CBR}	CBR (%)	Fibre contribution to CBR (%)	I_{CBR}	CBR (%)	Fibre contribution to CBR (%)	I_{CBR}
0	0	2.89	--	--	2.54	--	--	2.33	--	--
10	0.25	3.75	0.86	0.29	3.38	0.84	0.33	3.28	0.95	0.40
	0.5	4.61	1.72	0.59	3.86	1.30	0.52	3.49	1.16	0.50
	0.75	5.92	3.03	1.05	4.53	1.99	0.78	4.24	1.91	0.82
	1	5.36	2.47	0.85	4.21	1.67	0.66	4.20	1.87	0.80
20	0.25	4.98	2.09	0.72	3.97	1.43	0.56	4.03	1.70	0.73
	0.5	6.89	4.00	1.38	5.81	3.27	1.29	4.34	2.01	0.86
	0.75	8.23	5.34	1.85	6.24	3.70	1.45	4.62	2.29	0.98
	1	7.62	4.73	1.63	5.58	3.04	1.19	4.17	1.84	0.79
30	0.25	5.06	2.17	0.75	4.51	1.97	0.77	4.21	1.88	0.80
	0.5	5.97	3.08	1.06	5.23	2.69	1.06	4.54	2.21	0.95
	0.75	6.93	4.04	1.40	5.72	3.18	1.25	5.03	2.70	1.16
	1	6.36	3.47	1.20	5.60	3.06	1.20	4.53	2.20	0.94

5.3.2.2 Effect of Moulding Moisture Content on Unsoaked CBR of Specimens at MDU (Series 1)

Figure 5.4 presents the effect of moulding moisture content variation on CBR values of unsoaked specimens reinforced with varying lengths of 0.75% fibres. For all fibre lengths, the CBR value is the highest for the specimen moulded at 19.4% moisture content (OMC), followed by the CBR values at dry side (w = 17.4%) of OMC and at the wet side (w = 21.4%) of OMC. Similar behaviour of moulded moisture content variation on unconfined compressive strength was noted, where the compressive strength of glass fibre-reinforced clayey soil specimen was found to be greater at OMC and then decreased on either side of OMC (Section 3.2.1.3).

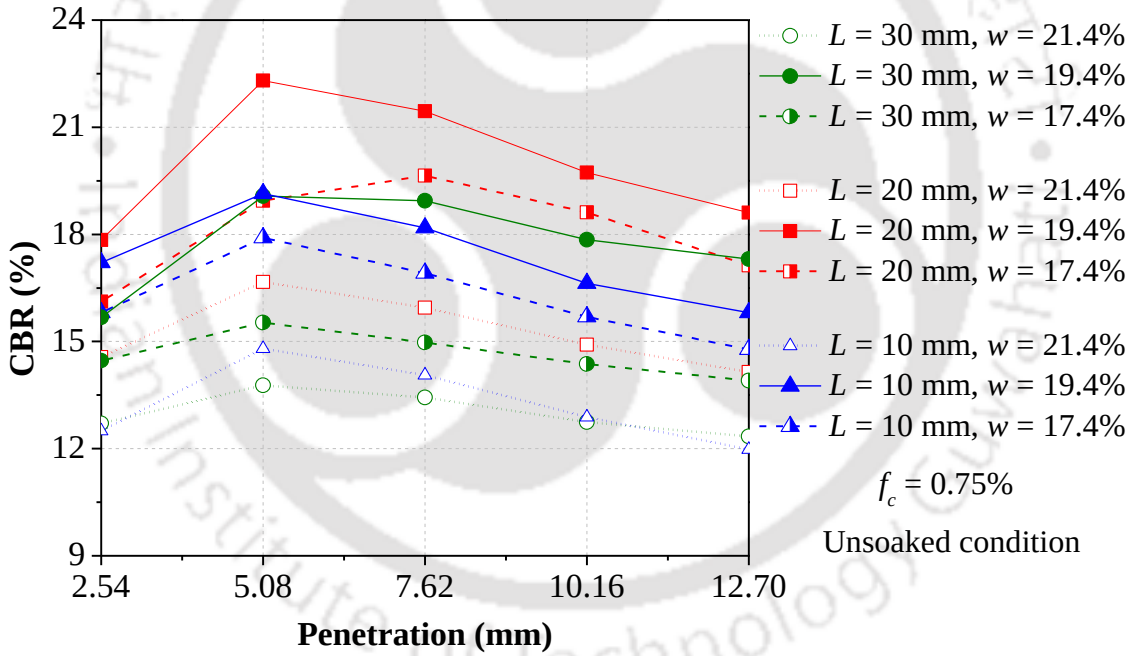

Fig. 5.4 Effect of moulding moisture content on unsoaked CBR variation at different penetration depths for specimens reinforced with 0.75% fibres and at MDU (Series 1)

For any moulded moisture content, the contribution to CBR is the maximum with 20 mm long fibres at any fibre content, and also with 0.75% fibres of any fibre length. The maximum fibre contributions to unsoaked CBR values (6.45, 8.06 and 4.67% of the unreinforced clayey soil) are 12.49, 14.25 and 12.00% (with corresponding improvement

factors of 1.94, 1.77 and 2.57 times) at OMC, dry of OMC and wet of OMC, respectively (Table 5.2).

5.3.2.3 Effect of Soaking Period on Soaked CBR of Specimens Moulded at OMC and MDU (Series 2)

Figure 5.5 shows the effect of soaking period variation on the CBR values of soil specimens reinforced with different lengths of 0.75% fibre content. The soaking period of the specimens was increased up to 40 days, as in the rainy season there may be prolonged rainfall and the soil may be submerged in the field for more than 4 days due to flooding. For specimens under 4 and 20 days soaking, the CBR is the maximum with 20 mm fibre length, at all penetration depths (Fig. 5.5). For 40 days soaking, the CBR of the specimens is the maximum with 30 mm fibre length. The CBR values under 20 and 40 days soaking with 10 mm long fibres are almost similar. Although the fibre contribution to CBR decreases with increasing soaking period, longer fibres are more effective in retaining the reinforcement effect even at higher penetration depth.

The CBR value tends to decrease with increase of soaking days. With increased soaking period, specimens tend to absorb more moisture within itself which causes more lubrication effect and this may result in easier slippage between soil-fibre interfacial surfaces. However, under the action of piston load, the longer fibres can sustain greater pullout prior to failure even under increasing soaking period. The maximum fibre contributions to soaked CBR values (2.89, 2.54 and 2.33% of the unreinforced clayey soil) are 5.34, 3.70 and 2.29% (with corresponding improvement factors of 1.85, 1.45 and 1.16 times) after 4, 20 and 40 days soaking, respectively (Table 5.3).

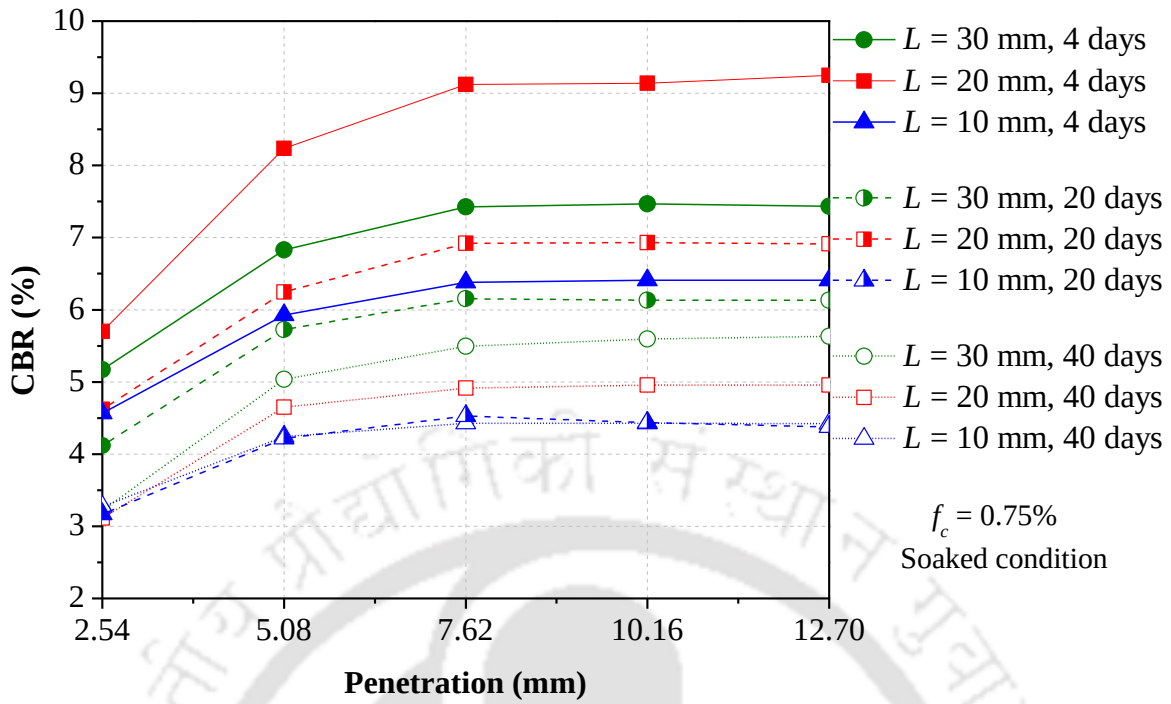

Fig. 5.5 Effect of soaking period on soaked CBR variation at different penetration depths for specimens reinforced with 0.75% fibres and moulded at OMC and MDU (Series 2)

5.3.3 Bearing Pressure Ratio

Increase in bearing pressure of soil due to fibre reinforcement at the maximum penetration depth of 12.70 mm has been evaluated in terms of bearing pressure ratio (*BPR*), defined as:

$$BPR = \frac{P_r}{P_u} \tag{5.2}$$

where P_r is the piston load for fibre-reinforced specimen at 12.70 mm penetration and P_u is the corresponding piston load for the unreinforced specimen.

The bearing pressure ratios of all specimens for unsoaked and soaked conditions are presented in Tables 5.4 and 5.5, respectively. Under unsoaked condition with any moulding moisture content, the *BPR* of reinforced specimen is the maximum with 0.75% fibre content for any fibre length and with 20 mm fibres for any fibre content (Table 5.4). The maximum

BPR values are 2.68, 2.21 and 2.62 for unsoaked reinforced specimens moulded with 17.4%, 19.4% and 21.4% moisture content, respectively.

In case of soaked reinforced specimens, the *BPR* decreases with increasing soaking period. Similar to that of unsoaked condition, the *BPR* is the maximum with 0.75% fibre content. However, the *BPR* value is noted to be the maximum with 20 mm fibres for specimens soaked for 4 days, and with 30 mm fibres for specimens soaked for 20 and 40 days. The maximum *BPR* values are 2.83, 2.36 and 2.11 for specimens soaked for 4, 20 and 40 days, respectively (Table 5.5).

5.3.4 Secant Modulus and Subgrade Modulus

The deformability of the reinforced soil when used as pavement subgrade material can be evaluated from the variation of secant modulus with penetration depth, as it reflects the deformation response under wheel loads and other concentrated loads. The secant modulus (k) is expressed as the ratio of the bearing pressure (σ_δ) to the corresponding penetration depth (δ):

$$k = \frac{\sigma_\delta}{\delta} \tag{5.3}$$

The secant modulus for all specimens has been calculated at penetration depths ranging from 2.54 mm to 12.70 mm, and the subgrade modulus (k_s) is being defined as the secant modulus value corresponding to penetration depth of 5.08 mm, at which design CBR value has been considered. For obtaining optimum soil-fibre combination, the subgrade modulus values are presented in Tables 5.6 and 5.7, respectively for unsoaked and soaked conditions.

Table 5.4 Summary of piston load, increase in bearing pressure and bearing pressure ratio at 12.70 mm penetration depth for all unsoaked specimens moulded with varying moisture content and at MDU (Series 1)

***L* (mm)**	***f_c* (%)**	***w* = 17.4%**			***w* = 19.4% (OMC)**			***w* = 21.4%**		
		Piston Load (kPa)	**Increase in Bearing Pressure (kPa)**	***BPR***	**Piston Load (kPa)**	**Increase in bearing Pressure (kPa)**	***BPR***	**Piston Load (kPa)**	**Increase in bearing Pressure (kPa)**	***BPR***
0	0	1170	--	1	1537	--	1	754	--	1
10	0.25	1861	691	1.59	2122	585	1.38	965	211	1.28
	0.5	2247	1077	1.92	2755	1218	1.79	1360	606	1.80
	0.75	2675	1505	2.29	2892	1355	1.88	1696	942	2.25
	1	2187	1017	1.87	2434	897	1.58	1571	817	2.08
20	0.25	2321	1151	1.98	2773	1236	1.80	1465	711	1.94
	0.5	2688	1518	2.30	2967	1430	1.93	1714	960	2.27
	0.75	3134	1964	2.68	3405	1868	2.21	1973	1219	2.62
	1	2548	1378	2.18	3091	1554	2.01	1611	857	2.14
30	0.25	1995	825	1.70	2241	704	1.46	1005	251	1.33
	0.5	2462	1292	2.10	2923	1386	1.90	1578	824	2.09
	0.75	2854	1684	2.44	3187	1650	2.07	1794	1040	2.38
	1	2334	1164	2.00	2575	1038	1.67	1571	817	2.08

Table 5.5 Summary of piston load, increase in bearing pressure and bearing pressure ratio at 12.70 mm penetration depth for all specimens moulded at OMC and MDU and soaked for different periods (Series 2)

***L* (mm)**	***f_c* (%)**	**4 days soaking**			**20 days soaking**			**40 days soaking**		
		Piston Load (kPa)	**Increase in Bearing Pressure (kPa)**	***BPR***	**Piston Load (kPa)**	**Increase in Bearing Pressure (kPa)**	***BPR***	**Piston Load (kPa)**	**Increase in Bearing Pressure (kPa)**	***BPR***
0	0	524	--	1	397	--	1	341	--	1
10	0.25	616	92	1.17	448	51	1.13	385	44	1.13
	0.5	684	160	1.30	564	167	1.42	496	155	1.45
	0.75	772	248	1.47	617	220	1.55	592	251	1.74
	1	697	173	1.33	602	205	1.52	541	200	1.59
20	0.25	1109	585	2.12	538	141	1.35	457	116	1.34
	0.5	1326	802	2.53	719	322	1.81	576	235	1.69
	0.75	1483	959	2.83	844	447	2.12	650	309	1.91
	1	1135	611	2.17	806	409	2.03	618	277	1.81
30	0.25	779	255	1.49	581	184	1.46	479	138	1.40
	0.5	948	424	1.81	712	315	1.79	598	257	1.75
	0.75	1043	519	1.99	939	542	2.36	719	378	2.11
	1	974	450	1.86	884	487	2.23	661	320	1.94

Table 5.6 Summary of subgrade modulus values for all unsoaked specimens moulded at MDU and varying moisture content (Series 1)

L (mm)	f_c (%)	k_s (MN/m^3) at w = 17.4%	k_s (MN/m^3) at w = 19.4% (OMC)	k_s (MN/m^3) at w = 21.4%
0	0	13.28	19.63	9.46
10	0.25	29.86	31.54	25.52
	0.5	37.91	40.93	32.06
	0.75	43.61	46.63	36.08
	1	35.23	36.90	32.71
20	0.25	38.58	41.01	31.89
	0.5	40.59	44.20	36.40
	0.75	46.13	53.51	40.59
	1	39.08	41.09	33.71
30	0.25	26.59	28.18	23.57
	0.5	36.15	39.92	30.19
	0.75	37.83	46.47	33.55
	1	28.35	30.36	25.66

Table 5.7 Summary of subgrade modulus for all specimens moulded at OMC and MDU and soaked for different periods (Series 2)

L (mm)	f_c (%)	k_s (MN/m^3) at 4 days soaking	k_s (MN/m^3) at 20 days soaking	k_s (MN/m^3) at 40 days soaking
0	0	6.68	6.08	5.29
10	0.25	7.62	6.98	6.23
	0.5	8.00	7.58	7.04
	0.75	9.42	8.40	8.11
	1	8.91	7.51	7.29
20	0.25	12.43	8.35	7.67
	0.5	15.51	10.54	8.04
	0.75	16.61	12.20	8.64
	1	12.77	10.87	8.31
30	0.25	8.48	7.43	7.84
	0.5	10.11	9.36	8.59
	0.75	11.83	11.83	9.23
	1	11.14	11.08	8.81

5.3.4.1 Variation with Fibre Content and Fibre Length

The effect of fibre content on secant modulus variation of reinforced specimens moulded at OMC and MDU with 20 mm fibres is presented in Fig 5.6 for both unsoaked and 4 days soaked conditions. At any penetration depth, the secant modulus gradually increases

with fibre content up to 0.75% fibres and then decreases with addition of 1% fibres. For any fibre content, the secant modulus tends to decrease with penetration depth. The reduction of secant modulus with penetration depth for unsoaked specimens (Fig. 5.6a) is greater than that of soaked specimens (Fig. 5.6b).

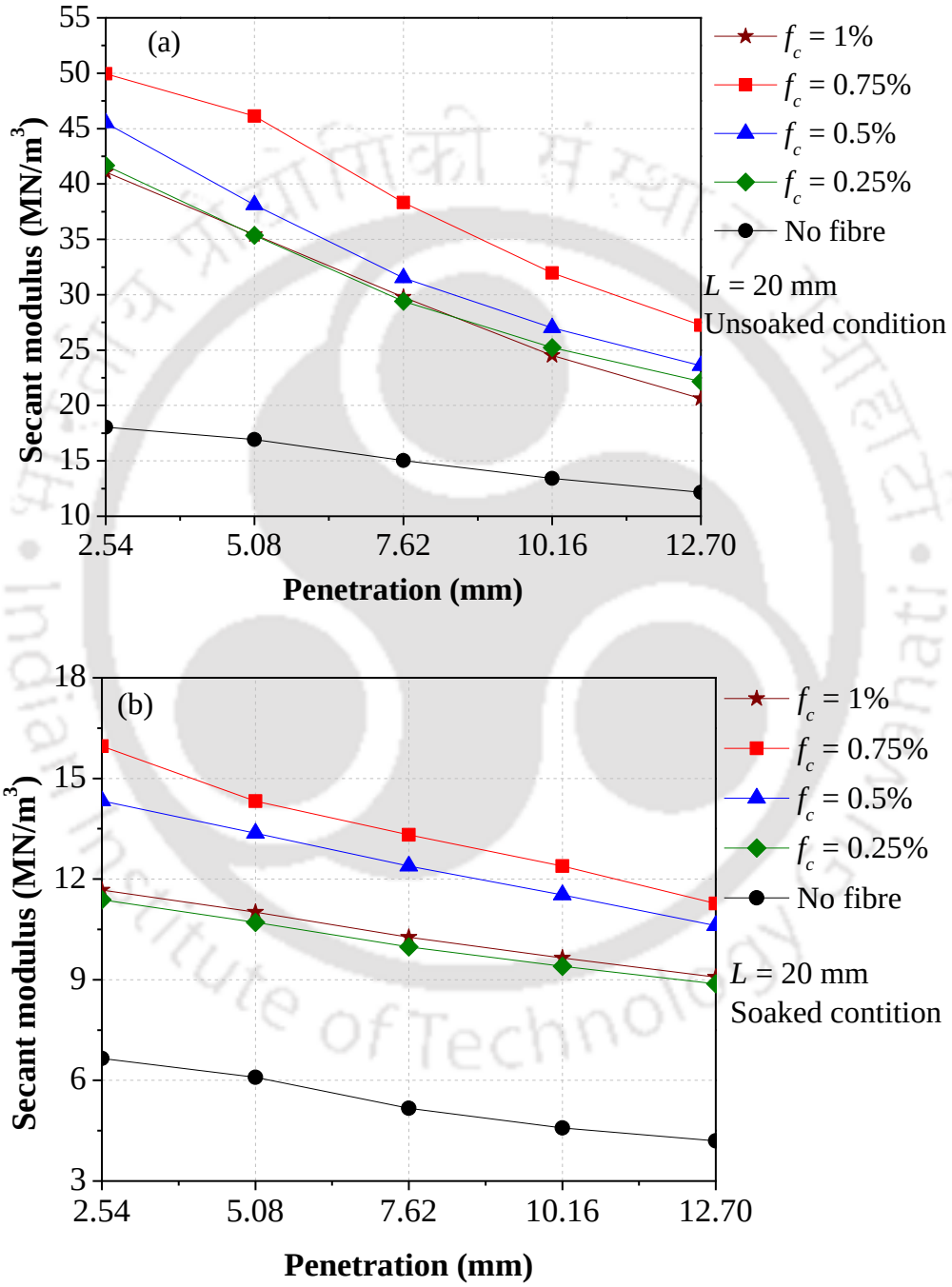

Fig. 5.6 Effect of fibre content on secant modulus variation with penetration depth for specimens reinforced with 20 mm fibres and moulded at OMC and MDU: (a) unsoaked condition; (b) soaked for 4 days

The effect of fibre length on secant modulus variation of specimens reinforced with 0.75%fibres is shown in Fig 5.7 for both unsoaked and 4 days soaked conditions. Under both conditions, at all penetration depths, the secant modulus is found to increase with fibre length up to 20 mm and then decreases with 30 mm fibres (Figs. 5.7a and 5.7b). Further, under both conditions, for any fibre length, the secant modulus decreases with increasing penetration depth.

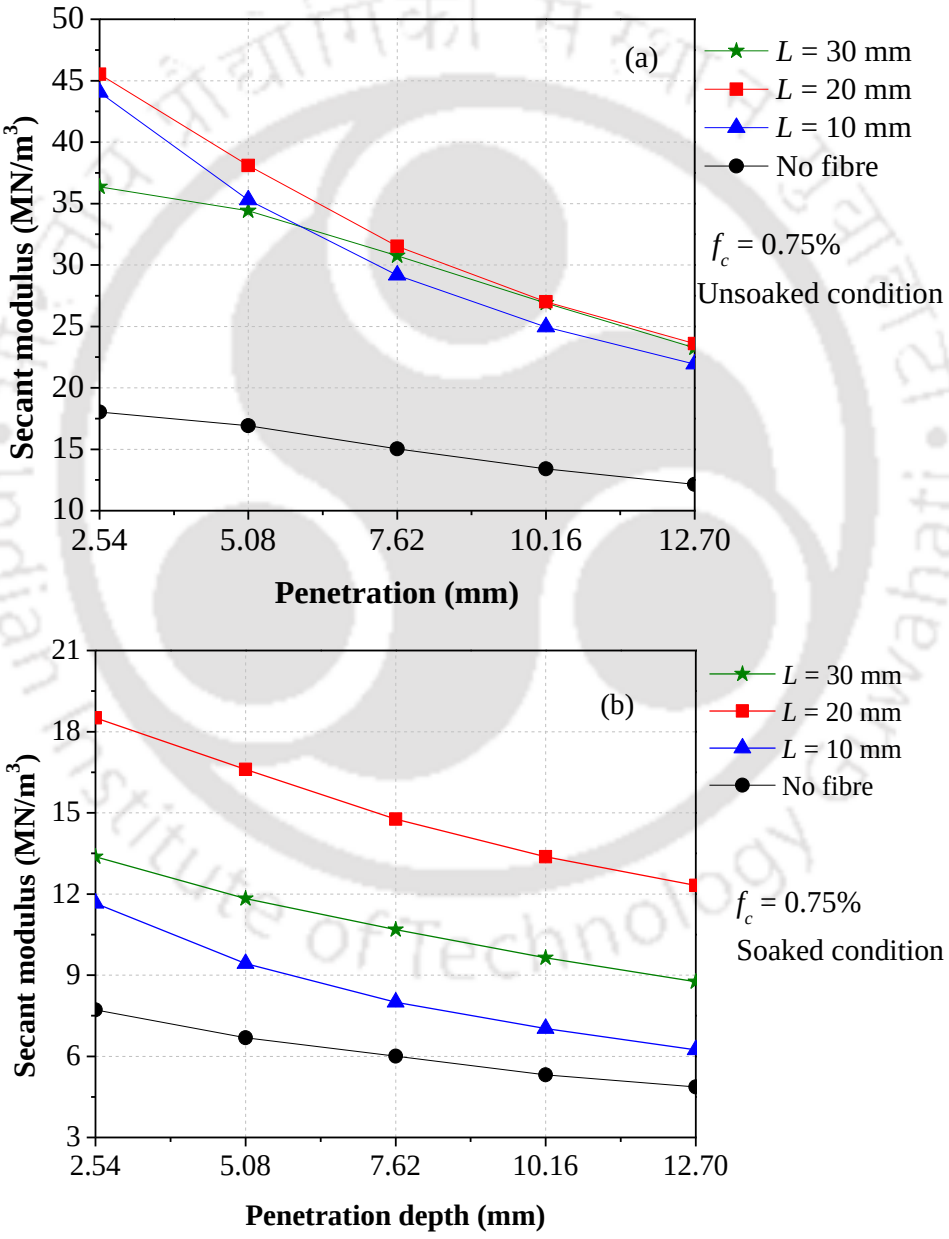

Fig. 5.7 Effect of fibre length on secant modulus variation with penetration depth for specimens reinforced with 0.75% fibres and moulded at OMC and MDU: (a) unsoaked condition; (b) soaked for 4 days

5.3.4.2 Variation with Moulded Moisture Content

The typical effect of moulded moisture content on the secant modulus is shown in Fig. 5.8 for unsoaked specimens with 0.75% fibres. At any penetration depth, the secant modulus with 20 mm fibres is greater irrespective of moulded moisture content. For any fibre length, the secant modulus is the highest for the specimen at OMC, and the value decreases on either drier or wetter moulded state. The maximum values of subgrade modulus are 46.13, 53.51 and 40.59 MN/m^3 at moulded moisture contents of 17.4%, 19.4% and 21.4%, respectively (Table 5.6).

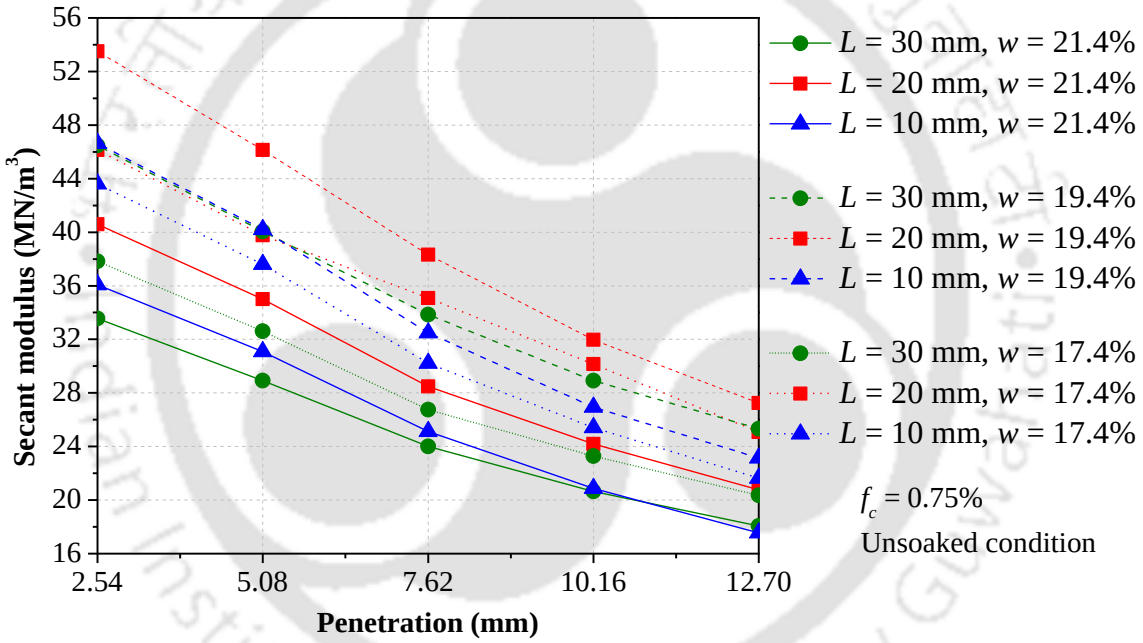

Fig. 5.8 Variation of secant modulus with moisture content for unsoaked specimens reinforced with 0.75% fibres and moulded at MDU (Series 1)

5.3.4.3 Variation with Soaking Period

Figure 5.9 presents the typical effect of soaking period on the secant modulus of fibre-reinforced soil with 0.75% fibres. Secant modulus decreases with increasing soaking period for any soil-fibre mix. The secant modulus variation is similar to that of CBR under different soaking conditions. As the soaking period increases to 20 and 40 days, the specimen reinforced with longer fibres (L = 30 mm) shows higher secant modulus value. For specimens

soaked for 40 days, the difference in secant modulus variation with fibre length is minimal, and the values with 10 and 20 mm fibres are close.

The subgrade modulus for varying soaking periods have been presented in Table 5.7. With increasing soaking period, the subgrade modulus value decreases for any combination of fibre length and fibre content. At any soaking period, subgrade modulus increases up to 0.75% fibres content. Under 4 and 20 days soaking, 20 mm fibre-reinforced specimen shows maximum subgrade modulus values of 16.61 and 12.20 MN/m^3, whereas for 40 days soaking, 30 mm fibre-reinforced specimens have highest subgrade modulus (9.23 MN/m^3).

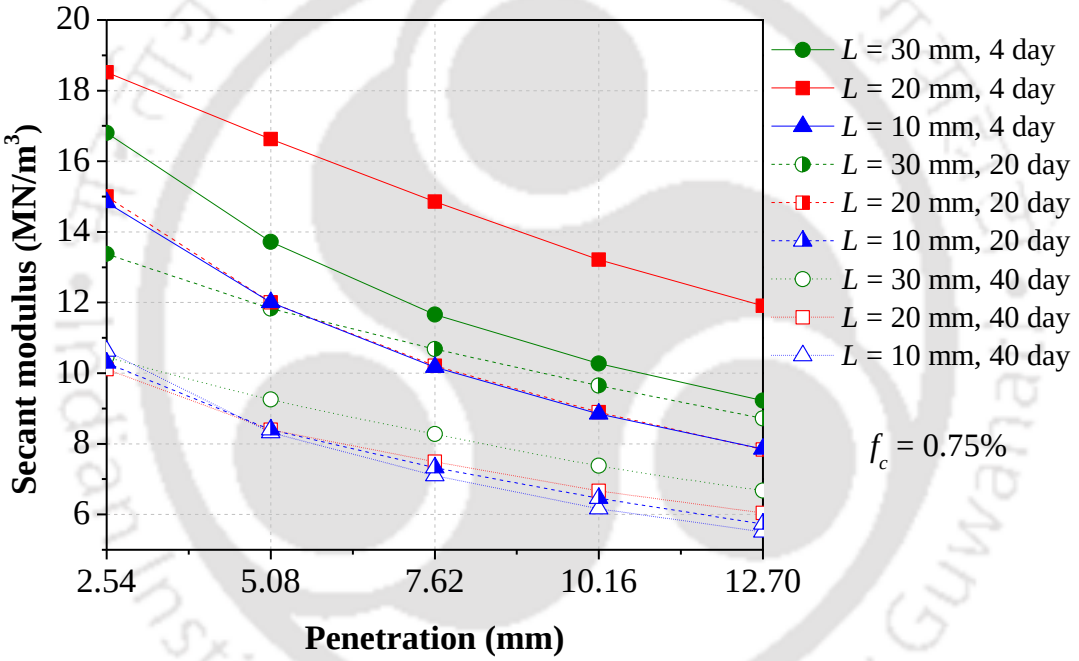

Fig. 5.9 Variation of secant modulus with soaking period for specimens reinforced with 0.75% fibres and moulded at OMC and MDU (Series 2)

Using the values of CBR and subgrade modulus (k_s) of all specimens, a correlation has been developed between k_s and CBR (Fig 5.10), expressed as:

$$k_s = 1.536 CBR^{1.162} \qquad (R^2 = 0.98) \qquad (5.5)$$

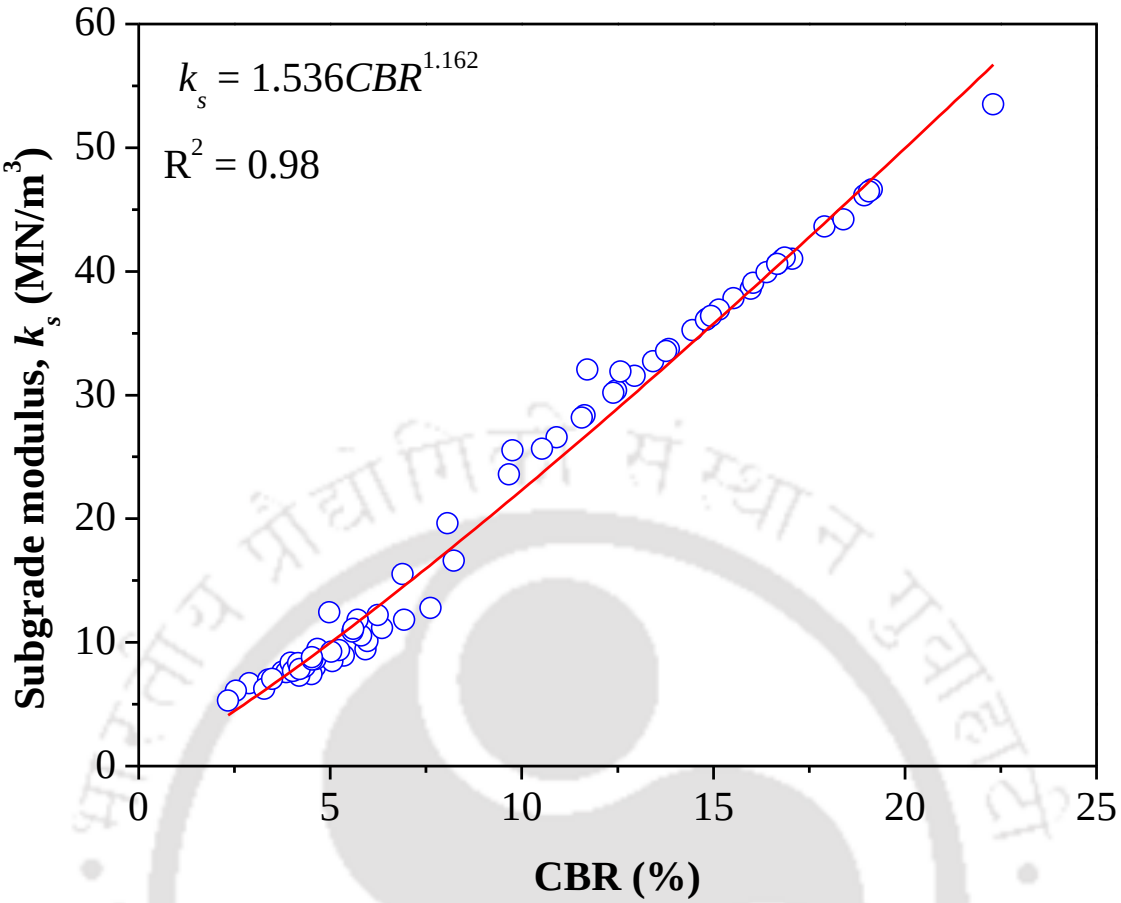

Fig. 5.10 Correlation between subgrade modulus and design CBR values

5.3.5 Effect of Fibre Reinforcement in Reduction of Pavement Thickness

The benefit of reinforcing subgrade soil with glass fibres for field application has been analysed by evaluating the reduction of required pavement thickness due to fibre reinforcement. The pavement thickness was calculated as per IRC:37-2001 for traffic values of 10, 30 and 150 million standard axles (msa) and for CBR values at 4 days soaking. The calculated pavement thicknesses are summarized in Table 5.8 with percentage reduction of pavement thickness for different soil-fibre mixes.

The required minimum pavement thicknesses above the unreinforced soil subgrade are 760, 820 and 900 mm for traffic values of 10, 30 and 150 msa, respectively. This required thickness decreases with increasing fibre content for any fibre length, and it decreases the maximum to 540, 585 and 660 mm with 0.75% fibres of 20 mm length for traffic values of

10, 30 and 150 msa, respectively. The corresponding reductions in thickness are 29, 28.6 and 26.6%, respectively which are greater than one quarter of the required pavement thickness over the unreinforced soil.

Table 5.8 Minimum pavement thickness for different traffic values as per IRC:37-2001 based on CBR of specimens moulded at OMC and MDU and soaked for 4 days (Series 2)

L (mm)	f_c (%)	CBR (%)	10 msa traffic		30 msa traffic		150 msa traffic	
			Thickness (mm)	Reduction (%)	Thickness (mm)	Reduction (%)	Thickness (mm)	Reduction (%)
-	0	2.89	760	-	820	-	900	-
10	0.25	3.75	720	5.3	760	7.3	835	7.2
	0.5	4.61	670	11.8	730	11.0	790	12.2
	0.75	5.92	625	17.8	660	19.5	725	19.4
	1	5.36	640	15.8	680	17.1	750	16.6
20	0.25	4.98	650	14.5	700	14.6	760	15.5
	0.5	6.89	585	23.0	625	23.8	690	23.3
	0.75	8.23	540	29.0	585	28.6	660	26.6
	1	7.62	560	26.3	605	26.2	670	25.5
30	0.25	5.06	650	14.5	700	14.6	760	15.5
	0.5	5.97	615	19.1	660	19.5	715	20.5
	0.75	6.93	585	23.0	625	23.8	690	23.3
	1	6.36	600	21.0	645	21.3	710	21.1

5.4 SUMMARY

The effect of glass fibre content, glass fibre length, compacted moisture content and soaking time variation on CBR and secant modulus of the clayey soil was investigated. The effect of pistion penetration depth on the CBR and secant modulus values was studied and the benefit of glass fibre on reduction of pavement thickness was evaluated. The following conclusions have been drawn from the test results:

1. At any moulded state, the unsoaked CBR of both unreinforced and reinforced soil specimens increases with penetration depth to reach peak value at 5.08 mm and then decreases at higher depths. However, the soaked CBR increases up to a greater penetration depth of 7.67 mm and then remains nearly constant up to 12.7 mm.

2. With increasing soaking period, the soaked CBR value reduces for both unreinforced and reinforced soil specimens. After 4, 20 and 40 soaking days, the maximum soaked CBR values (at 5.08 mm penetration depth) of the unreinforced specimens are respectively 2.89%, 2.54% and 2.33%, and the corresponding maximum soaked CBR values of the fibre-reinforced soil are 8.23%, 6.24% and 5.03%.
3. For any moulding moisture content, the optimum glass fibre content contributing to CBR is 0.75%. Under unsoaked condition, the optimum fibre length is 20 mm. However, for soaked condition, 20 mm long fibres give maximum contribution after 4 and 20 soaking days, whereas 30 mm long fibres provide greater improvement after 40 soaking days.
4. The subgrade modulus of the reinforced specimen at 5.08 mm penetration depth is the maximum when moulded at OMC, and the value is lower on either side of OMC with more reduction on the wet side. The subgrade modulus value decreases gradually with increasing soaking period.
5. The inclusion of 0.75% fibres of 20 mm length effectively improves the quality of the unreinforced soil as subgrade material from very poor (soaked CBR value of 2.89%) to good (soaked CBR value of 8.23%). When this particular soil-fibre mix is compacted at OMC as subgrade layer in the field, the overlying pavement thickness for low-volume flexible pavements can be reduced up to 25% even under a traffic value of 150 msa. As the minimum required soaked CBR value is 6% for use in the subgrade layer of such pavements, the soil mix with 0.75% fibres and longer length of 30 mm (soaked CBR value of 6.93%) is also practical.

CHAPTER 6

SHEAR STRENGTH BEHAVIOUR OF FIBRE-REINFORCED CLAYEY SOIL

6.1 INTRODUCTION

The load-deformation, stiffness and shear strength behaviour of the randomly distributed glass fibre-reinforced clayey soil have been investigated by conducting consolidated undrained (CU) triaxial compression tests. The effects of fibre content, fibre length, confining pressure and moulding states have been evaluated.

6.2 EXPERIMENTAL PROGRAMME

Two series of consolidated undrained (CU) triaxial tests were conducted as per ASTM D4767-11. The details of test specimens (38 mm diameter and 76 mm height) are presented in Table 6.1. For the first test series (Series 1), the clayey soil specimens were moulded at OMC (19.4%) and MDU (16.8 kN/m^3) with all combinations of fibre contents and fibre lengths as used in unconfined compression and CBR tests. For the second test series (Series 2), the specimens were prepared only at OMC but with varying dry unit weight (14.3, 15.1 and 16.0 kN/m^3) corresponding to 85, 90 and 95% of MDU, and reinforced with only 20 mm fibres. Thus, all specimens had the same initial moisture content of 19.4% before saturation in the triaxial cell.

Table 6.1 Summary of CU test specimens of clayey soil

Series	Moisture content, w (%)	Dry unit weight, γ_d (kN/m^3)	Fibre content, f_c (%)	Fibre length, L (mm)
1	19.4	16.8	0, 0.25, 0.5, 0.75, 1	10, 20, 30
2	19.4	14.3, 15.1, 16.0	-do-	20

6.3 RESULTS AND DISCUSSION

6.3.1 Stress-Strain Response

6.3.1.1 Effect of Fibre Content on Specimens Moulded at OMC and MDU

Typical effect of fibre content on deviator stress-strain and pore water pressure-strain response of reinforced specimens from Series 1, with 20 mm fibres and sheared under 100 kPa confining pressure, are shown in Fig. 6.1a and Fig. 6.1b, respectively. The deviator stress is found to increase significantly with fibre content up to 0.75%. With 1% fibre content, deviator stress remains close to that of with 0.75% fibre content. No peak has been noticed till 20% axial strain for the reinforced specimens as they continue to show some strain-hardening behaviour. Similar deviator stress response was observed by Andersland and Khattak (1979), Ranjan et al. (1996) and Estabragh et al. (2011 & 2013) on fibre-reinforced soils, where no clear peak was observed even at an axial strain of about 20%. With increasing fibre content, the number of fibres within the specimen increases and provides more soil-fibre surficial friction, and thus the mobilization of additional fibre tensile strength ultimately increases the specimen strength.

In Fig. 6.1b, the evolution of pore water pressure at the time of specimen shearing, as related to the tendency for contractive or dilative behaviour, can be determined by examining the slope of pore water pressure curve. As the pore water pressure remains positive throughout, it can be concluded that fibre reinforcement increases the contractive tendency of the soil. With increasing fibre content, the positive pore water pressure is observed to be greater.

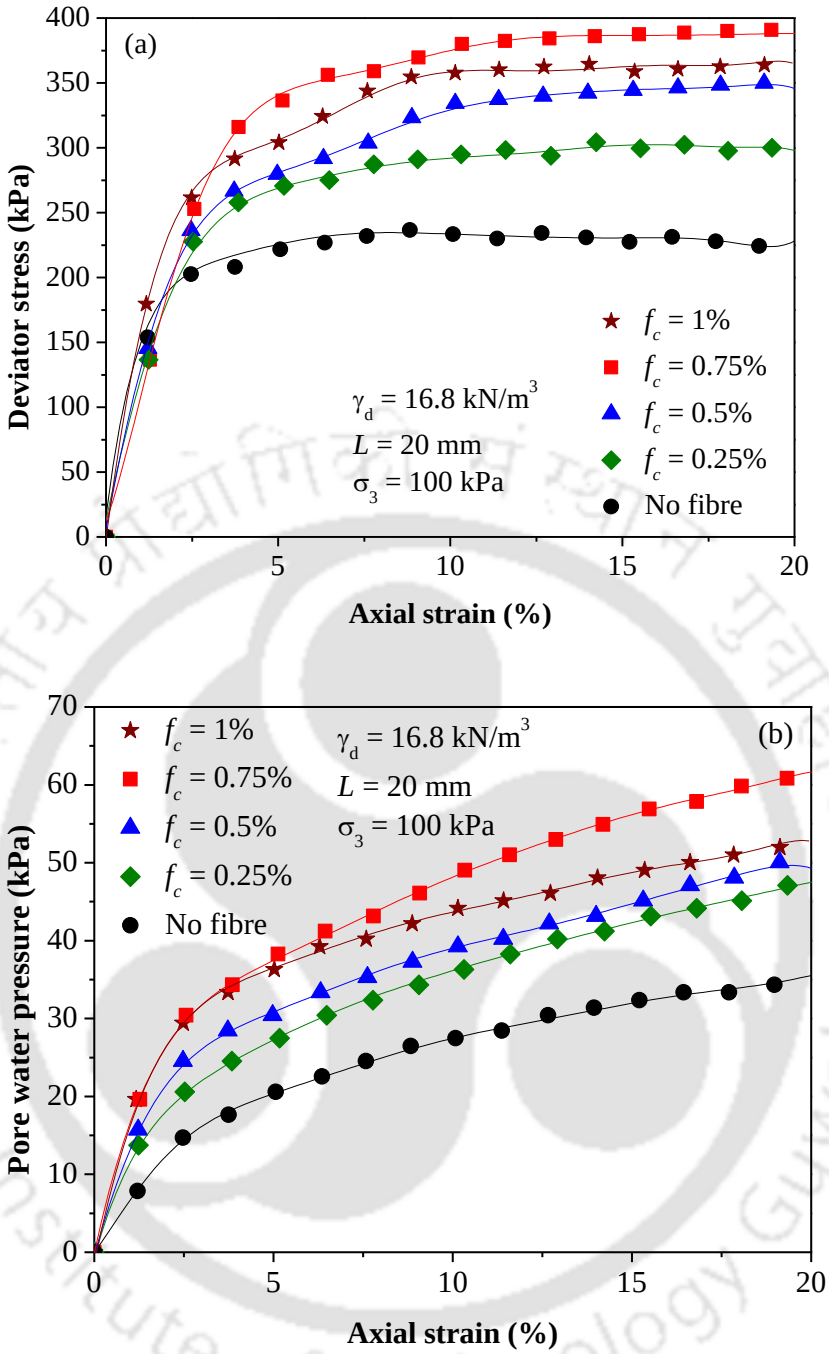

Fig. 6.1 Effect of fibre content under 100 kPa confining pressure on behaviour of specimens reinforced with 20 mm fibres and moulded at OMC and MDU (Series 1): (a) deviator stress response; (b) pore water pressure response

Typical effect of fibre content on the deformation modes of the specimens of Fig. 6.1 is presented in Fig. 6.2. The unreinforced soil specimen shows bulging in only a part of its length (Fig 6.2a). As the specimen is reinforced with 0.5% fibres, the bulging tends to get

distributed along its full length (Fig 6.2b). This indicates fibre reinforcement leads to a more uniform distribution of stresses within the specimen. As the fibre content is increased further to 1%, the bulging is restricted to the maximum and the specimen seems to stand like a column (Fig 6.2c). This is due to the reason that more of the soil particles are interlocked by the fibres. In contrast to the observed failure modes, Ozkul and Bykal (2007) found that rubber fibre-reinforced clayey soil showed barrelling type failure under drained condition and partial development of a shear plane under undrained condition.

(a) (b) (c)

Fig. 6.2 Effect of fibre content under 100 kPa confining pressure on deformation patterns of specimens reinforced with 20 mm fibres and moulded at OMC and MDU (Series 1): (a) unreinforced; (b) f_c = 0.5%; (c) f_c = 1%

6.3.1.2 Effect of Fibre Length on Specimens Moulded at OMC and MDU

Typical effect of fibre length on deviator stress-strain and pore water pressure variation of reinforced specimens from Series 1, with 0.75% fibres and sheared under 100 kPa confining pressure, are depicted in Fig. 6.3a and Fig. 6.3b, respectively. Compared to the unreinforced specimens, the fibre-reinforced specimens show higher deviator stress which is found to increase with fibre length up to 20 mm, and then to reduce with 30 mm fibres. Similar effect of fibre length was noted by Ahmad et al. (2010) where the shear stress increased non-linearly with increasing length of fibre up to 30 mm and decreased with 45 mm

length in 50 mm diameter specimens. Similar effect was noted in sand, in which the shear strength improvement reached a limiting level at some fibre length (Gray and Ohashi 1983).

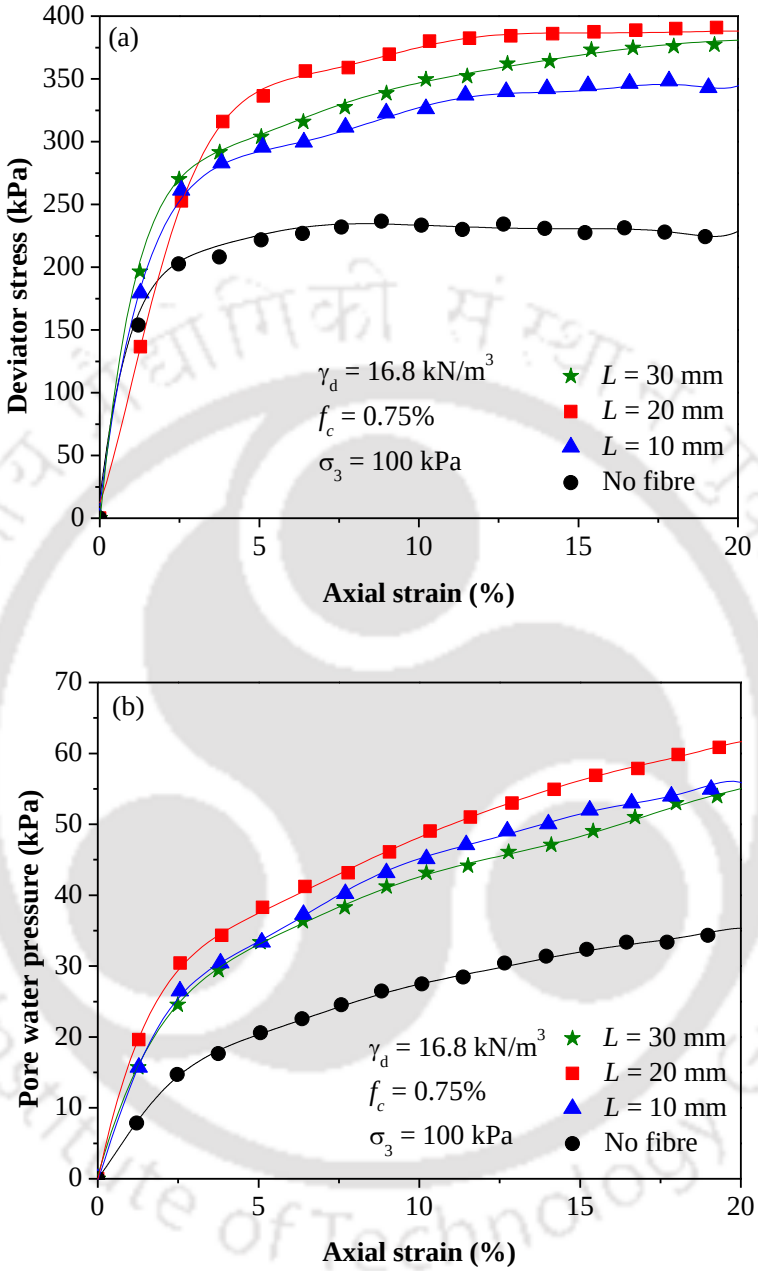

Fig. 6.3 Effect of fibre length under 100 kPa confining pressure on behaviour of specimens reinforced with 0.75% fibres and moulded at OMC and MDU (Series 1): (a) deviator stress response; (b) pore water pressure response

From pore pressure response (Fig. 6.3b), one observes that the positive pore pressure continues to increase with fibre length indicating more contractive behaviour of the specimen. The saturated clayey specimens have not undergone any volume change as the

shearing phase is carried out in an undrained condition, and there are only changes in the cross-sectional area over the length of the specimen, as observed from the deformation modes.

Typical effect of fibre length on the deformation modes of specimens of Fig. 6.3 is presented in Fig. 6.4. The unreinforced specimen exhibits bulging in only a part of its length (Fig. 6.4a). As fibres of 10 mm length are added to the unreinforced specimen, the bulging gets more distributed along its length (Fig. 6.4b). With longer fibres of 20 mm and 30 mm lengths (Figs. 6.4c and 6.4d), the specimen bulging progressively reduces. This is due to the reason that with increasing fibre length, bond strength and frictional resistance between soil and fibres increase. This bonding provides resistance against fibre sliding with more interlock of the soil particles, and limits the specimen bulging.

(a) (b) (c) (d)

Fig. 6.4 Effect of fibre length under 100 kPa confining pressure on deformation patterns of specimens reinforced with 0.75% fibres and moulded at OMC and MDU (Series 1): (a) unreinforced; (b) L = 10 mm; (c) L = 20 mm; (d) L = 30 mm

6.3.1.3 Effect of Confining Pressure on Specimens Moulded at OMC and MDU

Typical effect of confining pressure on deviator stress-strain and pore water pressure-strain variation of reinforced specimens from Series 1, with 0.75% fibres of 20 mm length, are presented in Fig. 6.5a and Fig. 6.5b, respectively. With higher confining pressure, both

the initial stiffness and peak deviator stress increase for the reinforced specimens (Fig. 6.5a). This is due to the reason that with increasing confining pressure, the interface surface area between soil particles and fibres increases and effective contact area directly influences the magnitude of the interfacial friction and adhesion (Dove and Frost 1999). Based on pullout tests of geotextile strips embedded in soil, Racana et al. (2003) found that the friction between soil and reinforcement increases with increasing normal stress.

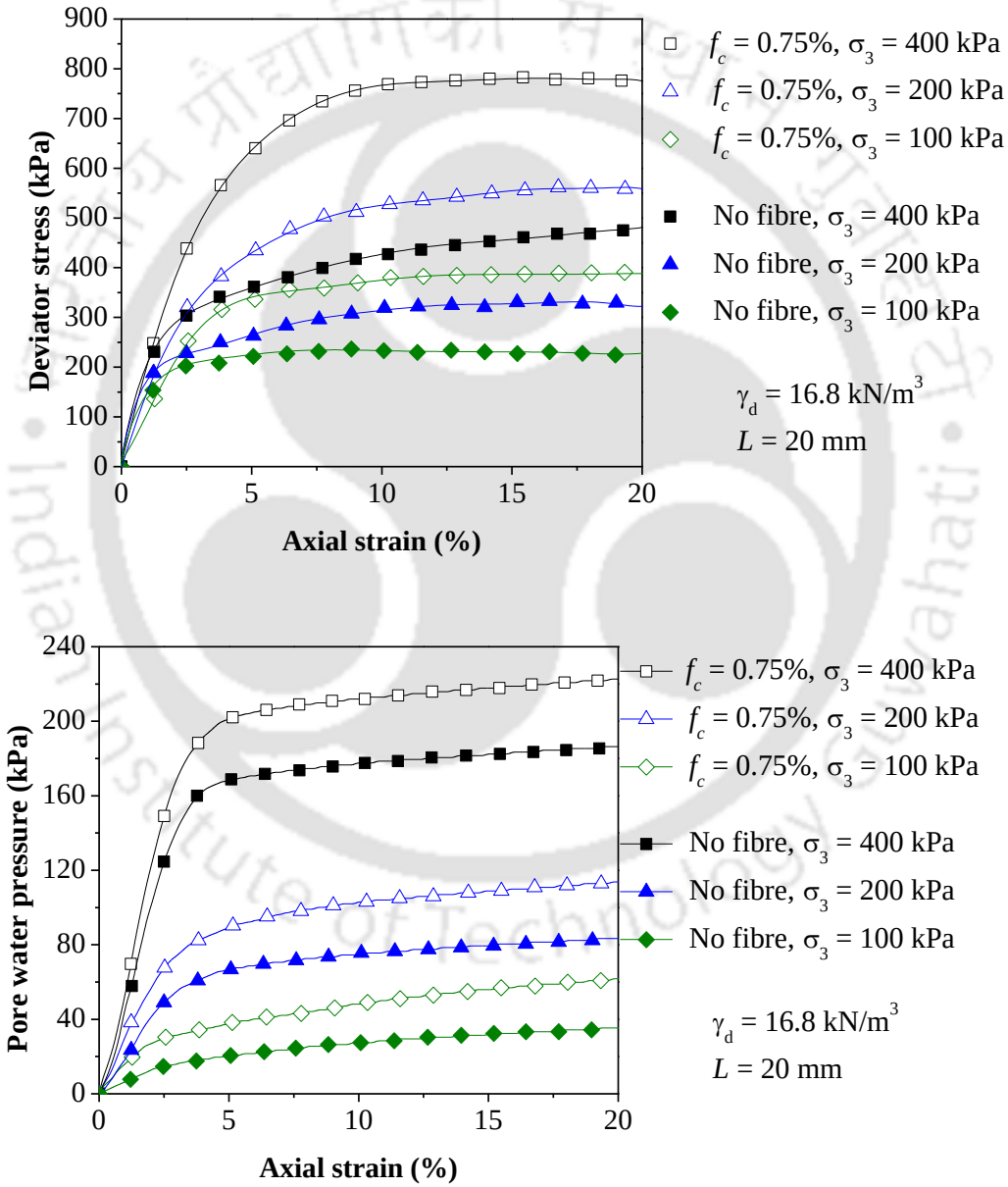

Fig. 6.5 Effect of confining pressure on behaviour of specimens reinforced with 0.75% fibres of 20 mm length and moulded at OMC and MDU (Series 1): (a) deviator stress response; (b) pore water pressure response

Thus, with higher confining pressure the surficial friction between the clayey soil and glass fibres have increased, leading to a rise in the specimen strength (Fig. 6.5a). The better interfacial bond strength and associated friction between soil and the glass fibres increases the contraction of the specimen, and this is noted as more positive pore pressure accumulation with increasing confining pressure (Fig. 6.5b). Similar effects of confining pressure on the initial stiffness and peak deviator stress have also been observed for the unreinforced specimens.

The effect of higher confining pressure on the deformation modes of specimens of Fig. 6.5, can be noted from Fig. 6.6. The specimens show bulging along its entire length under all confining pressures. However, the bulging progressively reduces with increasing confining pressure, as noted from the deformation at high confining pressure of 400 kPa (Fig. 6.6c) which is distinctly less than that at the low confining pressure of 100 kPa (Fig. 6.6a).

(a) (b) (c)

Fig. 6.6 Effect of confining pressure on deformation patterns of specimens reinforced with 0.75% fibres of 20 mm length and moulded at OMC and MDU (Series 1): (a) σ_3 = 100 kPa; (b) σ_3 = 200 kPa; (c) σ_3 = 400 kPa

6.3.1.4 Effect of Dry Unit Weight on Specimens Moulded at OMC

Typical effect of initial dry unit weight on deviator stress-strain and pore water pressure-strain variation of reinforced specimens from Series 1 & 2, with 0.75% fibres of 20

mm length and sheared under 100 kPa confining pressure, are depicted in Fig. 6.7a and Fig. 6.7b, respectively. The deviator stress is found to increase significantly with increasing dry unit weight from initial axial strain level. The interface friction angle between sand and polymer was noted to increase with increasing density of specimen during interface shear test (Frost and Han 1999). With increasing dry unit weight of specimen, the effective interfacial contact area between fibres and clayey soil increased (Tang et al. 2010), improving the fibre-soil interfacial shear strength.

Similarly, more surficial friction would have developed between the glass fibres and the clayey soil particles with increasing dry unit weight of specimen during shearing, resulting in enhanced deviator stress (Fig. 6.7a). From Fig. 6.7b, it can be observed that with the increase in dry unit weight, there is a lowering of positive pore water pressure generation within the specimen, which is also indicative of lower contractive behaviour. However, as the pore pressure curves are in a narrow range, it is noticeable from the deformation modes shown in Fig. 6.8 that the extent of bulging in the specimens is comparable irrespective of dry unit weight. This indicates that for same fibre content in fibre-reinforced clayey soil, the effect of initial dry unit weight (from 85% to 100% of MDU) on specimen deformation mode is not that significant, and is less than the influence of the variation of fibre content, fibre length or confining pressure.

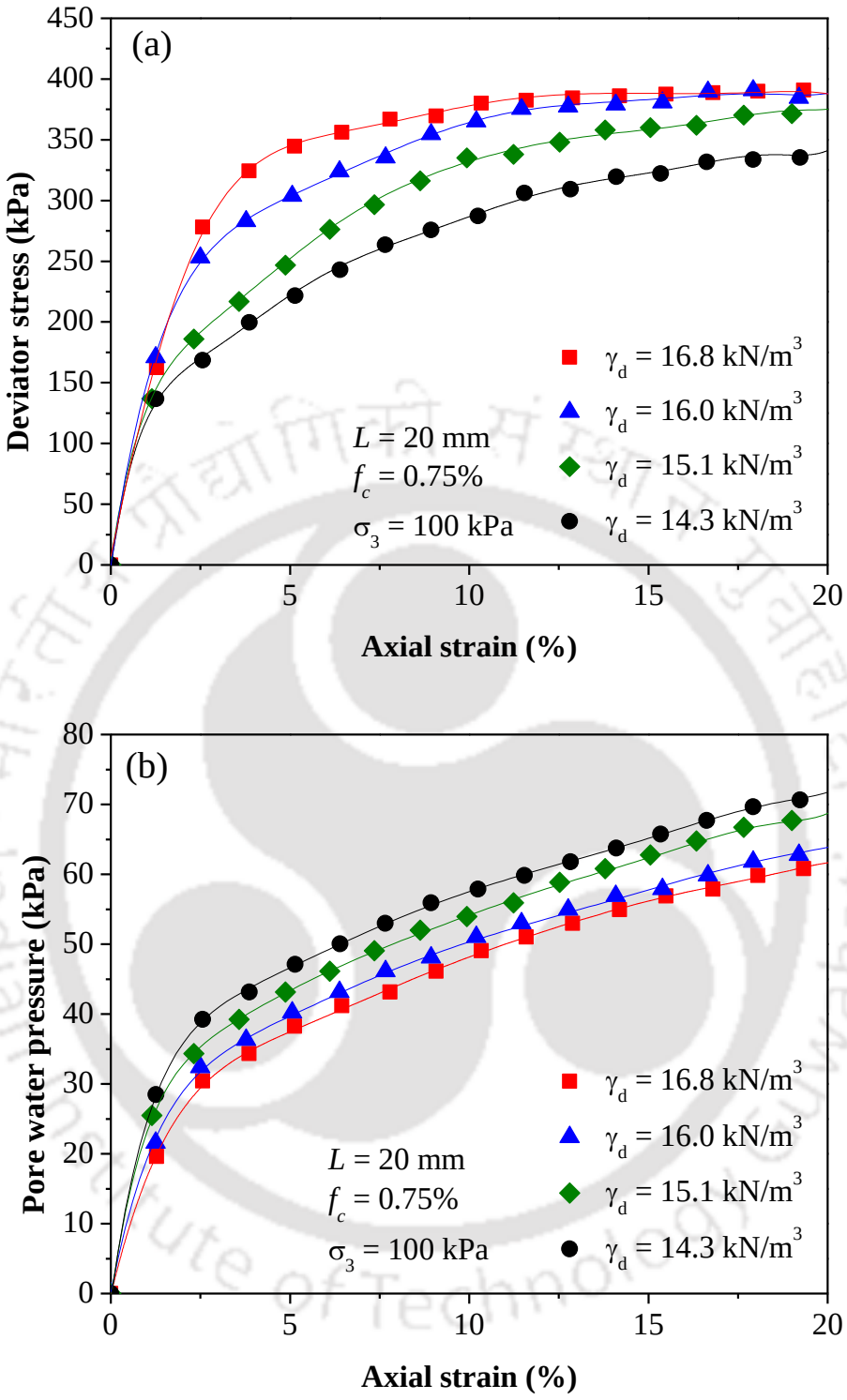

Fig. 6.7 Effect of dry unit weight under 100 kPa confining pressure on behaviour of specimens reinforced with 0.75% fibres of 20 mm length and moulded at OMC (Series 1 & 2): (a) deviator stress response; (b) pore water pressure response

(a) (b) (c) (d)

Fig. 6.8 Effect of dry unit weight under 100 kPa confining pressure on deformation patterns of specimens reinforced with 0.75% fibres of 20 mm length and moulded at OMC (Series 1 & 2): (a) γ_d = 14.3 kN/m^3; (b) γ_d = 15.1 kN/m^3; (c) γ_d = 16.0 kN/m^3; (d) γ_d = 16.8 kN/m^3

6.3.2 Failure Deviator Stress Ratio

As shown in Figs. 6.1a, 6.3a, 6.5a & 6.7a, no peak is observed in the deviator stress curves of all the glass fibre-reinforced clayey soil specimens. For further analysis of the test results, deviator stress corresponding to 10% axial strain has been considered as failure deviator stress. The effect of fibre contribution on the strength of the soil specimen at failure during undrained shearing can be quantified in terms of deviator stress ratio (*DSR*) defined as:

$$DSR = \frac{\sigma_{d,fibre}}{\sigma_{d,un}} \tag{6.1}$$

where $\sigma_{d,fibre}$ is the failure deviator stress of reinforced soil and $\sigma_{d,un}$ is the failure deviator stress of unreinforced soil.

The failure deviator stress and *DSR* values under different confining pressures for all soil-fibre specimens moulded at OMC and MDU (Series 1) are tabulated in Table 6.2. The combined effect of fibre content and confining pressure on *DSR* of specimens reinforced with

20 mm fibres is shown in Fig. 6.9. For the same confining pressure, the *DSR* is noted to increase with fibre content up to 0.75% and then reduce with 1% fibre content. However, at any fibre content, this ratio is noted to decrease with increasing confining pressure. with 0.75% fibres of 20 mm length, the maximum *DSR* values are 1.70, 1.66, 1.63 and 1.61 under 100, 200, 300 and 400 kPa confining pressures, respectively (Table 6.2).

The combined effect of fibre length and confining pressure on *DSR* of specimens from Series 1, reinforced with 0.75% fibres, is depicted in Fig. 6.10. The *DSR* increases with increasing fibre length up to 20 mm and then decreases with 30 mm fibres; yet the *DSR* of 30 mm fibre-reinforced specimen is greater than that with 10 mm fibres. With any fibre length, the *DSR* is noted to decrease with increasing confining pressure. The maximum and minimum *DSR* values under 100 kPa and 400 kPa confining pressures are 1.58, 1.70, 1.59 and 1.40, 1.61, 1.47 with 0.75% fibres of 10, 20 and 30 mm lengths, respectively (Table 6.2). Similar trends of variation with fibre length and confining pressure have been observed at other fibre contents.

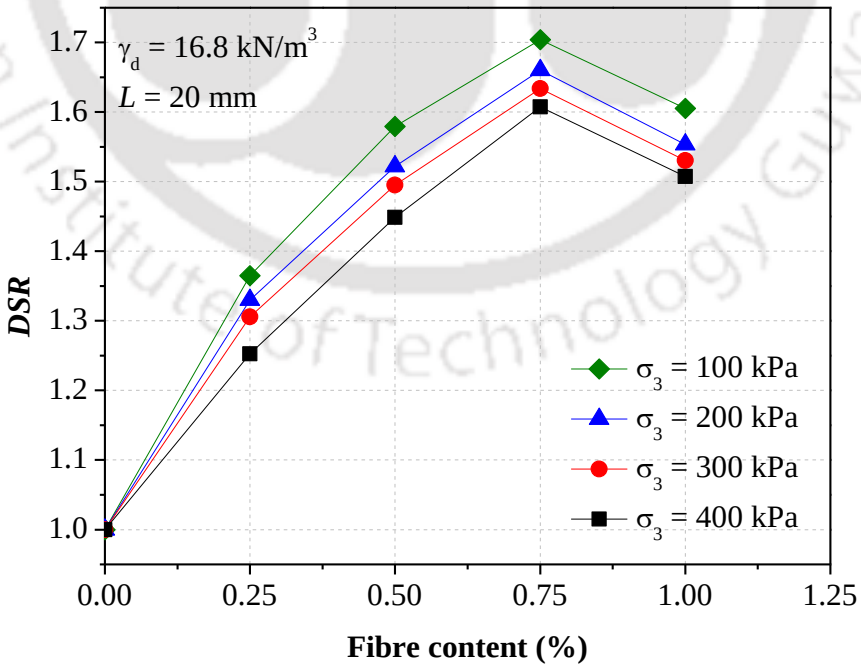

Fig. 6.9 Variation of deviator stress ratio with fibre content and confining pressure for specimens reinforced with 20 mm fibres and moulded at OMC and MDU (Series 1)

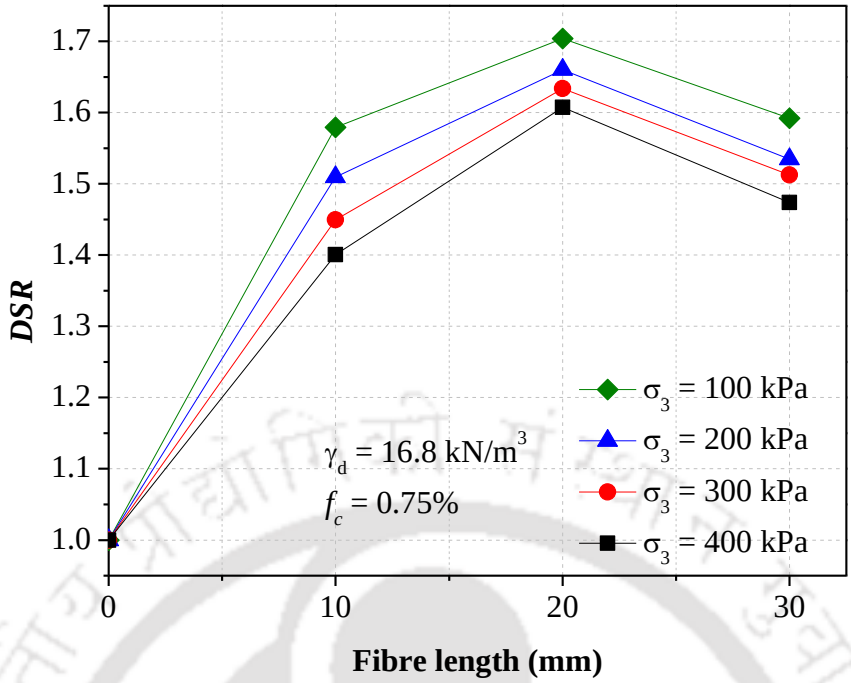

Fig. 6.10 Variation of deviator stress ratio with fibre length and confining pressure for specimens reinforced with 0.75% fibres and moulded at OMC and MDU (Series 1)

Table 6.2 Summary of failure deviator stress and *DSR* values under different confining pressures of all reinforced specimens moulded at OMC and MDU (Series 1)

Fibre length, *L* (mm)	**Fibre content, f_c (%)**	**σ_3 = 100 kPa**		**σ_3 = 200 kPa**		**σ_3 = 300 kPa**		**σ_3 = 400 kPa**	
		σ_d (kPa)	***DSR***	**σ_d (kPa)**	***DSR***	**σ_d (kPa)**	***DSR***	**σ_d (kPa)**	***DSR***
0	0	233	--	318	--	396	--	479	--
10	0.25	278	1.19	376	1.18	454	1.15	520	1.08
	0.5	332	1.42	441	1.38	533	1.34	628	1.31
	0.75	368	1.58	480	1.51	574	1.45	671	1.40
	1	341	1.46	456	1.43	546	1.38	643	1.34
20	0.25	318	1.36	423	1.33	517	1.30	600	1.25
	0.5	368	1.58	484	1.52	592	1.49	694	1.45
	0.75	397	1.70	528	1.66	647	1.63	770	1.61
	1	374	1.60	494	1.55	606	1.53	722	1.51
30	0.25	294	1.26	391	1.23	478	1.21	558	1.16
	0.5	349	1.50	459	1.44	558	1.41	652	1.36
	0.75	371	1.59	488	1.53	599	1.51	706	1.47
	1	353	1.51	465	1.46	573	1.45	684	1.43

The failure deviator stress and *DSR* values under different confining pressures for all specimens reinforced with 20 mm fibres and moulded at OMC and with varying dry unit weight (Series 1 & 2) are tabulated in Table 6.3. Typical effect of dry unit weight and confining pressure on *DSR* of specimens reinforced with 0.75% fibres of 20 mm length is presented in Fig. 6.11. Under any confining pressure, with increasing dry unit weight, the *DSR* reduces gradually from a maximum value at 14.3 kN/m^3 dry unit weight to a minimum value at 16.0 kN/m^3 dry unit weight, and then increases at 16.8 kN/m^3 (MDU). However, for the same moulding dry unit weight, the *DSR* value is noted to decrease with increasing confining pressure.

With 0.75% fibres of 20 mm length, the maximum and minimum *DSR* values under 100 kPa and 400 kPa confining pressures are 1.89, 1.74, 1.66, 1.70 and 1.77, 1.66, 1.59, 1.61 at 14.3, 15.1, 16.0 and 16.8 kN/m^3 dry unit weights, respectively (Table 6.3). Similar trends of variation with dry unit weight and confining pressure have been noted at other fibre contents.

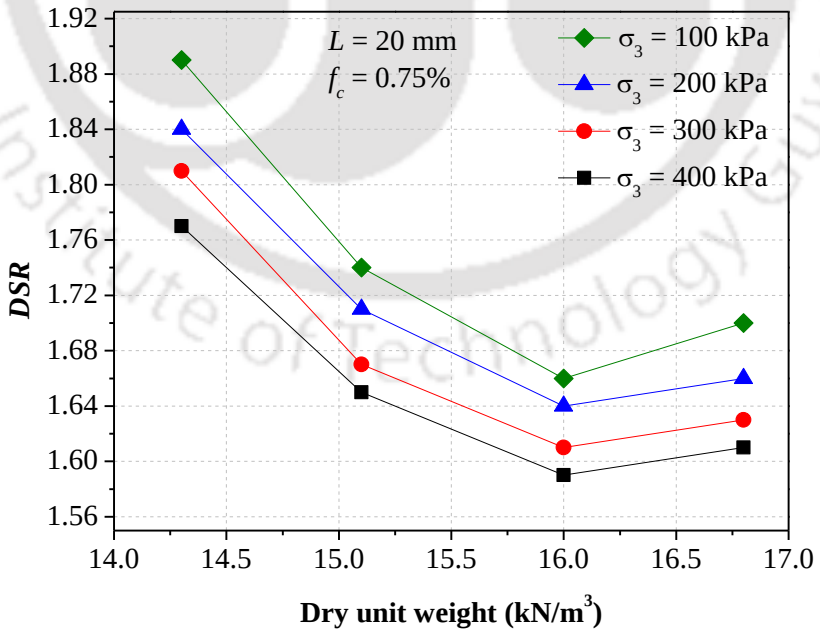

Fig. 6.11 Variation of deviator stress ratio with confining pressure for specimens reinforced with 0.75% fibres of 20 mm length and moulded at OMC with varying dry unit weight (Series 1 & 2)

Table 6.3 Summary of failure deviator stress and *DSR* values under different confining pressures for all specimens reinforced with 20 mm fibres and moulded at OMC with varying dry unit weight (Series 1 & 2)

Dry unit weight, γ_d (kN/m^3)	Fibre content, f_c (%)	σ_3 = 100 kPa		σ_3 = 200 kPa		σ_3 = 300 kPa		σ_3 = 400 kPa	
		σ_d (kPa)	*DSR*	σ_d (kPa)	*DSR*	σ_d (kPa)	*DSR*	σ_d (kPa)	*DSR*
14.3	0	161	--	238	--	298	--	347	--
	0.25	219	1.36	312	1.31	386	1.29	448	1.29
	0.5	268	1.66	384	1.61	472	1.58	546	1.57
	0.75	304	1.89	432	1.84	529	1.81	615	1.77
	1	295	1.83	422	1.77	524	1.76	606	1.75
15.1	0	193	--	265	--	332	--	398	--
	0.25	248	1.28	332	1.25	410	1.23	488	1.23
	0.5	306	1.58	414	1.56	514	1.55	619	1.55
	0.75	336	1.74	453	1.71	556	1.67	660	1.66
	1	324	1.69	439	1.66	549	1.65	643	1.62
16.0	0	222	--	302	--	377	--	457	--
	0.25	289	1.30	386	1.28	480	1.27	556	1.22
	0.5	336	1.51	448	1.48	553	1.47	660	1.44
	0.75	369	1.66	495	1.64	609	1.61	726	1.59
	1	354	1.59	471	1.56	586	1.55	703	1.54
16.8	0	233	--	318	--	396	--	479	--
	0.25	318	1.36	423	1.33	517	1.30	600	1.25
	0.5	368	1.58	484	1.52	592	1.49	694	1.45
	0.75	397	1.70	528	1.66	647	1.63	770	1.61
	1	374	1.60	494	1.55	606	1.52	722	1.51

6.3.3 Shear Strength Parameters

Shear strength parameters for all soil-fibre specimens have been obtained by plotting modified failure envelopes (K_f line) in terms of p'-q' plots, with the variables, p' and q', defined as:

$$p' = \frac{(\sigma_1' + \sigma_3')}{2} \tag{6.2}$$

$$q' = \frac{(\sigma_1' + \sigma_3')}{2} \tag{6.3}$$

where σ_1' = major principal effective stress, and σ_3' = minor principal effective stress.

The intercept of the K_f line with the Y-axis is d, and the angle that the K_f line makes with the X-axis is α. The equation of the K_f line and the equation of the shear strength envelope are related as follows:

$$\tan\alpha = \sin\phi' \tag{6.4}$$

$$c' = \frac{d}{\cos\phi'} \tag{6.5}$$

where ϕ' = angle of shearing resistance, and c' = cohesion intercept.

The shear strength parameters of all soil specimens of Series 1 are tabulated in Table 6.4. Typical shear strength envelopes showing the effects of fibre content and fibre length for specimens moulded at OMC and MDU are presented in Fig. 6.12. The failure envelopes indicate a general trend of shear strength improvement with fibre reinforcement, with noticeable increase in both cohesion intercept and friction angle. Within the range of fibre contents used, the shear strength is the maximum with 0.75% fibres and decreases with 1% fibres (Fig. 6.12a). Similarly, within the range of fibre lengths used, the shear strength is the maximum with 20 mm fibres, and reduces with 30 mm fibres (Fig. 6.12b). The cohesion intercept and friction angle of the unreinforced specimen are 45 kPa and 25.8°, respectively. With the optimum reinforcement (0.75% fibres of 20 mm length), the cohesion intercept and

friction angle have increased by magnitudes of 22 kPa and 9.4˚ to maximum values of 67 kPa and 35.2˚ (Table 6.4).

Table 6.4 Shear strength parameters and fibre contribution for all reinforced soil specimens moulded at OMC and MDU (Series 1)

f_c (%)		L = 10 mm		L = 20 mm		L = 30 mm	
		c' (kPa)	ϕ' (˚)	c' (kPa)	ϕ'(˚)	c' (kPa)	ϕ' (˚)
0		45	25.8	45	25.8	45	25.8
0.25		52	27.1	56	30.4	51	28.8
	Fibre contribution	7	1.3	11	4.6	6	3.0
0.5		62	29.8	63	33.3	59	31.7
	Fibre contribution	17	4.0	18	7.5	14	5.9
0.75		67	32.1	67	35.2	67	32.8
	Fibre contribution	22	6.3	22	9.5	22	7.0
1		63	30.7	66	33.1	62	31.6
	Fibre contribution	18	4.9	21	7.3	17	5.8

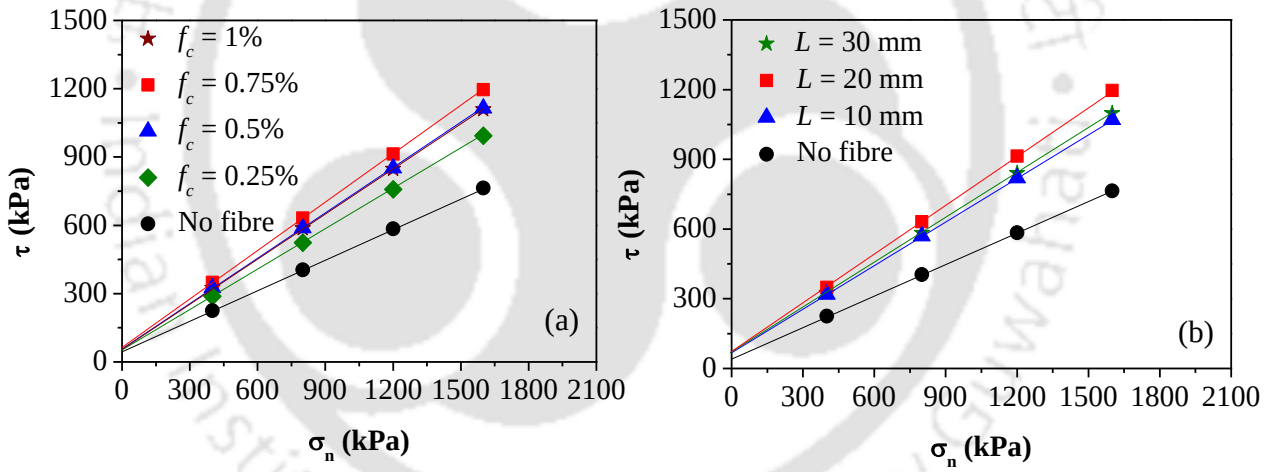

Fig. 6.12 Shear strength envelopes of reinforced specimens moulded at OMC and MDU (Series 1): (a) Variation with fibre content of 20 mm length; (b) Variation with fibre length of 0.75% content

The effect of moulding dry unit weight (Series 1 & 2) on shear strength envelopes of the specimens with optimum reinforcement (0.75% fibres of 20 mm length) is shown in Fig. 6.13. The shear strength is noted to increase continuously with increasing dry unit weight.

For unreinforced specimens, the cohesion intercept and friction angle values of 28 kPa and 22.9˚ at 14.3 kN/m^3 dry unit weight increase to maximum values of 45 kPa and 25.8˚

at 16.8 kN/m^3, i.e. an increase of 17 kPa and 2.9˚. For the reinforced specimen moulded at the lowest dry unit weight (γ_d = 14.3 kN/m^3), the maximum effective cohesion and friction angle are 57 kPa and 32.8˚ with 0.75% fibres, which are very much higher than the values of unreinforced specimens moulded at 15.1, 16.0 and 16.8 kN/m^3 dry unit weights (Table 6.5), indicating the beneficial effect of fibre reinforcement at all moulding states. As summarized in Table 6.5, the maximum fibre contribution to cohesion and friction angle are 29 kPa, 9.9˚; 25 kPa, 10.3˚; 25 kPa, 10.3˚ and 22 kPa, 9.4˚, respectively for dry unit weights of 14.3, 15.1, 16.0 and 16.8 kN/m^3.

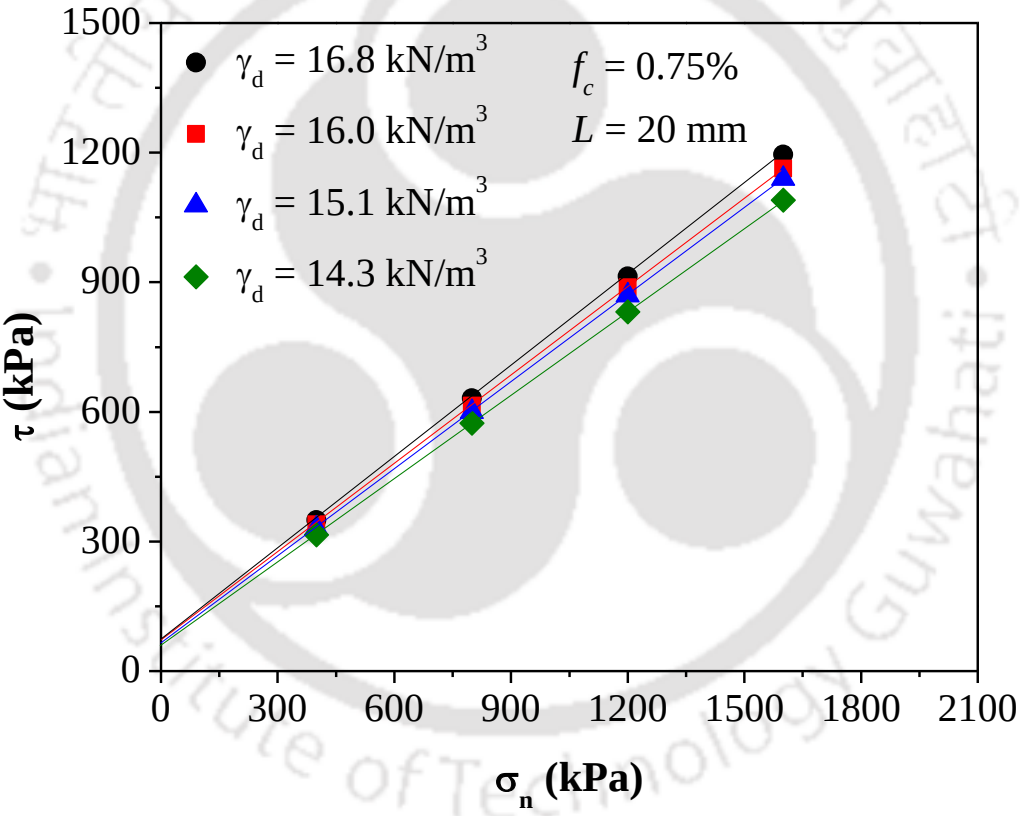

Fig. 6.13 Variation of shear strength envelope with dry unit weight for specimens reinforced with 0.75% fibres of 20 mm length (Series 1 & 2)

Table 6.5 Shear strength parameters and fibre contribution for all reinforced soil specimens with 20 mm fibres and moulded at OMC with varying dry unit weight (Series 1 & 2)

f_c (%)		γ_d = 14.3 kN/m^3		γ_d = 15.1 kN/m^3		γ_d = 16.0 kN/m^3		γ_d = 16.8 kN/m^3	
		c' (kPa)	ϕ' (°)	c' (kPa)	ϕ' (°)	c' (kPa)	ϕ' (°)	c' (kPa)	ϕ' (°)
0		28	22.9	35	23.7	40	24.2	45	25.8
0.25		40	25.6	45	26.9	46	29.8	56	30.4
	Fibre contribution	12	2.7	10	3.2	6	5.6	11	4.6
0.5		49	29.3	54	30.7	55	31.6	62	33.3
	Fibre contribution	21	6.4	19	7.0	15	7.4	17	7.5
0.75		57	32.8	60	34.0	65	34.5	67	35.2
	Fibre contribution	29	9.9	25	10.3	25	10.3	22	9.4
1		58	31.6	59	32.2	64	33.2	66	33.2
	Fibre contribution	30	8.7	24	8.5	24	9.0	21	7.4

6.3.4 Secant Modulus Response

Soil experiences irrecoverable (plastic) deformation even at low stress levels and shows nonlinear behavior very early in the stress-strain curve. The deformation characteristics of both the unreinforced and glass fibre-reinforced clayey soil specimens can be quantified through a deformation modulus, as a measure of its resistance against deformation in response to any external applied load.

The soil modulus of the soil at any deformation level can be determined from the stress-strain curve by drawing a secant line from the origin to the point considered on the stress-strain curve, and is the ratio of deviator stress level to its corresponding strain level. The stress-strain curves of reinforced soil, and therefore the soil modulus, are influenced by fibre parameters (content and length), moulding state factors (moisture content and dry unit weight) and and confining pressure. The secant modulus has been calculated at different axial strain values (0.5, 1, 2.5, 5, 10 and 20%).

For soil specimens of Series 1, with varying fibre content of 20 mm length, the secant modulus values at 2.5, 5, 10 and 20% axial strain are tabulated in Table 6.6. For any specimen, the secant modulus is higher at small axial strain and decreases with increasing

axial strain. The secant modulus values of the unreinforced soil at 2.5% axial strain are 8.08, 9.10, 11.94 and 14.84 MPa under 100, 200, 300 and 400 kPa confining pressures, respectively. The corresponding values decrease to 1.13, 1.61, 2.17 and 2.52 MPa at 20% axial strain.

Typical effect of fibre content on secant modulus variation under 100 kPa confining pressure, for specimens of Series 1 reinforced with 20 mm fibres, is shown in Fig. 6.14. At any axial strain level, the secant modulus increases with fibre content up to 0.75% and then decreases with 1% fibres. Under 100 kPa confining pressure, the secant modulus is the maximum with 0.75% fibres of 20 mm length (Table 6.6). The corresponding maximum value is 12.15 MPa at 2.5% axial strain which decreases to the minimum value of 1.93 MPa at 20% axial strain.

Typical effect of fibre length on secant modulus variation under 100 kPa confining pressure, for specimens of Series 1 reinforced with 0.75% fibres, is shown in Fig. 6.15. At any strain level, the secant modulus increases with fibre length to reach maximum value with 20 mm fibres, and then decreases with 30 mm fibres. However the secant modulus values with 30 mm fibres is higher than that of with 10 mm fibres. Under 100 kPa confining pressure, the maximum values of secant modulus with 0.75% fibres are 10.26, 12.15 and 11.48 MPa at 2.5% axial strain with 10, 20 and 30 mm fibres, respectively (Table 6.6).

Table 6.6 Summary of secant modulus values under different confining pressures for specimens reinforced with fibres of 20 mm length and moulded at OMC and MDU (Series 1)

Axial strain (%)	f_c (%)	Secant modulus (MPa)											
		L = 10 mm				L = 20 mm				L = 30 mm			
		100 kPa	200 kPa	300 kPa	400 kPa	100 kPa	200 kPa	300 kPa	400 kPa	100 kPa	200 kPa	300 kPa	400 kPa
2.5	0	8.08	9.10	11.94	14.84	8.08	9.10	11.94	14.84	8.08	9.10	11.94	14.84
	0.25	8.81	11.37	14.06	15.58	9.11	11.72	14.76	17.04	8.31	10.83	13.32	15.95
	0.5	8.87	12.68	15.10	17.54	12.05	12.72	16.44	20.49	9.91	12.31	14.58	18.89
	0.75	10.96	13.83	16.77	19.90	12.15	14.12	17.20	20.58	10.85	13.24	16.92	19.86
	1	8.63	11.78	15.86	19.56	10.51	12.32	15.64	18.12	9.96	13.03	15.86	19.71
5	0	4.38	5.17	6.51	8.22	4.38	5.17	6.51	8.22	4.38	5.17	6.51	8.22
	0.25	4.70	6.68	7.81	8.94	5.42	7.19	9.45	10.16	5.69	6.71	8.29	9.24
	0.5	5.02	7.72	9.39	10.83	5.93	8.34	10.03	12.89	5.95	7.74	9.56	11.41
	0.75	5.81	8.55	9.88	12.45	7.02	8.87	10.48	13.31	6.19	8.01	9.99	12.58
	1	5.26	7.49	9.41	11.93	6.05	8.49	10.12	13.18	5.91	7.70	9.74	11.93
10	0	2.32	3.18	3.95	4.78	2.32	3.18	3.95	4.78	2.32	3.18	3.95	4.78
	0.25	2.62	3.81	4.58	5.20	2.96	4.11	5.33	6.03	2.85	3.77	4.86	5.32
	0.5	3.01	4.48	5.31	6.42	3.35	4.75	6.06	7.19	3.16	4.45	5.81	6.56
	0.75	3.24	4.82	5.70	6.96	3.81	5.27	6.39	7.65	3.47	4.56	6.61	7.06
	1	3.08	4.44	5.49	6.56	3.54	4.78	6.22	7.19	3.35	4.39	5.69	6.78
20	0	1.13	1.61	2.17	2.52	1.13	1.61	2.17	2.52	1.13	1.61	2.17	2.52
	0.25	1.41	2.07	2.52	2.88	1.48	2.16	2.73	3.36	1.46	1.99	2.70	2.87
	0.5	1.54	2.27	2.82	3.53	1.75	2.46	3.22	3.68	1.62	2.41	3.08	3.16
	0.75	1.72	2.52	2.99	3.63	1.93	2.78	3.55	3.94	1.89	2.53	3.19	3.76
	1	1.61	2.45	2.92	3.30	1.84	2.44	3.19	3.59	1.71	2.45	2.92	3.62

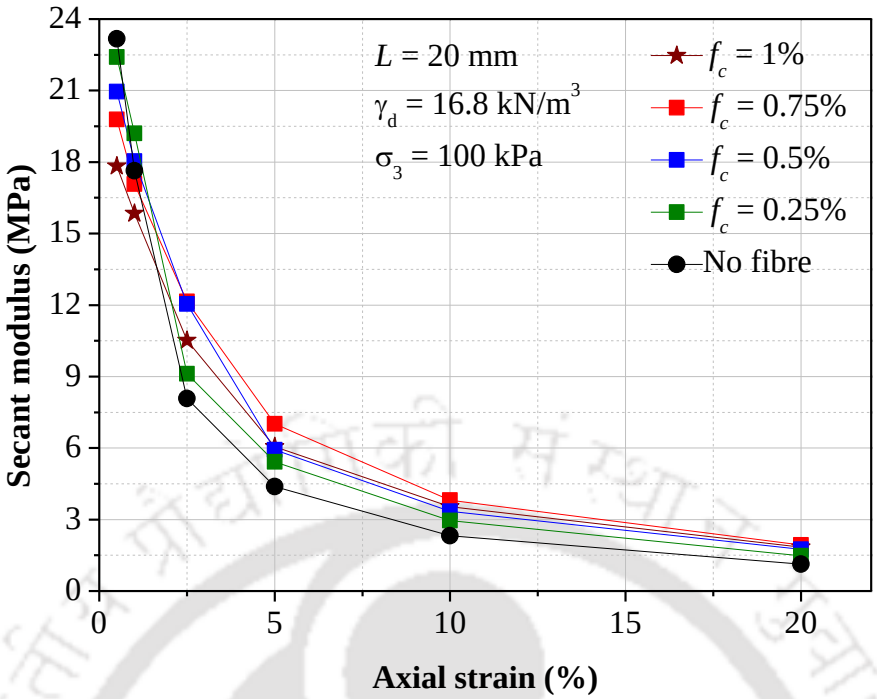

Fig. 6.14 Effect of fibre content on secant modulus variation under 100 kPa confining pressure for specimens reinforced with 20 mm fibres and moulded at OMC and MDU (Series 1)

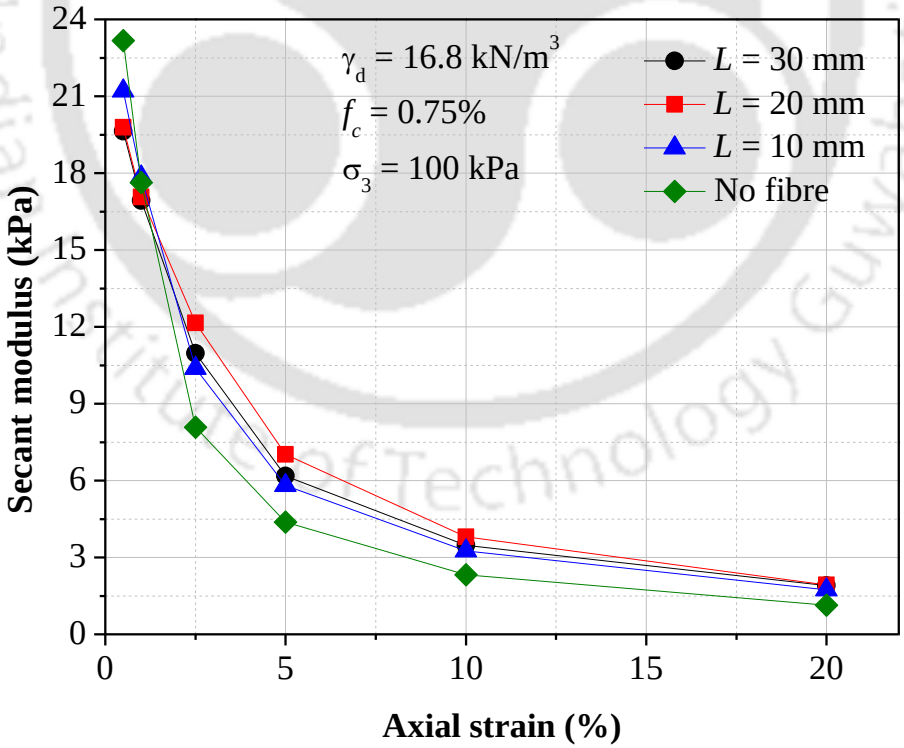

Fig. 6.15 Effect of fibre length on secant modulus variation under 100 kPa confining pressure for specimens reinforced with 0.75% fibres and moulded at OMC and MDU (Series 1)

Typical effect of confining pressure on secant modulus variation for specimens of Series 1, reinforced with 0.75% fibres of 20 mm length, is presented in Fig. 6.16. At any axial strain level, the secant modulus is greater with increasing confining pressure. The maximum secant modulus values at 2.5% axial strain are 12.15, 14.12, 17.20 and 20.58 MPa under 100, 200, 300 and 400 kPa confining pressures, respectively (Table 6.6).

The secant modulus values for specimens of Series 1 & 2, with fibres of 20 mm length and different dry unit weights, under the four confining pressures (100 to 400 kPa) are presented in Tables 6.7 & 6.8. The secant modulus is observed to increase with increasing confining pressure at any dry unit weight. At any dry unit weight, secant modulus values increase with fibre content up to 0.75% fibre and decreases with 1% fibres.

At 100 kPa confining pressure, secant modulus values of the unreinforced soil at 2.5% axial strain are 4.45, 5.14, 6.00 and 8.08 MPa for dry unit weights of 14.3, 15.1, 16.0 and 16.8 kN/m^3, respectively (Table 6.7). The corresponding values increase with confining pressure to reach maximum values of 9.16, 11.04, 14.21 and 14.84 MPa at 400 kPa confining pressure (Table 6.8). For the reinforced specimens, secant modulus values are the maximum with 0.75% fibres of 20 mm length, and the secant modulus variation under 400 kPa confining pressure is shown in Fig. 6.17. The corresponding maximum secant modulus values at 2.5% axial strain are 11.93, 15.41, 18.29 and 20.58 MPa for dry unit weights of 14.3, 15.1, 16.0 and 16.8 kN/m^3, respectively.

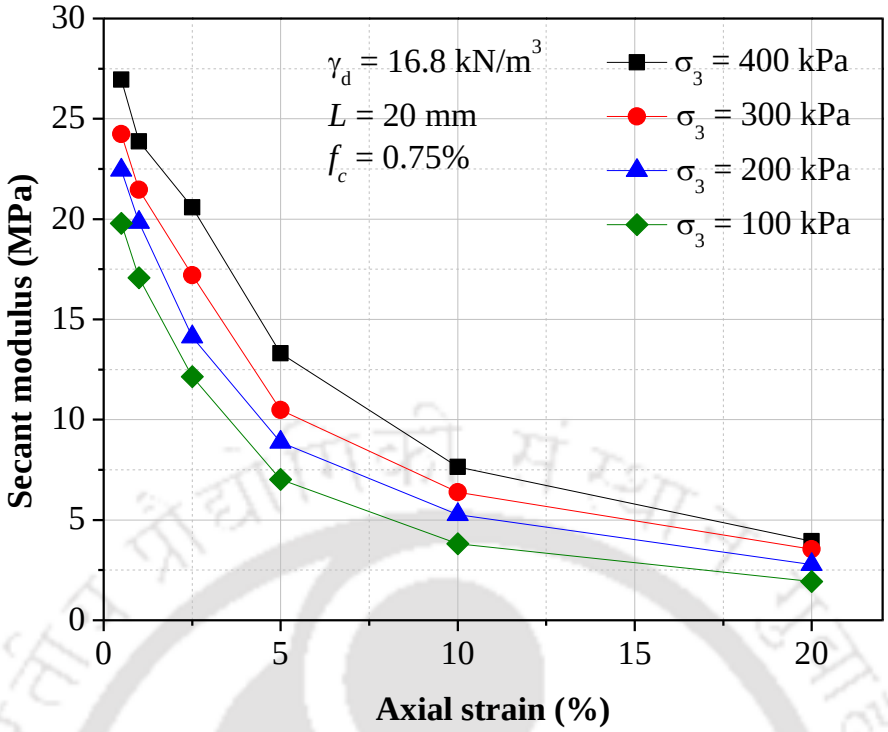

Fig. 6.16 Effect of confining pressure on secant modulus variation for specimens reinforced with 0.75% fibres of 20 mm length and moulded at OMC and MDU (Series 1)

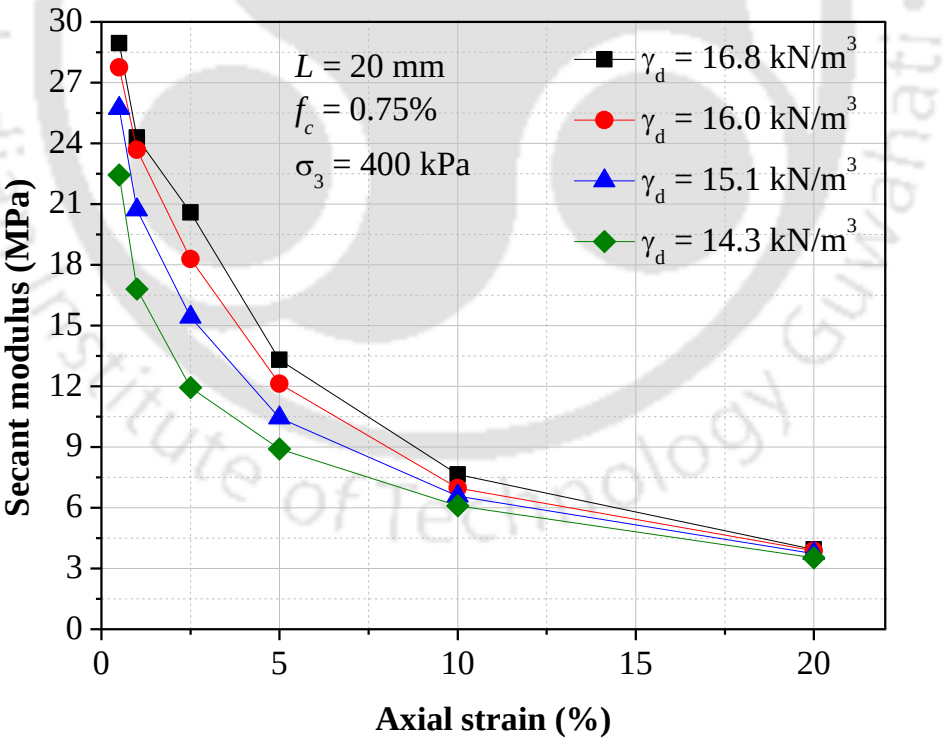

Fig. 6.17 Effect of dry unit weight on secant modulus variation under 400 kPa confining pressure for specimens reinforced with 0.75% fibres of 20 mm length and moulded at OMC (Series 1 & 2)

Table 6.7 Secant modulus values under 100 and 200 kPa confining pressures for specimens reinforced with 20 mm fibres and moulded at OMC with varying dry unit weight (Series 1 & 2)

Axial strain (%)	f_c (%)	Secant modulus (MPa)							
		γ_d = 14.3 kN/m^3		γ_d = 15.1 kN/m^3		γ_d = 16.0 kN/m^3		γ_d = 16.8 kN/m^3	
		100 kPa	200 kPa	100 kPa	200 kPa	100 kPa	200 kPa	100 kPa	200 kPa
2.5	0	4.45	6.08	5.14	7.25	6.00	9.18	8.08	9.10
	0.25	5.85	7.41	6.32	8.64	8.72	11.21	9.11	11.72
	0.5	6.18	7.96	8.54	10.28	9.54	12.05	12.05	12.72
	0.75	6.61	8.54	8.73	11.45	10.40	13.45	12.15	14.12
	1	5.75	7.21	7.46	8.85	10.12	11.8	10.51	12.32
5	0	2.81	3.65	3.27	4.38	3.77	5.45	4.38	5.17
	0.25	3.59	5.26	4.11	5.45	5.30	6.71	5.42	7.19
	0.5	4.08	5.6	5.19	6.99	5.58	7.47	5.93	8.34
	0.75	4.63	6.06	5.21	7.16	6.08	7.98	7.02	8.87
	1	3.63	5.79	4.91	6.55	5.98	7.58	6.05	8.49
10	0	1.63	2.31	1.94	2.62	2.16	2.99	2.32	3.18
	0.25	2.18	3.11	2.49	3.31	2.85	3.84	2.96	4.11
	0.5	2.72	3.81	3.09	4.11	3.31	4.50	3.35	4.75
	0.75	3.01	4.35	3.31	4.49	3.65	4.73	3.81	5.27
	1	2.92	3.95	3.24	4.33	3.45	4.65	3.54	4.78
20	0	0.86	1.37	1.03	1.44	1.11	1.54	1.13	1.61
	0.25	1.16	1.61	1.42	1.96	1.48	1.99	1.48	2.16
	0.5	1.44	2.13	1.76	2.37	1.73	2.37	1.75	2.46
	0.75	1.83	2.55	1.86	2.64	1.93	2.66	1.93	2.78
	1	1.31	2.07	1.79	2.53	1.73	2.41	1.84	2.44

Table 6.8 Secant modulus values under 300 and 400 kPa confining pressures for specimens reinforced with 20 mm fibres and moulded at OMC with varying dry unit weight (Series 1 & 2)

Axial strain (%)	f_c (%)	Secant modulus (MPa)							
		γ_d = 14.3 kN/m^3		γ_d = 15.1 kN/m^3		γ_d = 16.0 kN/m^3		γ_d = 16.8 kN/m^3	
		300 kPa	400 kPa	300 kPa	400 kPa	300 kPa	400 kPa	300 kPa	400 kPa
2.5	0	7.86	9.16	8.09	11.04	10.85	14.21	11.94	14.84
	0.25	8.43	10.25	10.61	13.42	13.85	16.35	14.76	17.04
	0.5	10.17	11.78	12.16	14.06	15.15	18.07	16.44	20.49
	0.75	10.35	11.93	12.75	15.41	17.02	18.29	17.20	20.58
	1	9.26	11.06	11.43	14.21	14.30	15.72	15.64	18.12
5	0	4.92	5.69	5.16	5.91	6.87	8.09	6.51	8.22
	0.25	6.07	7.29	6.58	8.25	8.55	9.75	9.45	10.16
	0.5	7.19	8.03	8.31	9.59	9.98	11.31	10.03	12.89
	0.75	7.41	8.91	8.39	10.44	10.26	12.12	10.48	13.31
	1	6.81	7.32	7.96	10.16	8.95	10.56	10.12	13.18
10	0	3.01	3.47	3.32	3.91	3.75	4.56	3.95	4.78
	0.25	3.81	4.39	4.06	4.91	4.81	5.57	5.33	6.03
	0.5	4.67	5.43	5.12	6.19	5.58	6.67	6.06	7.19
	0.75	5.27	6.09	5.58	6.57	5.81	6.98	6.39	7.65
	1	5.06	4.63	5.42	6.43	5.47	6.55	6.22	7.19
20	0	1.75	2.06	1.89	2.26	1.99	2.45	2.17	2.52
	0.25	2.09	2.46	2.44	2.92	2.41	2.85	2.73	3.36
	0.5	2.61	2.91	2.96	3.69	2.93	3.41	3.22	3.68
	0.75	3.09	3.52	3.31	3.87	3.25	3.88	3.55	3.94
	1	2.58	3.01	3.14	3.60	2.84	3.59	3.19	3.59

With the optimum reinforcement (0.75% fibres of 20 mm length), the relative effects of the ranges of moulded dry unit weight and confining pressure on secant modulus improvement can be compared at the considered failure axial strain level of 10%. At the considered failure axial strain level of 10%, the relative effects of the optimum reinforcement (0.75% glass fibres of 20 mm length), dry unit weight and confining pressure on secant modulus improvement can be compared. At 16.8 kN/m^3 dry unit weight and under 100 kPa confining pressure, the failure secant modulus of the unreinforced specimen which is 2.32 MPa has increased to a maximum value of 3.81 MPa (i.e. 1.49 MPa improvement).

At 100 kPa confining pressure, the failure secant modulus of the reinforced specimen is found to increase from 3.01 to 3.81 MPa (i.e. 0.80 MPa improvement) when dry unit weight is increased from 14.3 kN/m^3 to 16.8 kN/m^3. Further, at 16.8 kN/m^3 dry unit weight, the failure secant modulus of the reinforced specimen is noted to increase from 3.81 MPa to 5.27 MPa (1.46 MPa improvement) as confining pressure is increased from 100 kPa to 400 kPa. Comparing the stiffness improvement at failure strain, it can be concluded that the effect of confining pressure is higher than that of dry unit weight or fibre content.

6.3.5 Energy Absorption Capability

The energy absorption capability of the fibre-reinforced soil specimen can be obtained from the area under the deviatoric stress-axial deformation curve up to a deformation level, similar to the determination of toughness as per ASTM C1018-97 for fibre-reinforced concrete under flexural loading condition, from the area under the load-deflection curve up to a specified deflection. In the shearing phase of triaxial testing, the amount of energy applied in inducing deformation is absorbed by the soil specimens. The total energy absorption capability (*EAC*) of the reinforced soil specimen is thus related to its deviator stress-axial strain response, and it is the combination of energy dissipated in the deformation of soil

matrix and the energy dissipated through friction along the soil-fibre interface and the stretching of fibres. The *EAC* for the fibre-reinforced soil can be expressed as:

$$EAC = (EAC)_s + (EAC)_f \tag{6.6}$$

where $(EAC)_s$ is the energy dissipated in deformation of soil matrix only, and $(EAC)_f$ is the energy dissipated in soil-fibre interaction and fibre stretching.

Fig. 6.18 shows a typical representation of stress-strain curve of triaxial compression test for both unreinforced and fibre-reinforced specimens. Inclusion of fibre increases the stress carrying capacity of soil, increasing the *EAC* of reinforced soil. Considering the energy absorbed by soil matrix is same for both unreinforced and reinforced specimens up to the selected reference aial xstrain level (ε_f), the shaded area representing the difference between absorbed energy is showing the contribution of fibre reinforcement. The effects of fibre content, fibre length, dry unit weight and confining pressure on the *EAC* have been evaluated considering the maximum deformation of 15.2 mm, corresponding to the maximum strain level of 20% in the tests.

The *EAC* and $(EAC)_f$ values for all reinforced specimens of Series 1 moulded at 16.8 kN/m^3 (MDU) are tabulated in Table 6.9, and the energy dissipated in soil matrix deformation is always greater than the energy dissipated in soil-fibre interaction and fibre stretching. Under any confining pressure, both the *EAC* and $(EAC)_f$ values increase with fibre content only up to 0.75%, and also with fibre length only up to 20 mm. Further, for any combination of fibre content and fibre length, both the values are noted to increase with increasing confining pressure.

At MDU, the *EAC* value of 4439 kJ/m^3 for the unreinforced specimen has increased to 7045 kJ/m^3 with optimum reinforcement (0.75% fibres of 20 mm length), under 100 kPa confining pressure. Under 400 kPa confining pressure, this *EAC* value increases further to maximum values of 8945 and 13996 kJ/m^3, respectively for unreinforced and fibre-reinforced

specimens (Table 6.9). The trends of variations of both *EAC* and $(EAC)_f$ values are the same with fibre content, fibre length and confining pressure.

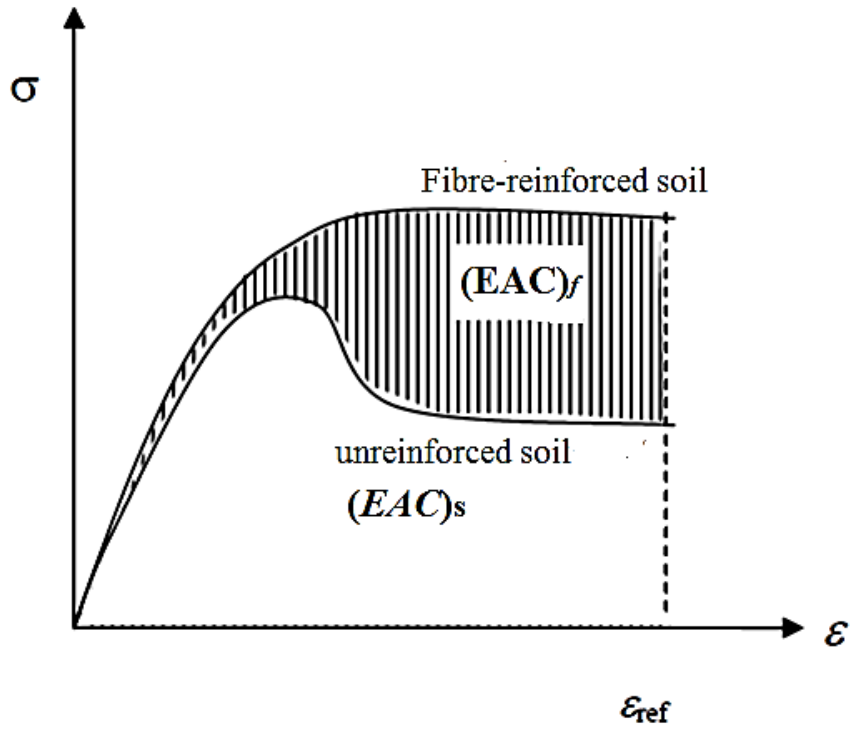

Fig. 6.18 Typical representation of energy absorption capability calculation from deviator stress-axial strain plot of CU test

Table 6.9 Summary of *EAC* and $(EAC)_f$ of all specimens moulded at OMC and MDU (Series 1)

f_c (%)		***EAC* and $(EAC)_f$, (kJ/m^3)**											
		σ_3 = 100 kPa			**σ_3 = 200 kPa**			**σ_3 = 300 kPa**			**σ_3 = 400 kPa**		
		***L* (mm)**			***L* (mm)**			***L* (mm)**			***L* (mm)**		
		10	**20**	**30**	**10**	**20**	**30**	**10**	**20**	**30**	**10**	**20**	**30**
0	*EAC*	4439	4439	4439	5867	5867	5867	7427	7427	7427	8945	8945	8945
0.25	*EAC*	4991	5457	5215	7055	7610	7210	8644	9725	9057	10421	11314	10080
	$(EAC)_f$	552	1018	776	1188	1743	1343	1217	2298	1630	1476	2369	1135
0.5	*EAC*	5557	6196	5625	8211	8665	8305	9910	10870	10572	12064	13323	12680
	$(EAC)_f$	1118	1757	1186	2344	2798	2438	2483	3443	3145	3119	4378	3735
0.75	*EAC*	6114	7045	6577	8542	9670	8852	10440	11655	11045	12772	13996	13906
	$(EAC)_f$	1675	2606	2138	2675	3803	2985	3013	4228	3618	3827	5051	4961
1	*EAC*	5775	6485	6234	8232	8582	8449	10299	11135	10560	12196	13127	13184
	$(EAC)_f$	1336	2046	1795	2365	2715	2582	2872	3708	3133	3251	4182	4239

The *EAC* and $(EAC)_f$ values for all reinforced specimens moulded at varying dry unit weight (Series 1 & 2) are tabulated in Table 6.10, and the effect of fibre content under 100 kPa confining pressure on the *EAC* of specimens is shown in Fig 6.19. At any dry unit weight, the *EAC* increases with increasing fibre content to a maximum value with 0.75% fibres and then reduces with 1% fibres. With greater dry unit weight, there is continuous increase in *EAC* for any soil-fibre mix. The maximum *EAC* values under 100 kPa confining pressure for specimens of 14.3, 15.1, 16.0 and 16.8 kN/m^3 dry unit weights are 5623, 5983, 6662 and 7045 kJ/m^3, respectively with the optimum reinforcement (0.75% fibres of 20 mm length). The same trends can be noted under all other confining pressures (Table 6.10).

The effect of confining pressure on *EAC* of specimen with 0.75% fibres of 20 mm length under varying dry unit weights (Series 1 & 2) is presented in Fig. 6.20. For the same fibre reinforcement and dry unit weight, the *EAC* of specimen increases with increasing confining pressure. The maximum *EAC* values of specimens at dry unit weights of 14.3, 15.1, 16.0 and 16.8 kN/m^3 are 10989, 12060, 13087 and 13996 kJ/m^3, respectively under 400 kPa confining pressure. From Figs. 6.19 & 6.20, it can be inferred that for any combination of fibre content and fibre length, the *EAC* will be greater with increasing dry unit weight.

The variation of $(EAC)_f$ with fibre content under 100 kPa confining pressure for specimens, reinforced with 20 mm fibres and moulded at varying dry unit weight is shown in Fig. 6.21 (Series 1 & 2). At any dry unit weight, the $(EAC)_f$ value is observed to increase only up to 0.75% fibre content. However, for the same fibre content, no particular trend can be noted for the $(EAC)_f$ variation with dry unit weight as it is not the maximum at MDU (Table 6.10). This is in contrast to the consistent trend of *EAC* variation with dry unit weight.

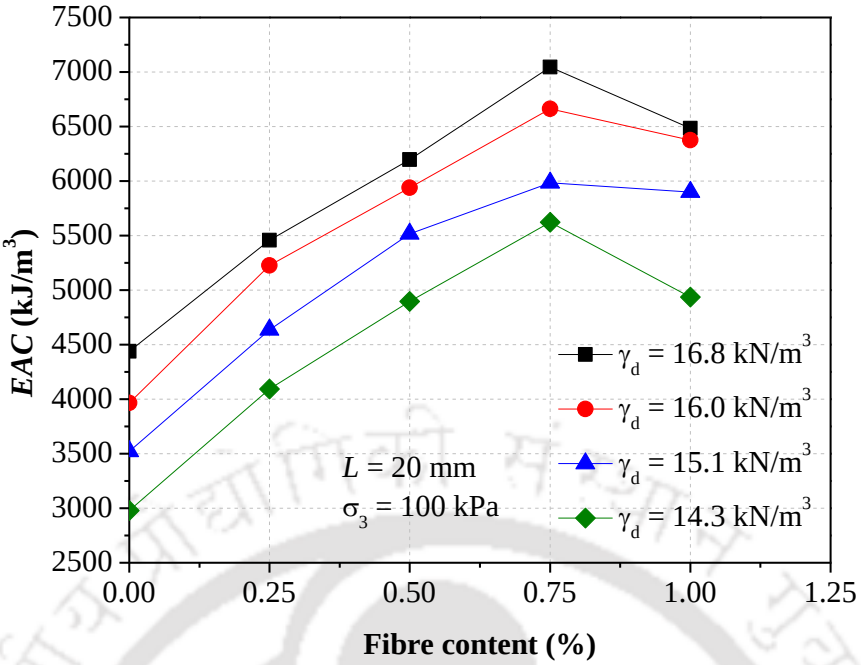

Fig. 6.19 Effect of fibre content on *EAC* variation under 100 kPa confining pressure for specimens reinforced with 20 mm fibres and moulded at OMC with varying dry unit weight (Series 1 & 2)

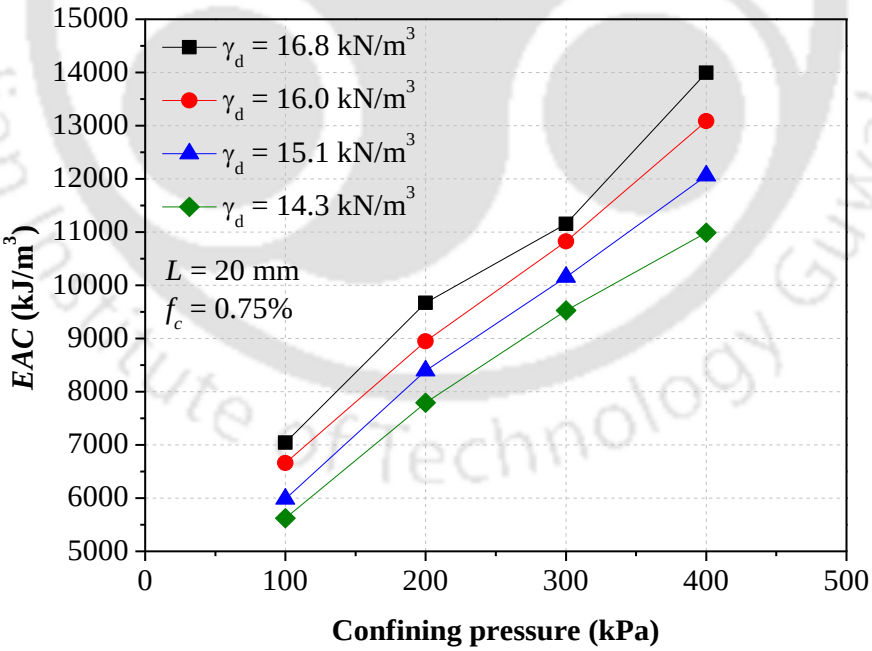

Fig. 6.20 Effect of confining pressure on *EAC* variation for specimens reinforced with 0.75% fibres of 20 mm length and moulded at OMC with varying dry unit weight (Series 1 & 2)

Table 6.10 Summary of *EAC* and $(EAC)_f$ of all specimens moulded at OMC with varying dry unit weight (Series 1 & 2)

f_c (%)		***EAC* and $(EAC)_f$, (kJ/m^3)**															
		σ_3 = 100 kPa				**σ_3 = 200 kPa**				**σ_3 = 300 kPa**				**σ_3 = 400 kPa**			
		γ_d (kN/m^3)				**γ_d (kN/m^3)**				**γ_d (kN/m^3)**				**γ_d (kN/m^3)**			
		14.3	**15.1**	**16.0**	**16.8**	**14.3**	**15.1**	**16.0**	**16.8**	**14.3**	**15.1**	**16.0**	**16.8**	**14.3**	**15.1**	**16.0**	**16.8**
0	*EAC*	2978	3520	3965	4439	4382	4156	5710	5867	5740	6268	7157	7427	6652	7228	8565	8945
0.25	*EAC*	4092	4636	5425	5457	5623	6264	7135	7610	6980	7735	8860	9725	8256	9422	10375	11314
	$(EAC)_f$	1114	1116	1460	1018	1241	2108	1425	1743	1240	1467	1703	2298	1604	2194	1810	2369
0.5	*EAC*	4896	5815	5940	6196	6922	7972	8460	8665	8402	9648	10284	10870	9661	11455	12090	13323
	$(EAC)_f$	1918	2295	1975	1757	2540	3816	2750	2798	2662	3380	3127	3443	3009	4227	3525	4378
0.75	*EAC*	5623	5983	6662	7045	7791	8396	8948	9670	9520	10124	10836	11655	10989	12060	13087	13996
	$(EAC)_f$	2645	2463	2697	2606	3409	4240	3238	3803	3780	3856	3679	4228	4337	4832	4522	5051
1	*EAC*	4935	5998	6376	6485	6608	8090	8582	8582	7465	9890	10610	11135	9490	11926	12685	13127
	$(EAC)_f$	1957	2478	2411	2046	2226	3934	2872	2715	1725	3622	3453	3708	2838	4698	4120	4182

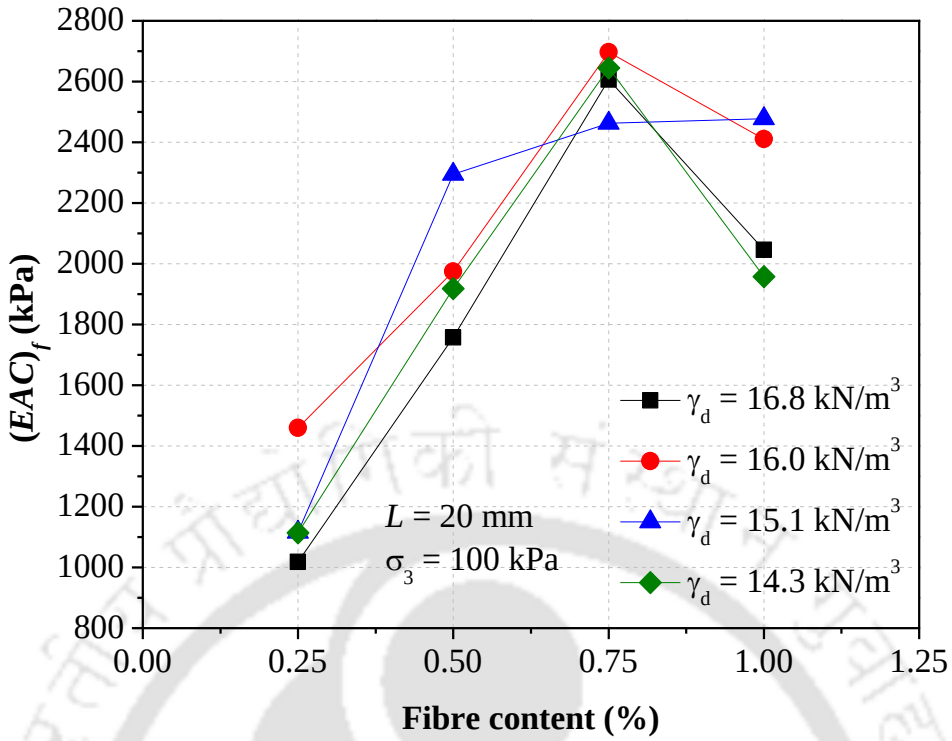

Fig. 6.21 Effect of fibre content on $(EAC)_f$ variation under 100 kPa confining pressure for specimens reinforced with 20 mm fibres and moulded at OMC with varying dry unit weight (Series 1 & 2)

The variation of $(EAC)_f$ with fibre content under varying confining pressure for specimens, reinforced with 20 mm fibres and moulded at MDU, is presented in Fig. 6.22. Under any confining pressure, the $(EAC)_f$ value increases with fibre content up to 0.75%. At any fibre content, the $(EAC)_f$ value is greater for a higher confining pressure. With optimum reinforcement and under 100 kPa confining pressure, the maximum $(EAC)_f$ values of the specimens are 2645, 2463, 2697 and 2606 kJ/m^3, respectively at 14.3, 15.1, 16.0 and 16.8 kN/m^3 dry unit weight (Table 6.10). The $(EAC)_f$ value further increases to maximum values of 4337, 4832, 4522 and 5051 kJ/m^3, respectively at 14.3, 15.1, 16.0 and 16.8 kN/m^3 dry unit weight at 400 kPa confining pressure.

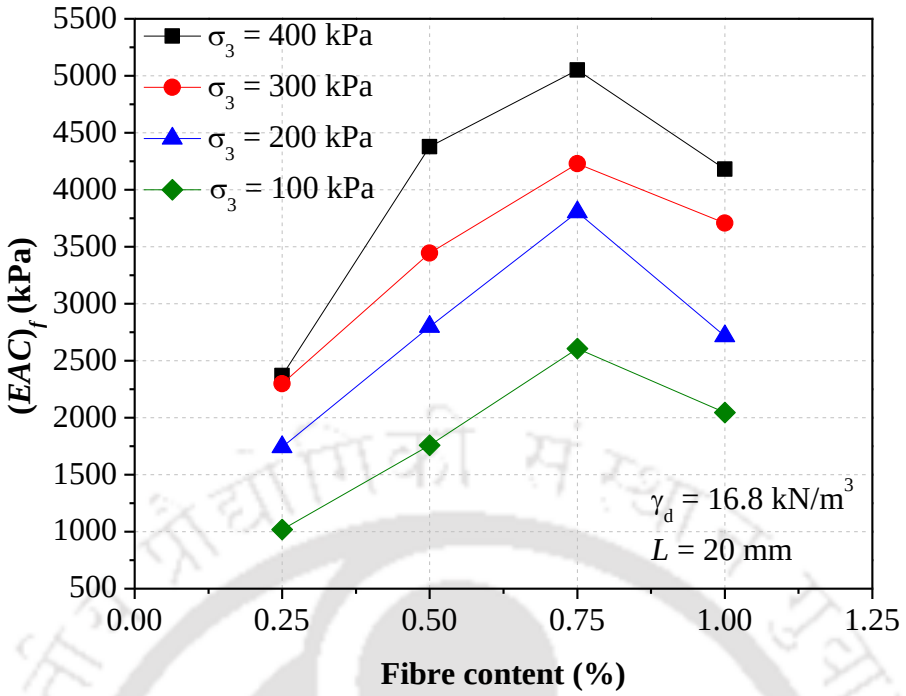

Fig. 6.22 Effect of fibre content on $(EAC)_f$ variation under varying confining pressure for specimens reinforced with 20 mm fibres and moulded at OMC and MDU (Series 1 & 2)

6.4 Regression Analysis

Multiple regression analysis is a statistical tool for the investigation of relationship between dependent and independent variables. The relationship between dependent and independent variables is expressed as follows:

$$y_i = a_o + a_1 x_{i1} + a_2 x_{i2} + \ldots\ldots + a_k x_{ik} \tag{6.7}$$

where i = 1, 2, 3……., n is the number of observations; y_i is dependent variable; x_{i1}, x_{i2},….,x_{ik} are independent variables; and a_0, a_1, a_2,….,a_k are regression coefficients.

The major principal stress at failure of the glass fibre-reinforced clayey soil is influenced by fibre content, fibre aspect ratio, dry unit weight and confining pressure. On the basis of the experimental data, an attempt has been made to develop a relationship to estimate the major principal stress at failure as a function of the influencing parameters. The developed representative equation is as follows:

$$\log_{10}(\sigma_{1f}) = 0.371 + 0.121\log_{10}(f_c) + 0.037\log_{10}(\frac{L}{d}) + 0.773\log_{10}(\gamma_d) + 0.636\log_{10}(\sigma_3) \quad (6.8)$$

$$\Rightarrow \sigma_{1f} = 2.35(f_c)^{0.121}(\frac{L}{d})^{0.037}(\gamma_d)^{0.773}(\sigma_3)^{0.636} \quad (6.9)$$

where σ_{1f} = major principal stress at failure (kPa); f_c = fibre content (%); L/d = fibre aspect ratio; γ_d = dry unit weight of specimen (kN/m^3) and σ_3 = confining pressure (kPa).

Statistic for goodness of fit such as multiple coefficient of determination R^2, adjusted value of R^2 (i.e. R_a^2) and standard error (E_s) have been determined to check how well the model fits the experimental data. The expression yielding the largest value of R^2, R_a^2 and the smallest value of E_s is considered the best fit. The values of R^2, R_a^2 and E_s for the best fit expression obtained from the regression analysis are given in Table 6.11. The respective values of R^2, R_a^2 and standard error for Eqn. 6.9 are 0.99, 0.98 and 0.018, indicating excellent quality of the fit for the representative equation.

Table 6.11 Goodness of fit statics for major principal stress at failure

Regression Statistics	
Multiple R	0.99
R Square	0.99
Adjusted R Square	0.98
Standard Error	0.018
Observations	96

To determine the effectiveness of the entire representative equation, significance tests have been performed by applying F-test. The significance of individual regression coefficient can be assessed through t-test. The significance level α has been set to be 0.05, and the results of analysis of variance (ANOVA) are given in Table 6.12. For the F-test, the null hypothesis implies that none of the independent variables are related to the dependent variable, whereas the alternate hypothesis suggests that at least one of the independent variables is related to the

dependent variable. From F distribution table with α = 0.05 and degrees of freedom df = (4, 91), the critical value of F (i.e. F_{crt}) for the present analysis is found to be 2.32 for Eqn. 6.9. As F_{crt} is smaller than the calculated value of F, the null hypothesis is rejected, indicating that at least one of the independent variables of Eqn. 6.9 explains the variation of the dependent variable.

Table 6.12 ANOVA table for major principal stress at failure

	Degree of freedom (df)	**Sum of Squares**	**Mean Squares**	**F**	**Significance F**
Regression	4	2.102	0.526	1543.857	0.0
Residual	91	0.031	0.0		
Total	95	2.133			

Table 6.13 Summary of t-statistics for major principal stress of failure

	Coefficient	**Standard Error**	**T stat**	**P-value**
Intercept	0.370	0.095	3.908	0.0
Variable 1 (log f_c)	0.121	0.008	14.549	0.0
Variable 2 (log L/d)	0.037	0.013	2.774	0.0
Variable 3 (log γ_d)	0.773	0.008	76.432	0.0
Variable 4 (log σ_3)	0.636	0.070	10.950	0.0

The summary of the t-value for various individual predictor parameters are given in Tables 6.13 for Eqn. 6.9. From the student's t-table, the critical value of t (i.e. t_{crt}) with α/2 = 0.025 and df = 96 is found to be 1.985 for Eqn. 6.9. For the t-test, the null hypothesis implies that the particular predictor variable is not related to the dependent variable. The alternative hypothesis suggests that the individual predictor variable is related to the dependent variable. Similar hypothesis has been assumed for all the independent variables. From Table 6.13, it is noted that t values for all independent predictor variables lie in the range of:

$$|t_{cal}| \geq t_{crit} \tag{6.10}$$

The above test results confirm that the proposed representative equation is valid.

6.5 SUMMARY

Consolidated undrained (CU) triaxial test was carried out to study the effect of glass fibre reinforcement and dry unit weight variation of compacted clayey soil specimens. The effect of reinforcement and specimen dry unit weight variation on deviator stress-axial strain, specimen deformation mode, pore pressure generation, secant modulus, shear strength and *EAC* behaviour under varying confining pressure was studied. The following conclusions have been drawn from the test results:

1. At any moulding dry unit weight and confining pressure, the failure deviator stress of reinforced specimens increases with increasing fibre content or fibre length to reach a maximum value with 0.75% fibres of 20 mm length. With increasing dry unit weight or confining pressure, the failure deviator stress increases.
2. For constant initial dry unit weight, under undrained condition, the positive pore water pressure of reinforced specimens at failure increases with the increase of any of fibre content, fibre length or confining pressure keeping the others constant. With increasing specimen dry unit weight, the magnitude of positive pore water pressure decreases.
3. For the same initial dry unit weight, the bulging deformation of unreinforced specimen is reduced more with increasing fibre content, fibre length or confining pressure. The reinforced specimen shows least bulging resembling an intact column, with 1% fibres of 30 mm length under 400 kPa confining pressure.
4. The shear strength of the clayey soil is the maximum with 0.75% fibres of 20 mm length. At dry unit weights of 14.3, 15.1, 16.0, and 16.8 kN/m^3, the maximum fibre contributions to the cohesion intercept and friction angle are 29 kPa and 9.9˚, 25 kPa and 10.3˚, 25 kPa and 10.3˚, and 22 kPa and 9.4˚, respectively.

5. The maximum shear strength parameters (c' = 57 kPa and ϕ' = 32.8°) of the reinforced specimen with the lowest dry unit weight of 14.3 kN/m^3 are greater than that of the unreinforced specimen (c' = 45 kPa and ϕ' = 25.8°) with the highest dry unit weight of 16.8 kN/m^3.

CHAPTER 7

SHEAR STRENGTH BEHAVIOUR OF FIBRE-REINFORCED SANDY SOIL

7.1 INTRODUCTION

The load-deformation, stiffness and shear strength behaviour of randomly distributed glass fibre-reinforced sandy soil specimens have been studied by carrying out consolidated drained (CD) triaxial compression tests. The effects of fibre content, fibre length, relative density and confining pressure have been evaluated, and the details are presented in the following sections.

7.2 EXPERIMENTAL PROGRAMME

The summary of all test specimens is given in Table 7.1. Sand specimens (38 mm diameter and 76 mm height) of different relative densities (D_r = 35, 65 and 85%) and reinforced with varying fibre content (f_c = 0, 0.5, 1, 2, 3 and 4%) and varying fibre length (L = 10, 20 and 30 mm), were tested under varying confining pressure (σ_3 = 100, 200, 300 and 400 kPa). The results of the unreinforced sand have been used as reference for quantifying the effects of fibre reinforcement. Both the unreinforced and fibre-reinforced specimens were prepared on the pedestal of the triaxial base plate using a split sampler, as elaborated in Section 3.4. All the triaxial tests were carried out as per ASTM D 4767-11.

Table 7.1 Summary of CD test specimens of sandy soil

Series	Fibre content, f_c (%)	Fibre length, L (mm)	Relative density, D_r (%)
1	0, 0.5, 1, 2, 3, 4	10, 20, 30	35, 65, 85

7.3 RESULTS AND DISCUSSION

7.3.1 Stress-Strain Response

7.3.1.1 Effect of Fibre Content

Typical effect of fibre content on the deviator stress-axial strain and volumetric strain-axial strain behaviour of the sand specimens at relative densities of 35% and 85% are presented in Figs. 7.1 and 7.2, under low (σ_3 = 100 kPa) and high (σ_3 = 400 kPa) confinement pressures, respectively. Even though the initial stiffness has decreased with fibre addition, the stress-strain curves show clear improvement in peak stress at both relative densities under low and high confining pressures. Failure strain also increases with fibre content indicating an increase in the ductility of the reinforced sand. The loss of initial stiffness is attributed to the change of specimen fabric with inclusion of fibres which causes non-homogeneous porosity, resulting in the lower porosity of soil matrix away from the fibres (Michalowski and Cermak 2003). During hydrostatic loading, the fibres experience compression and bending. Later, at the time of shear loading, the fibres undergo gradual stretching, resulting in improved stiffness and strength.

The effect of fibre content on initial stress-strain response of reinforced specimen is marginal up to about 2% axial strain (Figs. 7.1 & 7.2). The contribution of fibres to the strength of specimen is observed to start at a higher strain level above 2% with mobilization of tensile strength of fibres. Thus, at small strain levels, the resistance to the applied load is mostly taken by the soil particles and the contribution of fibres start after some initial soil deformation, as fibres work in tension only (Maher and Gray 1990; Zornberg 2002).

The improvement in strength reaches the optimum at 3% fibre content and thereafter shows reduction or only marginal additional strength gain with 4% fibres. At 4% fibre content, the homogeneous mixing of the glass fibres was also found to be difficult during specimen preparation as lumping of the fibres was noticeable. In this way, it can be stated

that fibre mixing difficulty can give information regarding the optimum fibre content.

During shearing, the fibres within the specimen locally stitch up potential slip planes that start to develop. With continuous shearing, the fibres get stretched on both sides of developing potential shear zone, and transfer some shear stress and strain to zones further away in the reinforced specimen, resulting in improved overall performance (Ozkul and Baykal 2007). In these zones, the additional tensile restraint of the fibres provide more effective interlocking in the soil matrix which increases the overall strength. With increasing fibre content, the number of fibres crossing the shear plane increases and the stress-strain response is further enhanced with increasing fibre content.

For specimens of 85% relative density, a clear post-peak stress drop appears, which reaches residual stress level around 15-20% axial strain (Figs. 7.1a & 7.2a). In case of specimens of 35% relative density, the reduction in post-peak stress after peak is very small up to 20% axial strain. Nevertheless, the residual stress of reinforced specimen is higher than that of unreinforced specimen. This indicates that the glass fibre-reinforced sand can bear greater load even at larger deformation compared to unreinforced soil.

From volumetric strain-axial strain response (Figs. 7.1b & 7.2b), it is evident that the specimens of 35% relative density have undergone mainly contraction, and the magnitude increases with fibre content. Fibre-reinforced specimens with 85% relative density have shown contraction at low axial strain followed by dilation at larger axial strain. With increasing fibre content, the initial volumetric compression is noted to increase whereas the dilation is noted to decrease. Thus, the effect of fibre reinforcement is to increase the specimen compression at 35% relative density sand and to restrain the dilation of the sand at 85% relative density, which results in better mobilization of soil-fibre surficial interaction leading to strength improvement.

The results are in agreement with the findings of Michalowski and Zhao (1996),

Consoli et al. (1998), Michalowski and Cermak (2003) and Mashiri et al. (2015), in which the dilation of sand decreased with reinforcement inclusion. On the other hand, from direct shear tests, Kaniraj and Havanagi (2001) and Sadek et al. (2010) found increase in dilation due to fibre reinforcement of fly ash-soil and sand, respectively.

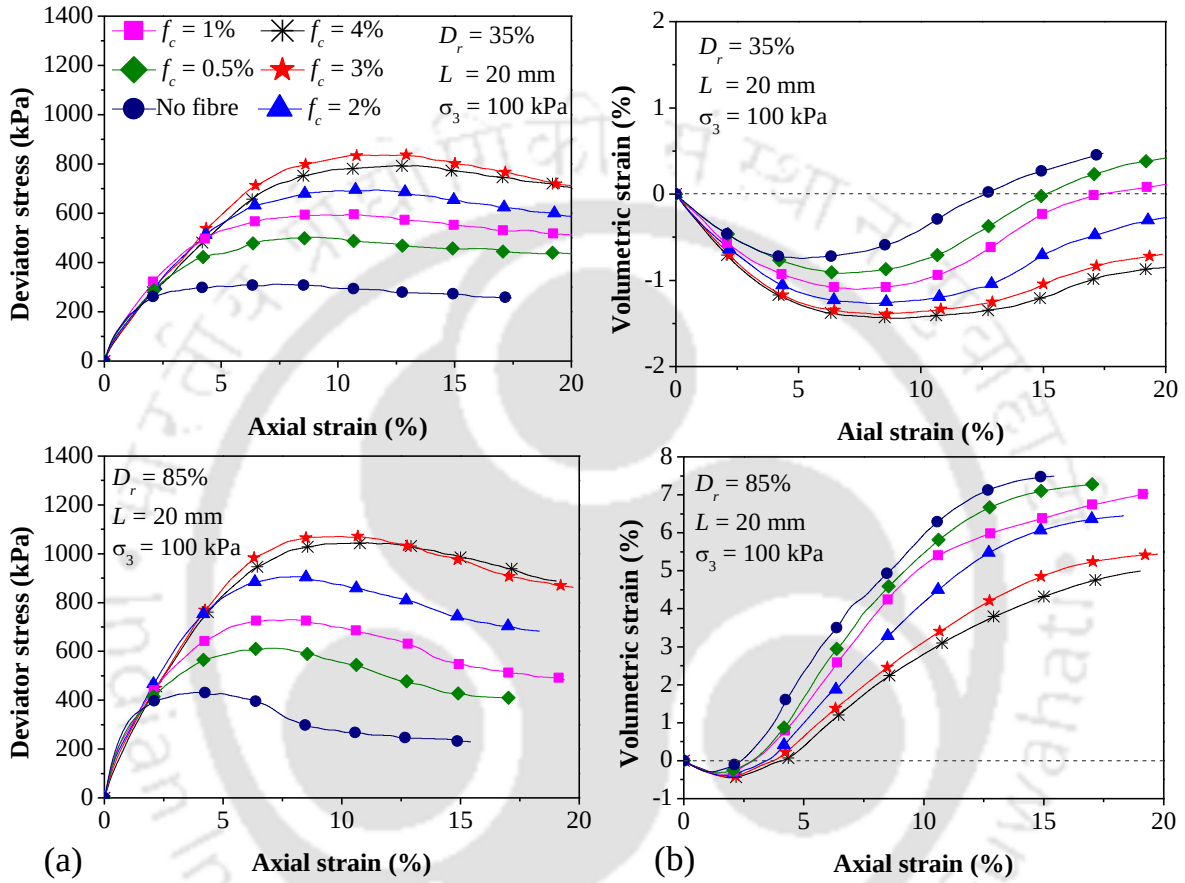

Fig. 7.1 Effect of fibre content under 100 kPa confining pressure on behaviour of specimens reinforced with 20 mm fibres and moulded at low (D_r = 35%) and high (D_r = 85%) relative densities: (a) deviator stress-axial strain response; (b) volumetric strain-axial strain response

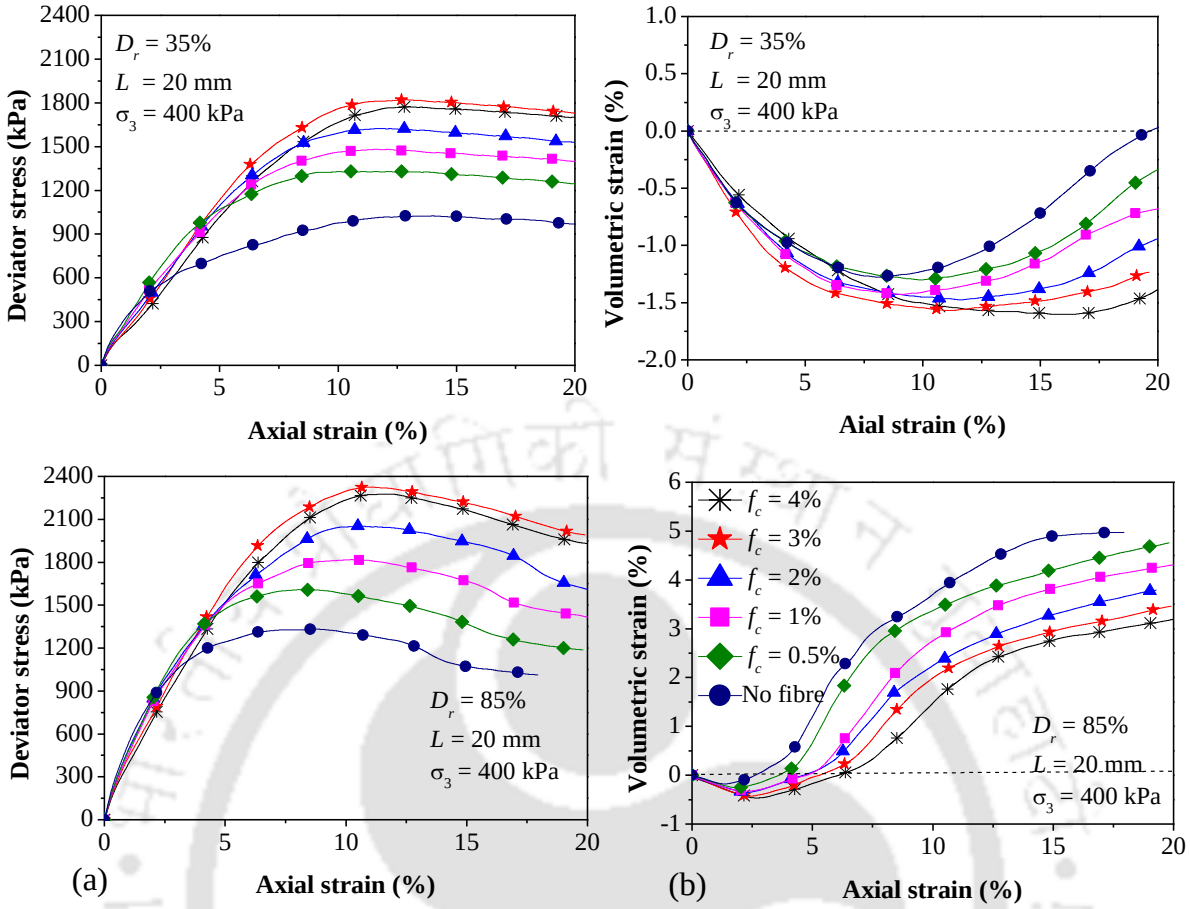

Fig. 7.2 Effect of fibre content under 400 kPa confining pressure on behaviour of specimens reinforced with 20 mm fibres and moulded at low (D_r = 35%) and high (D_r = 85%) relative densities: (a) deviator stress-axial strain response; (b) volumetric strain-axial strain response

The effect of fibre content on stress-strain behaviour can be further analyzed from the failure modes shown in Figs. 7.3 and 7.4 for specimens of 35% and 85% relative density. It must be noted that these pictures of the failure modes were taken at the end of the test when the specimens were in the residual state, much beyond the peak stress axial strain. At 35% relative density, the unreinforced specimen shows bulging failure (Fig. 7.3a). As the specimen is reinforced with fibres, the bulging gradually decreases with 2% fibres (Fig. 7.3b) to a minimum with 4% (Fig. 7.3c).

At 85% relative density, the unreinforced specimen undergoes shear failure and the failure plane extends over the entire specimen height from top to bottom (Fig. 7.4a). For the

fibre-reinforced specimen, the rupture is localized in a relatively smaller height (Figs. 7.4b & 7.4c), and this is indicative of less brittleness of the reinforced specimen. The residual strain levels corresponding to Figs. 7.4a, 7.4b & 7.4c are in an increasing order (Fig. 7.1a). Consoli et al. (2009b) found that fibre-reinforced sand specimen shows typically a ductile response by bulging failure.

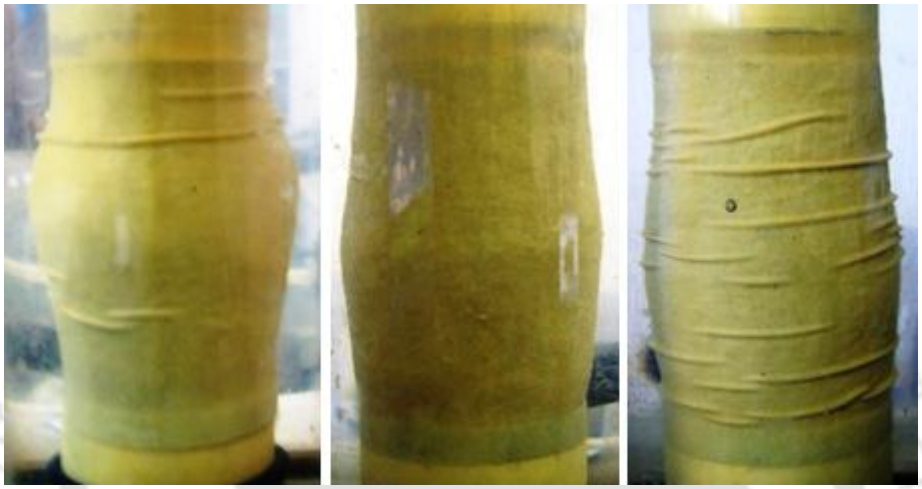

(a) (b) (c)

Fig. 7.3 Effect of fibre content under 100 kPa confining pressure on failure mode of sand specimens reinforced with 20 mm fibres and moulded at 35% relative density: (a) unreinforced; (b) f_c = 2%; (c) f_c = 4%

(a) (b) (c)

Fig. 7.4 Effect of fibre content under 100 kPa confining pressure on failure mode of sand specimens reinforced with 20 mm fibres and moulded at 85% relative density: (a) unreinforced; (b) f_c = 2%; (c) f_c = 4%

7.3.1.2 Effect of Fibre Length

Typical effect of fibre length on the deviator stress-axial strain and volumetric strain-axial strain response of the sand specimens at relative densities of 35% and 85% are presented in Figs. 7.5 and 7.6, under low (100 kPa) and high (400 kPa) confining pressures, respectively. The stress-strain response of specimen increases with increasing fibre length up to 20 mm fibres for all relative densities and confining pressures (Figs. 7.5a & 7.6a), and then decreases with the 30 mm long fibres. The improvement in strength with fibre length is due to the increased surface area of individual fibre, which provides more surface interaction between soil and fibres, and better mobilization of fibre tensile strength at the time of shearing (Maher and Gray 1990, Maher and Ho 1994). With 30 mm fibres, it was noted during specimen preparation that there was more folding and bending of the fibres in the 38 mm diameter specimen, both at the perimeter surface as well as between the three moulded layers of about 25 mm each. This has not allowed the utilization of full fibre length for mobilization of tensile strength, resulting in drop of stress-strain response. This indicates that fibre length around 50% of the diameter of specimen can provide maximum strength improvement.

The peak stress occurs when fibre-induced distributed tension reaches its maximum. If the developed maximum interface friction is lower than the tensile strength of the fibre, failure of specimen is due to the pullout of fibres. With increase in fibre length, the failure axial strain of the reinforced specimens has not varied noticeably for the same relative density and confining pressure (Figs. 7.5a & 7.6a). As longer fibres can facilitate larger shear deformation to mobilize greater interface friction between soil and fibres, the macroscopic axial strain at peak stress will increase with fibre length, in case there are no boundary effects (Michalowski 2008). Stress-strain response after peak is followed by stress drop, which is greater for specimens of 85% relative density under both low and high confining pressures (Figs. 7.5a and 7.6a). Nevertheless, the residual strength remains much higher than that of

unreinforced soil at both relative densities and confining pressures.

Observing the volumetric strain-axial strain response, it can be noted that the specimen of 35% relative density undergoes mainly contraction which increases only up to 20 mm. Specimens of 85% relative density exhibit contraction at small axial strain followed by dilation at larger axial strain (Figs. 7.5b & 7.6b). With increase in fibre length, initial volumetric contraction is noted to increase whereas the dilation is observed to decrease. This indicates that if the compression of specimen is increased or the dilation of specimen is restrained due to the varying fibre length, it should result in better surficial interaction between soil and fibres causing overall strength improvement.

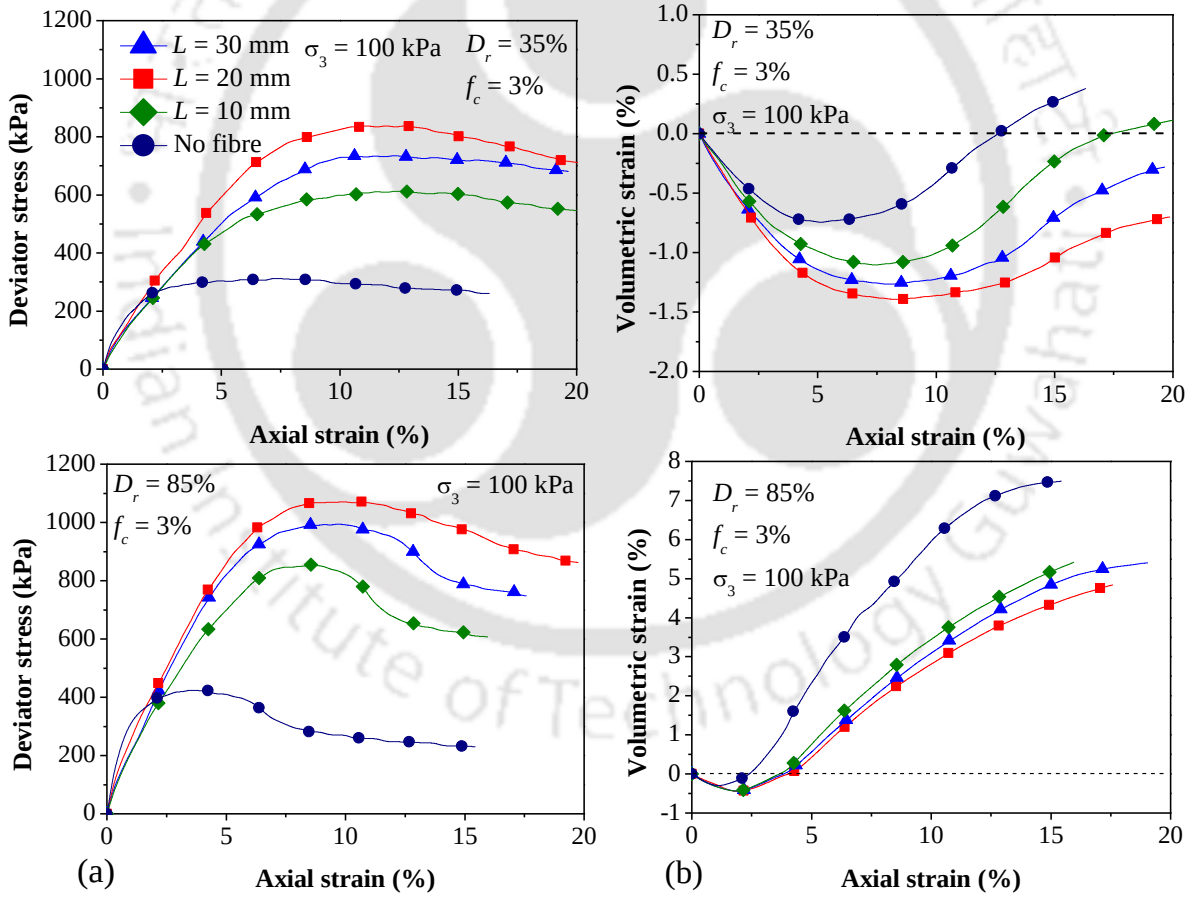

Fig. 7.5 Effect of fibre length under 100 kPa confining pressure on behaviour of sand specimens reinforced with 3% fibres and moulded at low (D_r = 35%) and high (D_r = 85%) relative densities: (a) deviator stress-axial strain response; (b) volumetric strain-axial strain response

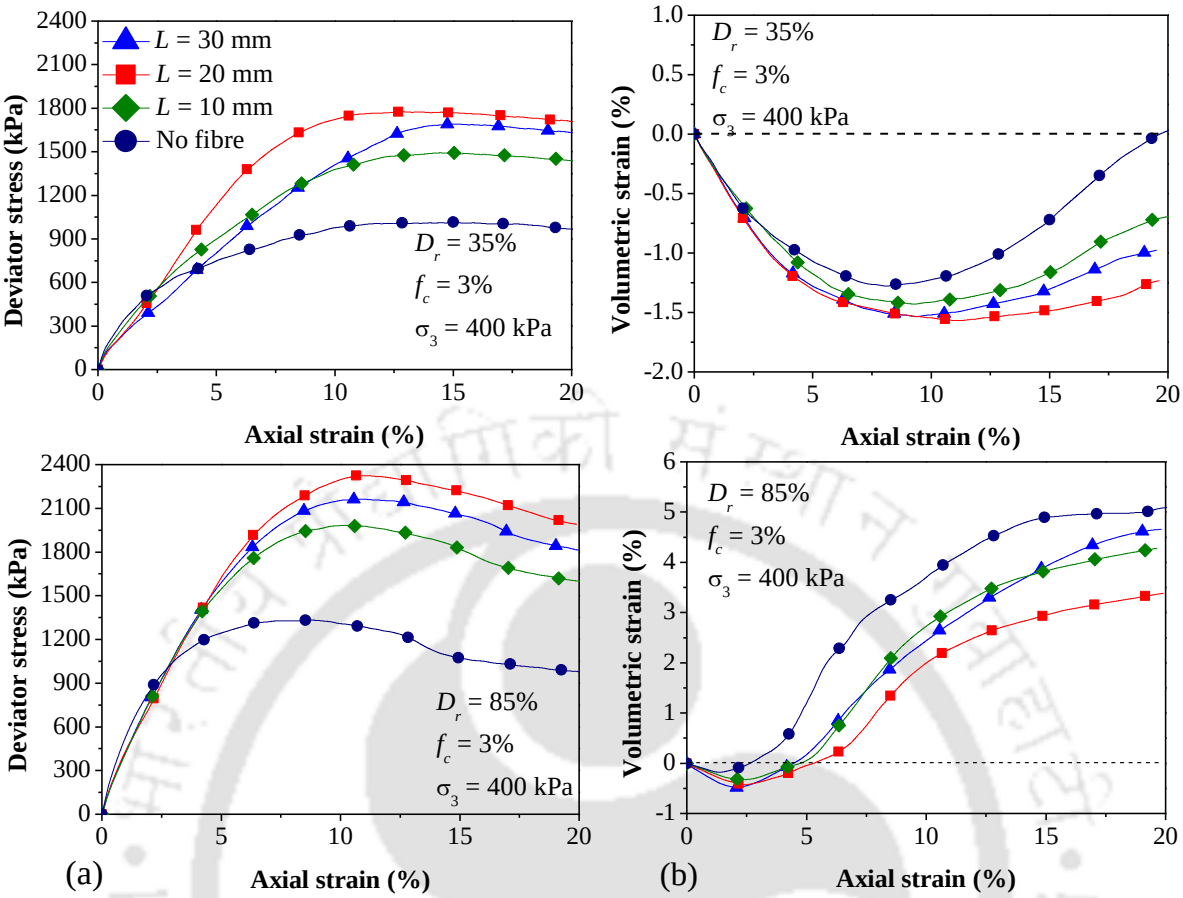

Fig. 7.6 Effect of fibre length under 400 kPa confining pressure on behaviour of sand specimens reinforced with 3% fibres and moulded at low (D_r = 35%) and high (D_r = 85%) relative densities: (a) deviator stress-axial strain response; (b) volumetric strain-axial strain response

Typical failure patterns under 100 kPa confining pressure, depicting the effect of fibre length for reinforced specimens of 85% relative density with 3% fibre content are presented in Fig. 7.7. In contrast to the unreinforced specimen experiencing clear shear failure (Fig. 7.7a), the specimen with short fibres (i.e. L = 10 mm) showed initial bulging followed by mild shearing failure near to the residual state (Fig. 7.7b) This is attributed to the reason that at the time of axial loading in the test, though there will always be a tendency for the development of a shear plane in a specimen of 85% relative density, a large number of the short 10 mm fibres has been capable in stitching up the developing shear plane and thus restrict its formation till the residual type.

For the same 3% fibre content and with 20 mm and 30 mm fibres, even though the soil-fibre composite sustains higher load prior to its failure, the number of fibres is not sufficient for preventing the shear plane development (Figs. 7c & 7d). As the fibre length increases, increased surface area of individual fibre exhibits increased resistance against fibre pullout and in response it holds the soil mass against volume expansion. As a result, the soil-fibre composite sustains higher load prior to its failure at larger strain level when fibres start getting pulled out, mostly along some critical plane and this appears as local rupture of specimen at higher axial strain (Figs. 7c & 7d).

(a) (b) (c) (d)

Fig. 7.7 Effect of fibre length under 100 kPa confining pressure on failure mode of sand specimens reinforced with 3% fibres and moulded at 85% relative density: (a) unreinforced; (b) L = 10 mm; (c) L = 20 mm; (d) L = 30 mm

Typical failure patterns under 100 kPa confining pressure, depicting the effect of fibre length for reinforced specimens of 35% relative density with 3% fibre content are presented in Fig. 7.8. All specimens experienced bulging failure with any fibre length (Figs. 7.8a to 7.8d). However, the extent of bulging reduces progressively with increasing fibre length and with longest fibre of 30 mm length the specimen shows least bulging (Fig. 7.8d).

(a) (b) (c) (d)

Fig. 7.8 Effect of fibre length under 100 kPa confining pressure on failure mode of sand specimens reinforced with 3% fibres and moulded at 35% relative density: (a) unreinforced; (b) L = 10 mm; (c) L = 20 mm; (d) L = 30 mm

7.3.1.3 Effect of Confining Pressure

Figs. 7.9a and 7.9b show a comparison under varying confining pressure of the deviator stress-axial strain and volumetric strain-axial strain response of unreinforced and fibre-reinforced sand specimens, of different relative densities (35%, 65% and 85%). At the same confining pressure, for specimens of all relative densities, the initial stiffness of the reinforced specimen is lower than that of the unreinforced specimen whereas the peak deviator stress and corresponding failure axial strain are higher. With increasing confining pressure, the initial stiffness, peak deviator stress and failure axial strain have increased for all unreinforced and fibre-reinforced specimens. Thus, it can be said that the specimen shows more smooth failure with increase in confining pressure. For the specimens of 35%, 65%, 85% relative densities, the contribution of 3% fibres leads to increase of peak deviator stress by 526 and 568 kPa; 576 and 799 kPa; 860 and 983 kPa; respectively under 100 and 400 kPa confining pressures (Figs. 7.9a).

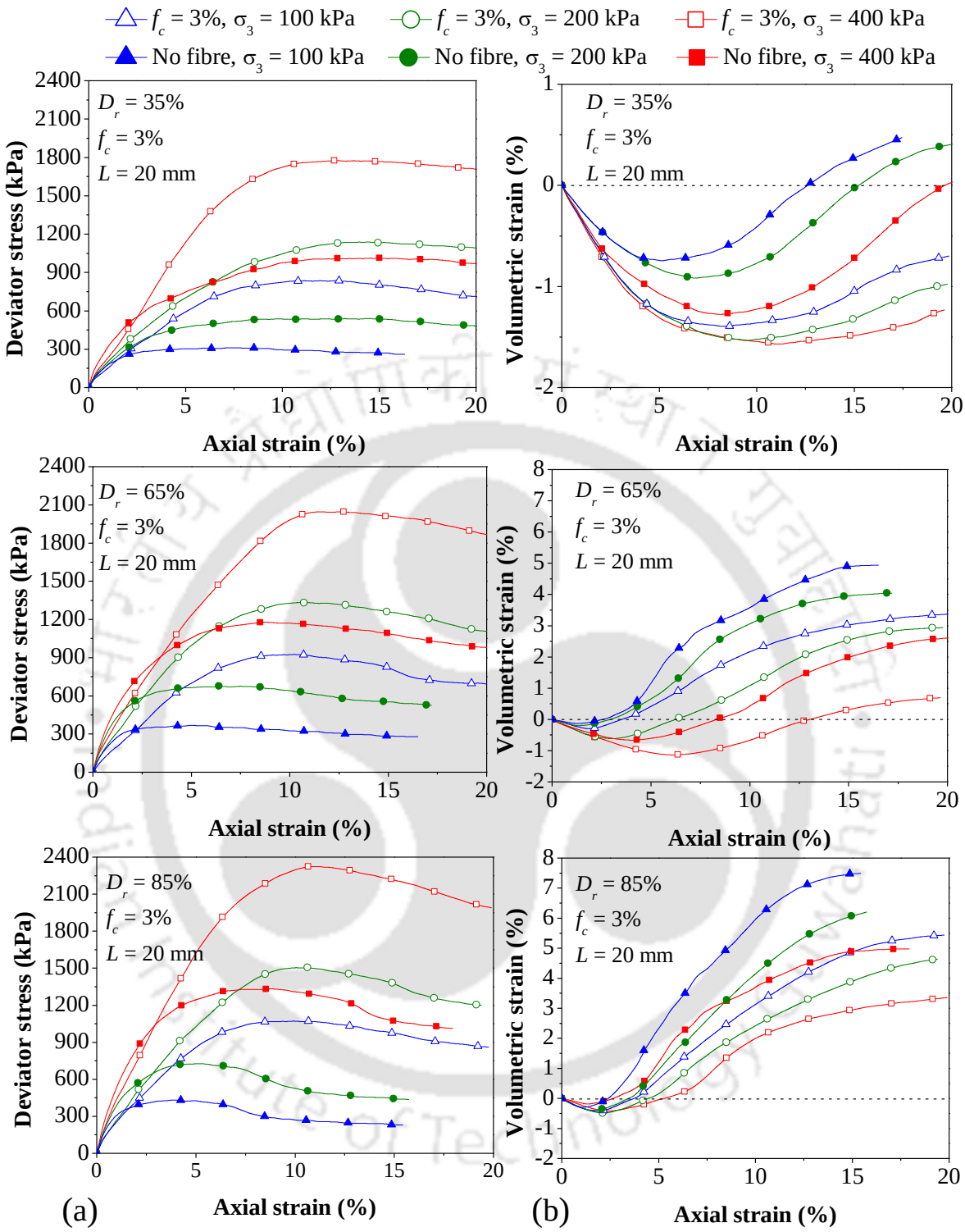

Fig. 7.9 Effect of confining pressure on behaviour of sand specimens reinforced with of 3% fibres of 20 mm length and moulded at varying relative density: (a) deviator stress-axial strain response; (b) volumetric strain-axial strain response

Observing the volumetric strain-axial strain curves, for the specimens of all relative densities, it has been noted that with increasing confining pressure, there is increase in contraction at smaller axial strain and reduction in dilation at larger axial strain (Fig. 7.9b). The increase in specimen contraction and reduction of specimen dilation with increasing confining pressure enhances the soil-fibre and soil-soil surficial interaction, resulting in strength improvement for both unreinforced and reinforced specimens. Similar effect with confining pressure has been reported by Michalowski and Zhao (1996), Consoli et al. (1998), Michalowski and Cermak (2003), Hamidi and Hooresfand (2013) and Mashiri et al. (2015).

The effect of confining pressure on the failure patterns of fibre-reinforced sand specimens of 35%, 65% and 85% relative densities are shown in Figs. 7.10, 7.11 and 7.12, respectively. For the unreinforced specimen of 35% relative density, under 100 kPa confining pressure, bulging failure is observed (Fig. 7.10a), and specimen bulging noted to reduce with inclusion of 3% fibres (Fig. 7.10b). At 400 kPa confining pressure, the unreinforced specimen also shows prominent bulging failure (Fig. 7.10c), and this bulging gets reduced with fibre inclusion and found to be least (Fig. 7.10d). This is a clear indication of the increase in specimen ductility with increasing confining pressure.

For the unreinforced specimen of 65% relative density, under 100 kPa confining pressure, a noticeable shear failure plane appears (Fig. 7.11a) but the shear plane becomes marginal with 3% fibres (Fig. 7.11b). However, at 400 kPa confining pressure, the unreinforced specimen shows prominent bulging failure (Fig. 7.11c), and this bulging gets reduced with fibre inclusion (Fig. 7.11d).

At 85% relative density under 100 kPa confining pressure, a noticeable shear failure plane appears in the unreinforced specimen (Fig. 7.12a), which becomes less prominent in the fibre-reinforced specimen (Fig. 7.12b). However, at 400 kPa confining pressure, the shear plane becomes marginal for unreinforced specimen (Fig. 7.12c), and with fibre inclusion it

diminishes further along with some bulging (Fig. 7.12d).

(a) (b) (c) (d)

Fig. 7.10 Effect of low and high confining pressures on failure mode of unreinforced and reinforced sand specimens with 3% fibres of 20 mm length and moulded at 35% relative density: (a) unreinforced, σ_3 = 100 kPa; (b) reinforced, σ_3 = 100 kPa; (c) unreinforced, σ_3 = 400 kPa; (d) reinforced, σ_3 = 400 kPa

(a) (b) (c) (d)

Fig. 7.11 Effect of low and high confining pressures on failure mode of unreinforced and reinforced sand specimens with 3% fibres of 20 mm length and moulded at 65% relative density: (a) unreinforced, σ_3 = 100 kPa; (b) reinforced, σ_3 = 100 kPa; (c) unreinforced, σ_3 = 400 kPa; (d) reinforced, σ_3 = 400 kPa

(a) (b) (c) (d)

Fig. 7.12 Effect of low and high confining pressures on failure mode of unreinforced and reinforced sand specimens with 3% fibres of 20 mm length and moulded at 85% relative density: (a) unreinforced, σ_3 = 100 kPa; (b) reinforced, σ_3 = 100 kPa; (c) unreinforced, σ_3 = 400 kPa; (d) reinforced, σ_3 = 400 kPa

7.3.1.4 Effect of Relative Density

A comparison of the deviator stress-axial strain and volumetric strain-axial strain response of unreinforced and fibre-reinforced sand specimens of different relative densities are depicted in Figs. 7.13a & 7.13b, under varying confining pressure (100, 200 and 400 kPa). At 35% relative density, under all confining pressures, no clear peak is noted for both unreinforced and reinforced specimens (Fig. 7.13a). With increasing soil relative density, under any confining pressure, the initial stiffness of both specimen types increases, and a clear peak appears at a smaller failure axial strain followed by post-peak stress drop. The peak deviator stress and post-peak stress reduction are most prominent for the specimens of 85% relative density. The improvement in response of sand specimen with increasing relative density is due to more initial interlocking of soil particles. At the time of specimen shearing, the relative inter-sliding of grains is higher for sand of relative density 85%, and the mobilized stress due to surficial interaction between soil-soil and soil-fibre is also greater leading to higher strength.

The failure axial strain values are close to 10%, 4%, 3% and 13%, 10%, 9%, respectively for the unreinforced and reinforced specimens of 35%, 65%, 85% relative densities, under 100 kPa confining pressure (Fig. 7.13a). The corresponding failure strain values of the unreinforced soil under 400 kPa confining pressure are about 13%, 7% and 5%, and they increase expressively with fibre reinforcement to values beyond 15%, 12% and 11%, respectively for specimens of 35%, 65% and 85% relative densities.

For all relative densities, in the case of the unreinforced specimens, the residual stress approaches the same stress level at a large value of shearing strain, at any confining pressure (Fig. 7.13a). As expected, at a large value of shearing strain, the unreinforced sand will reach the same void ratio by volume expansion for the specimen at 85% relative density and by volume contraction for the specimen at 35% relative density. However, in the presence of the interlocking fibres, the specimens at different relative densities are expected to have different void ratios even at a large shearing strain. Thus, the residual stress is greater for a higher relative density at both low and high confining pressures. It has also been found that the residual strength of fibre-reinforced sand of 35% relative density is much higher than the peak stress of unreinforced sand of 85% relative density at all confining pressures (Fig. 7.13a). As the specimen moulded at higher dry unit weight gains greater strength at comparatively low strain level, adequate compaction of fibre-reinforced sand is recommended for field applications.

From volumetric strain-axial strain response, it can be noted that both unreinforced and reinforced soil specimens of 35% relative density mainly undergo compression throughout, at any confining pressure (Fig. 7.13b). With increasing relative densities of 65% and 85%, the contraction is relatively smaller at initial small strain level, and the specimens undergo dilation at higher axial strain, at all confining pressures. Similar behaviour of volumetric strain has been noted by Mashiri et al. (2015) for sand-tyre chip mixtures with

varying relative density.

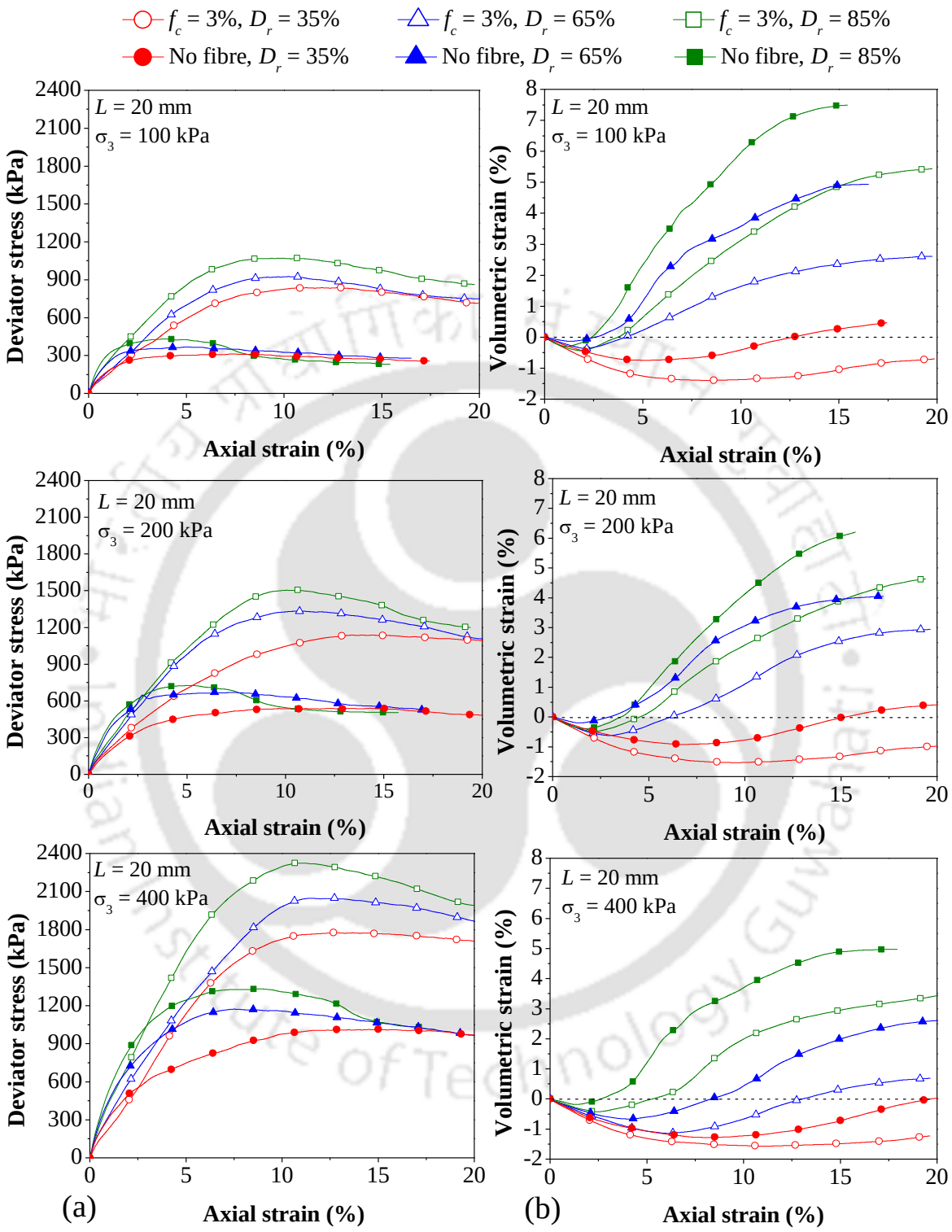

Fig. 7.13 Effect of relative density on behaviour of sand specimens reinforced with 3% fibres of 20 mm length and tested under varying confining pressure: (a) deviator stress-axial strain response; (b) volumetric strain-axial strain response

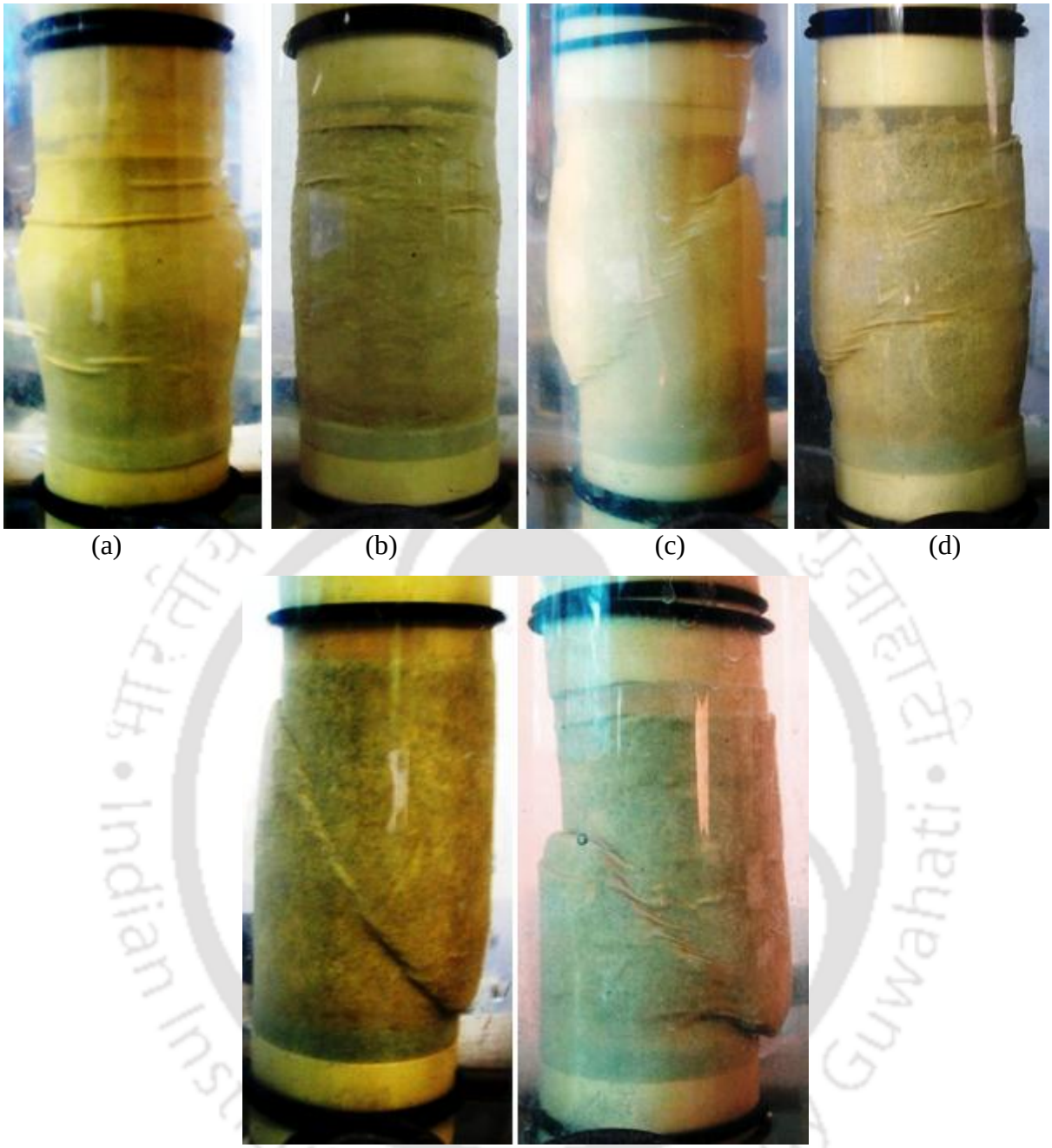

Fig. 7.14 Effect of relative density on failure mode of unreinforced and reinforced sand specimens with 3% fibres of 20 mm length and tested under 100 kPa confining pressure: (a) D_r = 35%, unreinforced; (b) D_r = 35%, reinforced; (c) D_r = 65%, unreinforced; (d) D_r = 65%, reinforced; (e) D_r = 85%, unreinforced; (f) D_r = 85%, reinforced

Typical effect of relative density on failure modes under 100 kPa confining pressure, for unreinforced and fibre-reinforced specimens with 3% fibres, is presented in Figs. 7.14a to 7.14f. At 35% relative density, the unreinforced sand specimen has undergone bulging failure

(Fig. 7.14a), whereas the fibre-reinforced specimen exhibits restricted bulging failure, as the fibres have restrained the lateral spreading (Fig. 7.14b).

At 65% relative density, a clear shear failure plane has been observed for the unreinforced sand specimen (Fig. 7.14c), whereas the fibre-reinforced specimen has shown partially developed slip plane (Fig. 7.14d) that appears at a higher axial strain than that of the unreinforced specimen. At 85% relative density, the unreinforced sand specimen develops a clear shear failure plane (Fig. 7.14e). Though the fibre-reinforced sand specimen also shows clear slip plane, the height of the shear failure zone has been reduced by the fibre inclusion indicating strain localization in a smaller zone (Fig. 7.14f). This has also been observed in the case of reinforced specimens with 2% and 4% fibres under 100 kPa confining pressure (See Figs. 7.4b &7.4c).

7.3.2 Failure Deviator Stress Ratio

In the deviator stress-axial strain response of all the glass fibre-reinforced sand specimens, a peak has been observed. The effect of fibre contribution on the sand strength at failure during drained shearing can also be presented in terms of deviator stress ratio (*DSR*) already defined in Section 6.3.2 as:

$$DSR = \frac{\sigma_{d,fiber}}{\sigma_{d,un}} \tag{7.1}$$

where $\sigma_{d,fiber}$ is the peak deviator stress of fibre-reinforced soil and $\sigma_{d,un}$ is the peak deviator stress of unreinforced soil, under similar test conditions. The peak deviator stress and failure axial strain values under different confining pressures for unreinforced and reinforced specimens are summarized in Tables 7.2 & 7.3, respectively.

The peak deviator stress values of unreinforced sand under 100, 200, 300 and 400 kPa confining pressures are 312, 540, 782 and 1016 kPa, respectively for 35% relative density; 358, 665, 926 and 1169 kPa, respectively for 65% relative density; and 429, 727, 1034 and

1335 kPa, respectively for 85% relative density (Table 7.2). The maximum increase in strength is with 3% fibres of 20 mm length and the corresponding peak values are 838, 1135, 1465 and 1815 kPa for 35% relative density; 926, 1321, 1695 and 2029 kPa for 65% relative density; and 1068, 1503, 1902 and 2318 kPa for 85% relative density.

At any relative density, the failure axial strain is noted to be higher with increasing fibre content, fibre length and confining pressure. With increasing specimen relative density, the failure axial strain shows a decreasing trend. The failure axial strain values of unreinforced sand under 100, 200, 300 and 400 kPa confining pressures are 7.5, 9.6, 12.4 and 13.7%, respectively for 35% relative density; 5.6, 7.4, 8.7 and 9.3%, respectively for 65% relative density; and 3.4, 5.0, 7.1 and 8.3%, respectively for 85% relative density (Table 7.3). The failure axial strain increase to reach the maximum value with glass fibre reinforcement of 4% content and 30 mm length, and the corresponding values under 100, 200, 300 and 400 kPa confining pressures are 13.3, 15.8, 16.6 and 17.0% for 35% relative density; 11.2, 11.9, 13.6 and 14.6% for 65% relative density; and 10.7, 11.5, 12.0 and 12.4% for 85% relative density. Increasing failure strain due to fibre reinforcement indicates improved ductility of the sand. This may restrict inconvenience regarding any permissible strain limit in the design of fibre-reinforced structure.

The *DSR* values of all reinforced sand specimens are summarized in Table 7.4. Typical plots of *DSR* variation with fibre content and relative density are presented in Fig. 7.15, and with fibre length and relative density in Fig. 7.16, under different confining pressures. For all relative densities and confining pressures, the *DSR* value increases with fibre content up to 3% (Fig. 7.15) and with fibre length up to 20 mm fibre (Fig. 7.16). With any fibre content or fibre length, the *DSR* value is the highest at 100 kPa confining pressure and then decreases up to 400 kPa confining pressure, indicating that the relative benefit of fibres is more at low confining pressure. With 3% fibres of 20 mm length, the *DSR* value is

the highest at 35% relative density.

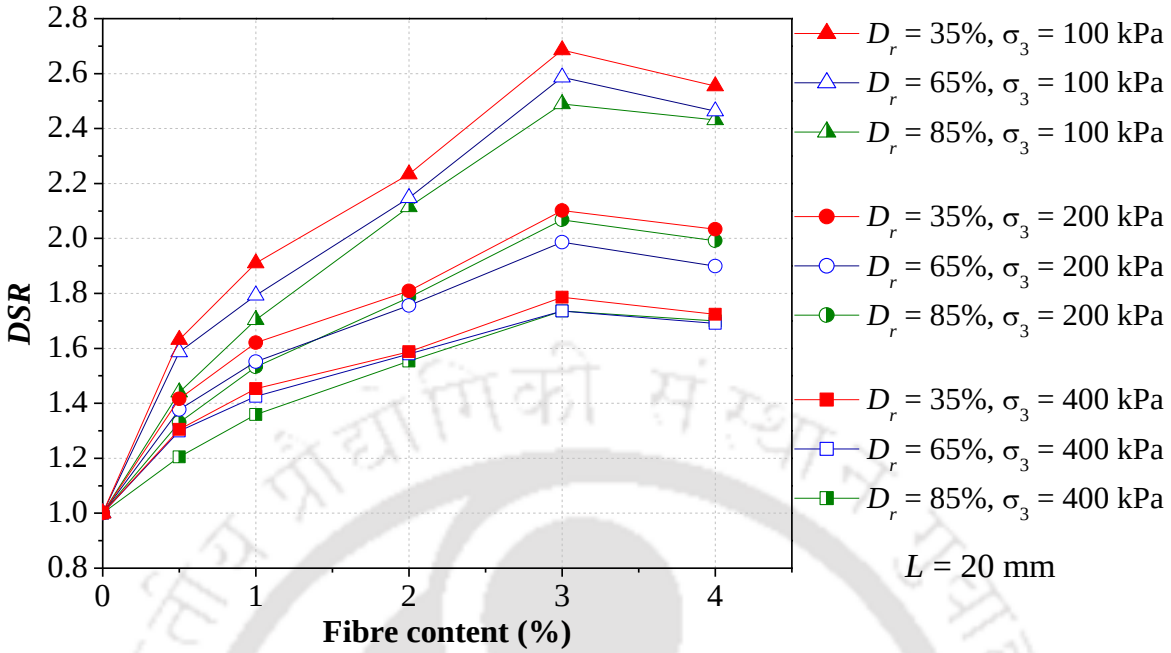

Fig. 7.15 Variation of deviator stress ratio with fibre content and relative density for specimens reinforced with 20 mm fibres under varying confining pressure

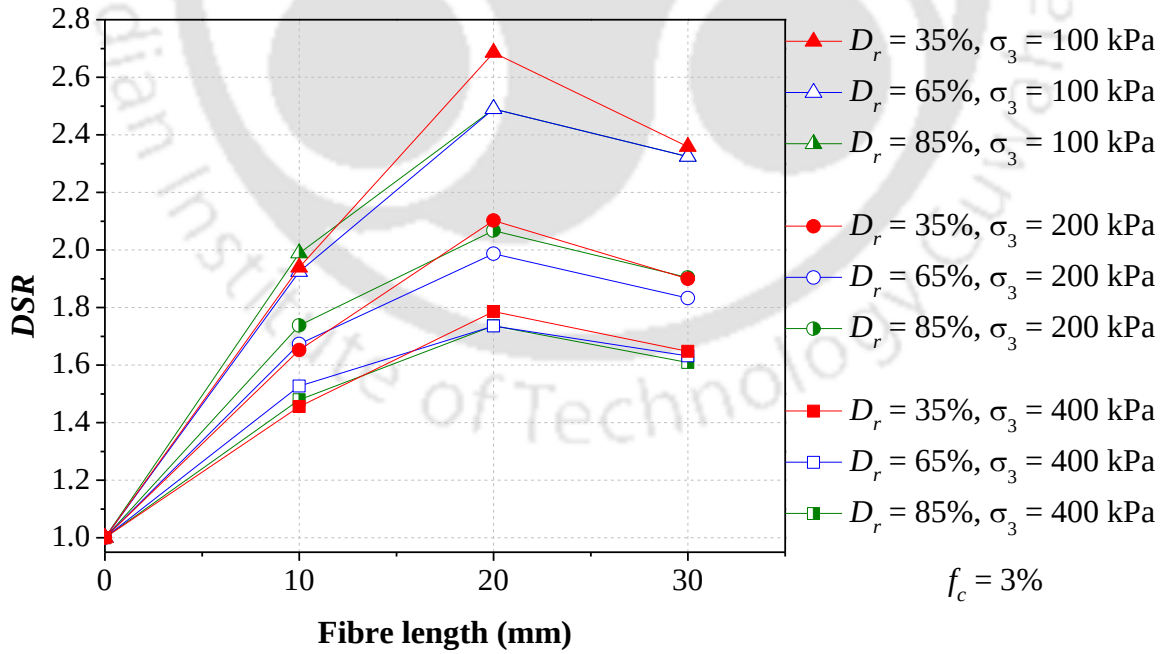

Fig. 7.16 Variation of deviator stress ratio with fibre length and relative density for specimens reinforced with 3% fibres under varying confining pressure

At higher confining pressure, the soil is already apparently stiff and the effectiveness of fibre contribution is less (Maher and Ho 1993). Similar response has been observed by Ozkul and Baykal (2007) on rubber fibre-reinforced clayey soil, where the contribution of rubber fibres to the strength of clay decreases with increasing levels of confinement. Hamidi and Hooresfand (2013) has also reported a decrease in principal stress ratio at failure $(\sigma_1/\sigma_3)_f$ with increasing confining pressure for polypropylene fibre-reinforced sandy soil.

With the optimum reinforcement (3% fibres of 20 mm length), maximum *DSR* values of the glass fibre-reinforced sand under 100 kPa confining pressure are 2.68, 2.59 and 2.49, respectively for specimens of 35%, 65% and 85% relative densities. They decrease to 1.78, 1.74 and 1.73, respectively under 400 kPa confining pressure.

Table 7.2 Summary of peak deviator stress of all fibre-reinforced sand specimens

Fibre length, L (mm)	Fibre content, f_c (%)	Peak deviator stress (kPa)											
		D_r = 35%				D_r = 65%				D_r = 85%			
		σ_3 (kPa)				σ_3 (kPa)				σ_3 (kPa)			
		100	200	300	400	100	200	300	400	100	200	300	400
0	0	312	540	782	1016	358	665	926	1169	429	727	1034	1335
10	0.5	398	648	902	1149	462	829	1118	1386	534	861	1198	1506
	1	476	723	992	1256	539	917	1236	1518	621	981	1316	1634
	2	563	838	1091	1387	620	1002	1334	1642	737	1116	1485	1792
	3	605	892	1192	1479	689	1113	1476	1785	853	1263	1638	1975
	4	584	855	1159	1424	636	1049	1389	1697	844	1241	1596	1936
20	0.5	509	765	1050	1326	568	916	1226	1518	618	967	1292	1608
	1	596	875	1172	1477	642	1032	1372	1666	731	1114	1458	1815
	2	697	977	1306	1613	769	1168	1523	1846	907	1298	1677	2074
	3	838	1135	1465	1815	926	1321	1695	2029	1068	1503	1902	2318
	4	797	1098	1408	1751	882	1263	1628	1977	1043	1448	1845	2269
30	0.5	459	714	969	1187	494	852	1156	1428	592	914	1223	1557
	1	523	816	1078	1338	603	973	1296	1587	709	1043	1367	1698
	2	626	902	1196	1489	727	1081	1427	1744	851	1190	1565	1906
	3	736	1026	1346	1674	843	1219	1584	1908	997	1384	1756	2148
	4	704	975	1306	1621	796	1159	1521	1862	972	1347	1724	2113

Table 7.3 Summary of failure axial strain of all fibre-reinforced sand specimens

Fibre length, L (mm)	Fibre content, f_c (%)	Failure axial strain (%)											
		D_r = 35%				D_r = 65%				D_r = 85%			
		σ_3 (kPa)				σ_3 (kPa)				σ_3 (kPa)			
		100	200	300	400	100	200	300	400	100	200	300	400
0	0	7.5	9.6	12.4	13.7	5.6	7.4	8.7	9.3	3.4	5.0	7.1	8.3
10	0.5	8.8	11.3	13.7	14.0	7.6	8.0	9.3	9.6	4.5	6.2	7.9	8.9
	1	9.7	12.1	14.1	14.8	8.5	8.8	9.9	10.3	5.9	7.7	8.8	9.9
	2	11.0	12.7	14.9	15.8	9.4	9.6	10.2	10.9	7.3	8.8	9.4	10.3
	3	11.8	13.3	15.3	16.3	10.1	10.2	10.6	12.2	8.6	9.6	9.8	10.7
	4	12.6	14.5	15.8	16.7	10.6	10.7	11.2	12.6	9.3	10.4	10.6	10.9
20	0.5	9.8	12.3	14.3	14.5	8.0	8.8	9.5	9.7	5.7	7.7	8.9	9.1
	1	10.6	13.4	14.6	15.3	9.2	9.5	10.5	10.8	6.9	8.2	9.5	10.3
	2	11.6	14.1	15.1	15.6	9.8	10.1	11.2	11.4	8.0	9.5	10.2	10.8
	3	12.5	14.7	15.7	16.4	10.6	11.0	11.7	12.1	9.3	10.4	11.1	11.3
	4	13.1	15.2	16.5	16.9	11.0	11.3	12.3	13.0	10.5	10.8	11.7	11.9
30	0.5	10.9	13.0	13.1	14.5	8.8	9.0	9.9	10.1	6.6	6.7	9.2	9.5
	1	11.3	13.9	14.3	15.7	9.2	9.5	10.7	10.9	7.6	7.8	9.5	10.2
	2	11.9	14.7	15.1	16.2	10.4	10.6	11.5	12.3	8.8	9.6	10.9	11.0
	3	12.7	15.5	15.7	16.6	10.9	11.1	12.6	13.3	9.6	10.5	11.3	12.1
	4	13.3	15.8	16.6	17.0	11.2	11.9	13.6	14.6	10.7	11.5	12.0	12.4

Table 7.4 Summary of deviator stress ratio of all fibre-reinforced sand specimens

Fibre length, L (mm)	Fibre content, f_c (%)	Deviator stress ratio, *DSR*											
		D_r = 35%				D_r = 65%				D_r = 85%			
		σ_3 (kPa)				σ_3 (kPa)				σ_3 (kPa)			
		100	200	300	400	100	200	300	400	100	200	300	400
0	0	1.00	1.00	1.00	1.00	1.00	1.00	1.00	1.00	1.00	1.00	1.00	1.00
10	0.5	1.27	1.20	1.15	1.13	1.29	1.25	1.21	1.18	1.24	1.18	1.16	1.13
	1	1.52	1.34	1.27	1.24	1.50	1.38	1.33	1.30	1.45	1.35	1.27	1.22
	2	1.80	1.55	1.39	1.36	1.73	1.50	1.44	1.40	1.72	1.53	1.44	1.34
	3	1.94	1.65	1.52	1.45	1.92	1.67	1.59	1.53	1.99	1.74	1.58	1.48
	4	1.87	1.58	1.48	1.40	1.78	1.58	1.50	1.45	1.97	1.71	1.54	1.45
20	0.5	1.63	1.41	1.34	1.26	1.58	1.37	1.32	1.30	1.44	1.33	1.25	1.20
	1	1.91	1.62	1.49	1.30	1.79	1.55	1.48	1.42	1.70	1.53	1.41	1.36
	2	2.23	1.81	1.67	1.59	2.15	1.75	1.64	1.58	2.11	1.78	1.62	1.55
	3	2.68	2.10	1.87	1.78	2.59	1.98	1.83	1.73	2.49	2.07	1.84	1.74
	4	2.55	2.03	1.80	1.72	2.46	1.90	1.76	1.69	2.43	1.99	1.78	1.70
30	0.5	1.47	1.32	1.24	1.17	1.38	1.28	1.25	1.22	1.38	1.26	1.18	1.16
	1	1.67	1.51	1.38	1.32	1.68	1.46	1.40	1.36	1.65	1.43	1.32	1.27
	2	2.00	1.67	1.53	1.46	2.03	1.62	1.54	1.49	1.98	1.64	1.51	1.43
	3	2.36	1.90	1.72	1.65	2.35	1.83	1.71	1.63	2.32	1.90	1.70	1.61
	4	2.25	1.80	1.67	1.59	2.22	1.74	1.64	1.59	2.26	1.85	1.67	1.58

7.3.3 Shear Strength Parameters

The shear strength parameters (c' and ϕ') for all glass fibre-reinforced sand specimens have been obtained from modified failure envelopes (K_f line), as in Section 6.3.3. The values of cohesion intercept and friction angle for all unreinforced and reinforced specimens, determined at both peak stress and residual stress levels, along with the fibre contributions are tabulated in Tables 7.5 and 7.6, respectively. The cohesion of the unreinforced sand is due to its composition of 4% silt size fraction, 93% fine sand fraction and 3% medium sand fraction. It can be noted that the improvement in peak and residual shear strength of the reinforced specimen is associated with the increase in both cohesion intercept and friction angle. At 35%, 65% and 85% relative densities, the values of cohesion intercept and internal friction angle for the unreinforced sand specimens are 19 kPa and 32.7°, 26 kPa and 35.0°, and 30 kPa and 37.0°, respectively at peak stress level (See Table 7.5). At residual stress level, the corresponding values are 4 kPa and 33.0°, 9 kPa and 32.8°, and 0 kPa and 33.3°.

Fig. 7.17 presents the peak shear strength envelopes for specimens reinforced with varying content of 20 mm fibres and moulded at different relative densities. At all relative densities, both the cohesion intercept and friction angle are noted to increase to the maximum values with 3% fibres, and then decrease with 4% fibres. The shear strength parameters with 4% fibres are still greater than those with 2% fibres. However, at the same fibre content, the specimen with higher relative density has greater shear strength (Tables 7.5 & 7.6). Similar trends have been observed with the other fibre lengths of 30 mm and 10 mm. The maximum values of peak cohesion intercept and peak friction angle are 120 kPa and 38.3˚, 132 kPa and 40.4˚, and 145 kPa and 42.4˚, respectively at 35%, 65% and 85% relative densities, with 3% fibres of 20 mm length (Tables 7.4 and 7.5). The corresponding fibre contributions to cohesion intercept and friction angle are 100 kPa and 5.6˚, 106 kPa and 5.4˚, and 115 kPa and 5.4˚, respectively.

Table 7.5 Comparison of peak and residual cohesion intercepts of fibre-reinforced sand and fibre contributions at different relative densities

L (mm)	f_c (%)		Peak cohesion intercept (kPa)			Residual cohesion intercept (kPa)		
			D_r = 35%	D_r = 65%	D_r = 85%	D_r = 35%	D_r = 65%	D_r = 85%
0	0		20	26	30	4	9	0
10	0.5		39	43	51	20	29	16
		Fibre contribution	19	17	21	16	20	16
	1		55	57	70	34	33	35
		Fibre contribution	35	31	50	30	24	35
	2		72	71	93	50	38	63
		Fibre contribution	52	45	63	46	29	63
	3		79	81	114	61	45	74
		Fibre contribution	59	55	84	57	36	74
	4		76	73	115	67	49	79
		Fibre contribution	56	47	85	63	40	79
20	0.5		59	65	72	40	36	38
		Fibre contribution	39	39	42	36	27	38
	1		74	77	89	56	41	56
		Fibre contribution	54	51	59	52	32	56
	2		94	100	117	70	57	86
		Fibre contribution	74	74	87	66	48	86
	3		120	132	145	94	70	107
		Fibre contribution	100	106	115	90	61	107
	4		115	122	140	96	78	105
		Fibre contribution	95	96	110	92	69	105
30	0.5		60	50	66	35	22	25
		Fibre contribution	40	24	36	31	13	25
	1		68	70	90	48	41	44
		Fibre contribution	48	44	60	44	32	44
	2		84	94	116	64	60	64
		Fibre contribution	64	68	86	60	51	64
	3		101	116	140	83	74	93
		Fibre contribution	81	90	110	79	65	93
	4		94	104	134	77	73	86
		Fibre contribution	74	78	104	73	64	86

Table 7.6 Comparison of peak and residual friction angles of fibre-reinforced sand and fibre contributions at different relative densities

L (mm)	f_c (%)		Peak friction angle (°)			Residual friction angle (°)		
			D_r = 35%	D_r = 65%	D_r = 85%	D_r = 35%	D_r = 65%	D_r = 85%
0	0		32.7	35.0	37.0	33.0	32.8	33.3
10	0.5		33.8	37.4	38.3	34.4	34.0	34.8
		Fibre contribution	1.1	2.4	1.3	1.4	1.2	1.5
	1		34.5	38.3	38.9	35.1	36.4	35.8
		Fibre contribution	1.8	3.3	1.9	2.1	3.6	2.5
	2		35.4	39.0	39.7	35.9	37.7	36.7
		Fibre contribution	2.7	4.0	2.7	2.9	4.9	3.4
	3		36.4	40.3	40.7	36.3	39.5	38.5
		Fibre contribution	3.7	5.3	2.7	3.3	6.7	5.2
	4		35.8	39.7	40.2	35.8	38.5	37.8
		Fibre contribution	3.1	4.7	2.2	2.8	5.7	4.5
20	0.5		35.3	37.8	38.5	35.3	35.6	35.5
		Fibre contribution	2.6	2.8	1.5	2.3	2.8	2.2
	1		36.5	39.1	40.0	36.8	38.0	37.0
		Fibre contribution	3.8	4.1	3.0	3.8	5.2	3.7
	2		37.3	40.0	41.3	37.8	39.7	37.7
		Fibre contribution	4.6	5.0	4.3	4.8	6.9	4.4
	3		38.3	40.4	42.4	38.7	41.5	40.6
		Fibre contribution	5.6	5.4	5.4	5.7	8.7	7.3
	4		37.8	40.2	42.1	38.2	40.8	40.1
		Fibre contribution	5.1	5.2	5.1	5.2	8.0	6.8
30	0.5		33.3	37.5	38.0	34.2	36.6	35.8
		Fibre contribution	0.6	2.5	1.0	1.2	3.8	2.5
	1		35.1	38.4	38.7	35.8	38.1	36.8
		Fibre contribution	2.4	3.4	1.7	2.8	5.3	3.5
	2		36.2	39.0	39.7	36.6	39.3	38.4
		Fibre contribution	3.5	4.0	2.7	3.6	6.5	5.1
	3		37.6	39.8	41.0	38.0	41.1	39.7
		Fibre contribution	4.9	4.8	4.0	5.0	8.3	6.4
	4		37.3	39.8	40.9	37.9	40.6	40.1
		Fibre contribution	4.6	4.8	3.9	4.9	7.8	6.8

At any relative density, the residual cohesion intercept and friction angle values also increase with increasing fibre content and fibre length only up to 3% fibres and 20 mm length (Fig. 7.18). However, they do not indicate any specific trends with the soil relative density as in the case of peak shear strength parameters (Tables 7.4 & 7.5), similar to the results of Li and Zornberg (2013). In case of reinforced specimens of 35% relative density, residual

friction angles are noted to be marginally greater than that peak friction angles (Table 7.5), as the specimens undergo mostly volumetric contraction. For specimens of 65% and 85% relative densities, as the specimens undergo mostly dilation up to residual strain level, the residual friction angle is noted to be lower than the peak friction angle value. However, at all relative densities, it can be noted that the fibre contribution to friction angle improvement is higher at residual stress level than that at peak stress level. The maximum fibre contributions to friction angle at peak stress level are 5.6˚, 5.4˚ and 5.4˚, respectively for 35%, 65% and 85% relative densities with 3% fibres of 20 mm length (See Table 7.6), which is the optimum glass fibre reinforcement. The corresponding maximum fibre contributions at residual stress level are 5.7˚, 8.7˚ and 7.3˚, respectively.

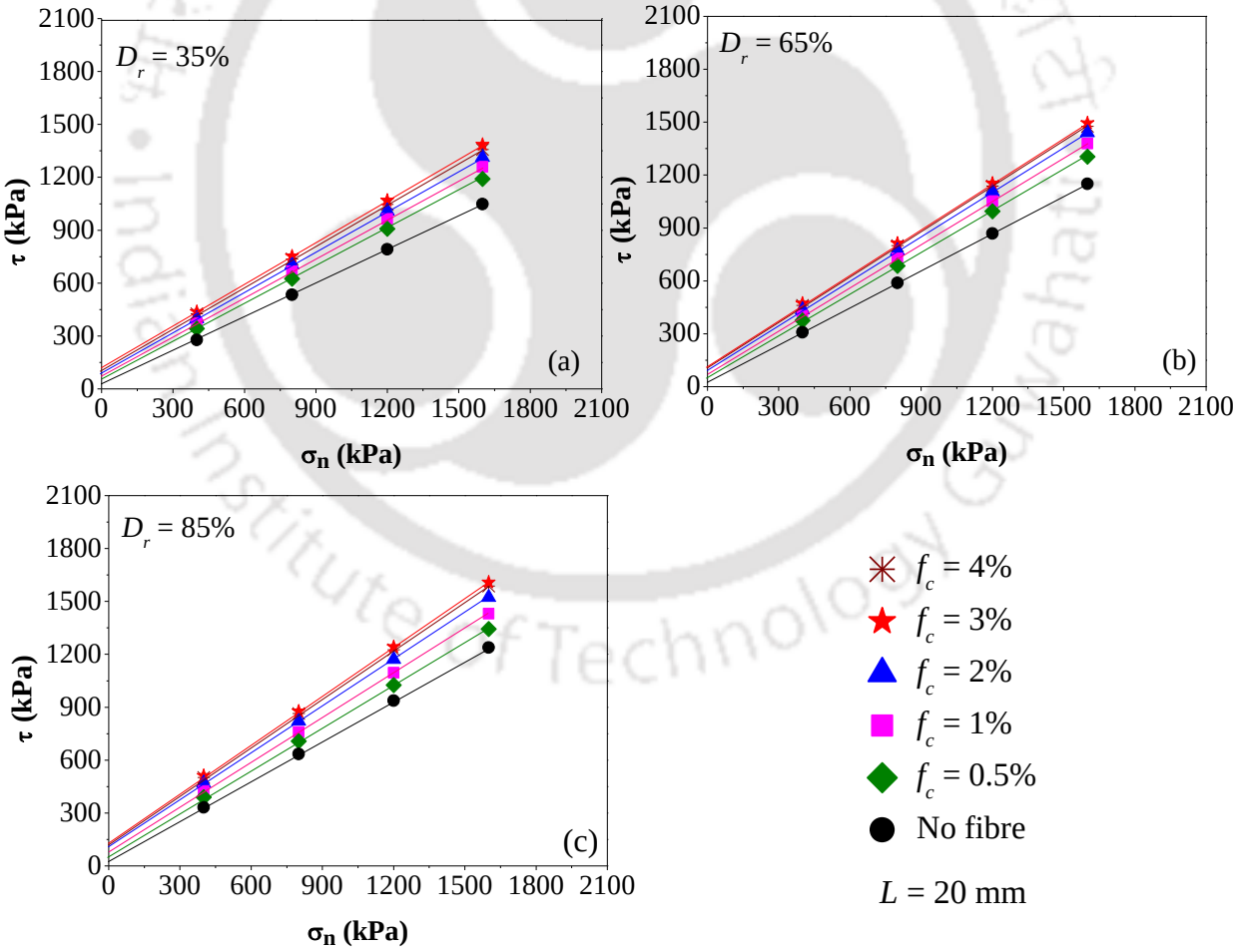

Fig. 7.17 Peak shear strength envelopes of sand reinforced with varying content of 20 mm fibres and moulded at different relative densities: (a) D_r = 35%; (b) D_r = 65%; (c) D_r = 85%

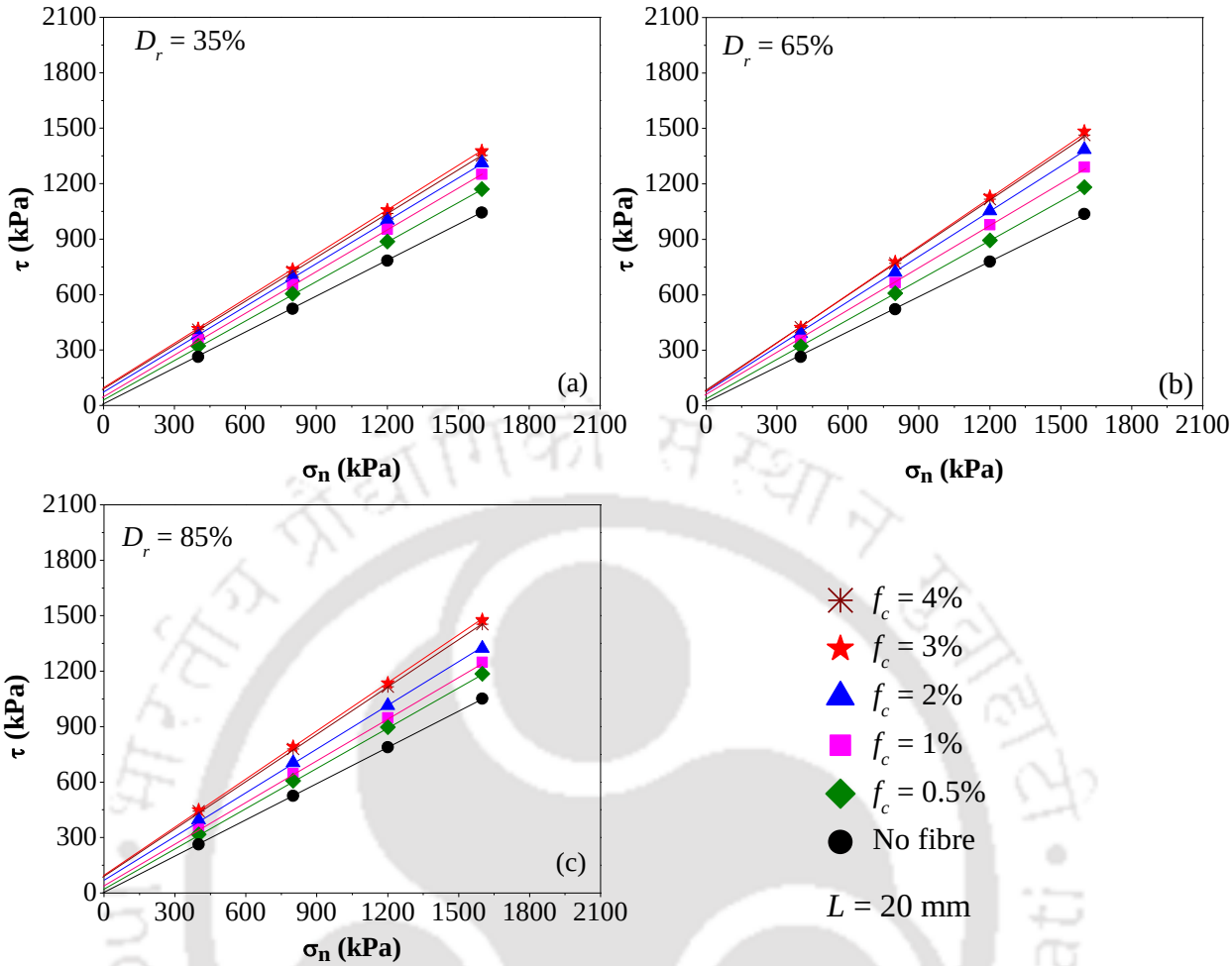

Fig. 7.18 Residual shear strength envelopes of sand reinforced with varying content of 20 mm fibres and moulded at different relative densities: (a) D_r = 35%; (b) D_r = 65%; (c) D_r = 85%

7.3.4 Secant Modulus Response

The stress-strain curves of the reinforced sand, and therefore the secant modulus, are influenced by fibre parameters (content and length), moulding state factor (relative density) and confining pressure. The secant modulus values for all unreinforced and glass fibre-reinforced sand specimens have been determined at different axial strain values (0.5, 1, 2.5, 5, 10 and 15%), as in Section 6.3.4.

The effect of fibre content (20 mm length) under both low (100 kPa) and high (400 kPa) confining pressures on secant modulus variation of specimens moulded at 35% and 85%

relative densities are shown in Figs. 7.19a and 7.19b, respectively. For specimens of both relative densities, secant modulus is noted to decrease with increasing axial strain, under any confining pressure. Further, at any axial strain level, the secant modulus tends to increase with fibre content and also with confining pressure. At the low confining pressure of 100 kPa, the secant modulus of unreinforced specimen at 2.5% axial strain is lower than or comparable to that of the reinforced specimens. At the high confining pressure of 400 kPa, the secant modulus of the unreinforced specimen at 2.5% axial strain is distinctly greater than that of the reinforced specimens. At the low relative density of 35%, the secant modulus is the maximum with 3% fibre content at 2.5% and 5% axial strains, and with 4% fibre content at 10% and 15% axial strain levels. In the case of high relative density of 85%, the secant modulus values with 3% and 4% fibre contents are comparable at all axial strain levels.

The effect of fibre length (3% content) under both low (100 kPa) and high (400 kPa) confining pressures on secant modulus variation of specimens moulded at 35% and 85% relative densities are presented in Figs. 7.20a and 7.20b, respectively. At any axial strain, the secant modulus increases with fibre length to reach maximum value with 20 mm fibres and then decreases with 30 mm fibres. With increasing confining pressure, the secant modulus is noted to increase.

The combined effect of relative density and confining pressure on secant modulus is shown in Figs. 7.21a to 7.21d, for sand specimens reinforced with 3% fibres of 20 mm length. At any axial strain, the secant modulus for both unreinforced and reinforced specimens is noted to be greater for higher relative density, and is also found to further increase with higher confining pressure. Under 100 kPa confining pressure (Fig. 7.21a), at 2.5% axial strain, the secant modulus of reinforced specimen for any relative density is higher than that of the corresponding unreinforced specimen. However, under confining pressures of

200, 300 and 400 kPa (Figs. 7.21b to 7.21d), the secant modulus of the reinforced specimen at 2.5% axial strain is lower than that of the corresponding unreinforced specimen.

At axial strain of 10% or more, the secant modulus of the reinforced soil of 65% relative density is found to be greater than that of unreinforced soil of 85% relative density, under all confining pressures. Hence, for geotechnical structures which can withstand large deformation, fibre-reinforced soil with relatively lower compaction density may fulfill the required stiffness criterion, in comparison to the use of the unreinforced soil in field application.

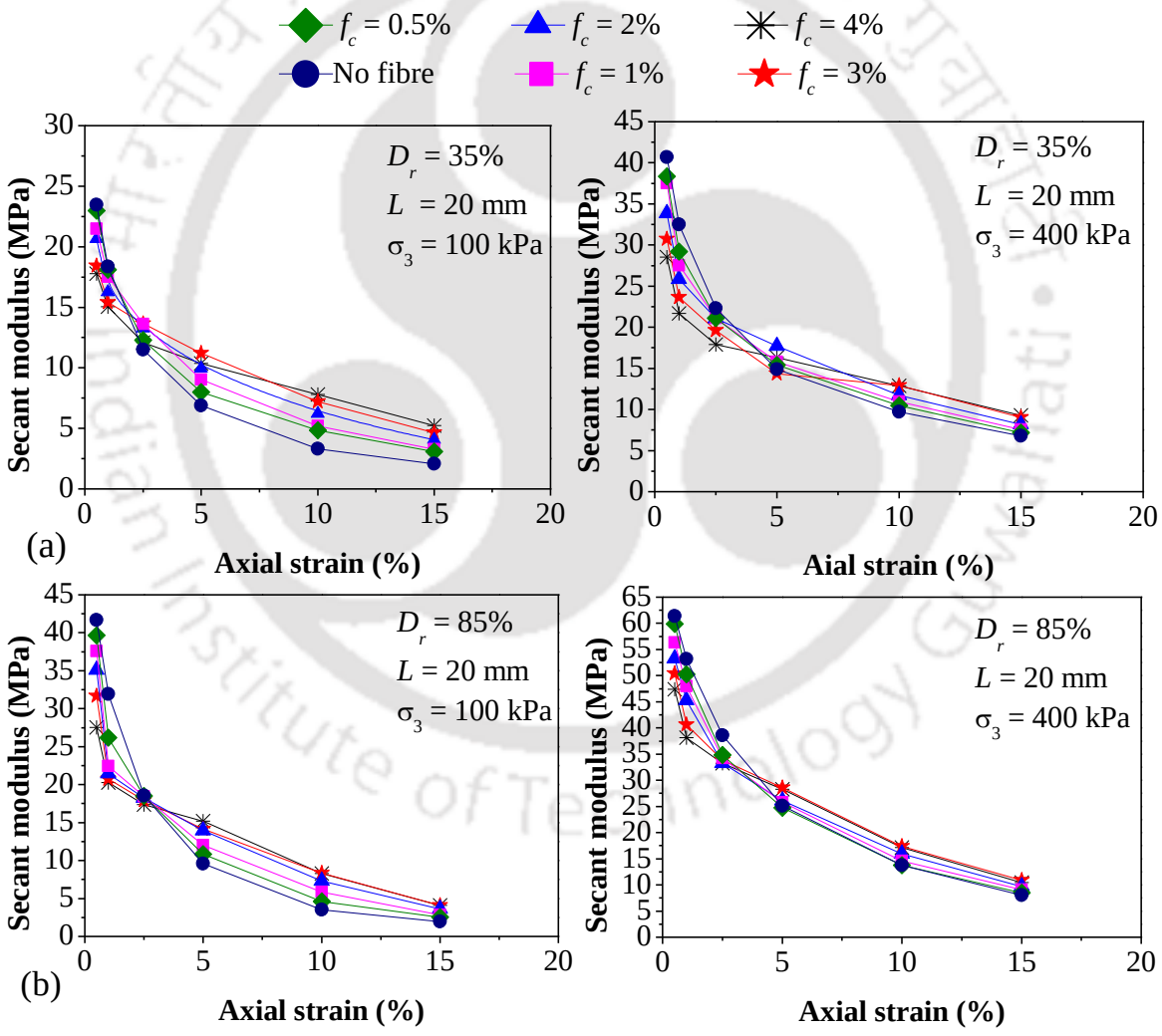

Fig. 7.19 Effect of fibre content on secant modulus variation under 100 and 400 kPa confining pressures for sand specimens reinforced with 20 mm fibres and moulded at different relative densities: (a) D_r = 35%; (b) D_r = 85%

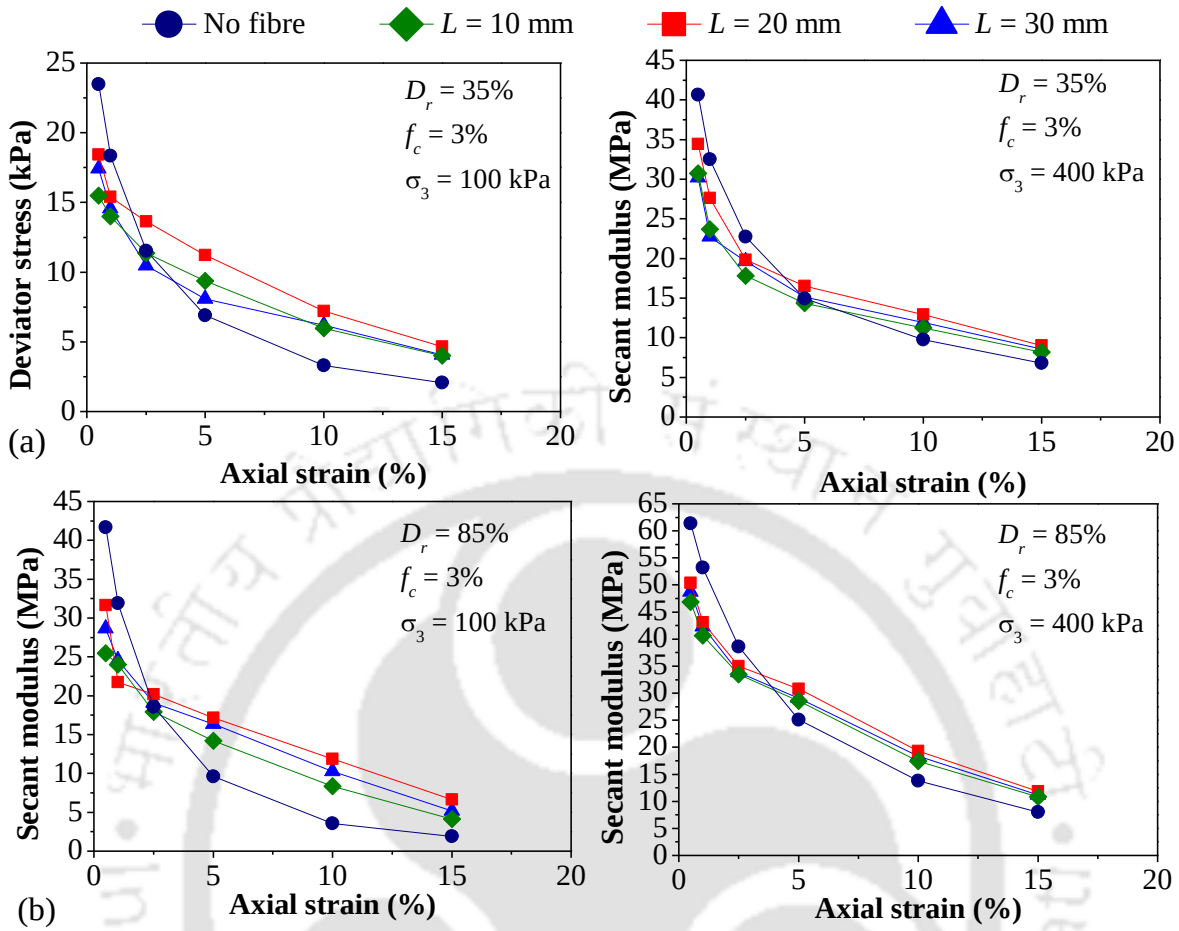

Fig. 7.20 Effect of fibre length on secant modulus variation under 100 and 400 kPa confining pressures for sand specimens reinforced with 3% fibres and moulded at different relative densities: (a) D_r = 35%; (b) D_r = 85%

The secant modulus values at all axial strain under varying relative density and confining pressure for unreinforced and fibre-reinforced specimens with 3% fibres of 20 mm length are summarized in Table 7.7. The secant modulus value is noted to increase with increasing specimen relative density and confining pressure. For unreinforced sand, the secant modulus values at 100 kPa confining pressure and at 2.5%, 5%, 10% and 15% axial strain are 11.52, 6.90, 3.32 and 2..09 MPa; 14.29, 7.23, 3.18 and 1.89 MPa; 18.55, 9.61, 3.55 and 1.93 MPa respectively for 35%, 65% and 85% relative densities. The corresponding

values increase maximum to 22.29, 14.91, 9.73 and 6.81 MPa; 31.56, 21.20, 11.58 and 7.05 MPa; 38.63, 25.09, 13.78 and 8.03 MPa under 400 kPa confining pressure.

At any relative density, the secant modulus value increases with fibre content up to 3% fibres for any fibre length, and with fibre length up to 20 mm length for any fibre content. Under 100 kPa confining pressure, the maximum secant modulus values with 3% fibres of 20 mm length at 2.5%, 5%, 10% and 15% axial strain are 13.68, 11.22, 7.79 and 5.22 MPa; 14.31, 13.99, 9.12 and 5.31 MPa; 17.92, 17.39, 8.36 and 4.11 MPa, respectively for 35%, 65% and 85% relative densities. The corresponding maximum values under 400 kPa confining pressure are 19.64, 17.70, 12.91 and 9.28 MPa; 28.12, 24.67, 19.69 and 13.41 MPa; 33.86, 29.07, 17.41 and 10.88 MPa, respectively.

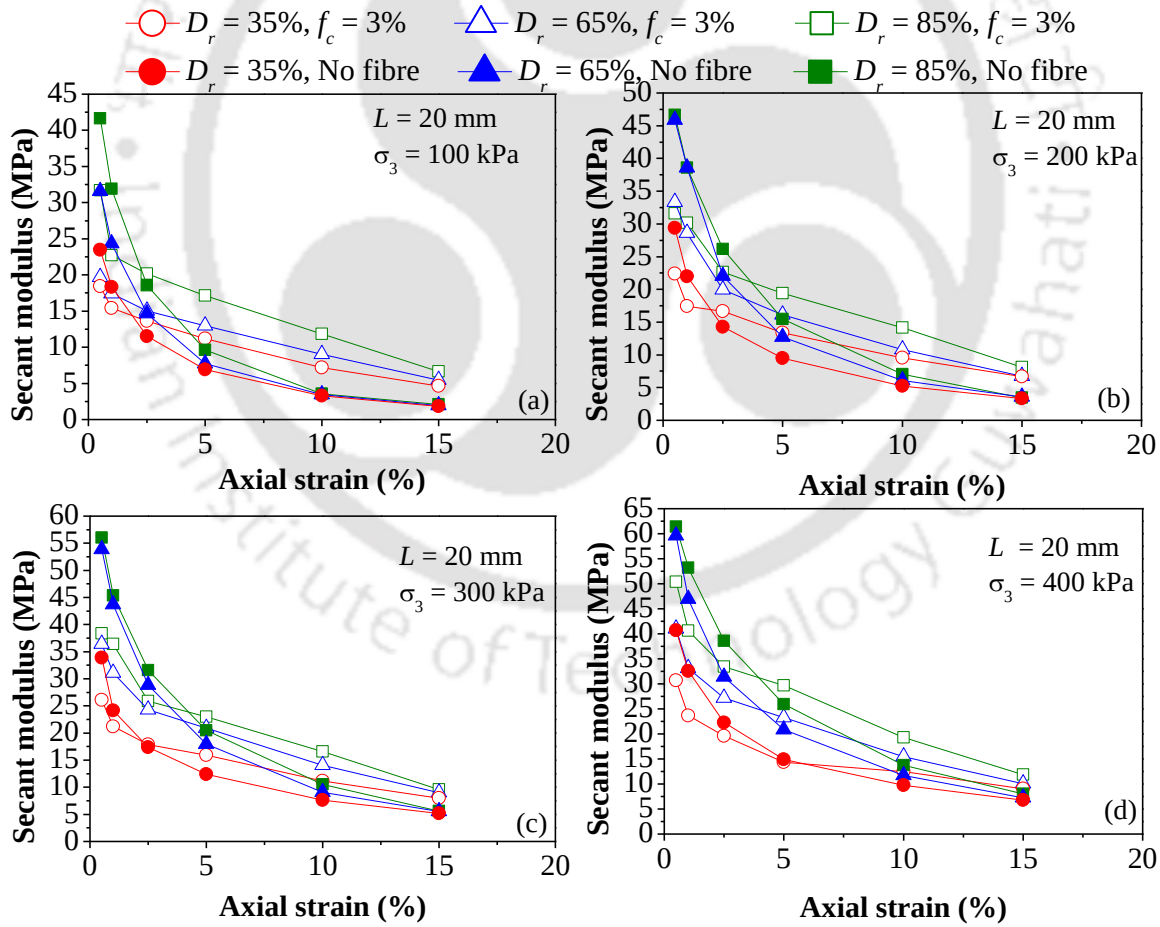

Fig. 7.21 Effect of relative density on secant modulus variation under all confining pressures of sand specimens reinforced with 3% fibres of 20 mm length: (a) σ_3 = 100 kPa; (b) σ_3 = 200 kPa; (c) σ_3 = 300 kPa; (d) σ_3 = 400 kPa

Table 7.7 Summary of secant modulus values for unreinforced and fibre-reinforced specimens with optimum fibre reinforcement (3% fibres of 20 mm length) at all relative densities and confining pressures

Axial strain (%)	**Fibre content, f_c (%)**	**Secant Modulus (MPa)**											
		D_r = 35%				**D_r = 65%**				**D_r = 85%**			
		σ_3 (kPa)				**σ_3 (kPa)**				**σ_3 (kPa)**			
		100	**200**	**300**	**400**	**100**	**200**	**300**	**400**	**100**	**200**	**300**	**400**
2.5	0	11.52	14.03	17.38	22.29	14.29	22.04	29.87	31.56	18.55	26.14	31.57	38.63
	3	13.64	16.64	16.92	19.64	14.31	21.42	25.87	28.12	17.92	26.31	32.16	33.86
5	0	6.90	9.48	11.73	14.91	7.23	12.98	17.79	21.20	9.61	15.45	20.48	25.09
	3	11.22	13.37	14.93	17.70	13.99	19.72	22.11	24.67	17.39	19.43	22.97	29.07
10	0	3.32	5.23	7.64	9.73	3.18	6.30	8.98	11.58	3.55	7.04	10.56	13.78
	3	7.79	9.56	11.85	12.91	9.12	13.16	16.74	19.69	8.36	12.04	15.08	17.41
15	0	2.09	3.57	5.19	6.81	1.89	3.69	5.56	7.05	1.93	3.45	5.63	8.03
	3	5.22	6.69	8.29	9.28	5.31	8.36	11.09	13.41	4.11	6.28	8.37	10.88

7.3.5 Brittleness Index

As reported by Consoli et al. (1998), the post-peak behaviour of fibre-reinforced specimens can be quantified in terms of brittleness index (I_B) defined as:

$$I_B = \frac{\sigma_{d,peak}}{\sigma_{d,res}} - 1 \tag{7.2}$$

where $\sigma_{d,peak}$ is the peak deviator stress and $\sigma_{d,res}$ is residual deviator stress of the specimen. A decreasing value of I_B indicates a less brittle or more ductile nature of the specimen failure behaviour. The brittleness index values calculated for all soil-fibre mixes are summarized in Table 7.8.

Typical brittleness index variation, showing the effect of fibre content and relative density under low (100 kPa) and high (400 kPa) confining pressures, is presented in Fig. 7.22. With increasing fibre content, the brittleness index decreases for all relative densities and confining pressures. The brittleness index of the unreinforced specimen of 85% relative density under 100 kPa confining pressure, has reduced from 0.852 to 0.213 with 4% fibres of 20 mm length (Table 7.8). This can also be noted from their failure modes, as shown already in Fig. 7.4.

With increasing confining pressure from 100 to 400 kPa, the brittleness index decreases for any relative density indicating inducement of ductility in specimen. The brittleness index of the unreinforced specimen of 85% relative density under 100 kPa confining pressure is 0.852, which has reduced to 0.405 under 400 kPa confining pressure (Table 7.8). The corresponding values are 0.213 and 0.166 for specimens reinforced with 4% fibres of 20 mm length. This can also be noted from the failure modes, as shown already in Figs. 7.11 & 7.12.

With the same fibre content, as the specimen relative density is increased to 65% and 85%, the brittleness index increases. At 35% relative density, the brittleness index values are

less than 0.2 and their variation with fibre content is noted to be the least, and all the specimens have shown true ductile behaviour in the failure modes (Figs. 7.3 & 7.10) with no visible shear plane. For the unreinforced specimen under 100 kPa confining pressure, as the specimen relative density is increased from 35% to 65% and 85%, the brittleness index increases from 0.2 to 0.491 and 0.852, respectively. The same can be noted from the failure modes (Fig. 7.14), where the specimen at 35% relative density has shown pure bulging failure which has progressively changed to shear failure mode at 65% and 85% relative densities, indicating increasing brittle behaviour.

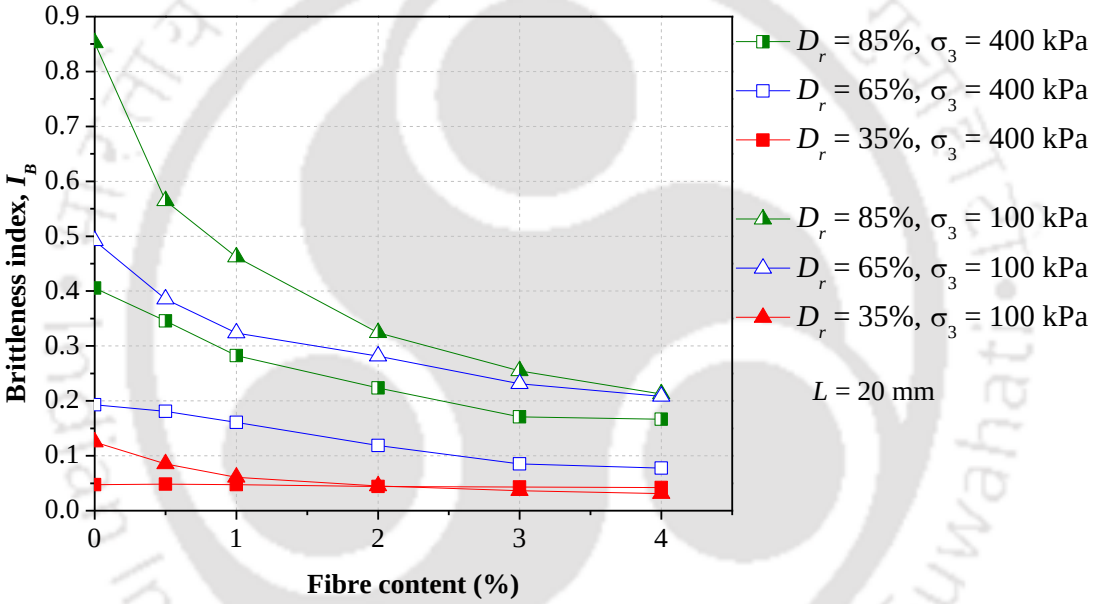

Fig. 7.22 Variation of brittleness index with fibre content under low and high confining pressures for sand specimens reinforced with 20 mm fibres and moulded at different relative densities

From the brittleness index values summarized in Table 7.8, the maximum values of brittleness index for unreinforced specimens are under 100 kPa confining pressure, and they are 0.200, 0.491 and 0.852, respectively at 35%, 65% and 85% relative densities. However, the minimum values of brittleness index for unreinforced specimens are under 400 kPa confining pressure, and those values are 0.016, 0.037 and 0.166, respectively with 4% fibre of 30 mm length.

Table 7.8 Summary of brittleness index (I_B) values of all reinforced sand specimens

Fibre length, L (mm)	Fibre content, f_c (%)	Brittleness index, I_B											
		D_r = 35%				D_r = 65%				D_r = 85%			
		σ_3 (kPa)				σ_3 (kPa)				σ_3 (kPa)			
		100	200	300	400	100	200	300	400	100	200	300	400
0	0	0.200	0.120	0.049	0.047	0.491	0.371	0.268	0.193	0.852	0.671	0.520	0.405
10	0.5	0.188	0.110	0.048	0.042	0.359	0.295	0.235	0.173	0.618	0.484	0.426	0.309
	1	0.147	0.100	0.047	0.038	0.298	0.256	0.200	0.150	0.496	0.391	0.322	0.297
	2	0.097	0.090	0.044	0.035	0.278	0.222	0.186	0.136	0.404	0.268	0.280	0.262
	3	0.070	0.070	0.041	0.031	0.252	0.217	0.162	0.119	0.376	0.257	0.246	0.247
	4	0.043	0.050	0.039	0.017	0.223	0.192	0.143	0.109	0.361	0.247	0.242	0.229
20	0.5	0.170	0.085	0.034	0.048	0.385	0.327	0.232	0.186	0.564	0.465	0.389	0.345
	1	0.168	0.061	0.032	0.047	0.323	0.282	0.193	0.161	0.462	0.410	0.356	0.283
	2	0.152	0.045	0.028	0.044	0.281	0.236	0.149	0.119	0.324	0.304	0.266	0.223
	3	0.132	0.036	0.024	0.043	0.251	0.190	0.130	0.085	0.235	0.242	0.231	0.171
	4	0.107	0.031	0.020	0.042	0.208	0.164	0.126	0.077	0.213	0.227	0.206	0.166
30	0.5	0.133	0.098	0.036	0.041	0.372	0.235	0.133	0.103	0.480	0.417	0.337	0.251
	1	0.101	0.081	0.031	0.033	0.269	0.179	0.117	0.098	0.390	0.346	0.277	0.217
	2	0.098	0.074	0.026	0.030	0.222	0.150	0.089	0.076	0.350	0.315	0.262	0.191
	3	0.082	0.068	0.023	0.027	0.204	0.118	0.049	0.040	0.303	0.247	0.211	0.183
	4	0.075	0.048	0.020	0.016	0.162	0.093	0.045	0.037	0.279	0.230	0.177	0.167

7.3.6 Energy Absorption Capability

As in Section 6.3.5, the total energy absorption capability (*EAC*) for the fibre-reinforced sand specimen is the sum of the energy dissipated through the deformation of soil matrix $(EAC)_s$ and the energy dissipated through soil-fibre interface friction and fibre stretching $(EAC)_f$. For the fibre-reinforced sand specimen, the energy absorption capability (*EAC*) is related to both its peak strength and post-peak response, and the magnitude would depend on the geometrical characteristics (diameter and length) of the test specimen. The effects of fibre content, relative density and confining pressure on the energy absorption capability of the specimen size used in this study have been evaluated at 11.4 mm deformation, corresponding to a strain level of 15% in the tests. The *EAC* values of all reinforced specimens for different relative densities under varying confining pressure are summarized in Table 7.9.

The effects of fibre content and fibre length on *EAC* of the specimens at 85% relative density, under varying confining pressure, are shown in Figs. 7.23a and 7.23b, respectively. At any confining pressure, the *EAC* value increases with increase in fibre content up to 3% and with fibre length up to 20 mm. Further, with increasing confining pressure up to 400 kPa, the *EAC* increases with any combination of fibre content and fibre length. Under 400 kPa confining pressure, the maximum *EAC* values of unreinforced specimens are 12164, 15492 and 17153 kJ/m^3, respectively for 35%, 65% and 85% relative densities (Table 7.9), and the corresponding maximum values among all reinforced specimens are 19849, 22576 and 26964 kJ/m^3 with 3% fibres of 20 mm length.

Due to random distribution of fibres, the progressive absorption of energy takes place during loading, and higher energy is required to deform the reinforced specimen. The stretching of fibres under loading requires more energy, resulting in greater *EAC* with increasing fibre content. As the shear stress exceeds the shear strength of sand in any zone

within the specimen, the fibres in the vicinity develop resisting force, resulting in continuous energy absorption.

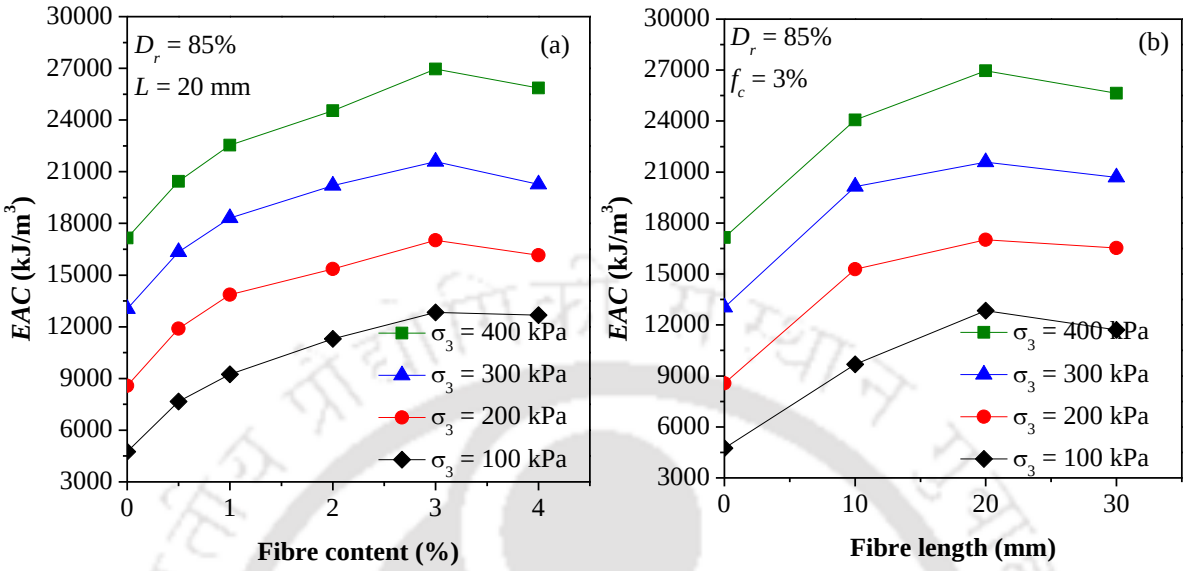

Fig. 7.23 *EAC* variation under different confining pressures for reinforced sand specimens at 85% relative density: (a) Effect of varying fibre content of 20 mm length; (b) Effect of varying fibre length of 3% content

Typical *EAC* variation, showing the effect of fibre content and relative density under low (100 kPa) and high (400 kPa) confining pressures, is presented in Fig. 7.24. Under any confining pressure, the *EAC* of any reinforced specimen is greater with increasing relative density. Hamidi and Hooresfand (2013) and Consoli et al. (2002) have reported similar behaviour of *EAC* for cement treated polypropylene fibre-reinforced sand with increasing specimen relative density. The maximum contribution of reinforcement on the *EAC* is found with limiting fibre content of 3%. However, *EAC* is noted to increase continuously with relative density and confining pressure.

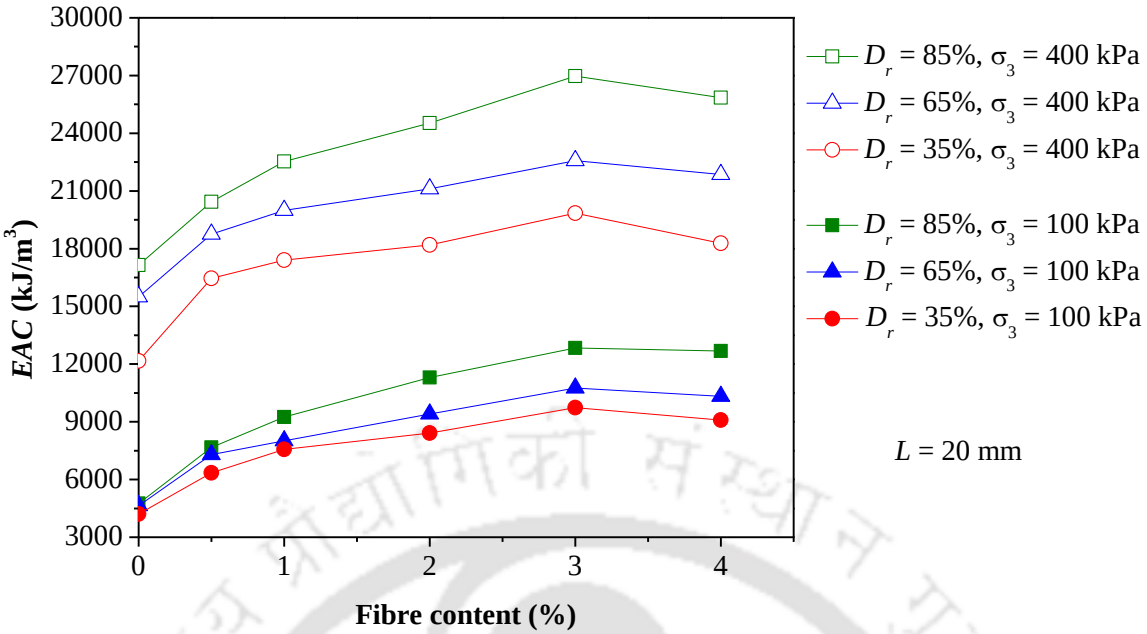

Fig. 7.24 *EAC* variation with fibre content of 20 mm length under 100 kPa and 400 kPa confining pressures for sand specimens moulded at different relative densities

The values of $(EAC)_f$ for all specimens are summarized in Table 7.10. For any combination of relative density and confining pressure, it can be noted that the $(EAC)_f$ increases with fibre content up to 3%, and the maximum is with 20 mm length. However, for any combination of fibre content and length, no consistent trends have been noted for $(EAC)_f$ with the increase of either specimen relative density or confining pressure, keeping the other constant. With the optimum fibre reinforcement (3% fibres of 20 mm length) and 35% relative density, the maximum $(EAC)_f$ values are 5530, 5326, 5712 and 7685 kJ/m^3, respectively under 100, 200, 300 and 400 kPa confining pressures. The corresponding values with 65% relative density are 6118, 7276, 7048 and 7084 kJ/m^3, and with 85% relative density are 8088, 8443, 8549 and 9811 kJ/m^3.

At the same fibre contents of 0.5% and 1%, the contribution of glass fibre inclusion to *EAC* is relatively higher for sandy soil specimens (Table 7.10) compared to that of clayey soil specimens (Table 6.8).

Table 7.9 Summary of energy absorption capability (*EAC*) values of all reinforced-sand specimens

Fibre length, *L* (mm)	Fibre content, f_c (%)	Energy Absorption Capability, *EAC* (kJ/m^3)											
		D_r = 35%				D_r = 65%				D_r = 85%			
		σ_3 (kPa)				σ_3 (kPa)				σ_3 (kPa)			
		100	200	300	400	100	200	300	400	100	200	300	400
0	0	4205	6986	9365	12164	4644	8370	12416	15492	4754	8572	13034	17153
10	0.5	5120	7811	10829	13793	5941	10496	14361	17524	6536	10672	14863	18606
	1	6108	8939	11937	15427	6800	11659	15639	18539	7436	12028	15997	20455
	2	6936	9933	12707	16190	7622	12508	16802	19495	8836	13551	18171	22257
	3	7319	9846	13469	16209	8389	13475	17737	20168	9681	15285	20140	24072
	4	6825	8669	13031	15289	7716	12720	16446	18652	9874	14446	19550	23980
20	0.5	6345	9390	12048	16451	7290	11887	15851	18751	7667	11893	16347	20438
	1	7565	10438	13476	17411	8018	13109	17284	19985	9245	13866	18308	22534
	2	8415	11329	14589	18201	9409	14559	18223	21110	11305	15353	20188	24534
	3	9735	12312	15077	19849	10762	15646	19464	22576	12842	17015	21583	26964
	4	9096	11498	14423	18278	10328	15104	18340	21852	12683	16158	20262	25852
30	0.5	5955	8414	11156	13630	6552	11223	14873	18005	7269	11461	15475	19795
	1	6492	9452	12005	14396	7745	12814	16094	18953	9007	12784	17165	21193
	2	7648	9855	12740	15304	8915	13663	17136	20568	10385	14074	19006	23237
	3	8372	10813	13939	16321	10102	14929	18196	21480	11717	16530	20682	25635
	4	8116	10368	12922	15284	9829	14240	17406	20082	11589	15323	19625	24884

Table 7.10 Summary of $(EAC)_f$ values of all reinforced-sand specimens

L (mm)	f_c (%)	$(EAC)_f$ (kJ/m^3)											
		D_r = 35%				D_r = 65%				D_r = 85%			
		σ_3 (kPa)				σ_3 (kPa)				σ_3 (kPa)			
		100	200	300	400	100	200	300	400	100	200	300	400
10	0.5	915	825	1464	1629	1297	2126	1945	2032	1782	2100	1829	1453
	1	1903	1953	2572	3263	2156	3289	3223	3047	2682	3456	2963	3302
	2	2731	2947	3342	4026	2978	4138	4386	4003	4082	4979	5137	5104
	3	3114	2860	4104	4045	3745	5105	5321	4676	4927	6713	7106	6919
	4	2620	1683	3666	3125	3072	4350	4030	3160	5120	5874	6516	6827
20	0.5	2140	2404	2683	4287	2646	3517	3435	3259	2913	3321	3313	3285
	1	3360	3452	4111	5247	3374	4739	4868	4493	4491	5294	5274	5381
	2	4210	4343	5224	6037	4765	6189	5807	5618	6551	6781	7154	7381
	3	5530	5326	5712	7685	6118	7276	7048	7084	8088	8443	8549	9811
	4	4891	4512	5058	6114	5684	6734	5924	6360	7929	7586	7228	8699
30	0.5	1750	1428	1791	1466	1908	2853	5508	5841	2515	2889	2441	2642
	1	2287	2466	2640	2232	3101	4444	6729	6789	4253	4212	4131	4040
	2	3443	2869	3375	3140	4271	5293	7771	8404	5631	5502	5972	6084
	3	4167	3827	4574	4157	5458	6559	8831	9316	6963	7958	7648	8482
	4	3911	3382	3557	3120	5185	5870	8041	7918	6835	6751	6591	7731

The change in ductility of the reinforced soil specimens can be evaluated from the variation of failure axial strain, or from the variation of the brittleness index. In addition, the soil ductility can also be assessed by measuring the variation of energy absorption along the complete stress-strain curve, and expressing in terms of normalized energy absorption $[(EAC)_\varepsilon/(EAC)_{\varepsilon ref}]$. For any stress-strain plot, $(EAC)_\varepsilon$ is the area below the stress-deformation curve up to any axial strain ε, whereas $(EAC)_{\varepsilon ref}$ is the area up to the deformation corresponding to the reference strain (ε_{ref}) of 15%.

At any axial deformation or strain level, while comparing for different specimens of varying fibre contents, the normalized energy absorption capability $[(EAC)_\varepsilon/(EAC)_{\varepsilon ref}]$ will be higher for a greater ratio of post-peak stress loss to residual stress. Therefore, at a given strain level, the specimen with a lower value of normalized energy absorption indicates more ductile behaviour and vice versa.

Fig. 7.25 shows typical normalized *EAC* plots for reinforced specimens of 85% relative density with varying fibre content of 20 mm length, under varying confining pressure. Under any confining pressure, as the fibre content increases up to 4%, the normalized energy absorption becomes progressively lower. This indicates that at the same confining pressure, increasing fibre content up to 4% leads to a more ductile behaviour of reinforced soil, though the maximum peak strength is with 3% fibre content (Table 7.2). Similar behaviour has been noted earlier in case of brittleness index (Table 7.8) and specimen failure mode (Figs. 7.4, 7.11 & 7.12), where specimens have shown more ductile behaviour with increasing fibre content and confining pressure.

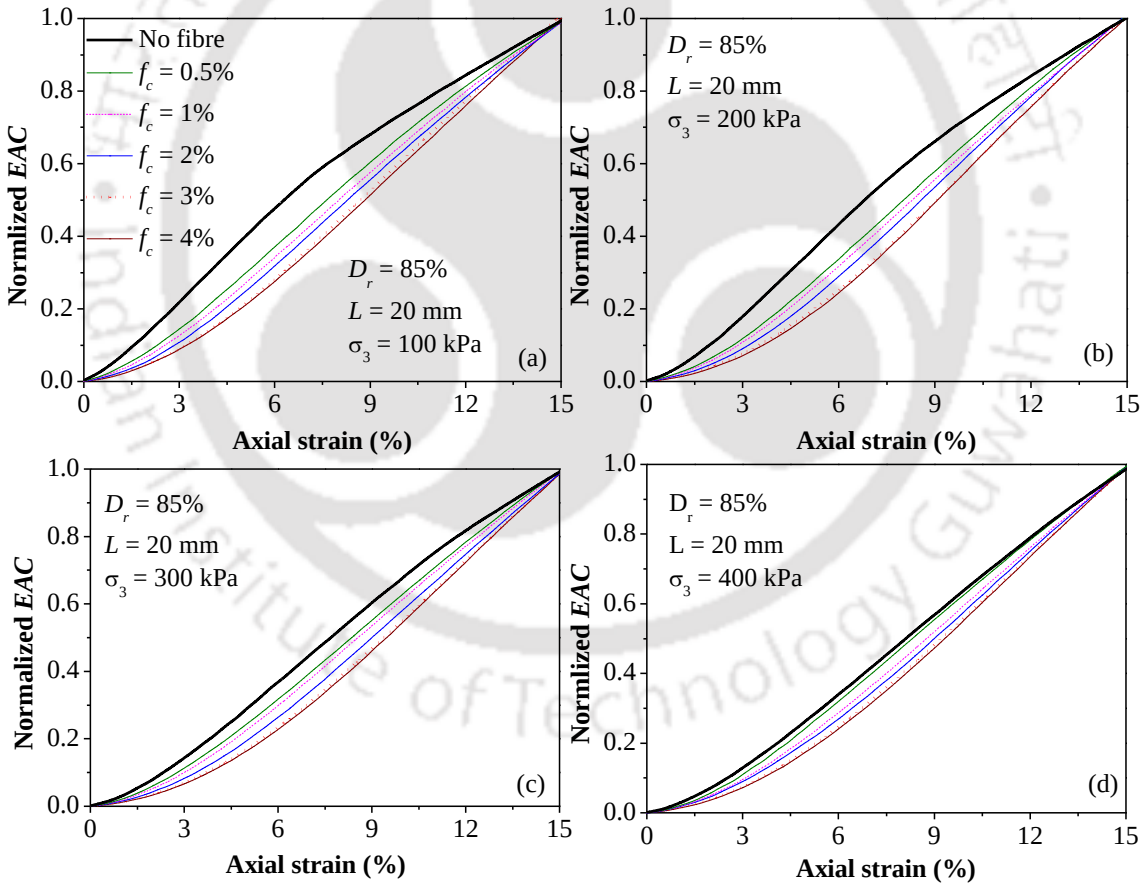

Fig. 7.25 Effect of fibre content of 20 mm length on normalized *EAC* variation under all confining pressures for sand specimens moulded at 85% relative density: (a) σ_3 = 100 kPa; (b) σ_3 = 200 kPa; (c) σ_3 = 300 kPa; (d) σ_3 = 400 kPa

7.4 REGRESSION ANALYSIS

As in Section 6.4, a representative equation has been developed to find out the major principal stress at failure (σ_{1f}) of the glass fibre-reinforced sand by carrying out multiple regression analysis. The major principal stress at failure is influenced by fibre content, fibre aspect ratio, relative density (or dry unit weight) and confining pressure. The expression developed by multiple regression analysis using least square method is:

$$\log_{10}(\sigma_{1f}) = -1.384 + 0.148\log_{10}(f_c) + 0.084\log_{10}(\frac{L}{d}) + 2.2461\log_{10}(\gamma_d) + 0.7\log_{10}(\sigma_3) \quad (7.3)$$

$$\Rightarrow \sigma_{1f} = 0.041(f_c)^{0.148}(\frac{L}{d})^{0.084}(\gamma_d)^{2.246}(\sigma_3)^{0.7} \quad (7.4)$$

where σ_{1f} = major principal stress at failure (kPa); f_c = fibre content (%); L/d = fibre aspect ratio; γ_d = dry unit weight of specimen (kN/m^3) and σ_3 = confining pressure (kPa).

Statistic for goodness of fit such as multiple coefficient of determination R^2, adjusted value of R^2 (i.e. R_a^2) and standard error (E_s) are determined to check how well the equation fits the experimental data. The values of R^2, R_a^2 and E_s for the representative equation obtained from regression analysis are given in Table 7.11. The respective values of R^2, R_a^2 and standard error for Eqn. 6.9 are 0.99, 0.98 and 0.018, and they indicate excellent quality of the fit for the equation.

Table 7.11 Goodness of fit statics for major principal stress at failure

Regression Statistics	
Multiple R	0.99
R Square	0.99
Adjusted R Square	0.98
Standard Error	0.022
Observations	180

Significance tests of the overall model are performed by applying F-test to determine the effectiveness of the representative equation. The significance of individual regression

coefficients in the multiple regression model has been assessed through t-test, by setting the significance level α to 0.05. The results obtained from the analysis of variance (ANOVA) are given in Table 7.12.

From F distribution table with α = 0.05 and degrees of freedom df = (4, 175), the critical value of F (i.e. F_{crt}) for Eqn. 7.4 is found to be 2.28. As the calculated value of F is greater than F_{crt}, the null hypothesis is rejected, and this indicates that at least one of the independent variables of Eqn. 7.4 explains the variation of the dependent variable.

Table 7.12 ANOVA table for major principal stress at failure

	Degree of freedom (df)	**Sum of Squares**	**Mean Squares**	**F**	**Significance F**
Regression	4	5.334	1.067	2189.689	0.0
Residual	175	0.084	0.0		
Total	179	5.419			

Table 7.13 Summary of t-statistics for major principal stress of failure

	Coefficient	**Standard Error**	**T stat**	**P-value**
Intercept	-1.384	0.143	-12.742	0.0
Variable 1 (log f_c)	0.148	0.006	14.196	0.0
Variable 2 (log L/d)	0.084	0.010	6.173	0.0
Variable 3 (log γ_d)	2.246	0.117	1.555	0.0
Variable 4 (log σ_3)	0.700	0.009	13.640	0.0

The summary of the t value for various individual predictor parameters are given in Tables 7.13 for Eqn. 7.4. From the student's t-table, the critical value of t (i.e. t_{crt}) with α/2 = 0.025 and df = 175 for Eqn. 7.4 is found to be 1.984. Similar hypothesis are assumed for all independent variable. From Table 7.13, it can be observed that t value for all independent predictor variables lies in the range of:

$$|t_{cal}| \geq t_{crit} \tag{7.5}$$

The above test results confirm that the proposed representative equation is valid for the material considered in the study.

7.7 SUMMARY

The shear strength behavior of glass fiber-reinforced sandy soil of varying relative density was investigated by conducting consolidated drained (CD) triaxial compression test. The effect of glass fibre and specimen compacted density on deviatoric stress-axial strain, specimen failure mode, failure axial strain, post peak behaviour, shear strength, secant modulus, brittleness index and *EAC* under varying confining pressure was studied. The following conclusions have been drawn from the test results:

1. For the same initial relative density and confining pressure, the peak deviator stress increases with fibre content up to 3% and with fibre length up to 20 mm. With increasing relative density or confining pressure, the peak deviator stress of all specimens also increases.
2. At any relative density, failure axial strain increases with increasing fibre content, fibre length and confining pressure.
3. With increasing fibre content, fibre length and confining pressure, the specimen contractive behaviour at 35% relative density increases, whereas the specimen dilative behaviour at 65% and 85% relative densities decreases.
4. At any relative density, though the initial stiffness of the sand specimen decreases with fibre reinforcement, the residual stress of the reinforced sand specimen increases with increasing fibre content and fibre length with reduction in post-peak stress drop. With increasing confining pressure, the failure deviator stress ratio of the sand specimen decreases for any fibre content or fibre length, indicating that fibre contribution is relatively higher under low confining pressure. However, the *EAC* and ductility of the specimens increase under higher confining pressure.
5. The shear strength of reinforced sandy soil specimen is the maximum with 3% fibres of 20 mm length. At initial relative densities of 35%, 65%, and 85%, the maximum fibre

contributions to effective cohesion intercept and friction angle are 100 kPa and 5.6˚, 106 kPa and 5.4˚, and 115 kPa and 5.4˚, respectively.

6. With increasing fibre content or fibre length, the bulging failure of the sand specimens at 35% relative density is progressively reduced, whereas for the specimens at 65% and 85% relative densities, shear failure is restricted to a smaller zone. With increasing confining pressure, the bulging and shearing of the specimens are further restrained.

CHAPTER 8
SUMMARY AND CONCLUSIONS

8.1 SUMMARY

In this research work, the strength and deformation behaviour of a glass fibre-reinforced clayey soil was studied by conducting UC, CBR and CU triaxial tests, and that of a glass fibre-reinforced sandy soil through CD triaxial tests. The reinforced clayey soil specimens were prepared at varying moulded states (close to OMC and MDU of the unreinforced soil) with different fibre contents (f_c = 0, 0.25, 0.5, 0.75 and 1%) and fibre lengths (L = 10, 20 and 30 mm). The reinforced sandy soil specimens were prepared at varying relative densities (D_r = 35%, 65% and 85% of the unreinforced soil) with different fibre contents (f_c = 0, 0.5, 1, 2, 3 and 4%) and fibre lengths (L = 10, 20 and 30 mm).

The laboratory results were analysed to evaluate the effect of the glass fibres on the compressive strength, CBR, shear strength, failure axial strain, specimen deformation and failure modes, secant modulus and energy absorption capability.

8.2 CONCLUSIONS

Based on the test results and the analyses carried out, the following conclusions have been drawn:

1. The compaction behaviour of the clayey soil is insignificantly affected by glass fibre addition, with only a small reduction in MDU and a marginal increase in OMC with increase in fibre content.
2. Glass fibre reinforcement can effectively increase the UCS, CBR and shear strength of both clayey and sandy soils. For the clayey soil, the optimum glass fibre reinforcement is 0.75% fibre of 20 mm length at any moulding state, and for the sandy soil, it is 3% fibre content of 20 mm length at any relative density.

3. At any dry unit weight, an increase in moulding moisture content up to OMC results in an increase of UCS of reinforced specimens, whereas moisture content above OMC leads to a reduction of UCS. In contrast, at any moulding moisture content, an increase in dry unit weight always results in increase of UCS.
4. At any moulded state of the reinforced specimens, the secant modulus at failure strain level decreases with increasing fibre content keeping the fibre length constant, while the energy absorption capability (EAC) increases with higher fibre content or fibre length or moisture content keeping the others unchanged. However, at any dry unit weight, the secant modulus at failure strain level increases with increasing moisture content only up to OMC and then decreases.
5. The failure pattern of clayey soil specimen is affected by fibre reinforcement and moulding states. Single distinct shear band of unreinforced specimen gradually changed to multi-shear planes along with barrelling in a part of the specimen at 0.25 and 0.5% fibre content, which further transformed to predominantly plastic bulging with a network of minor fissures at higher fibre contents (f_c = 0.75 & 1%) of any length.
6. At low moisture content (w = 19.4 & 21.4%) localized multiple cracks appears around the specimen surface which disappear at higher moisture content (w = 19.4 & 21.4%). At low dry unit weights (γ_d = 14.3 & 15.1 kN/m^3), the failure pattern of the reinforced specimen is characterized with bulging and the appearance of prominent multiple shear cracks, which transformed to plastic bulging with smaller shear cracks at higher dry unit weights (γ_d = 16.0 & 16.8 kN/m^3). However, at the highest dry unit weight (γ_d = 17.6 kN/m^3), the reinforced specimen undergoes distinct shear failure.
7. At any moulded state, the unsoaked CBR of both unreinforced and reinforced clayey soil specimens increases with penetration depth to reach peak value at 5.08 mm and then decreases at higher depths. However, the soaked CBR increases up to a greater

penetration depth of 7.67 mm and then remains nearly constant up to 12.7 mm and CBR value decreases with increasing soaking period.

8. The subgrade modulus of the reinforced clayey soil specimen at 5.08 mm penetration depth is the maximum when moulded at OMC, and the value is lower on either side of OMC with more reduction on the wet side. The subgrade modulus value decreases gradually with increasing soaking period.
9. The inclusion of 0.75% fibres of 20 mm length effectively improves the quality of the unreinforced clayey soil as subgrade material from very poor (soaked CBR = 2.89%) to good (soaked CBR = 8.23%). When this particular soil-fibre mix is compacted at OMC as subgrade layer in the field, the overlying pavement thickness for low-volume flexible pavements can be reduced up to 25% even under a traffic value of 150 msa.
10. At any moulding dry unit weight and confining pressure, the failure deviator stress of reinforced specimens increases only up to limiting magnitudes of fibre content (f_c = 0.75%) or fibre length (L = 20 mm).
11. For the same dry unit weight, under undrained condition, the positive pore water pressure of reinforced specimens increases with the increase of any of fibre content, fibre length or confining pressure keeping other parameters constant.
12. At the same dry unit weight, the bulging deformation of unreinforced specimen is reduced more with increasing fibre content, fibre length or confining pressure. As the confining pressure is increased, the influence of the fibres reduces as the strength of the soil itself increases. If the confining pressure is increased to higher levels, the soil may not show bulging due to compressive volume changes even without addition of fibres.
13. For the same initial relative density and confining pressure, the peak deviator stress of sandy soil specimen increases with fibre content up to 3% and with fibre length up to 20 mm. With increasing relative density or confining pressure, the peak deviator stress of all

specimens also increases. However the failure axial strain increases with increasing fibre content, fibre length and confining pressure at any relative density.

14. With increasing fibre content, fibre length and confining pressure, the specimen contractive behaviour at 35% relative density increases, whereas the specimen dilative behaviour at 65% and 85% relative densities decreases.
15. At any relative density, though the initial stiffness of the sand specimen decreases with fibre reinforcement, the residual stress of the reinforced sand specimen increases with increasing fibre content and fibre length with reduction in post-peak stress drop. With increasing confining pressure, the failure deviator stress ratio of the sand specimen decreases for any fibre content or fibre length, indicating that fibre contribution is relatively higher under low confining pressure. However, the *EAC* and ductility of the specimens increase under higher confining pressure.
16. With increasing fibre content or fibre length, the bulging failure of 35% relative density sand specimens is progressively reduced, whereas for the specimens at 65% and 85% relative densities, shear failure is restricted to a smaller zone. With increasing confining pressure, the bulging and shearing are further restrained.

8.3 SCOPE FOR FURTHER RESEARCH

Resilient modulus tests can be conducted on the glass fibre-soil mixes of varying moulded states to evaluate their behaviour under cyclic loading states that simulate the conditions of moving vehicular wheel loads.

REFERENCES

1. Abdullah, M. N., Normaniza Osman, N and Ali, F.H. (2011). "Soil-root shear strength properties of some slope plants." *Sains Malaysiana*, 40(10), 1065-1073.
2. Abbott, S. (2017). "Railway geotechnical asset management in Great Britain." *Geostrata*, January/February, pp. 50-55.
3. Ahmad, F., Bateni, F. and Azmi, M. (2010). "Performance evaluation of silty sand reinforced with fibres." *Geotextiles and Geomembranes*, 28(1), 93-99.
4. Ahmad, F., Mujah, F., Hazarika, H. and Safari, A. (2012). "Assessing the potential reuse of recycled glass fibre in problematic soil applications." *Journal of Cleaner Production*, 35, 102-107.
5. Akbulut, S., Arasan, S. and Kalkan, E. (2007). "Modification of clayey soils using scrap tire rubber and synthetic fibres." *Applied Clay Science*, 38(1), 23-32.
6. Andersland, O.B. and Khattak, A.S. (1979). "Shear strength of kaolinite/ fiber soil mixture." *In: Proceedings of international conference on soil reinforcement*. Paris, 1, pp. 11-16.
7. Anagnostopoulos, C.A., Tzetzis, D. and Berketis, K. (2014). "Shear strength behaviour of polypropylene fibre reinforced cohesive soils." *Geomechanics and Geoengineering*, 9(3), 241-251.
8. Ang, E.C. and Loehr, J.E. (2003). "Specimen Size Effects for Fibre-Reinforced Silty Clay in Unconfined Compression." *Geotechnical Testing Journal*, 26(2), 191-200.
9. Al-Refeai, T.O. (1991). "Behavior of granular soils reinforced with discrete randomly oriented inclusions." *Geotextiles and Geomembranes*, 10(4), 319-333.
10. Al-Refeai, T.O. and Al- Suhaibani, A. (1998). "Dynamic and static characterization of polypropylene fiber-reinforced dune sand." *Geosynthetics International*, 5(5), 443-458.

11. ASTM C1018 (1997). Standard test method for flexural toughness and first-crack strength of fibre-reinforced concrete (using beam with third-point loading). ASTM International, West Conshohocken, PA, USA.
12. ASTM D 422-63 (2007). Standard test method for particle-size analysis of soils. ASTM International, West Conshohocken, PA, USA.
13. ASTM D 698 (2012). Standard test methods for laboratory compaction characteristics of soil using standard effort (12,400 ft-lbf/ft^3 (600 kN-m/m^3)). ASTM International, West Conshohocken, PA, USA.
14. ASTM D 792 (2008). Standard test methods for density and specific gravity (relative density) of plastics by displacement. ASTM International, West Conshohocken, PA, USA.
15. ASTM D 854 (2010). Standard test methods for specific gravity of soil solids by water pycnometer. ASTM International, West Conshohocken, PA, USA.
16. ASTM D 1883 (2016). Standard test method for California Bearing Ratio (CBR) of laboratory-compacted soils. West Conshohocken, PA, USA.
17. ASTM D 2166/D 2166M (2013) Standard test method for unconfined compressive strength of cohesive soil. ASTM International, West Conshohocken, PA, USA.
18. ASTM D 2487 (2011). Standard Practice for Classification of Soils for Engineering Purposes (Unified Soil Classification System). ASTM International, West Conshohocken, PA USA.
19. ASTM D 4254 (2006). Standard test methods for minimum index density and unit weight of soils and calculation of relative density. ASTM International, West Conshohocken, PA, USA.
20. ASTM D 4318 (2010). Standard test methods for liquid limit, plastic limit, and plasticity index of soils. ASTM International, West Conshohocken, PA, USA.

21. ASTM D 4767 (2011). Standard test method for consolidated undrained triaxial compression test for cohesive soils. ASTM International, West Conshohocken, PA, USA.
22. ASTM D 6913 (2009). Standard test methods for particle-size distribution (gradation) of soils using sieve analysis. ASTM International, West Conshohocken, PA, USA.
23. Attom, M.F., Al-Akhras, N.M. and Malkawi, A.I.H. (2009). "Effect of fibres on the mechanical properties of clayey soil." *Proceedings of the Institution of Civil Engineers-Geotechnical Engineering*, 162(5), 277-282.
24. Ayyappan, S., Hemlatha, K. and Sundaram, M. (2010). "Investigation of engineering behavior of soil, polypropylene fibres and fly ash -mixtures for road construction." *International Journal of Environmental Science and Development*, 1(2), 171-175.
25. Benson, C.H. and Khire, M.V. (1994). "Reinforcing sand with strips of reclaimed high-density polyethylene." *Journal of Geotechnical Engineering*, 120(5), 838-855.
26. Buckingham, E. (1914). "On physically similar systems: illustrations of the use of dimensional equations." *Physical Review*, 4(4), 345-376.
27. Butterfield, R. (1999). "Dimensional analysis for geotechnical engineers." *Geotechnique*, 49(3), 357-366.
28. Cetin, H., Fener, M. and Gunaydin, O. (2006). "Geotechnical properties of tire-cohesive clayey soil mixtures as a fill material." *Engineering Geology*, 88(1), 110-120.
29. Chandra, S., Viladkar, M.N. and Nagrale, P.P. (2008). "Mechanistic approach for fibre-reinforced flexible pavements." *Journal of Transportation Engineering*, 134(1), 15-23.

30. Choudhary, A.K., Jha, J.N. and Gill, K.S. (2010). "A study on CBR behavior of waste plastic strip reinforced soil." *Emirates Journal for Engineering Research*, 15(1), 51-57.

31. Claria, J.J. and Vettorelo P.V. (2016). "Mechanical behavior of loose sand reinforced with synthetic fibers." *Soil Mechanics and Foundation Engineering*, 53(1), 12-18.

32. Consoli, N.C., Prietto, P.D.M. and Ulbrich, L.A. (1998). "Influence of fibre and cement addition on behavior of sandy soil." *Journal of Geotechnical and Geoenvironmental Engineering*, 124(12), 1211-1214.

33. Consoli, N.C., Montardo, J.P., Prietto, P.D.M. and Pasa, G.S. (2002). "Engineering behavior of a sand reinforced with plastic waste." *Journal of Geotechnical and Geoenvironmemtal Engineering*, 128(6), 462-472.

34. Consoli, N.C., Vendruscolo, M.A. and Prietto, P.D.M. (2003a). "Behavior of plate load tests on soil layers improved with cement and fibre." *Journal of Geotechnical and Geoenvironmental Engineering*, 129(1), 96-101.

35. Consoli, N.C., Casagrande, M.D.T., Prietto, P.D.M. and Thome, A. (2003b). "Plate load test on fibre-reinforced soil." *Journal of Geotechnical and Geoenvironmental Engineering*, 129(10), 951-955.

36. Consoli, N.C., Heineck, K.S., Casagrande, M.D.T. and Coop, M.R. (2007). "Shear strength behavior of fibre-reinforced sand considering triaxial tests under distinct stress paths." *Journal of Geotechnical and Geoenvironmental Engineering*, 133(11), 1466-1469.

37. Consoli, N.C., Casagrande, M.D.T., Thome, T., Dalla Rosa, F. and Fahey, M. (2009a). "Effect of relative density on plate loading tests on fibre-reinforced sand." *Geotechnique*, 59(5), 471-476.

38. Consoli, N.C., Vendruscolo, M.A., Fonini, A. and Rosa, F.D. (2009b). "Fibre reinforcement effects on sand considering a wide cementation range." *Geotextiles and Geomembranes*, 27(3), 196-203.

39. Consoli, N.C., Festugato, L. and Heineck, K.S. (2009c). "Strain-hardening behaviour of fibre-reinforced sand in view of filament geometry." *Geosynthetics International*, 16(2), 109-115.

40. Consoli, N.C., Montardo, J.P., Donato, M. and Prietto, P.D.M. (2004). "Effect of material properties on the behaviour of sand cement fibre composites." *Proceedings of the Institution of Civil Engineers-Ground Improvement*, 8(2), 77-90.

41. Crockford, W.W., Grogan, W.P. and Chill, D.S. (1993). "Strength and life of stabilized layers containing fibrillated polypropylene." *Transportation Research Record 1418*, 60-66.

42. Dove, J.E. and Frost, J.D. (1999). "Peak friction behavior of smooth geomembrane-particle interface." *Journal of Geotechnical and Geoenvironmental Engineering*, 129(7), 544-555.

43. Edincliler, A. and Cagatay, A. (2013). "Weak subgrade improvement with rubber fibre inclusions." *Geosynthetics International*, 20(1), 39-46.

44. Eldesouky, H., Morsy, M.M. and Mansour, M.F. (2016). "Fibre-reinforced sand strength and dilation characteristics." *Ain Shams Engineering Journal*, 7(2), 517-526.

45. Estabragh, A.R., Bordbar, A.T. and Javadi, A.A. (2011). "Mechanical behavior of a clay soil reinforced with nylon fibres." *Geotech and Geological Engineering*, 29(5), 899-908.

46. Estabragh, A.R., Bordbar, A.T. and Javadi, A.A. (2013). "A study on the mechanical behavior of a fibre-clay composite with natural fibre." *Geotechnical and Geological Engineering*, 31(2), 501-510.

47. Fakher, A., Jones, C.J.F.P. (1996). "Discussion of bearing capacity of rectangular footings on geogrid reinforced sand." by Yetimoglu, T., Wu, J.T.H., Saglamer, A. *Journal of Geotechnical Engineering*, 122(4), 326-327.

48. Falorca, I.M.C.F.G. and Pinto, M.I.M. (2011). "Effect of short, randomly distributed polypropylene microfibres on shear strength behaviour of soils." *Geosynthetics International*, 18(1), 2-11.

49. Falorca, I.M.C.F.G., Pinto, M.I.M. and Ferreira Gomes, L.M.F. (2006). "Residual shear strength of sandy clay reinforced with short polypropylene fibres randomly oriented." *Proceedings of the 8th International Conference on Geosynthetics*, pp. 18-22.

50. Falorca, I.M.C.F.G., Gomes, L.M.F. and Pinto, M.I.M. (2011). "A full-scale trial embankment construction with soil reinforced with short randomly distributed polypropylene microfibers." *Geosynthetics International*, 18(5), 280-288.

51. Fletcher, C.S. and Humphries, W.K. (1991). "California bearing ratio improvement of remoulded soils by the addition of polypropylene fibre reinforcement." *Transportation Research Record 1295*, pp 80-86.

52. Freilich, B.J., Li, C. and Zornberg, J.G. (2010). "Effective Shear Strength of Fibre-Reinforced Clays." *9th International Conference on Geosynthetics*, Brazil, pp 1997-2000.

53. Freitag, D.R. (1986). "Soil randomly reinforced with fibres." *Journal of Geotechnical Engineering*, 112(8), 823-826.

54. Frost, J.D. and Han, J. (1999). "Behavior of interfaces between fibre reinforced polymers and sands." *Journal of Geotechnical and Geoenvironmental Engineering*, 125(8), 633-640.

55. Gray G.H. and Ohashi H. (1983). "Mechanics of fibre reinforcement in sand." *Journal of Geotechnical Engineering*, 109(3), 335-353.

56. Gray, G.H. and Al Refeai, T. (1986). "Behavior of fabric- versus fibre reinforced sand." *Journal of Geotechnical Engineering*, 112(8), 804-820.

57. Gregory, G.H. (2011). "Sustainability and the fibre-reinforced soil repair of a roadway embankment." *Geosynthetic*, 29(4), 18-22.

58. Greenwood, J.R., Norris, J.E. and Wint, J. (2004). "Assessing the contribution of vegetation to slope stability." *Geotechnical Engineering*, 157(4), 199-207.

59. Hataf, N. and Rahimi, M.M. (2006). "Experimental investigation of bearing capacity of sand reinforced with randomly distributed tire shreds." *Construction and Building Materials*, 20, 910-916.

60. Hamidi, A. and Hooresfand, M. (2013). "Effect of fibre reinforcement on triaxial shear behavior of cement treated sand." *Geotextiles and Geomembranes*, 36, 1-9.

61. Hazirbaba, K. and Gullu, H. (2010). "California Bearing Ratio improvement and freeze-thaw performance of fine-grained soils treated with geofibre and synthetic fluid." *Cold Regions Science and Technology*, 63(1), 50-60.

62. Haeri, S.M., Noorzad, R. and Oskoorouchi, A.M. (2000). "Effect of geotextile reinforcement on the mechanical behavior of sand." *Geotextiles and Geomembranes*, 18(6), 385-402.

63. Hoover, J.M., Moeller, D.T., Pitt, J.M., Smith, S.G. and Wainaina, N.W. (1982). Performance of randomly oriented fibre-reinforced roadway soils. Lowa DOT Project-HR-211, Department of Transportation, Highway Division, Lowa State University.

64. http://www.chhajedgarden.com/blog/vetiver-planting-for-slope-stabilization/ Accessed on 15th may 2017.

65. IRC SP 20 (2002). Rural road manual. Indian Road Congress Special Publication 20. New Delhi, India.

66. IRC 37 (2001). Guidelines for the design of flexible pavements. The Indian Road Congress, New Delhi, India.

67. IRC SP 72 (2007). Guidelines for the design of flexible pavements for low volume rural roads. The Indian Road Congress, New Delhi, India.

68. Jha, J.N., Choudhary, A.K., Gill, K.S. and Shukla, S.K. (2014). "Behavior of plastic waste fibre-reinforced industrial wastes in pavement applications." *International Journal of Geotechnical Engineering*, 8(3), 277-286.

69. Jiang, H., Cai, Y. and Liu, J. (2010). "Engineering properties of soils reinforced by short discrete polypropylene fibre." *Journal of Materials in Civil Engineering*, 22(12), 1315-1322.

70. Kalantri, B., Huat, B.B.K. and Prasad, A. (2010). "Effect of polypropylene fibres on the california bearing ratio of air cured stabilized tropical peat soil." *American Journal of Engineering and Applied Sciences*, 3(1), 1-6.

71. Kaniraj, S.R. and Havanagi, V.J. (2001). "Behavior of cement-stabilized fibre-reinforced fly ash-soil mixtures." *Journal of Geotechnical and Geoenvironmental Engineering*, 127(7), 574-584.

72. Koerner, R.M. (1998). Designing with geosynthetics, 4th editionn, Prentice Hall, New Jersey, USA.

73. Kumar, P. and Singh, S.P. (2008). "Fibre-reinforced fly ash subbases in rural roads." *Journal of Transportation Engineering*, 134(4), 171-180.

74. Kumar, R., Kanaujia, V.K. and Chandra, D. (1999). "Engineering behaviour of fibre-reinforced pond ash and silty sand." *Geosynthetics International*, 6(6), 509-518.

75. Kumar, P., Mehndiratta, H.C., Chandranarayana, S. and Singh, S.P. (2005). "Effect of randomly distributed fibres on flyash embankments." *Journal of Institute of Engineers, India Part CV, Civil Engineering Division Board*, 86, (3), 113-118.

76. Ladd, R.S. (1978). "Preparing test specimens using undercompaction." *Geotechnical Testing Journal*, 1(1), 16-23.

77. Li, C. and Zornberg, j.G. (2013). "Mobilization of reinforcement forces in fibre reinforced soil." *Journal of Geotechnical and Geoenvironmental Engineering*, 139(1), 107-115.

78. Li, J., Tang, C., Wang, D., Pei, X. and Shi, B. (2014). "Effect of discrete fibre reinforcement on soil tensile strength." *Journal of Rock Mechanics and Geotechnical Engineering*, 6(2), 133-137.

79. Lovisa, J., Shukla, S.K. and Shivakugam, N. (2010). "Shear strength of randomly distributed moist fibrereinforced sand." *Geosynthetic International*, 17(2), 100-106.

80. Lutz, J.T. and Grossman, R.F. (2001). Polymer modifiers and additives. In: Roberto, A., -Anido, Lopez, Tarun, R.N., Gary, T.F., David, A.L. and Vistasp, M.K. (Eds.), Emerging Material for Civil Infrastructure: State of the Art. ACSE, USA. ISBN 0-7844-0583-7.

81. Maher, M.H. and Gray, D.H. (1990). "Static response of sands reinforced with randomly distributed fibres." *Journal of Geotechnical Engineering*, 116(11), 1661-1677.

82. Maher, M.H. and Ho, Y.C. (1993). "Behavior of Fibre-Reinforced Cemented Sand Under Static and Cyclic Loads." *Geotechnical Testing Journal*, 16(3), 330-338.

83. Maher, M.H. and Ho, Y.C. (1994). "Mechanical properties of kaolinite fibre soil composite." *Journal of Geotechnical Engineering*, 120(8), 1381-1393.

84. Mashiri, M.S., Vinod, V.S., Seikh, M.N. and Tsang, H.H. (2015). "Shear strength and dilatancy behavior of sand-tyre chip mixtures." *Soils and Foundations*, 55(3), 517-528.

85. McGown, A., Andrawes, K.Z. and Al-Hasani, M.M. (1978). "Effect of inclusion properties on the behavior of sand." *Geptechnique*, 28(3), 327-346.

86. Michalowsk, R.L. and Zhao, A. (1996). "Failure of fibre-reinforced granular soils." *Journal of Geotechnical Engineering*, 122(3), 226-234.

87. Michalowski, R.L. and Cermak, J. (2002). "Strength anisotropy of fibre-reinforced sand." *Computer and Geotechnics*, 29(4), 279-299.

88. Michalowaski, R.L. and Cermak, J. (2003). "Triaxial compression of sand reinforced with fibres." *Journal of Geotechnical and Geoenvironmental Engineering*, 129(2), 125-136.

89. Michalowaski R.L. (2008). "Limit analysis with anisotropic fibre-reinforced soil." *Geotechnique*, 58(6), 489-501.

90. Mirzababaei, M., Miraftab, M., Mohamed, M. and MacMohan, P. (2013). "Unconfined compression strength of reinforced clays with carpet waste fibres." *Journal of Geotechnical and Geoenvironmental Engineering*, 139(2), 483-493.

91. Mohanty, B., Chauhan, M.S. and Mittal, S. (2011). "California bearing ratio of randomly oriented fibre reinforced clayey subgrade for rural roads." *Proceedings of Indian Geotechnical Conference*, India, Paper No. J-354.

92. Moraci, N. and Recalcati, P. (2006). "Factors affecting the pullout behavior of extruded geogrids embedded in a compacted granular soil." *Geotextiles and Geomembranes*, 24(4), 220-242.

93. Mujah, D., Ahmad, F., Hazarika, H and Safari, A. (2013). "Evaluation of the mechanical properties of recycled glass fibers-derived three dimensional geomaterial for ground improvement." *Journal of Cleaner Production*, 52, 495-503.

94. Muntohar, A.S., Widiyanti, A., Hartono, E. and Diana, W. (2013). "Engineering properties of silty soil stabilized withLime and rice husk ash and reinforced with waste plastic fibre." *Journal of Materials in Civil Engineering*, 25(9), 1260-1270.

95. Nataraj, M.S. and McMain, K.L. (1997). "Strength and deformation properties of soils reinforced with fibrillated fibres." *Geosynthetic International*, 4(1), 65-79.

96. Najjar, S.S., Sadek, S. and Alcovero, A. (2013). "Quantification of model uncertainty in shear strength predictions for fiber-reinforced sand." *Journal of Geotechnical and Geoenvironmental Engineering*, 139(1), 116-133.

97. Nasr, A.M. (2014). "Behavior of strip footing on fiber-reinforced cemented sand adjacent to sheet pile wall." *Geotextiles and Geomembranes*, 42(6), 599-610.

98. Ozkul, Z.H. and Baykal, G. (2006). "Shear strength of clay with rubber fibre inclusions." *Geosynthetics International*, 13(5), 173-180.

99. Ozkul, Z.H. and Baykal, G. (2007). "Shear behavior of compacted rubber fibre-clay composite in drained and undrained loading." *Journal of Geotechnical and Geoenvironmental Engineering*, 133(7), 767-781.

100. Park, S. (2009). "Effect of fibre reinforcement and distribution on unconfined compressive strength of fibre-reinforced cemented sand." *Geotextiles and Geomembranes*, 27(2), 162-166.

101. Park, S. (2011). "Unconfined compressive strength and ductility of fibre-reinforced cemented sand." *Construction and Building Materials*, 25(2), 1134-1138.

102. Park, T. and Tan, S.A. (2005). "Enhanced performance of reinforced soil walls by the inclusion of short fibre." *Geotextiles and Geomembranes*, 23(4), 348-361.

103. Ple, O. and Le, T.N.H. (2012). "Effect of polypropylene fibre-reinforcement on the mechanical behavior of silty clay." *Geotextiles and Geomembranes*, 32, 111-116.

104. Prabakar, J. and Sridhar, R.S. (2002). "Effect of random inclusion of sisal fibre on strength behaviour of soil." *Construction and Building Materials*, 16(2), 123-131.

105. Pradhan, P.K., Kar. R.K. and Naik, A. (2012). "Effect of random inclusion of polypropylene fibres on strength characteristics of cohesive soil." *Geotechnical and Geological Engineering*, 30(1), 15-25.

106. Puppala, A.J. and Musenda, C. (2000). "Effects of fibre reinforcement on strength and volume change in expansive soils." *Transportation Research Record: Journal of Transportation Research Board*, TRB 1736, 134-140.

107. Qu, J., Li, C., Liu, B., Chen, X., Li, M. and Yao, Z. (2013). "Effect of random inclusion of wheat straw fibers on shear strength characteristics of Shanghai cohesive soil." *Geotechnical and Geological Engineering*, 31, 511-518.

108. Racana, N., Grédiac, M. and Gourvès, R. (2003). "Pull-out response of corrugated geotextile strips." *Geotextiles and Geomembranes*, 21(5), 265-288.

109. Rafalko, S.D., Brandon, T. L., Filz, G. M. and Mitchell, J. K. (2006). "Fibre reinforcement for rapid stabilization of soft clay soils." Technical Report AFRL-RX-TY-TP-2009-4603, Department of Civil and Environmental Engineering Virginia Polytechnic Institute and State University Blacksburg, VA 24060-0105.

110. Rao, S.V.K. and Nasar, A.M.A. (2012). "Laboratory study on the relative performance of silty-sand soils reinforced with linen fibre." *Geotechnical and Geological Engineering*, 30(1), 63-74.

111. Ranjan, G., Vasan, R.M. and Charan, H.D. (1994). "Behaviour of plastic fibre reinforced sand." *Geotextiles and Geomembranes*, 13(8), 555-565.

112. Ranjan, G., Vasan, R.M. and Charan, H.D. (1996). "Probabilistic analysis of randomly distributed fibre reinforced soil." *Journal of Geotechnical Engineering*, 122(6), 419-426.

113. Santoni, R.L. and Webster, S.L. (2001). "Airfields and roads construction using fibre stabilization of sands." *Journal of Transportation Engineering*, 127(2), 96-104.

114. Santoni, R.L., Tingle, J.S. and Webster, S.L. (2001). "Engineering properties of sand-fibre mixtures for road construction." *Journal of Geotechnical and Geoenvironmental Engineering*, 127(3), 258-268.

115. Sarbaz, H., Ghiassian, H. and Heshmati, A.K. (2014). "CBR strength of reinforced soil with natural fibres and considering environmental conditions." *International Journal of Pavement Engineering*, 15(7), 577-583.

116. Sarsby, R.W. (2007). Geosynthetic in civil engineering. 1st Edition, Woodhead Publication Ltd, Cambridge.

117. Sadek, S., Najjar. S.S. and Freiha, F. (2010). "Shear strength of fibre reinforced sands." *Journal of Geotechnical and Geoenvironmental Engineering*, 136(3), 490-499.

118. Schlosser, F. and Long, N.T. (1974). "Recent results in French research on reinforced earth." *Journal of Construction Division*, 100(3), 223-237.

119. Shewbridge S.E. and Sitar N. (1989). "Deformation characteristic of reinforced sand in direct shear" *Journal of Geotechnical Engineering*, 115(8), 1134-1147.

120. Shukla, S.K. (2002). Geosynthetics and their applications. Thomas Telford, London.

121. Shukla, S.K. (2017). Fundamentals of fibre-reinforced soil engineering. Springer Nature, Singapore.

122. Shukla S.K., Shivakugan N. and Singh A.K. (2010). "Analytical model for fibre-reinforced granular soil under high confining stress." *Journal of Material in Civil Engineering*, 22(9), 935-942.

123. Sivakumar Babu, G.L.S. and Chouskey, S.K. (2011). "Stress strain response of plastic waste mixed soil." *Waste Management*, 31(3), 481-488.

124. Sivakumar Babu G.L. and Vasudevan A.K. (2008). "Strength and stiffness response of coir fibre-reinforced tropical soil." *Journal of Materials in Civil Engineering*, 20(9), 571-577.

125. Sivakumar Babu, G.L., Vasudevan, A.K. and Sayida, M.K. (2008). "Use of coir fibres for improving the engineering properties of expansive soils." *Journal of Natural Fibres*, 5(1), 61-75.

126. Tafreshi, S.N.M. and Norouzi, A.H. (2012). "Bearing capacity of a square model footing on sand reinforced with shredded tire - An experimental investigation." *Construction and Building Materials*, 35, 547-556.

127. Take, W.A., Irving, J., Bischoff, P.H. and Valsangkar, A.J. (1997). "Synthetic fibre reinforcement of clayey sand and silt subgrade and sand sub base." *Proceedings of the International Conference on Ground Improvement Techniques*, pp 547-552.

128. Tang, C.S., Shi, B. and Zhao, L.Z. (2010). "Interfacial shear strength of fibre reinforced soil." *Geotextiles and Geomembranes*, 28(1), 54-62.

129. Tang, C., Shi, B., Gao, W., Chen, F. and Cai, Y. (2007). "Strength and mechanical behavior of short polypropylene fibre reinforced and cement stabilized clayey soil." *Geotextiles and Geomembranes*, 25(3), 194-202.

130. Tingle, J.S., Santoni, R.L. and Webster, S.L. (2002). "Full scale field tests of discrete fibre reinforced sand." *Journal of Transportation Engineering*, 128(1), 9-16.

131. Vidal, H. (1969). The principle of reinforced earth. Highway Research Record 282, 1-16.

132. Waldron L.J. (1977). "The shear resistance of root permeated homogeneous and stratified soil." *Soil Science Society of America Proceedings*, 41(5), 843-849.

133. Waldron, L.J. and Dakessian, S. (1981). "Soil reinforcement by roots: calculation of increased soil shears resistance from root properties." *Soil Science*, 132(6), 427-435.

134. Wasti, Y. and Butun, M.D. (1996). "Behaviour of model footings on sand reinforced with discrete inclusions." *Geotextiles and Geomembranes*, 14, 575-584.

135. White, D.J., Vennapusa, P.K.R., Becker, P., White, C. and Engineers, B.C. (2013). "Cement Stabilization with Fibre Reinforcement of Subbase." Technical Brief, Centre for CEER Earthworks Engineering Research, Iowa State University, Institute of Transportation.

136. Wu, T.H., McKinnell, W.P. and Swanston, D.N. (1979). "Strength of tree roots and landslides on Prince of Wales Island, Alaska." *Canadian Geotechnical Journal*, 16(1), 19-33.

137. Yetimoglu, T. and Salbas, O. (2003). "A study on shear strength of sands reinforced with randomly distributed discrete fibres." *Geotextiles and Geomembranes*, 21(2), 103-110.

138. Yetimoglu, T., Inanir, M. and Inanir, O. E. (2005). "A studyon bearing capacityof randomly distributed fibre-reinforced sand fills overlying soft clay." *Geotextiles and Geomembranes*, 23(2), 174-183.

139. Yoder, E.J., Witczak, M.W. (1975). Principles of Pavement Design. Wiley, New York.

140. Yoon, S., Prezzi, M., Siddiki, N.Z. and Kim, B. (2006). "Construction of a test embankment using a sand-tire shred mixture as fill material." *Waste Management*, 26(9), 1033-1044.

141. Zaimoglu, A.S. and Yetimoglu, T. (2012). "Strength behavior of fine grained soil reinforced with randomly distributed polypropylene fibres." *Geotechnical and Geological Engineering*, 30(1), 197-203.

142. Zhang, Z., Farrag, K. and Morvant, M. (2003). "Evaluation of effect of synthetic fibers and nonwoven geotextile reinforcement on the stability of heavy clay embankments." FHWA/La 03/373. Lousiana Transportation research centre, Balton Rouge, L.A., U.S.A.

143. Zhang, M.X., Javadib, A.A. and Min, X. (2006). "Triaxial tests of sand reinforced with 3D inclusions." *Geotextiles and Geomembranes*, 24(4), 201-209.

144. Zornberg, J.G. (2002). "Discrete framework for limit equilibrium analysis of fibre-reinforced soil, *Geotechnique*, 52(8), 593-604.

LIST OF PUBLICATIONS

Journals:

- Patel S.K. and Singh B. (2018). "Shear Strength and Deformation Behaviour of Glass Fibre-Reinforced Cohesive Soil with Varying Dry Unit Weight". *Indian Geotechnical Journal*. doi: 10.1007/s40098-018-0323-5
- Patel S.K. and Singh B. (2017). "Shear strength response of glass fibre-reinforced sand with varying compacted relative density". *International Journal of Geotechnical Engineering*. doi: 10.1080/19386362.2017.1352157
- Patel S.K. and Singh B. (2017). "Experimental investigation on the behaviour of glass fibre-reinforced cohesive soil for application as pavement subgrade material". *International Journal of Geosynthetics and Ground Engineering*, 3 (2), 1-12. doi: 10.1007/s40891-017-0090-x
- Patel S.K. and Singh B. (2017). "Strength and deformation behavior of fibre-reinforced cohesive soil under varying moisture and compaction states". *Geotechnical and Geological Engineering*. 35 (4), 1767-1781. doi: 10.1007/s10706-017-0207-y
- Patel, S.K. and Singh, B. (2016). "Experimental investigation on strength aspects of glass fibre-reinforced fine grained soil". *International Journal of Earth Sciences and Engineering*, 9 (3), 32-39.
- Patel, S.K. and Singh, B. (2015). "Review of predictive models for shear strength behaviour of fibre reinforced soils." *Journal of Environmental Research and Development*, 10 (1), 161-172.
- Patel, S.K. and Singh, B. (2015). "Strength and stiffness development of fibre-reinforced lateratic soil." *Journal of Environmental Research Development*, 9(3A), 995-1002.

- Patel, S.K. and Singh, B. (2014). "Unconfined compressive strength behaviour of fibre-reinforced lateritic soil." *Journal of Civil Engineering and Environmental Technology*, 1(4), 93-98.

Book Chapter:

- Patel S.K. and Singh B. (2018). Experimental study on shear strength behavior of Glass fiber-reinforced sand. In A. Sevi et al. (eds.), *Enhancements in Applied Geomechanics, Mining, and Excavation Simulation and Analysis*, Sustainable infrastructures, Springer. doi: 10.1007/978-3-319-95645-9_14
- Patel S.K. and Singh B. (2018). Investigation of glass fiber reinforcement effect on the CBR strength of cohesive soil. In T. Thyagaraj (ed.), *Ground Improvement Techniques and Geosynthetics*. doi: 10.1007/978-981-13-0559-7_8

Conferences:

- Patel S.K. and Singh B. (2017). "Effect of compacted moisture content variation on compressive strength of fibre-reinforced cohesive soil." *Proceedings of Indian Geotechnical Conference*, IIT Guwahati, India (CD-ROM).
- Patel S.K. and Singh B. (2016). "Investigation of Glass Fibre Reinforcement Effect on the CBR Strength of Cohesive Soil". *Proceedings of Indian Geotechnical Conference*, IIT Madras, India (CD-ROM).
- Patel, S.K. and Singh, B. (2016). "Effect of compaction state on unconfined compressive strength of glass fibre reinforced fine-grained soil." *Proceedings of International Conference on Soil and Environment*, IISc Bengaluru, India (CD-ROM).

- Jose, A., Patel, S.K. and Singh, B. (2015). "Laboratory investigation on strength characteristics of fibre reinforced cohesive soil." *Proceedings of 50th Indian Geotechnical Conference*, Pune, India (CD-ROM).
- Patel, S.K. and Singh, B. (2015). "Effect of fibre reinforcement on strength and stiffness improvement of cohesive soil." *Proceedings of International Conference on Infrastructure Development for Environmental Conservation and Sustenance*, India, 167-173.
- Patel, S.K and Singh, B. (2015). "CBR behaviour of randomly distributed glass fibre reinforced soil." *Proceedings of International Conference on Geo-Engineering and Climate Change Technologies for Sustainable Environment Management*, MNIT Allahabad, India.
- Patel, S.K and Singh, B. (2015). "Improvement in strength characteristic of fibre reinforced sandy soil." *Proceedings of 5th Indian Young Geotechnical Engineers Conference*, Vadodara, India, 190-193.
- Patel, S.K. and Singh, B. (2014). "Modification of strength behavior of sandy soil with synthetic fibre." *Proceedings of Indian Geotechnical Conference*, Kakinada, India, 683-689.
- Patel, S.K. and Singh, B. (2014). "Influence of glass fibre inclusion on strength characteristics of a sandy." *North East Students Geo-Congress on Advances in Geotechnical Engineering*, IIT Guwahati, India (CD-ROM).
- Patel, S.K. and Singh, B. (2014). "Models for Predicting Shear Strength of Fibre-Reinforced Soils." *Proceedings of 3rd International Conference on Sustainable Innovative Techniques in Architecture, Civil and Environmental Engineering*, JNU New Delhi, India, 335-342.